AD-A189 574 FROZEN ORBIT ANALYSIS IN THE MARTIAN SYSTEM(U) AIR FORCE INST OF TECH WRIGHT-PATTERSON AFB OH SCHOOL OF ENGINEERING J W FOISTER DEC 87 AFIT/GSO/AA/87D-2 1/2

UNCLASSIFIED F/G 3/3 NL

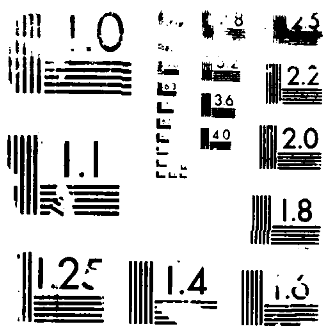
1.0
2.5
2.2
2.0
1.1
1.8
1.25
1.4
1.6

(1)

DEPARTMENT OF THE AIR FORCE

AIR UNIVERSITY

AIR FORCE INSTITUTE OF TECHNOLOGY

Wright-Patterson Air Force Base, Ohio

AFIT/GSO/AA/87D-2

FROZEN ORBIT ANALYSIS

IN THE

MARTIAN SYSTEM

THESIS

James W. Foister, III
Captain, USAF

AFIT/GSO/AA/87D-2

AFIT/GSO/AA/87D-2

FROZEN ORBIT ANALYSIS IN THE MARTIAN SYSTEM

THESIS

Presented to the Faculty of the School of Engineering

of the Air Force Institute of Technology

Air Universtiy

In Partial Fulfillment of the

Requirements for the Degree of

Master of Science in Space Operations

James W. Foister, III

Captain, USAF

December 1987

Preface

I wish to express my appreciation for the help I received from my advisor, Capt. Rodney D. Bain.

Table of Contents

List of Figures

Figure

Page

Figure

Page

Figure

Page

Figure

Page

Figure		Page
G.4	Delta ι, Delta ω vs. Semi Major Axis for e = .3, ι = 30	131
G.5	Delta ι, Delta ω vs. Semi Major Axis for e = .3, ι = 40	132
G.6	Delta ι, Delta ω vs. Semi Major Axis for e = .3, ι = 50	133
G.7	Delta ι, Delta ω vs. Semi Major Axis for e = .3, ι = 60	134
G.8	Delta ι, Delta ω vs. Semi Major Axis for e = .3, ι = 70	135
G.9	Delta ι, Delta ω vs. Semi Major Axis for e = .3, ι = 80	136
G.10	Delta ι, Delta ω vs. Semi Major Axis for e = .3, ι = 90	137
H.1	Delta a, Delta ω vs. Semi Major Axis for e = .3, ι = 1	138
H.2	Delta a, Delta ω vs. Semi Major Axis for e = .3, ι = 10	139
H.3	Delta a, Delta ω vs. Semi Major Axis for e = .3, ι = 20	140
H.4	Delta a, Delta ω vs. Semi Major Axis for e = .3, ι = 30	141
H.5	Delta a, Delta ω vs. Semi Major Axis for e = .3, ι = 40	142
H.6	Delta a, Delta ω vs. Semi Major Axis for e = .3, ι = 50	143
H.7	Delta a, Delta ω vs. Semi Major Axis for e = .3, ι = 60	144
H.8	Delta a, Delta ω vs. Semi Major Axis for e = .3, ι = 70	145

Figure

Page

Figure

Page

List of Tables

List of Symbols

A	The area.
a	The semi major axis.
$\vec{a}_g$	Acceleration due to gravity.
C_D	The coefficient of drag.
E	The eccentric anomaly.
e	The eccentricity.
exp	The exponential of the mathematical argument.
f	The true anomaly.
G	The Universal Gravitational constant.
g	The local acceleration due to gravity.
i	The angle of inclination.
J_n	The coefficient for the n th zonal harmonic (i.e. $J_2 = C_{20}$)
j	$\sqrt{-1}$
LHS	Left hand side of the equation.
M	Depending upon the context either the mass of the primary body, or the mean anomaly.
M_i	The molecular mass of type i molecule.
m	The mass of the secondary body.
$\underline{m}$	The mean molecular mass of the unit volume atmosphere.
N_i	The number of molecules of type i per unit volume.
p	The atmospheric pressure.
R	The Universal Gas Constant.
RE	The real part of the mathematical argument.
R_e	The equatorial radius of the planet.
RHS	Right hand side of the equation.
R_p	The radius of the primary body.
r	Radial distance from the center of the primary body to the center of the secondary body.

$\bar{s}$ The state vector.

$\bar{u}$ The velocity of the atmosphere relative to the planet.

V Volume, potential, or velocity depending upon context.

$\bar{V}$ The velocity of the satellite relative to the atmosphere.

$\bar{v}$ The velocity of the satellite relative to the planet.

α The angle from x axis of the inertial frame to the longitude of the projection of the secondary body onto the primary body.

δ and Δ The change in the mathematical argument.

θ The angle from x axis of the inertial frame to the prime meridian of the primary body (also known as the "local sidereal time").

λ Longitude

μ The mass of the primary body multiplied by the Universal Gravitational constant.

ρ The atmospheric density.

ϕ Latitude

Ω The longitude of the ascending node.

ω The argument of the periapsis.

∇ The gradient.

ϵ The eccentricity of the planet's shape.

Abstract

A frozen orbit is an orbit whose time rate of change of the argument of the periapsis (ω), the eccentricity (e), the semi major axis (a), or the angle of inclination (i) is approximately equal to zero. Martian frozen orbits are known to exist for polar trajectories with altitudes from 300 km to 1000 km. The objective of this study was to determine if other regions with characteristics similar to the known frozen orbits exist, taking into account the perturbative effects due to a 6 X 6 gravity field and atmospheric drag.

First, the geopotential equation was derived for both spherical coordinates and the classical orbital elements. Next, a model for the atmospheric drag was developed. Using these two models, a Fortran computer model named ASAP (Artificial Satellite Analysis Program) was analyzed for accuracy. This program proved to be highly reliable, and was used to carry out further analysis.

Two of the three trajectories planned for the future Mars Geoscience/Climatology Orbiter (MGCO) are frozen orbits. In order to determine the characteristics of ω, e, a, and i of a frozen orbit, one of the MGCO frozen orbits was examined in both a 6 X 0 and a 6 X 6 gravity field. The analysis showed that the above orbital elements are not periodic over one orbital period (when in the presence of a 6 X 6 gravity field), but they are bounded over one axial period.

Since the greatest change over an orbital period is in the argument of the periapsis and the eccentricity the effect of driving the change in these two parameters to approximately zero over one orbital period was investigated. Driving the change in ω to zero does not provide the desired level of control on the argument of the periapsis. Driving the change in e to zero can only be accomplished at the cost of relatively high

rates of change in ω over one orbital period. An orbit was found in which the change in ω and in e over one orbital period were both equal to approximately zero. Again the argument of the periapsis is not bounded, but rather periodic.

A search for a combination of orbital elements which would yield a zero change over one orbital period for all four of the above orbital elements was conducted for an eccentricity of 0.3. The results showed no such orbit exist; regions were found in which the change in 3 out of the 4 orbital elements were driven to zero or approximately zero.

Finally, the predominant characteristics of the elements for the MGCO frozen orbit are identified, and a region with these same characteristics was found.

FROZEN ORBIT ANALYSIS IN THE MARTIAN SYSTEM

I. Introduction

Background

Mars is the closest planet to Earth that is potentially habitable by man; however, Mars is, at its closest approach to Earth, approximately 78 million kilometers away. Even though the trip to Mars is made along keplerian trajectories which take advantage of the Sun's gravity, fuel is still consumed in trajectory correction maneuvers. When a probe arrives at Mars, fuel will again be required to establish, and maintain an orbit about the planet. The size of the probe that can be sent to Mars is dependent on the size of the booster used to get the probe out of the Earth's gravity field. Mission planners must make use of boosters currently available because both budget and time constraints do not allow for a booster to be designed for a specific mission. Therefore, the size of the payload is itself a constraint, part of which is taken up in mission required fuel. If the mission profile is such that the fuel required is minimized, then the mission duration can be increased. Having the capability to maintain probes in orbit about Mars for long periods will increase our knowledge of Mars' surface, climatology, gravity field, magnetic field, and the interaction of the magnetic field with the solar wind. Such a probe could also be used to better determine what and where Mars' resources are, a factor that may be critical to future manned missions to the planet.

One method of minimizing fuel is to select an orbit that takes advantage of Mars' gravity field in such a way as to minimize the effects of atmospheric drag upon the probe. In the 1960's H. W. West, R. T. Clapp, and H. Small were able to show that for Earth there exist a class of polar orbits with non zero eccentricity, and whose argument of the periapsis is over the south pole, such that the line of apsides does not rotate, but rather oscillates about its initial position. These orbits were called "frozen" because of the off setting effects of the odd and even zonal harmonics on the eccentricity and the argument of the periapsis yielding orbits whose shape, and whose orientation of the line of apsides is nearly constant over time (17:2). Since most planets are oblate, and since atmospheric drag is a function of altitude above the planet, the amount of atmospheric drag experienced will be less over the poles. This implies that a probe in an orbit that maintains its periapsis over a polar region will experience less drag, and hence require less fuel consumption to remain in orbit. For Mars, frozen orbits are known to exist for polar, or near polar orbits with altitudes from 300 to 1000 km (17:2).

Definition of a Frozen Orbit

This thesis defines a frozen orbit as any orbit whose time rate of change of the argument of the periapsis (ω), the eccentricity (e), the semi major axis (a), or the angle of inclination (ι) is equal to approximately zero.

Objective

Given the perturbing effects of the zonal and sectoral harmonics up to and including an order of six, and the perturbing effects of atmospheric drag, this thesis seeks to determine other regions where orbital stabilities similar to the polar frozen orbits may exist.

Methodology

First, in order to understand the relationship that exist between the orbital elements for a frozen orbit, a known Martian frozen orbit will be examined. From the understanding of the sensitivities of this orbit to changes in the orbital elements, manipulations of the orbital elements will be made in an effort to find other stable regions. This thesis will only consider the perturbing effects due to the geopotential and atmospheric drag upon orbits with altitudes from approximately 200 km to 20,000 km (Martian geosynchronous). Resonance effects will not be considered, nor will the effects due to solar pressure or third bodies.

II. The Geopotential

Although the derivations in this section already exist in the literature, in the interest of completeness they are presented in this chapter.

Derivation of the Geopotential Equation

Sir Isaac Newton showed that in inertial space the gravitational force of attraction between two bodies can be written as:

$$\frac{\vec{F}}{m} = -\frac{GM}{r^3}\vec{r} = \vec{a}_g \tag{2.1}$$

Newton also demonstrated that for a spherical body with a homogenous distribution of mass, the entire mass of the primary body acts as if its mass existed as a point particle located at the center of its sphere. If a planet is not perfectly spherical, and/or does not have a homogenous distribution of mass, then these irregularities will effect the motion of satellite about that planet. The acceleration which a satellite experiences (due to the mass of the primary body) can be written as (19:49):

$$\vec{a}_g = -\nabla V(x, y, z) \tag{2.2}$$

The $V(x,y,z)$ term in equation (2.2) can be solved using a special form of Poisson's Equation that is known as Laplace's Equation (the derivation of these equations is found in Appendix A) which in cartesian coordinates is:

$$\nabla^2 V = 0 \tag{2.3}$$

The equations of motion of a satellite in orbit around a planet are simpler if expressed in spherical polar coordinates, hence, equation (2.3) becomes (10:3):

$$\frac{1}{r^2}\frac{\partial}{\partial r}\left(r^2\frac{\partial V}{\partial r}\right)+\frac{1}{r^2\cos\phi}\frac{\partial}{\partial\phi}\left(\cos\phi\frac{\partial V}{\partial\phi}\right)+\frac{1}{r^2\cos^2\phi}\frac{\partial^2 V}{\partial\lambda^2}=0 \tag{2.4}$$

where r = radial distance from the center of the attracting body to the satellite

ϕ = the latitude

λ = the longitude

Equation (2.4) is a linear partial differential equation whose solution takes the form of (10:4):

$$V(r,\phi,\lambda) = R(r)\Phi(\phi)\Lambda(\lambda) \tag{2.5}$$

Because $V(r,\phi,\lambda)$ describes a smooth sphere certain boundary conditions must be imposed upon equation (2.5). First, in order to prevent a jump discontinuity in the Λ function it must have the same value at $\Lambda(0)$ and $\Lambda(2\pi)$. Second, to prevent discontinuities at the poles of the sphere, the first derivative of Φ with respect to ϕ must equal zero when ever the latitude is equal to odd multiples of $\pi/2$.

Substitution of equation (2.5) into equation (2.4) yields:

$$\frac{1}{r^2}\frac{\partial}{\partial r}\left(r^2\frac{\partial}{\partial r}\left(R(r)\Phi(\phi)\Lambda(\lambda)\right)\right)+\frac{1}{r^2\cos\phi}\frac{\partial}{\partial\phi}\left(\cos\phi\frac{\partial}{\partial\phi}\left(R(r)\Phi(\phi)\Lambda(\lambda)\right)\right)$$
$$+\frac{1}{r^2\cos^2\phi}\frac{\partial^2}{\partial\lambda^2}\left(R(r)\Phi(\phi)\Lambda(\lambda)\right)=0 \tag{2.6}$$

The right hand side (RHS) of the equation (2.6) can be written in terms of λ alone as:

$$\frac{\cos^2\phi}{R}\frac{d}{dr}\left(r^2\frac{dR}{dr}\right)+\frac{\cos\phi}{\Phi}\frac{d}{d\phi}\left(\cos\phi\frac{d\Phi}{d\phi}\right)=-\frac{1}{\Lambda}\frac{d^2\Lambda}{d\lambda^2} \tag{2.7}$$

Since the LHS and the RHS of equation (2.7) are independent, set them equal to the constant k. Hence equation (2.7) implies:

$$\frac{d^2\Lambda}{d\lambda^2} + k\Lambda = 0 \tag{2.8}$$

The solution to equation (2.8) has the form:

$$\Lambda = C\cos\left[(k)^{1/2}\lambda\right] + S\sin\left[(k)^{1/2}\lambda\right] \tag{2.9}$$

where, in addition to k being a constant, C and S are also constants. Further, unlike the constants C and S, k can not be an arbitrary value. The first boundary condition in equation (2.5) implies that $\sqrt{k}$ must be equal to a positive integer. Let this integer be m.

Hence the general solution to equation (2.8) has the form:

$$\Lambda_m(\lambda) = C_m \cos m\lambda + S_m \sin m\lambda \tag{2.10}$$

To obtain the next expression, set the LHS of equation (2.7) equal to k yielding:

$$\frac{1}{R}\frac{d}{dr}\left(r^2\frac{dR}{dr}\right) = \frac{m^2}{\cos^2\phi} - \frac{1}{\Phi\cos\phi}\frac{d}{d\phi}\left(\cos\phi\frac{d\Phi}{d\phi}\right) \tag{2.11}$$

Again the LHS and the RHS are independent of each other; therefore, equate both sides to a constant, denoted by T. Hence:

$$\frac{1}{R}\frac{d}{dr}\left(r^2\frac{dR}{dr}\right) = T \tag{2.12}$$

which implies

$$\frac{1}{\cos\phi}\frac{d}{d\phi}\left(\cos\phi\frac{d\Phi}{d\phi}\right) - \Phi\left(\frac{m^2}{\cos^2\phi} - T\right) = 0 \tag{2.13}$$

Here the second boundary condition in equation (2.5) imposes the already mentioned conditional values of $d\Phi/d\phi$.

Now let $x = \sin\phi$ which implies $dx = \cos\phi\, d\phi$. From this the mathematical operator:

$$\frac{d()}{d\phi} = \cos\phi \frac{d()}{dx} \tag{2.14}$$

is derived. Applying this operator to equation (2.13) yields:

$$\cos^2\theta \frac{d^2\Phi}{dx^2} - \Phi\left(\frac{m^2}{\cos^2\phi} - T\right) = 0 \tag{2.15}$$

Therefore, equation (2.15) becomes:

$$(1 - x^2)\frac{d^2\Phi}{dx^2} - \Phi\left(\frac{m^2}{(1 - x^2)} - T\right) = 0 \tag{2.16}$$

Equation (2.16) is the algebraic form known in the literature as Ferrier's form of Legendre's Associated Equation whose solution has the form (1:160-162):

$$P_L^m(x) = (1 - x^2)^{m/2} \frac{d^m}{dx^m} P_L(x) \tag{2.17}$$

When $x = \sin\phi$ equation (2.17) becomes:

$$P_L^m(\sin\phi) = (\cos^2\phi)^{m/2} \frac{d^m}{dx^m} P_L(\sin\phi) \tag{2.18}$$

where (1:132)

$$P_L(\sin\phi) = \frac{1}{2^L L!} \frac{d^L}{d(\sin\phi)^L}\left[(\sin^2\phi - 1)^L\right] \tag{2.19}$$

In equations (2.17) and (2.18), m is any non negative integer, and L is an integer value which is the number of times $P_L(\sin\phi)$ passes through zero as ϕ varies from 0 to π (4:57).

Equations (2.18) and (2.19) are Rodrigues formulas giving a representation of the Legendre polynomials. An alternate expression for the Legendre polynomials is (1:132):

$$P_L(x) = \sum_{k=0}^{[L/2]} \frac{(-1)^k (2L-2k)!}{2^L k!(L-k)!(L-2k)!} x^{L-2k} \tag{2.20}$$

where $[L/2]$ is the integer part of $L/2$.

Hence a solution to equation (2.13) is:

$$\Phi(\phi) = P_L^m(\sin\phi) \tag{2.21}$$

In order to find the last expression recall equation (2.12) written as:

$$\frac{d}{dr}\left(r^2 \frac{dR}{dr}\right) = RT \tag{2.22}$$

Returning to equation (2.16), it can be seen that this equation has the general form of Legendre's Associated Equation (1:160):

$$(1-x^2)y'' - 2xy' + \left(L(L+1) - \frac{m^2}{1-x^2}\right)y = 0 \tag{2.23}$$

This implies:

$$T = L(L+1) \tag{2.24}$$

Equation (2.22) becomes:

$$\frac{d}{dr}\left(r^2 \frac{dR}{dr}\right) = RL(L+1) \tag{2.25}$$

Now, let $R = r^p$. Then equation (2.25) produces:

$$p(p+1)r^p = r^p L(L+1) \tag{2.26}$$

Because $U(r,\phi,\lambda)$ decreases with increasing distance, equation (2.26) implies:

$$p = -(L+1) \tag{2.27}$$

therefore:

$$R(r) = r^{-(L+1)} \tag{2.28}$$

Combining equations (2.10), (2.21), and (2.28) into equation (2.5) yields the desired solution to equation (2.4). The results, equation (2.29), is the objective of this section (19:55).

$$U(r,\phi,\lambda) = -\frac{GM}{r}\sum_{L=0}^{\infty}\sum_{m=0}^{L}\left(\frac{r}{R_p}\right)^{-L} P_L^m(\sin\phi)\left(C_{Lm}\cos m\lambda + S_{Lm}\sin m\lambda\right) \tag{2.29}$$

where R_p = the equatorial radius of the primary body

G = the universal gravity constant

r = the distance from the center of the primary body to the satellite

The C_{Lm} and the S_{Lm} terms in the above equation are constants that describe the distribution of the primary body's mass, and are known in the literature as the primary body's "gravity model". These terms are dimensionless since the dimensional units are carried by the term GM.

As an example of the effects of a primary body's shape and distribution of mass upon its gravity field, an 18 by 18 gravity model for the planet Mars was input into equation (2.29). The result was solved for values of latitude and longitude that encompass the planet at an altitude of 500 km. (see the program Mars1 in Appendix E) The results are plotted in Figure 2.1. Note the checkerboard or "tesseral" pattern of alternating regions of higher and lower geopotential than would exist if Mars were a perfect, homogenous sphere.

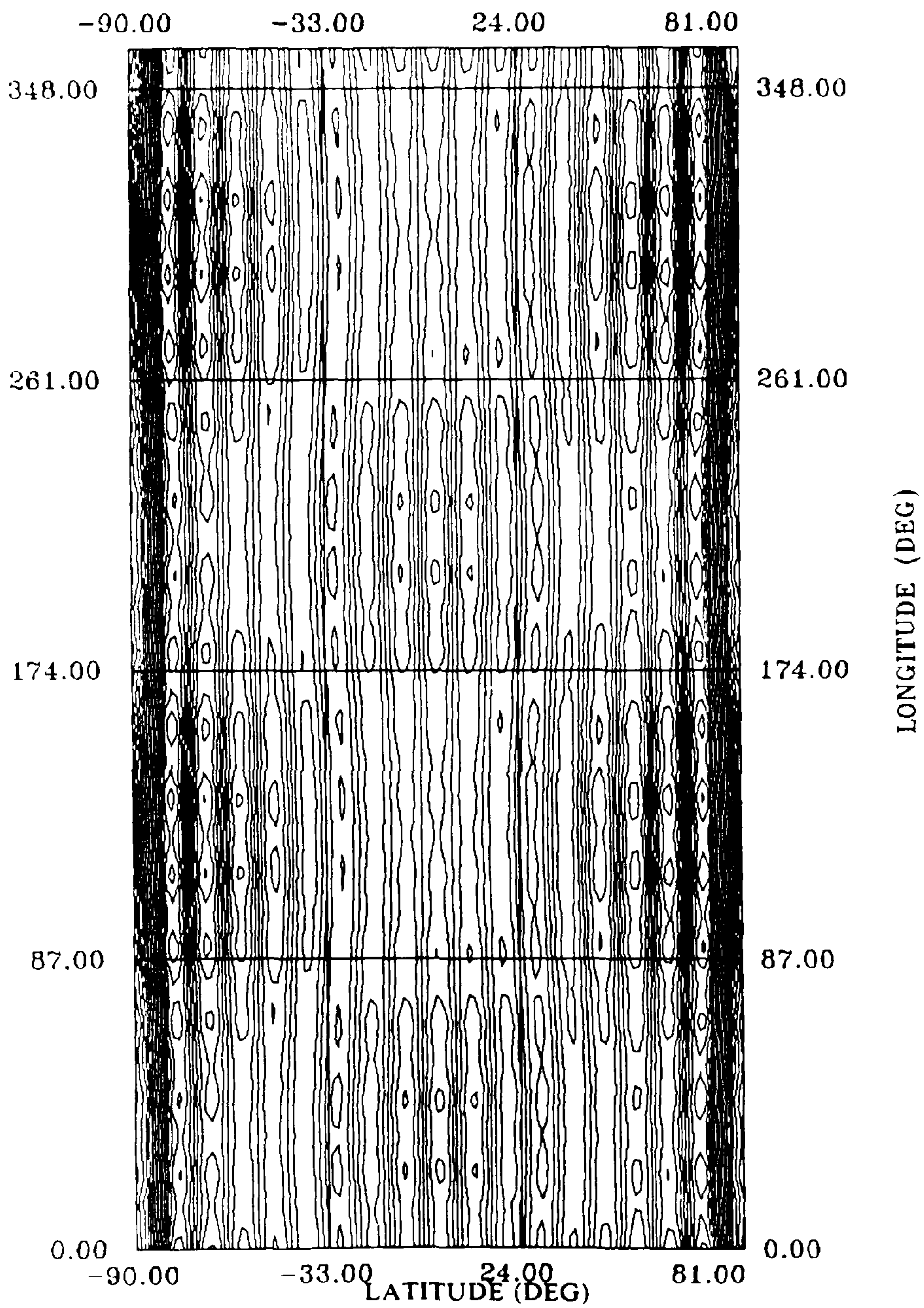

Mars' Geopotential Field at 500 KM Altitude

Figure 2.1

The Geopotential Equation as a Function of the Classical Orbital Elements

Equation (2.29) is given in spherical polar coordinates. Since satellite motion is often described in terms of the classical orbital elements, it is necessary to derive equation (2.29) into a function of the classical orbital elements. This derivation is structured on the work of Kaula, Born, and Hildebrand, see references 10 and 3.

Using equations (2.18) and (2.20) rewrite the $P_L^m(\sin\phi)$ term in the above equation to yield:

$$P_L^m(\sin\phi) = (1-\sin^2\phi)^{m/2}\frac{d^m}{d(\sin\phi)^m}P_L(\sin\phi) \tag{2.30}$$

where

$$P_L(\sin\phi) = \sum_{t=0}^{[L/2]}\frac{(-1)^t(2L-2t)!\sin^{L-2t}\phi}{2^L t!(L-t)!(L-2t)!} \tag{2.31}$$

Combining equations (2.30) and (2.31):

$$P_L^m(\sin\phi) = \cos^m\phi\sum_{t=0}^{[L/2]}\frac{(-1)^t(2L-2t)!}{2^L t!(L-t)!(L-2t)!}\frac{d^m\sin^{L-2t}\phi}{d(\sin\phi)^m} \tag{2.32}$$

Noting that (1:61)

$$\frac{d^m}{dx^m}x^a = D^m x^a = \frac{\Gamma(a+1)}{\Gamma(a-m+1)}x^{a-m} \tag{2.33}$$

Then

$$D^m(\sin\phi)^{L-2t} = \frac{\Gamma(L-2t+1)}{\Gamma(L-2t-m+1)}\sin^{L-2t-m}\phi = \frac{(L-2t)!}{(L-2t-m)!}\sin^{L-m-2t}\phi \tag{2.34}$$

Substituting equation (2.34) into equation (2.32), results in:

$$P_L^m(\sin\phi) = \cos^m\phi \sum_{t=0}^{[(L-m)/2]} \frac{(-1)^t (2L-2t)!\,\sin^{L-m-2t}\phi}{2^L t!\,(L-t)!\,(L-m-2t)!} \tag{2.35}$$

The upper limit of the summation changed from $[L/2]$ due to the denominator term, $(L-m-2t)!$. This term causes any value of t greater than $(L-m)/2$ to make the factorial $(L-m-2t)$ negative, driving the factorial to infinity, and thus driving the summation to zero.

Let (10:6):

$$T_{Lmt} = \frac{(-1)^t (2L-2t)!}{2^L t!\,(L-t)!\,(L-m-2t)!} \tag{2.36}$$

Then inserting equations (2.35) and (2.36) into equation (2.29) yields:

$$U = -\frac{GM}{r}\sum_{L=0}^{\infty}\sum_{m=0}^{L}\left(\frac{r}{R_p}\right)^L \cos^m\phi \sum_{t=0}^{[(L-m)/2]} T_{Lmt}\sin^{L-m-2t}\phi \tag{2.37}$$

$$\times\left[C_{Lm}\cos m\lambda + S_{Lm}\sin m\lambda\right]$$

In order to utilize Lagrange's Planetary Equations, equation (2.37) must be rewritten in terms of the six orbital elements, a, e, i, ω, Ω, and M. Figure 2.2 shows the relationships between the various angles.

The λ term will now be converted into the orbital elements. From Figure 2.2 it is easily seen that $\lambda = \alpha - \theta$; however, neither α nor θ are members of the orbital element set. Therefore, express λ as:

$$\lambda = (\alpha - \Omega) - (\theta - \Omega) = (\alpha - \Omega) + (\Omega - \theta) \tag{2.38}$$

where λ = the longitude of the projection of the secondary body onto the primary body

α = the angle from the x axis of the inertial frame to the longitude of the projection of the secondary body onto the primary body

θ = the angle from the x axis of the inertial frame to the prime meridian of the primary body (also known as the "local sidereal time")

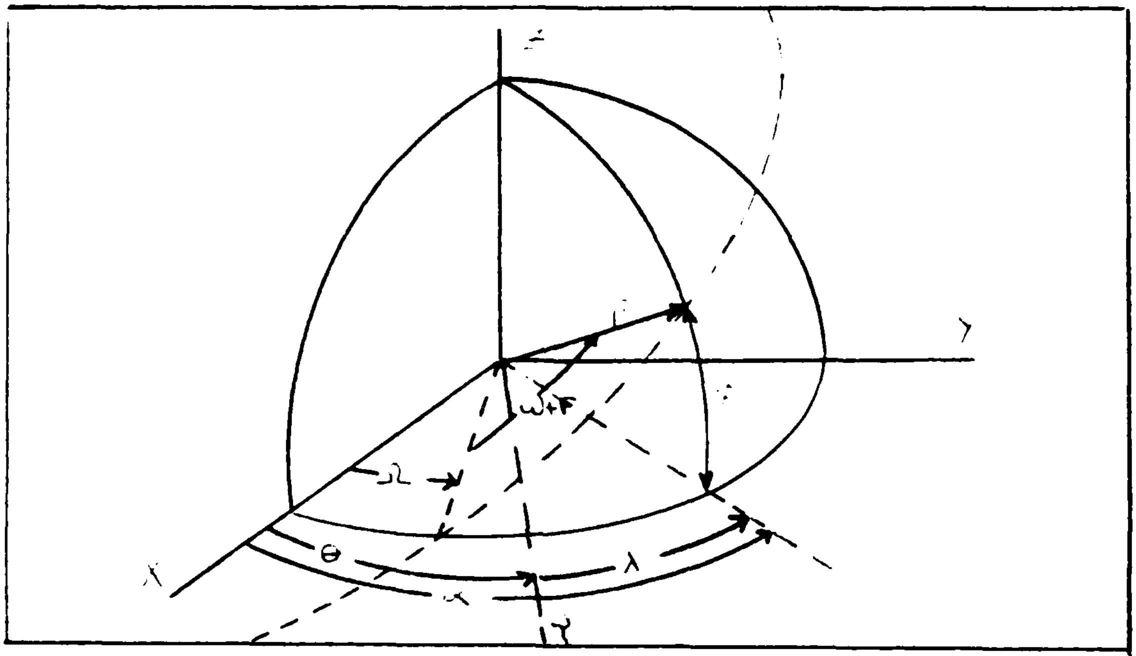

Orientation of Satellite Orbit Plane (3:4)

Figure 2.2

Applying equation (2.38) to the $\cos m\lambda$ and $\sin m\lambda$ terms of equation (2.37) yields:

$$\cos m\lambda = \cos[m(\alpha - \Omega) + m(\Omega - \theta)] \tag{2.39}$$

$$\sin m\lambda = \sin[m(\alpha - \Omega) + (\Omega - \theta)] \tag{2.39a}$$

Applying equations (B1.1) and (B1.2), found in Appendix B to equations (2.39) and (2.39a) yields:

$$\cos m\lambda = \cos m(\alpha - \Omega)\cos m(\Omega - \theta) - \sin m(\alpha - \Omega)\sin m(\Omega - \theta) \tag{2.40}$$

$$\sin m\lambda = \sin m(\alpha - \Omega)\cos m(\Omega - \theta) + \cos m(\alpha - \Omega)\sin m(\Omega - \theta) \tag{2.40a}$$

Noting the angular relationships in Figure 2.2, and using the properties of spherical trigonometry the following relationships are evident:

$$\cos(\alpha - \Omega) = \frac{\cos(\omega + f)}{\cos\phi} \tag{2.41}$$

$$\sin(\alpha - \Omega) = \tan\phi\cot i \tag{2.42}$$

$$\sin\phi = \sin(\omega + f)\sin i \tag{2.43}$$

Looking at the $\cos(\alpha - \Omega)$ terms of equation (2.40) and applying equations (B2.5), (B2.7), (2.41), and (2.42) yields:

$$\begin{aligned}\cos m(\alpha - \Omega) &= RE\sum_{s=0}^{m}\binom{m}{s} j^s \cos^{m-s}(\alpha - \Omega)\sin^s(\alpha - \Omega) \\ &= RE\sum_{s=0}^{m}\binom{m}{s} j^s \frac{\cos^{m-s}(\omega + f)}{\cos^{m-s}\phi}\tan^s\phi\cot^s i \\ &= RE\sum_{s=0}^{m}\binom{m}{s} j^s \frac{\cos^{m-s}(\omega + f)\sin^s(\omega + f)\cos^s i}{\cos^m\phi}\end{aligned} \tag{2.44}$$

The same process applied to the sine terms of equations (2.40) yields:

$$\sin m(\alpha - \Omega) = RE\sum_{s=0}^{m}\binom{m}{s} j^{s-1} \frac{\cos^{m-s}(\omega + f)\sin^s(\omega + f)\cos^s i}{\cos^m\phi} \tag{2.45}$$

Injecting equations (2.44) and (2.45) into equations (2.40) will result in:

$$\begin{aligned}\cos m\lambda = \Big[RE\sum_{s=0}^{m}\binom{m}{s} j^s &\frac{\cos^{m-s}(\omega + f)\sin^s(\omega + f)\cos^s i}{\cos^m\phi} \\ &\times \big(\cos m(\Omega - \theta) + j\sin m(\Omega - \theta)\big)\Big]\end{aligned} \tag{2.46}$$

$$\sin m\lambda = [RE \sum_{s=0}^{m} \binom{m}{s} j^{s} \frac{\cos^{m-s}(\omega+f)\sin^{s}(\omega+f)\cos^{s} i}{\cos^{m}\phi} \times (\sin m(\Omega-\theta) - j\cos m(\Omega-\theta))] \tag{2.47}$$

Applying equation (2.36), equation (2.35) can be written as:

$$P_{\ell}^{m}(\sin\phi) = \cos^{m}\phi \sum_{t=0}^{(L-m)/2} T_{Lmt} \sin^{L-m-2t}\phi \tag{2.48}$$

Inject equation (2.43) into equation (2.48) to yield:

$$P_{\ell}^{m}(\sin(\omega+f)\sin i) = \cos^{m}\phi \sum_{t=0}^{k} \sin^{L-m-2t}(\omega+f) \sin^{L-m-2t} i \, T_{Lmt} \tag{2.49}$$

where $k = (l-m)/2$

Substituting equations (2.46), (2.47), and (2.49) into equation (2.29) yields:

$$U = -\frac{GM}{r} \sum_{L=0}^{\infty} \sum_{m=0}^{L} \left(\frac{r}{R_p}\right)^{-L} \sum_{t=0}^{k} T_{Lmt} \sin^{L-m-2t} i \tag{2.50}$$

$$\times RE\{[(C_{Lm} - jS_{Lm})\cos m(\Omega-\theta) + (S_{Lm} + jC_{Lm})\sin m(\Omega-\theta)]$$

$$\times \sum_{s=0}^{m} \binom{m}{s} j^{s} \cos^{m-s}(\omega+f) \sin^{L-m-2t}(\omega+f) \cos^{s} i\}$$

The last term of equation (2.50) is in the form of $\sin^{a} x \cos^{b} x$. Applying equations (B3.2) and (B3.3), from Appendix B, to equation (2.50) yields:

$$U = -\frac{GM}{r} \sum_{L=0}^{\infty} \sum_{m=0}^{L} \left(\frac{r}{R_p}\right)^{-L} \sum_{t=0}^{k} T_{Lmt} \sin^{L-m-2t} i$$

$$\times RE\{[(C_{Lm} - jS_{Lm})\cos m(\Omega-\theta) + (S_{Lm} + jC_{Lm})\sin m(\Omega-\theta)] \tag{2.51}$$

$$\times \sum_{s=0}^{m} \binom{m}{s} j^{s} \frac{-j^{n}}{2^{L-2t}} \sum_{c=0}^{L-m-2t+s} \sum_{d=0}^{m-s} \binom{L-m-2t+s}{c} \binom{m-s}{d} (-1)^{c}$$

$$\times [\cos(L-2t-2c-2d)(\omega+f) + j\sin(L-2t-2c-2d)(\omega+f)] \cos^{s} i\}$$

Let $\delta = m(\Omega - \theta)$ and $\gamma = (l-2t-2c-2d)(\omega + f)$. Then applying trigonometry to the

$$[(C_{lm} - jS_{lm})\cos m(\Omega-\theta) + (S_{lm} + jC_{lm})\sin m(\Omega-\theta)]$$
$$\times [\cos(l-2t-2c-2d)(\omega+f) + j\sin(l-2t-2c-2d)(\omega+f)]$$

terms of equation (2.51) yields (3:5):

$$V = \frac{GM}{r}\sum_{l=2}^{\infty}\sum_{m=0}^{l}\left(\frac{r}{R_p}\right)^{l}\sum_{t=0}^{k} T_{lmt}\sin^{l-m-2t} i\, RE\Big\{\sum_{s=0}^{m}\binom{m}{s} j^s\cos^s i\,\frac{(-j)^{l-m-2t+s}}{2^{l-2t}} \tag{2.52}$$
$$\times \sum_{c=0}^{l-m-2t+s}\sum_{d=0}^{m-s}\binom{l-m-2t+s}{c}\binom{m-s}{d}(-1)^c[(C_{lm}-jS_{lm})\cos(\delta+\gamma)$$
$$+ (S_{lm}+jC_{lm})\sin(\delta+\gamma)]\Big\}$$

Since V in equation (2.52) is a real physical quantity it is necessary to determine the real part of the bracketed term. Consider the $j^s(-j)^{l-m-2t+s}$ term.

$$j^s(-j)^{l-m-2t+s} = j^s(1/j)^{l-m-2t+s} = j^s j^{-l+m+2t-s} \tag{2.53}$$
$$= j^{-l+m+2t} = j^{(-(l-m)/2+t)2}$$
$$= (-1)^{-(l-m)/2+t}$$

Remember that k is the integer part of $(l-m)/2$, so if $l-m$ is odd (3:7):

$$\frac{l-m}{2} = k + \frac{1}{2} \tag{2.54}$$

$$j^s(-j)^{l-m-2t+s} = (-1)^{-k+t-1/2} = -j(-1)^{-k+t} \tag{2.55}$$

When $(l-m)/2$ is even:

$$\frac{l-m}{2} = k \tag{2.56}$$

$$j^s(-j)^{l-m-2t+s} = (-1)^{-k+t} = (-1)^{k+t} \tag{2.57}$$

As a result of equations (2.55) and (2.57) equation (2.52) becomes:

$$
\begin{aligned}
V = &-\frac{GM}{r}\sum_{l=0}^{\infty}\sum_{m=0}^{l}\left(\frac{r}{R_p}\right)^{-l}\sum_{t=0}^{k}T_{lmt}\sin^{l-m-2t}i \\
&\times\sum_{s=0}^{m}\binom{m}{s}\frac{\cos^{s}i}{2^{l-2t}}\times\sum_{c=0}^{l-m-2t+s}\sum_{d=0}^{m-s}\binom{l-m-2t+s}{c}\binom{m-s}{d}(-1)^{c} \\
&\times\left\{\begin{vmatrix} C_{lm} \\ -S_{lm}\end{vmatrix}\begin{matrix}\mathrm{l-m,even} \\ \mathrm{l-m,odd}\end{matrix}\cos[(l-2t-2c-2d)(\omega+f)+m(\Omega-\theta)]\right. \\
&\left.+\begin{vmatrix} S_{lm} \\ C_{lm}\end{vmatrix}\begin{matrix}\mathrm{l-m,even} \\ \mathrm{l-m,odd}\end{matrix}\sin[(l-2t-2c-2d)(\omega+f)+m(\Omega-\theta)]\right\}
\end{aligned}
\tag{2.58}
$$

Transform equation (2.58) so terms of the form:

$$[(l-2p)(\omega+f)+m(\Omega-\theta)]$$

can be collected together. This is accomplished by letting (3:8):

$$p = t + c + d \tag{2.59}$$

This implies

$$l - 2t - 2c - 2d = l - 2p \tag{2.60}$$

Hence, equation (2.58) becomes:

$$
\begin{aligned}
V = &-\frac{GM}{r}\sum_{l=0}^{\infty}\sum_{m=0}^{l}\left(\frac{r}{R_p}\right)^{-l}\sum_{t=0}^{k}T_{lmt}\sin^{l-m-2t}i \\
&(-1)^{k+t}\sum_{s=0}^{m}\binom{m}{s}\frac{\cos^{s}i}{2^{l-2t}}\times\sum_{c=0}^{l-m-2t+s}\sum_{p=t+c}^{m-s}\binom{l-m-2t+s}{c}\binom{m-s}{p-t-c}(-1)^{c} \\
&\times\left\{\begin{vmatrix} C_{lm} \\ -S_{lm}\end{vmatrix}\begin{matrix} l-m,even \\ l-m,odd\end{matrix}\cos[(l-2p)(\omega+f)+m(\Omega-\theta)]\right. \\
&\left.+\begin{vmatrix} S_{lm} \\ C_{lm}\end{vmatrix}\begin{matrix} l-m,even \\ l-m,odd\end{matrix}\sin[(l-2p)(\omega+f)+m(\Omega-\theta)]\right\}
\end{aligned}
\tag{2.61}
$$

Evaluating equation (2.36) yields the following relationship:

$$0 \leq t \leq k \tag{2.62}$$

Likewise, an evaluation of the binomial coefficient terms of equations (2.58*) and (2.61) yields:

$$0 \leq s \leq m \tag{2.62a}$$

$$0 \leq c \leq L - m - 2t + s \tag{2.62b}$$

$$0 \leq d \leq m - s \tag{2.62c}$$

$$0 \leq p \leq L \tag{2.62d}$$

However, according to equation (2.59) $t = p - c - d$. Since both c and d have minimum values of zero, t_{max} is equal to p. This implies that the maximum value of t will be the smaller value of p or k, and equation (2.62) becomes:

$$0 \leq t \leq \text{the smaller of } k \text{ or } p \tag{2.62e}$$

Grouping selected terms from equation (2.61), and taking into account the possible values for t, s, c, and p from equations (2.62), leads to the definition (10:34):

$$F_{Lmp}(i) = \sum_{t} \frac{(2L-2t)!}{t!\,(L-t)!\,(L-m-2t)!\,2^{2L-2t}} \sin^{L-m-2t} i \times \sum_{s=0}^{m} \binom{m}{s} \cos^{s} i \sum_{c} \binom{L-m-2t+s}{c} \binom{m-s}{p-t-c} (-1)^{c-k} \tag{2.63}$$

$F_{Lmp}(i)$ is known in the literature as the Inclination Function. A table of values for this function is given in Appendix C. Rewriting equation (2.61) in terms of the inclination function gives:

$$V_{Lm} = -\frac{GMR_p^L}{r^{L+1}} \sum_{p=0}^{L} F_{Lmp}(i) \left\{ \begin{bmatrix} C_{Lm} \\ -S_{Lm} \end{bmatrix}_{L-m,\,odd}^{L-m,\,even} \cos[(L-2p)(\omega+f)+m(\Omega-\theta)] + \begin{bmatrix} S_{Lm} \\ C_{Lm} \end{bmatrix}_{L-m,\,odd}^{L-m,\,even} \sin[(L-2p)(\omega+f)+m(\Omega-\theta)] \right\} \tag{2.64}$$

Where equation (2.64) is in a form that is for a particular value of L and m.

Next, equation (2.64) must be written so that the r and f terms are expressed in terms of a, M, and e. From equation (2.64) isolate any particular

$$\frac{1}{r^{L+1}} \begin{bmatrix} \cos \\ \sin \end{bmatrix} [(L-2p)(\omega+f)+m(\Omega-\theta)] \tag{2.65}$$

term and let

$$\epsilon = (L-2p)\omega + m(\Omega-\theta) \tag{2.66}$$

Equation (2.65) becomes:

$$\frac{1}{r^{L+1}} \begin{bmatrix} \cos \\ \sin \end{bmatrix} [(L-2p)f+\epsilon] \tag{2.67}$$

Now, consider the term:

$$\frac{1}{r^{L+1}} \cos[(L-2p)f+\epsilon] = \{\cos[(L-2p)f]\cos\epsilon - \sin[(L-2p)f]\sin\epsilon\} \frac{1}{r^{L+1}} \tag{2.68}$$

Here Born et al. introduces the term:

$$\left(\frac{r}{a}\right)^n \exp(jmf) = \sum_{l=-\infty}^{\infty} X_l^{n,m} \exp(jlM) \tag{2.69}$$

Where $X_l^{n,m}$ is known as Hansen's coefficients (2:2):

$$X_l^{n,m} = \frac{1}{2\pi(1+\beta^2)^{n+1}} \int_0^{2\pi} y^{m-l}(1-\beta y)^{n-m+1}\left(1-\frac{\beta}{y}\right)^{n+m+1} \exp\left\{\frac{el}{2}\left[y-\frac{1}{y}\right]\right\} dE \tag{2.70}$$

where

$$\beta = \frac{e}{1+\sqrt{1-e^2}} = \frac{1-\sqrt{1-e^2}}{e} \tag{2.71}$$

$$y = \exp(jE) \tag{2.72}$$

E in the above equations is the Eccentric Anomaly. Employing equation (2.69) along with the following relationships:

$$\exp(jmf) = \cos mf + j\sin mf \tag{2.73}$$

$$\exp(jim) = \cos im + j\sin im \tag{2.73a}$$

$$i = l - 2p + q \qquad m = L - 2p \qquad n = -L - 1 \tag{2.74}$$

and noting that from equation (2.69) follows:

$$\left(\frac{r}{a}\right)^n \cos mf = \sum_{i=-\infty}^{\infty} X_i^{n,m} \cos iM \tag{2.75}$$

$$\left(\frac{r}{a}\right)^n \sin mf = \sum_{i=-\infty}^{\infty} X_i^{n,m} \sin iM \tag{2.75a}$$

changes equation (2.65) into:

$$\frac{1}{a}\left(\frac{a}{r}\right)^{L+1}\begin{bmatrix}\cos\\ \sin\end{bmatrix}\left[(L-2p)\omega + (L-2p)f + m(\Omega-\theta)\right] \tag{2.76}$$

$$= \frac{1}{a^{L+1}}\sum_{q=-\infty}^{\infty} X_{L-2p+q}^{-L-1,L-2p}\begin{bmatrix}\cos\\ \sin\end{bmatrix}\left[(L-2p)\omega + (L-2p+q)M + m(\Omega-\theta)\right]$$

Next a determination of the characteristics of Hansen's coefficients is necessary. It is beyond the scope of this chapter, but it can be shown that for the case at hand (2:5):

$$X^{n,m} = \left(\frac{e}{2}\right)^m (1-e^2)^{n+3/2} \sum_{q=0}^{\infty} \binom{-n-2}{m+2q}\binom{m+2q}{q}\left(\frac{e}{2}\right)^{2q} \tag{2.77}$$

If ... then direct substitution into equation (2.77) yields:

$$X_0^{-L-1,L-2p} = \frac{1}{(1-e^2)^{L-1/2}} \sum_{d=0}^{p-1} \binom{L-1}{2d+L-2p} \binom{2d+L-2p}{d} \left(\frac{e}{2}\right)^{2d+L-2p} \tag{2.78}$$

If $L-2p<0$ then equation (2.77) yields:

$$X_0^{-L-1,L-2p} = \frac{1}{(1-e^2)^{L-1/2}} \sum_{d=0}^{L-p-1} \binom{L-1}{2d+2p-L} \binom{2d+2p-L}{d} \left(\frac{e}{2}\right)^{2d+2p-L} \tag{2.79}$$

Here Born et al. makes the following definition:

$$p' = p \quad \text{for} \quad p \le L/2$$
$$p' = L-p \quad \text{for} \quad p > L/2 \tag{2.80}$$

This implies:

$$X_0^{-L-1,L-2p} = \frac{1}{(1-e^2)^{L-1/2}} \sum_{d=0}^{p'-1} \binom{L-1}{2d+L-2p'} \binom{2d+L-2p'}{d} \left(\frac{e}{2}\right)^{2d+L-2p'} \tag{2.81}$$

But

$$X_0^{-L-1,L-2p} \equiv G_{Lpq}(e) = G_{Lp(2p-L)}(e) \tag{2.82}$$

and when $q>0$ (3:A-13):

$$X_{L-2p+q}^{-L-1,L-2p} = C \sum_{k=0}^{\infty} \sum_{r=0}^{q+k} \sum_{t=0}^{k} \frac{(-1)^r}{r!\,t!} \binom{2p-2L}{q+k-r} \binom{-2p}{k-t} \nu^{r+t} \beta^{2k} \tag{2.83}$$

when $q<0$:

$$X_{L-2p+q}^{-L-1,L-2p} = C \sum_{k=0}^{\infty} \sum_{r=0}^{|q|+k} \sum_{t=0}^{k} \frac{(-1)^t}{r!\,t!} \binom{-2p}{|q|+k-r} \binom{2p-2L}{k-t} \nu^{r+t} \beta^{2k} \tag{2.84}$$

where

$$C = (-1)^{|q|} (1+\beta^2)^{L} \beta^{|q|}$$
$$\nu = \frac{(L-2p+q)\,e}{2\beta} \tag{2.85}$$

Substituting directly into equations (2.83) and (2.84) yields:

$$X_0^{-(L+1),L-2p} = C\sum_{k=0}^{\infty}\sum_{r=0}^{q+k}\sum_{t=0}^{k}\frac{(-1)^r}{r!\,t!}\binom{2p-2L}{q+k-r}\binom{-2p}{k-t}\nu^{r+t}\beta^{2k} \tag{2.86}$$

$$X_0^{-(L+1),L-2p} = C\sum_{k=0}^{\infty}\sum_{r=0}^{q+k}\sum_{t=0}^{k}\frac{(-1)^t}{r!\,t!}\binom{-2p}{q+k-r}\binom{2p-2L}{k-t}\nu^{r+t}\beta^{2k} \tag{2.87}$$

By examining the combination of cases for $q>0$, $q<0$, $p\leq L/2$, and $p>L/2$ it can be shown that (3:14-15):

$$X_{L-2p+q}^{-(L+1),L-2p} \equiv G_{Lpq}(e) = (-1)^{|q|}(1+\beta^2)^L\beta^{|q|}\sum_{k=0}^{\infty}P_{Lpqk}Q_{Lpqk}\beta^{2k} \tag{2.88}$$

where

$$P_{Lpqk} = \sum_{r=0}^{h}\binom{2p'-2L}{h-r}\frac{(-1)^r}{r!}\left(\frac{(L-2p'+q')e}{2\beta}\right)^r \tag{2.89}$$

$$Q_{Lpqk} = \sum_{r=0}^{h}\binom{-2p'}{h-r}\frac{1}{r!}\left(\frac{(L-2p'+q')e}{2\beta}\right)^r \tag{2.90}$$

In equations (2.89) and (2.90) the following conditions hold. $h=k+q'$ if $q'>0$. If $q'<0$ then $h=k$. Also, $p'=p$ and $q'=q$ if $p\leq L/2$. If $p>L/2$ then $p'=L-p$ and $q'=-q$.

The $G_{Lpq}(e)$ term is known as the Eccentricity Function. A list of this function's values is in Appendix C.

Equations (2.63), (2.64), and (2.88) allow equation (2.29) to be written into the form:

$$V_{Lm} = -\frac{GMR_p^L}{r^{L+1}}\sum_{p=0}^{L}F_{Lmp}(i)\sum_{q=-\infty}^{\infty}G_{Lpq}(e)S_{Lmpq}(\omega,M,\Omega,\theta) \tag{2.91}$$

where

$$S_{Lmpq} = \begin{bmatrix} C_{Lm} \\ -S_{Lm} \end{bmatrix}_{L-m,\,odd}^{L-m,\,even} \cos[(L-2p)\omega + (L-2p+q)M + m(\Omega-\theta)]$$

$$+ \begin{bmatrix} S_{Lm} \\ C_{Lm} \end{bmatrix}_{L-m,\,odd}^{L-m,\,even} \sin[(L-2p)\omega + (L-2p+q)M + m(\Omega-\theta)] \tag{2.92}$$

III. Atmospheric Drag

Atmospheric Drag Effects

A satellite moving through an atmosphere experiences a force perpendicular to its flight path ("lift"), and a force in the opposite direction to its flight path ("drag"). Because of variations in a satellite's attitude, the resultant lift force is usually zero. This is especially true for spherical satellites, or satellites whose length is greater than its diameter. Even if the resultant lift force is not zero, its effects, when compared with drag, are still negligible (15:295). Drag, on the other hand can have a profound effect on the orbit of a satellite.

In this analysis, the atmosphere is modeled as a locally exponential atmosphere. Therefore, the density of the atmosphere is decreasing exponentially with altitude, implying that drag's predominant effects occur when the satellite is near its closet approach to a planet. At this point the flight path angle is approximately zero. Thus, drag will be acting directly opposite to the satellite's velocity vector. This will have the effect of slowing the satellite down, and hence, decreasing its energy. The decrease in the satellite's energy will result in a decrease in the semi major axis a, and the eccentricity, e. Although periapsis altitude will decrease somewhat, this decrease is very small when compared with the resulting decrease in the apoapsis altitude. The over all effect of drag will to be to "circularize" the orbit.

If the atmosphere were perfectly spherical and nonrotating, the reduction in a and e would be drag's only effects on the orbit. However, atmospheres share the same propensity for oblateness as their planets and tend to rotate. The oblateness of the atmosphere will induce small changes in the argument of periapsis, ω, while the rotation of the atmosphere results in small lateral forces on the satellite. These lateral forces cause increasing changes in the angle of inclination, i, and small periodic changes in the longitude of the ascending node, Ω (11:6-7).

The atmospheric drag on a satellite may be expressed as (15:295):

$$D = \frac{\rho V^2 S C_D}{2m} \tag{3.1}$$

where D = the force of drag

ρ = the atmospheric density

V = the velocity of the satellite relative to the atmosphere

S = the effective area of the satellite

C_D = the coefficient of drag

m = the mass of the satellite

Atmospheric Density

Appendix D develops the expression used for a locally exponential atmosphere. This expression is:

$$\rho = \rho_0 \exp\left\{-\frac{gm}{RT} z\right\} \tag{3.2}$$

In equation (3.2), z is equal to the altitude above the planet. To write equation (3.2) in terms of the radial distance (r) from the center of the planet let:

$$z = r - R_p \tag{3.3}$$

where R_p is the radius of the planet. Using an expression for the rectangular components of a point on the surface of a planet as found in Escobal, page 26, R_p can be written as:

$$R_p = R_e \left(\frac{1 - \epsilon^2}{1 - \epsilon^2 \cos^2 \phi} \right)^{1/2} \tag{3.4}$$

where R_e = the equatorial radius of the planet

e = the eccentricity of the planet's shape

ϕ = the latitude

Applying equation (3.3) to equation (3.2) yields:

$$\rho = \rho_0 \exp\left(-\left\{ \frac{gm}{RT} \right\} (r - R_p) \right) \tag{3.5}$$

The bracketed term is equal to $1/H$, where H is the "scale height" and is equal to the change in altitude required in order for the density to change by one exponential. As can be seen from equation (3.5) it is not constant; however, at the altitudes that the satellite will experience significant air drag H is so large it can be treated as a constant. For example, using data obtain from the Viking 1 space craft, at 200 km altitude the scale height is 14.1387 km (16:4368-4373). It is because the scale height can be considered a constant over some small altitude band that the assumption of a locally exponential decreasing atmosphere may be made (18:4). Therefore, equation (3.5) becomes:

$$\rho = \rho_0 \exp\left\{ -\frac{r - R_p}{H} \right\} \tag{3.6}$$

Velocity With Respect to the Atmosphere

Let:

$\vec{V}$ = velocity of satellite relative to the atmosphere

$\vec{V}_p$ = velocity of the satellite relative to the planet

$\vec{V}_a$ = velocity of the atmosphere relative to the planet (atmosphere assumed to be moving west to east)

Figure 3.1 shows the angular relationships between these vectors.

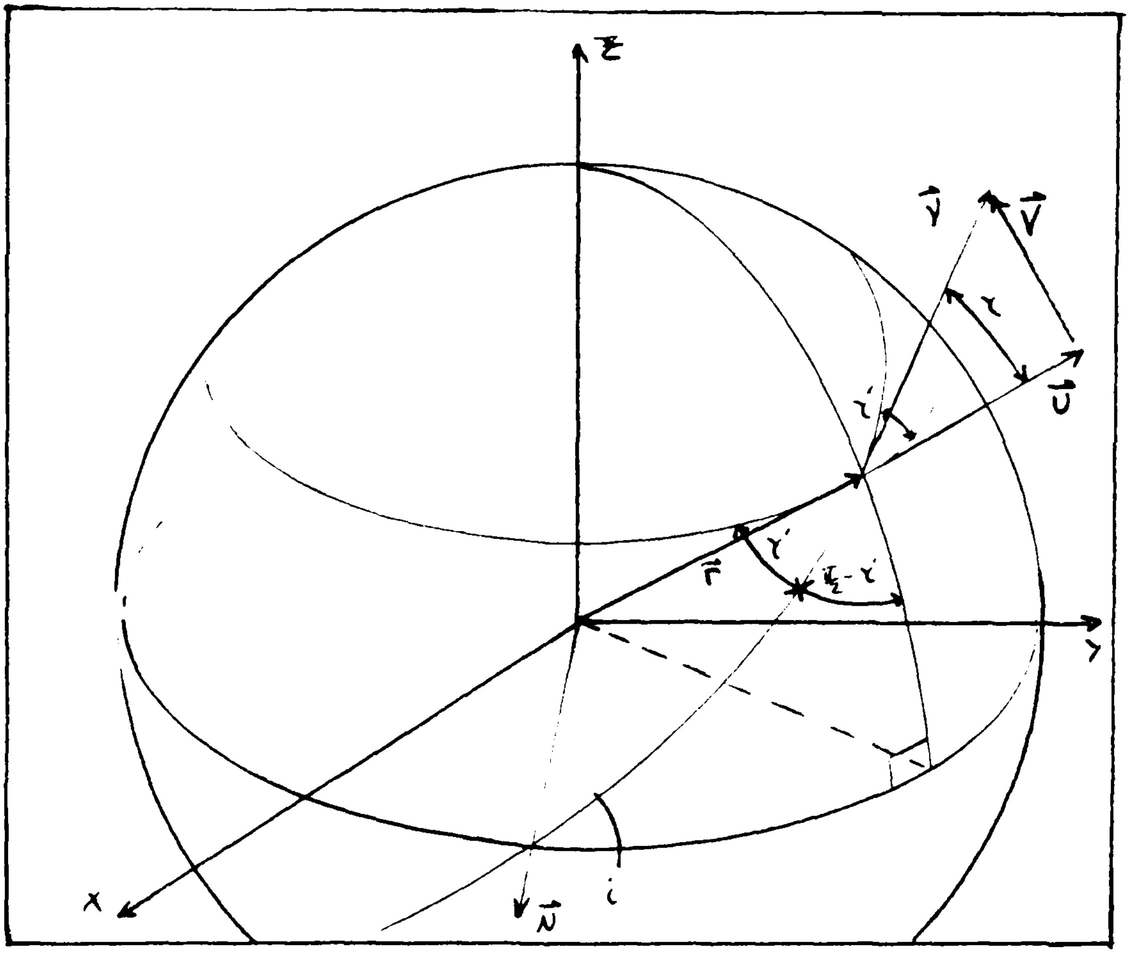

Angular Relationships Between the Different Types of Velocities

Figure 3.1.

From Figure 3.1 it can be seen that:

$$\vec{V} = \vec{v} - \vec{u} \tag{3.7}$$

Applying the law of cosines yields:

$$V^2 = v^2 + u^2 - 2vu\cos\gamma \tag{3.8}$$

Assume that the atmosphere rotates with an angular velocity ω about the planet. Then

$$u = r\omega\cos\phi \tag{3.9}$$

where r = radial distance from the center of the planet

ϕ = latitude

Using spherical trigonometry and the angular relationships in Figure 3.1:

$$\cos i = \cos\phi\cos\gamma' \tag{3.10}$$

This analysis assumes, since the most profound effects occur at periapsis, that the satellite is at its periapsis point. Thus implying that, $\gamma' \approx \gamma$. γ is still a good approximation for γ' even when the satellite is not at its periapsis point. However, the satellite must be with in two scale heights of periapsis altitude to keep the error of assuming $\gamma' \approx \gamma$ to less than one percent (11:23).

Therefore, assuming $\gamma' \approx \gamma$ and applying equation (3.10) to equation (3.9) yields:

$$\begin{aligned} u &= r\omega\cos\phi \\ &= r\omega\frac{\cos i}{\cos\gamma} \\ u\cos\gamma &= r\omega\cos i \end{aligned} \tag{3.11}$$

Substituting equations (3.9) and (3.11) into equation (3.8) yields:

$$V'^2 = V^2\left(1 - \frac{r\omega}{V}\cos i\right)^2 + r^2\omega^2\ \cos^2\phi - \cos^2 i \tag{3.12}$$

For the planet Mars, the atmosphere rotates with approximately the same angular velocity as the planet (18:3). Therefore, $\omega \approx .00008050$ radians per second (13:2-3). This small value for ω results in the $r^2\omega^2$ term in the above equation being vanishingly small when compared to V^2 and will be neglected. Further, since drag effects the periapsis altitude, velocity, and angle of inclination, equation (3.12) must be rewritten for some reference periapsis altitude, velocity, and inclination. This is accomplished by letting $r = r_{p0}$, $v = v_{p0}$, and $i = i_0$. Equation (3.12) becomes:

$$V \cong v\left(1 - \frac{r_{p0}\omega}{v_{p0}}\cos i_0\right) \tag{3.13}$$

The Cross Sectional Area, S

The cross sectional area effecting drag, S, will be a function of the satellite's shape and flight path angle. Due to the array of scientific sensors desired for a Mars mission, the satellite's shape will most likely be very irregular, implying that the effective cross sectional area may not be known. No matter what the shape, a satellite in uncontrolled flight will have a tendency to rotate about its axis of maximum moment of inertia (8:369-371). For cylindrical shaped satellites with a length to diameter (L/d) ratio greater than roughly 2, this rotation will cause the satellite to move through the atmosphere tumbling end over end, or revolving like an aircraft propeller (11:16).

In the first case a mean value of S is:

$$S = \frac{2}{\pi}\left(Ld + \frac{1}{4}\pi d^2\right) \tag{3.14}$$

and in the second case:

$$S = Ld \tag{3.15}$$

where L = the length of the satellite

d = the diameter of the satellite

If the direction of the spin axis is not known, then the mean value of S is somewhere in-between the values given in equation (3.14) and (3.15). Averaging these two equations yields:

$$S = ld\left(0.818 + 0.25\frac{d}{l}\right) \tag{3.16}$$

This value will never be more than 15 percent off the extreme case (satellite spinning like a propeller).

When L/d is less than 1/2, the spin axis becomes the axis of symmetry. In this case, if the spin axis is aligned with the satellite's direction of motion:

$$S = \pi r^2 \tag{3.17}$$

If the spin axis is perpendicular to the flight path, S is given by equation (3.15). In this case, if l is much smaller than d the value of S can become very small. This implies that the error associated in averaging the values of equations (3.15) and (3.17), when the direction of the spin axis is unknown, can yield differences between the actual and estimated values of S that are much greater than those of the previous case.

For this thesis, based on a rough estimate on the size of satellites currently orbiting the earth, a cross sectional area of $S = 10m^2$ will be used.

The Coefficient of Drag, C_D

The coefficient of drag is dependent upon the density of the atmosphere, the Reynolds number, angle of attack, the shape, and the speed of the satellite. These parameters not only vary from satellite configuration to satellite configuration, but can also vary through out the satellite's flight path.

As the density increases three distinct regions of atmospheric flow are encountered. First, continuum flow, is the region where the atmosphere deforms continuously under the shear force applied by the moving satellite. The Viking project found that for Mars this region exist from the surface to about 90 km altitude. For Viking the coefficient of drag in this region was approximately 1.47. Next, the slip flow region, which exist from about 90 km to 115 km, is a region of transition between continuum flow and free molecular flow, the third region. Free molecular flow exist when the distance that a molecule can travel with out striking another molecule, its mean free path, is greater than the dimensions of the satellite. For Mars this region exist for altitudes greater than roughly 115 km.

This thesis is concerned primarily with the region of free molecular flow. In this region the coefficient of drag can vary as the angle of attack of the satellite varies, and will be on the order of 2.0 to 2.25. A C_D of 2.0 will be used in this thesis. This value was chosen because it was the coefficient of drag used on the Viking mission (16:4369).

IV. Computer Program Validation

Description of the Program

Part of the analysis of this thesis was carried out using the Artificial Satellite Analysis Program (ASAP), see reference 13. This program uses Cowell's method. Essentially this involves taking the state vector of the satellite with respect to an x, y, z coordinate system whose origin is at the center of the central body, whose xy plane lies in the plane of the equator, and whose z axis goes through the north pole of the central body; and then solving the associated equations of motion via a numerical integration package. ASAP uses an 8th order Runge-Kutta integrator that requires the equations of motion be written as a set of first order differential equations. This process looks like (13:3-1):

$$\bar{S} = [x, y, z, \dot{x}, \dot{y}, \dot{z}]^T \tag{4.1}$$

where $\dot{x} = V_x$ = velocity in the X direction

$\dot{y} = V_y$ = velocity in Y direction

$\dot{z} = V_z$ = velocity in Z direction

Applying Newton's second law (to determine the equations of motion), and keeping in mind that the Runge-Kutta package used requires a set of first order differential equations yields (13:3-1):

$$\dot{V}_x = \ddot{x} = -\mu \frac{x}{r^3} + \text{Perturbations} \tag{4.2}$$

$$\dot{V}_y = \ddot{y} = -\mu \frac{y}{r^3} + \text{Perturbations} \tag{4.3}$$

$$\dot{V}_z = \ddot{z} = -\mu \frac{z}{r^3} + \text{Pertrubations} \tag{4.4}$$

where μ = the universal gravity constant multiplied by the mass of the central body

r = $\sqrt{x^2+y^2+z^2}$

This thesis will only consider those perturbing effects caused by the central body and atmospheric drag.

Perturbations due to the Central Body. ASAP uses equations (2.29), (2.91), and (2.92) in order to find the geopotential in terms of latitude, longitude, radial position, and the classical orbital elements, i, e, ω, ν, and Ω. The implementation of these equations into a form acceptable to the Runge-Kutta integrator requires the conversion to cartesian coordinates. This is accomplished by rewriting equation (2.29) such that only effects due to departures in the central body's shape from a perfect, homogenous sphere are considered. The resulting equation is:

$$\Phi(r,\phi,\lambda) = -\frac{GM}{r}\sum_{l=2}^{\infty}\sum_{m=0}^{l}\left(\frac{r}{R_p}\right)^{-l} P_l^m(\sin\phi)\left(C_{lm}\cos m\lambda + S_{lm}\sin m\lambda\right) \tag{4.5}$$

The perturbing portion of equations (4.2) through (4.4) due to the central body can now be written as (13:3-1):

$$\ddot{x} = \Gamma_x = \left(\frac{1}{r}\frac{\partial\Phi}{\partial r} - \frac{z}{r^2\sqrt{x^2+y^2}}\frac{\partial\Phi}{\partial\phi}\right)x - \left(\frac{1}{x^2+y^2}\frac{\partial\Phi}{\partial\lambda}\right)y \tag{4.6}$$

$$\ddot{y} = \Gamma_y = \left(\frac{1}{r}\frac{\partial\Phi}{\partial r} - \frac{z}{r^2\sqrt{x^2+y^2}}\frac{\partial\Phi}{\partial\phi}\right)y + \left(\frac{1}{x^2+y^2}\frac{\partial\Phi}{\partial\lambda}\right)x \tag{4.7}$$

$$\ddot{z} = \Gamma_z = \frac{1}{r}\left(\frac{\partial\Phi}{\partial r}\right)z + \frac{\sqrt{x^2+y^2}}{r^2}\frac{\partial\Phi}{\partial\phi} \tag{4.8}$$

where

$$\frac{\partial\Phi}{\partial r} = \frac{1}{r}\left(\frac{GM}{r}\right)\sum_{l=2}^{\infty}\sum_{m=0}^{l}\left(\frac{r}{R_p}\right)^{-l}(l+1)\,P_l^m(\sin\phi)\left(C_{lm}\cos m\lambda + S_{lm}\sin m\lambda\right) \tag{4.9}$$

$$\frac{\partial \Phi}{\partial \phi} = -\left(\frac{GM}{r}\right)\sum_{l=2}^{\infty}\sum_{m=0}^{l}\left(\frac{r}{R_p}\right)^{l} \left[P_l^{m+1} \sin\phi - m\tan\phi P_l^m \sin\phi\right] \left[C_{lm}\cos m\lambda + S_{lm}\sin m\lambda\right] \tag{4.10}$$

$$\frac{\partial \Phi}{\partial \lambda} = -\left(\frac{GM}{r}\right)\sum_{l=2}^{\infty}\sum_{m=0}^{l}\left(\frac{r}{R_p}\right)^{l} P_l^m \sin\phi \left[S_{lm}\cos m\lambda - C_{lm}\sin m\lambda\right] m \tag{4.11}$$

Perturbations due to Atmospheric Drag. Since atmospheric drag acts to retard the motion of a satellite, the equation of motion of atmospheric drag used by ASAP is the negative of equation (3.1). As a model for the atmospheric density change with altitude, equation (3.6) is employed; however, the selection of a reference height from which to base density calculations is allowed. This is implemented by replacing the R_r term in equation (3.6) with a reference height term, h_r. The program also takes into account the departure in the central body's shape from a perfect sphere by use of equation (3.4).

Program Validation.

The following equations were used in the validation of ASAP. They were derived from the Lagrange Planetary equations where the disturbing function is derived from equation (2.91), using only the zonal harmonics up to and including the 6th zonal (14:28-30):

$$\Delta e = 2\pi\left(\sum_n J_n\left(\frac{R_p}{p}\right)^n e_n + J_2^2\left(\frac{R_p}{p}\right)^4 e_{22}\right) \tag{4.12}$$

where

$$e_2 = 0 \tag{4.13}$$

$$e_3 = -\frac{3}{2}\left(1 - e^2\right)\sin i\cos\omega\left(1 - \frac{5}{4}\sin^2 i\right) \tag{4.14}$$

$$e_4 = -\frac{15}{16}\left(1 - e^2\right)\left(1 - \frac{7}{6}\sin^2 i\right)e\sin 2\omega\sin^2 i \tag{4.15}$$

$$e_5 = [illegible] \sin^2 i + \frac{21}{8}\sin^4 i\Big)\left(1 + \frac{3}{4}e^2\right)\cos\omega + \frac{7}{8}\left(1 - \frac{9}{8}\sin^2 i\right)e^2\cos 3\omega\sin^2 i\Big] \tag{4.16}$$

$$e_6 = \frac{525}{32}(1-e^2)\sin^2 i\left[\left(1-3\sin^2 i+\frac{33}{16}\sin^4 i\right)\left(1+\frac{1}{2}e^2\right)e\sin 2\omega+\frac{3}{16}\left(1-\frac{11}{10}\sin^2 i\right)e^3\sin 4\omega\sin^2 i\right] \tag{4.17}$$

$$e_{22} = -3\sin\omega\left[\frac{3}{2}\left(1-\frac{5}{4}\sin^2 i\right)(1+e\cos\omega)^2-\sin^2 i\,(1-e^2)\left\{\left(1-\frac{5}{4}\sin^2 i\right)-\left(\frac{7}{8}-\frac{15}{16}\sin^2 i\right)\right\}e\cos\omega\right] \tag{4.18}$$

$$\Delta i = 2\pi\left(\sum_n J_n\left(\frac{R_p}{p}\right)^n i_n + J_2^2\left(\frac{R_p}{p}\right)^4 i_{22}\right) \tag{4.19}$$

where

$$i_2 = 0 \tag{4.20}$$

$$i_3 = \frac{3}{2}\left(1-\frac{5}{4}\sin^2 i\right)e\cos\omega\cos i \tag{4.21}$$

$$i_4 = \frac{45}{32}\left(1-\frac{7}{6}\sin^2 i\right)e^2\sin 2\omega\sin 2i \tag{4.22}$$

$$i_5 = -\frac{15}{4}e\cos i\left[\left(1-\frac{7}{2}\sin^2 i+\frac{21}{8}\sin^4 i\right)\left(1+\frac{3}{4}e^2\right)\cos\omega+\frac{7}{8}\left(1-\frac{9}{8}\sin^2 i\right)e^2\cos 3\omega\sin^2 i\right] \tag{4.23}$$

$$i_{[illegible]} = -\frac{525}{64}e\sin 2i\left[\left(1-3\sin^2 i+\frac{33}{16}\sin^4 i\right)\left(1+\frac{1}{2}e^2\right)e\sin 2\omega+\frac{3}{16}\left(1-\frac{11}{10}\sin^2 i\right)e^3\sin 4\omega\sin^2 i\right] \tag{4.24}$$

$$i_{22} = -\frac{3}{2}\sin 2i\left[\left(1-\frac{5}{4}\sin^2 i\right)e\sin\omega+\left(-\frac{7}{16}+\frac{15}{32}\sin^2 i\right)e^2\sin 2\omega\right] \tag{4.25}$$

$$\Delta\Omega = 2\pi\left(\sum_n J_n\left(\frac{R_p}{p}\right)^n \Omega_n + J_2^2\left(\frac{R_p}{p}\right)^4 \Omega_{22}\right) \tag{4.26}$$

where

$$\Omega_2 = -\frac{3}{2}\cos i \tag{4.27}$$

$$\Omega_3 = \frac{3}{2}\left(1-\frac{15}{4}\sin^2 i\right)e\sin\omega\cot i \tag{4.28}$$

$$\Omega_4 = \frac{15}{4}\cos\iota\left[\left(1 - \frac{7}{4}\sin^2\iota\right)\left(1 + \frac{3}{2}e^2\right) - \frac{3}{4}\left(1 - \frac{7}{3}\sin^2\iota\right)e^2\cos 2\omega\right] \tag{4.29}$$

$$\Omega_5 = -\frac{15}{4}\cot\iota\left[\left(1 - \frac{21}{2}\sin^2\iota + \frac{105}{8}\sin^4\iota\right)\left(1 + \frac{3}{4}e^2\right)e\sin\omega + \frac{7}{8}\left(1 - \frac{15}{8}\sin^2\iota\right)e^3\sin 3\omega\right] \tag{4.30}$$

$$\begin{aligned}\Omega_6 = &-\frac{105}{16}\cos\iota\left[\left(1 - \frac{9}{2}\sin^2\iota + \frac{33}{8}\sin^4\iota\right)\left(1 + 5e^2 + \frac{15}{8}e^4\right)\right.\\ &\left.-\frac{5}{2}\left(1 - 6\sin^2\iota + \frac{99}{16}\sin^4\iota\right)\left(1 + \frac{1}{2}e^2\right)e^2\cos 2\omega - \frac{15}{32}\left(1 - \frac{33}{20}\sin^2\iota\right)e^4\cos 4\omega\sin^2\iota\right]\end{aligned} \tag{4.31}$$

$$\begin{aligned}\Omega_{22} = &\frac{3}{2}\cos\iota\left[\left(\frac{3}{4} - 5\sin^2\iota\right) + (4 - 10\sin^2 i)\, e\cos\omega + \left(-\frac{1}{4} - \frac{5}{16}\sin^2\iota\right)e^2\right.\\ &\left.+\left(-\frac{7}{8} + \frac{15}{8}\sin^2\iota\right)e^2\cos 2\omega\right]\end{aligned} \tag{4.32}$$

$$\Delta\omega = 2\pi\left(\sum_n J_n\left(\frac{R_p}{p}\right)^n\omega_n + J_2^2\left(\frac{R_p}{p}\right)^4\omega_{22}\right) \tag{4.33}$$

where

$$\omega_2 = 3\left(1 - \frac{5}{4}\sin^2\iota\right) \tag{4.34}$$

$$\omega_3 = \frac{3}{2}e^{-1}\sin\omega\sin i\left[\left(1 - \frac{5}{4}\sin^2\iota\right) + \left(\frac{35}{4}\cos^2\iota - \mathrm{cosec}^2\iota\right)e^2\right] \tag{4.35}$$

$$\begin{aligned}\omega_4 = &-\frac{15}{32}\left[16 - 62\sin^2\iota + 49\sin^4\iota + (6\sin^2\iota - 7\sin^4\iota)\cos 2\omega + \left(18 - 63^2\iota + \frac{189}{4}\sin^4\iota\right)e^2\right.\\ &\left.+\left(-6 + 35\sin^2\iota - \frac{63}{2}\sin^4\iota\right)e^2\cos 2\omega\right]\end{aligned} \tag{4.36}$$

$$\omega_5 = \frac{105}{16} e^{-1} \sin\omega \operatorname{cosec} i \Big[\Big(-\frac{4}{7} + 2\sin^2 i - \frac{3}{2}\sin^4 i\Big)\sin^2 i$$

$$+\Big(\frac{4}{7} - \frac{87}{7}\sin^2 i + \frac{67}{2}\sin^4 i - \frac{357}{16}\sin^6 i\Big)e^2 + \Big(-1 + \frac{9}{8}\sin^2 i\Big)e^2\cos 2\omega \sin^4 i \tag{4.37}$$

$$+\Big(\frac{3}{7} - 7\sin^2 i + \frac{267}{16}\sin^4 i - \frac{165}{16}\sin^6 i\Big)e^4 + \Big(1 - \frac{39}{8}\sin^2 i + \frac{33}{8}\sin^4 i\Big)e^4\cos 2\omega \sin^2 i$$

$$\omega_6 = \frac{525}{64}\Big[\frac{8}{5}\Big(1 - 8\sin^2 i + \frac{129}{8}\sin^4 i - \frac{297}{32}\sin^6 i\Big)$$

$$+\Big(2 - 6\sin^2 i + \frac{33}{8}\sin^4 i\Big)\cos 2\omega \sin^2 i + 6\Big(1 - \frac{43}{6}\sin^2 i + \frac{109}{8}\sin^4 i - \frac{121}{8}\sin^6 i\Big)e^2$$

$$+\Big(-2 + 25\sin^2 i - \frac{459}{8}\sin^4 i + \frac{561}{16}\sin^6 i\Big)e^2\cos 2\omega \tag{4.38}$$

$$+\frac{3}{8}\Big(1 - \frac{11}{10}\sin^2 i\Big)e^2\cos 4\omega \sin^4 i + \Big(2 - \frac{27}{2}\sin^2 i + \frac{99}{4}\sin^4 i - \frac{429}{32}\sin^6 i\Big)e^4$$

$$+\Big(-1 + \frac{21}{2}\sin^2 i - \frac{363}{16}\sin^4 i + \frac{429}{32}\sin^6 i\Big)e^4\cos 2\omega$$

$$+\frac{3}{8}\Big(-1 + \frac{22}{5}\sin^2 i - \frac{143}{40}\sin^4 i\Big)e^4\cos 4\omega \sin^2 i\Big]$$

$$\omega_{22} = \frac{9}{4}\Big[\Big(-2 + \frac{23}{6}\sin^2 i - \frac{5}{8}\sin^4 i\Big)e^{-1}\cos\omega$$

$$+\Big(\frac{95}{12}\sin^2 i - \frac{445}{48}\sin^4 i\Big) + \Big(-2 + \frac{23}{12}\sin^2 i + \frac{5}{8}\sin^4 i\Big)\cos 2\omega \tag{4.39}$$

$$+\Big(-\frac{25}{6} + \frac{461}{24}\sin^2 i - \frac{50}{3}\sin^4 i\Big)e\cos\omega + \Big(-\frac{1}{2} + \frac{5}{8}\sin^2 i\Big)e\cos 3\omega$$

$$+\Big(\frac{7}{12} - \frac{3}{8}\sin^2 i - \frac{15}{32}\sin^4 i\Big)e^2 + \Big(\frac{7}{12} - \frac{79}{24}\sin^2 i + \frac{45}{16}\sin^4 i\Big)e^2\cos 2\omega\Big]$$

Each of the above 4 orbital elements (e, i, Ω, ω) were analyzed and predictions were made as to what values will drive the change in each element to zero. These predictions were then tested by running ASAP with the appropriate elements. If ASAP is reliable both the predictions and the ASAP output should agree.

Because ω contributes only to the long term perturbations, which are periodic over one axial period (the time for the line of apsides to make one complete revolution), all trigonometric terms containing ω will be set equal to zero. This greatly simplifies the above equations, and is valid due to the method of averaging when applied to the ω terms of equation (2.91). Setting ω equal to zero causes all the odd zonal harmonics in equations (4.12) through (4.39) to go to zero, and eliminates many other terms from the even zonal harmonics.

Eccentricity and Inclination. Equations (4.12) through (4.25) do not have any non zero terms once trigonometric functions of ω have been set to zero. This implies that no matter what the size, shape, or orientation of the orbit the secular changes in eccentricity and inclination due to zonal harmonics are zero. Eccentricity and inclination will experience a short term change due to a change in the mean anomaly, and also a long term change due to precession of the line of apsides; however, since both these effects are periodic, and since the change in ω over one orbital period is small compared to the change in mean anomaly, the change in eccentricity and inclination over one orbital period will be almost zero while the change in eccentricity and inclination over on axial period will be zero. This prediction is also supported by Roy, page 290.

Several computer runs were made with ASAP using different input values. These data runs considered the perturbative effects due to zonal harmonics up to and including an order of six. In all cases the output was consistent with the above predictions. Figures 4.1 through 4.4 are a representative sample of the output, and indicates the change in eccentricity and inclination over one orbital period, and one axial period. Table 4.1 lists the input orbital elements used to generate Figures 4.1 through 4.10.

Input Orbital Elements for Figures 4.1 Through 4.10

Table 4.1

Input Orbital Elements	Figures 4.1 and 4.2	Figures 4.3 and 4.4	Figures 4.5 and 4.6	Figures 4.7 through 4.10
a km	4000	3992.6667	3992.6667	3992.6667
e	.10165	.1	.1	.1
i degrees	45	82.2464924	90	63.2604625464
Ω degrees	90	90	90	90
ω degrees	270	40	270	270
M degrees	90	90	90	90

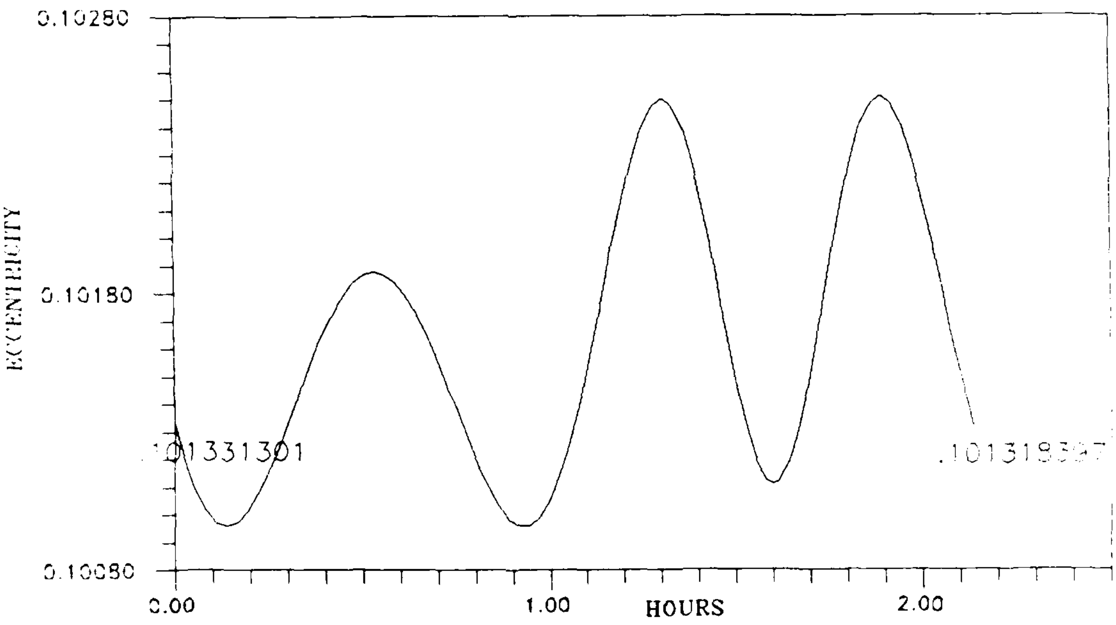

Change in Eccentricity Over One Orbital Period (6 X 0 Gravity Field)

Figure 4.1

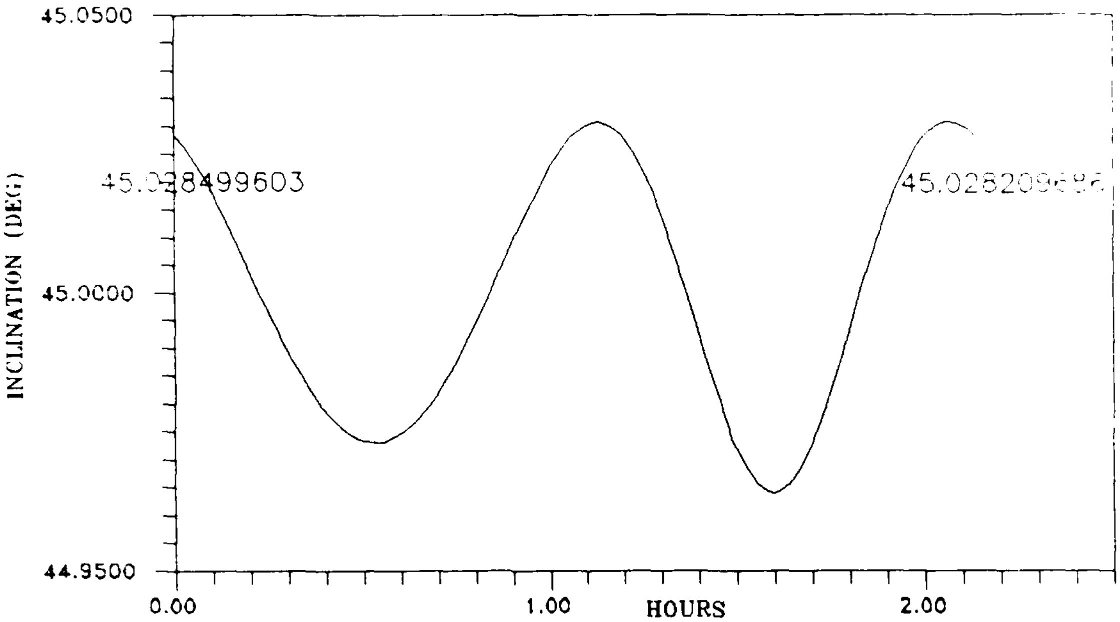

Change in Inclination Over One Orbital Period (6 X 0 Gravity Field)

Figure 4.2

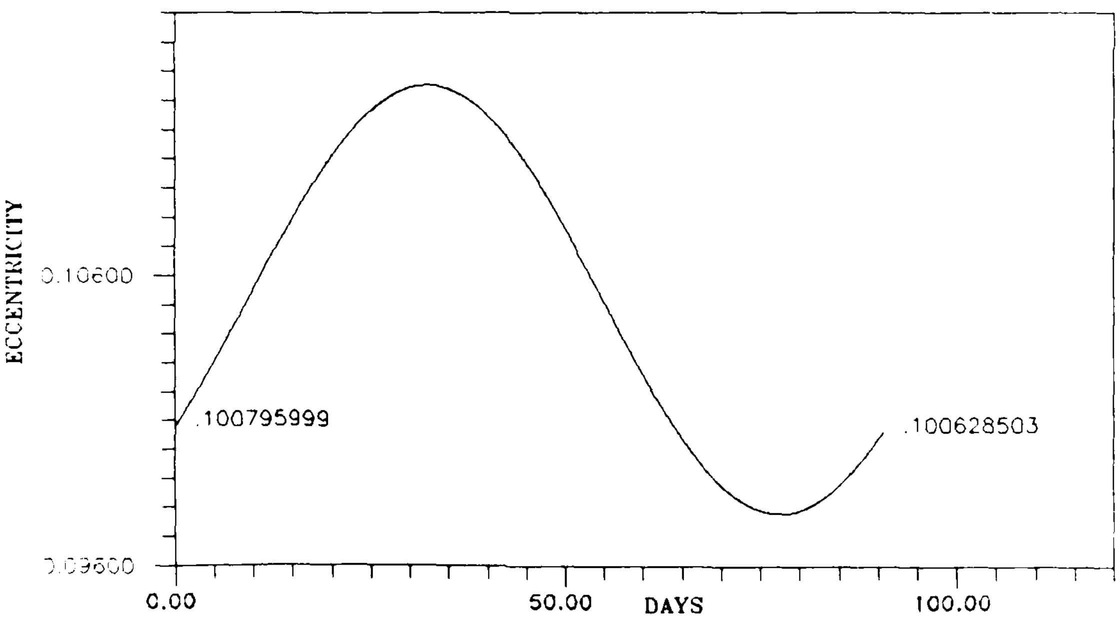

Change in Eccentricity Over One Axial Period (6 X 0 Gravity Field)

Figure 4.3

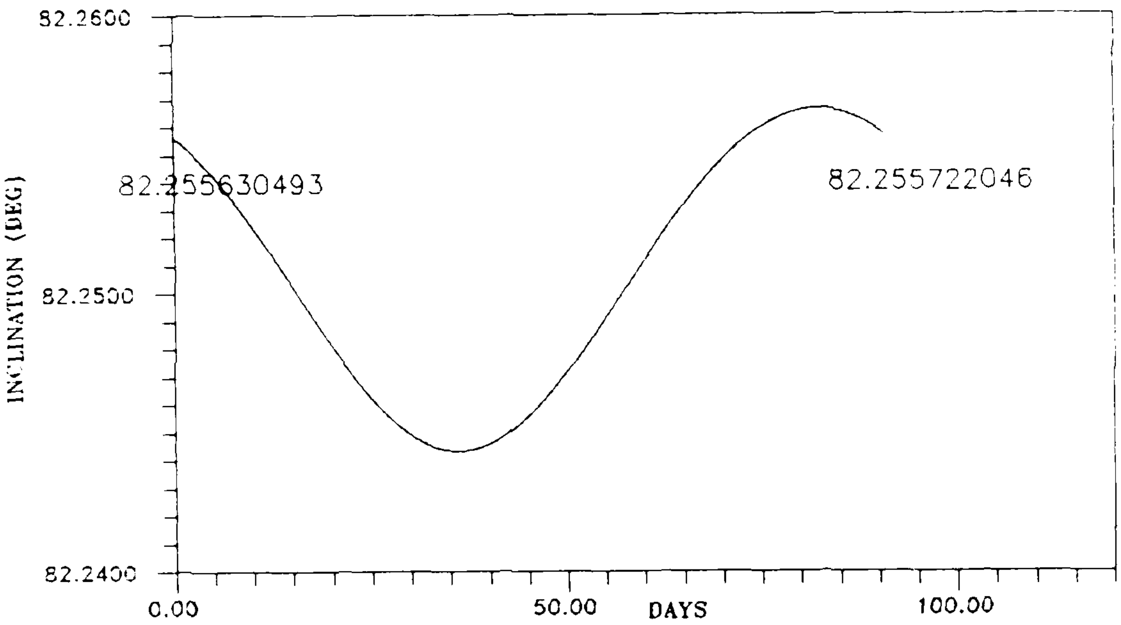

Change in Inclination Over One Axial Period (6 X 0 Gravity Field)

Figure 4.4

Note, due to inaccuracies in calculating the exact axial period, the change in eccentricity and inclination shown in Figures 4.3 and 4.4 are not exactly zero.

Longitude of the Ascending Node. Equations (4.26) and (4.32) have the term $\cos\iota$ as a common denominator. Thus, any value of the inclination that drives the $\cos\iota$ term to zero will cause the change in the Longitude of the Ascending Node (Ω) to also equal zero. A polar orbit ($\iota = 90$) has long been known to yield $\Delta\Omega$ equal zero. Figure 4.5 shows the ASAP output given an input value of ι equal to ninety degrees. As expected, throughout the orbital period there is no change in Ω.

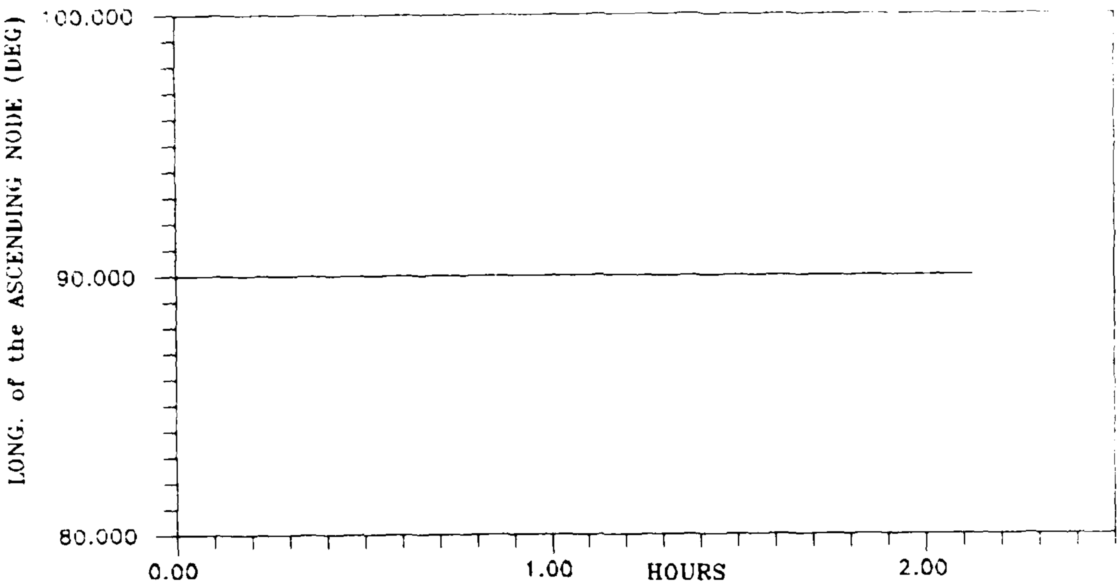

Change in Ascending Node for a Polar Orbit (6 X 0 Gravity Field)

Figure 4.5

In addition to the predominant $\cos\iota$ term, equations (4.27) through (4.32) also contain other trigonometric functions of ι. A search for values of ι (other than $\iota=90$, $\iota=270$) that will cause $\Delta\Omega$ to equal zero was made by inputting equations (4.27) through (4.32) into equation (4.26). The $\cos\iota$ terms were eliminated by setting $\Delta\Omega$ equal to zero and then dividing by $\cos\iota$. The only ι terms left in the equation are powers of $\sin\iota$. Terms were grouped by the power of their associated $\sin\iota$ terms thus producing a 4th degree polynomial. By making the change of variable $f=\sin^2\iota$ the polynomial is reduced to a quadratic. This quadratic was solved using the computer program Capmega given in Appendix E. The results show that for eccentricities from 0 to .9, and for inclinations from 0 to 90, there is no other value of ι that will yield $\Delta\Omega$ equal to zero other than those values of ι associated with a polar orbit.

Note that equations (4.21) through (4.25) also have a common denominator of $\cos\iota$, thus implying that the change in inclination will also be zero if in a polar orbit. This gives another opportunity to validate ASAP by noting its predicted change in inclination for a polar orbit. Figure 4.6 shows the results of this procedure.

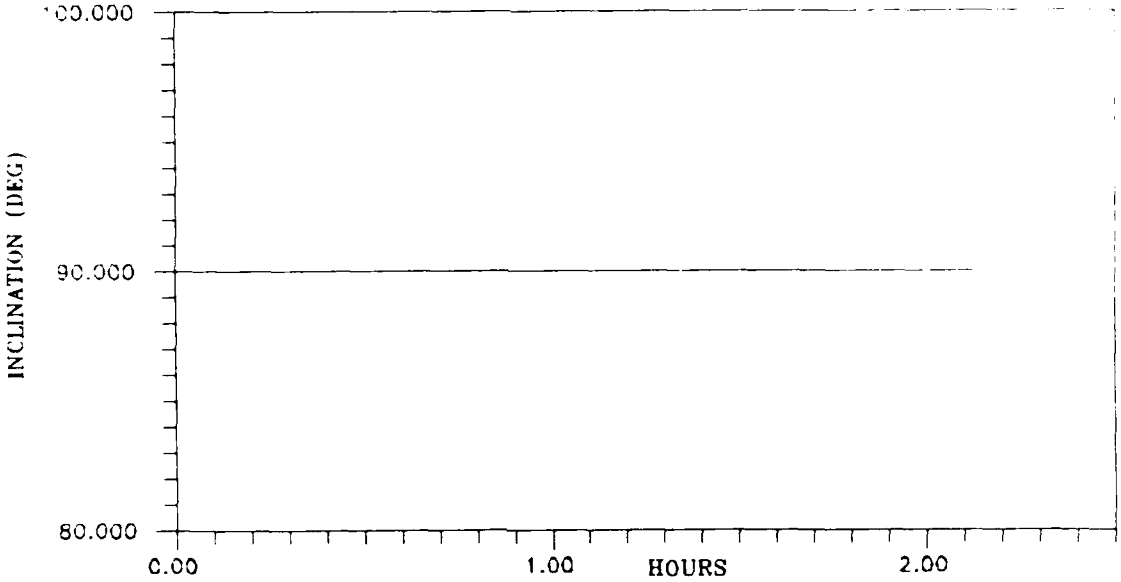

Change in Inclination for a Polar Orbit (6 X 0 Gravity Field)

Figure 4.6

<u>Argument of the Periapsis</u>. In a process similar to the one described above, equations (4.34) through (4.39) were substituted into equation (4.33), and terms of similar powers of $\sin\iota$ were grouped together. The program Omega (found in Appendix E) was used to solve the resulting polynomial. The results yielded a particular value for ι, taking into account the zonal harmonics up to order six, that causes $\Delta\omega$ to equal zero. This value is know as the critical value of ι, and is dependent on the semi major axis and the eccentricity of the orbit. A critical value of ι was determined for several different values of eccentricity and semi major axis. These values were inputted into ASAP. In each case ASAP yielded the proper result.

As with the eccentricity and inclination, ω is subject to short and long term perturbations; therefore, when the inclination is at its critical value, the change in ω over one orbital period should be close to zero, while the change over one axial period should be exactly zero. Figure 4.7 shows that the change in ω over one orbital period is indeed almost zero. Figures 4.8 through 4.9 demonstrate the closed nature of the change in eccentricity, and inclination vs. the change in the argument of the periapsis over one orbital period. Figure 4.10 shows that the same closed relationship exist between the semi major axis and the argument of the periapsis, agreeing with the literature (see Roy, page 290).

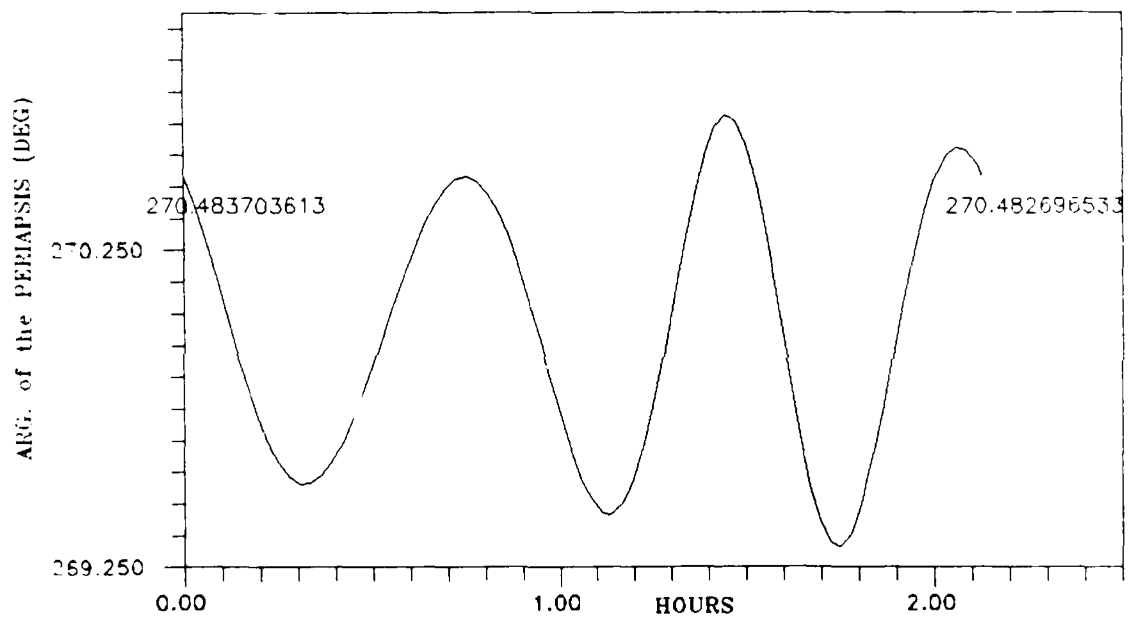

Change in Arg. of the Periapsis Over One Orbital Period for Critical Value of Inclination

Figure 4.7

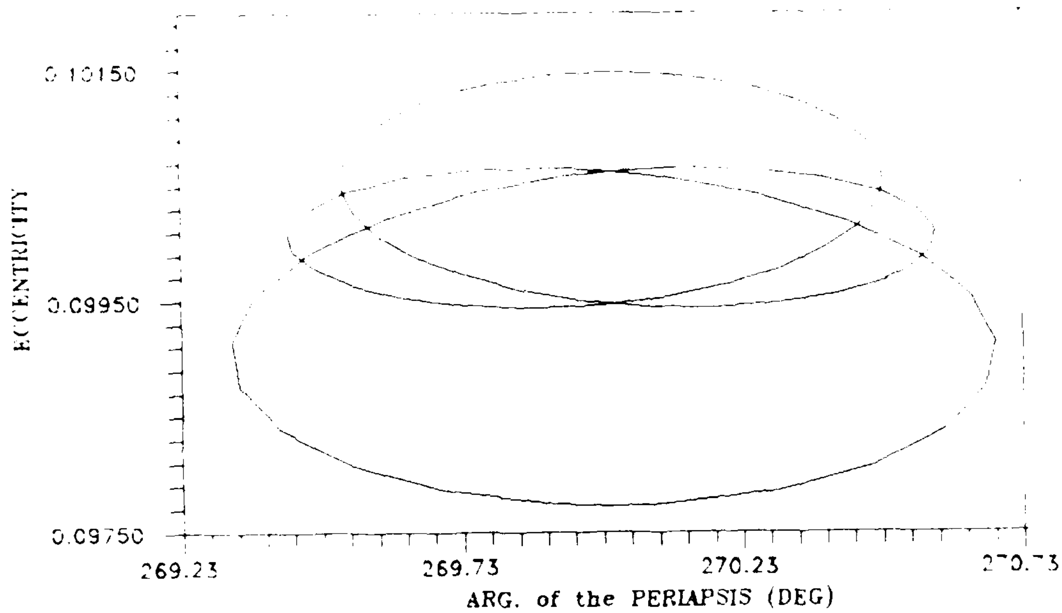

ω vs. Eccentricity Over One Orbital Period for Critical Value of i

Figure 4.8

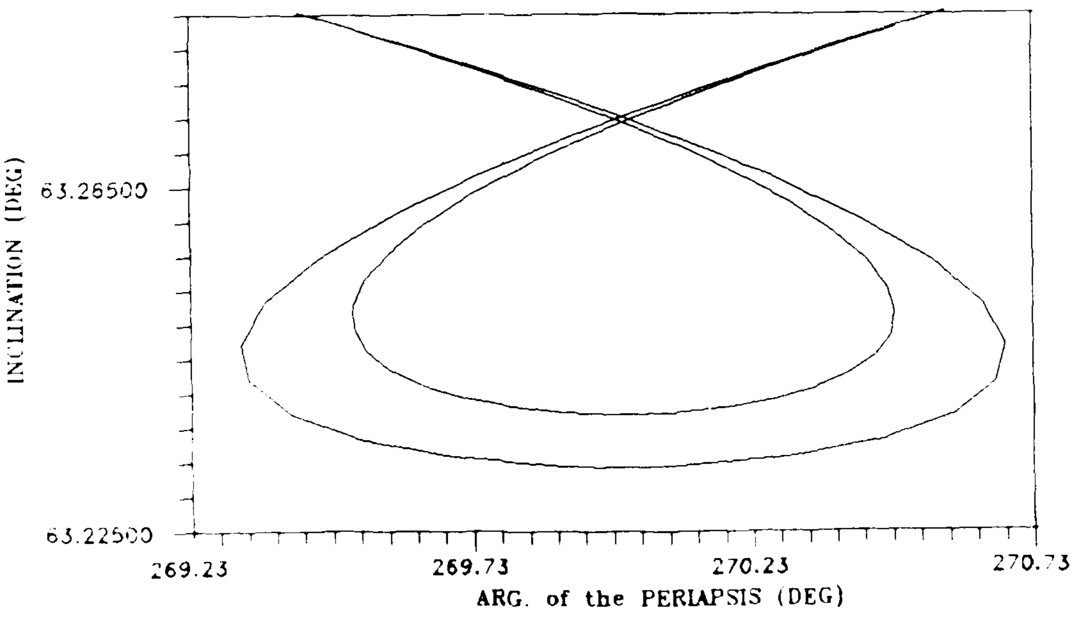

ω vs. Inclination Over One Orbital Period for Critical Value of i

Figure 4.9

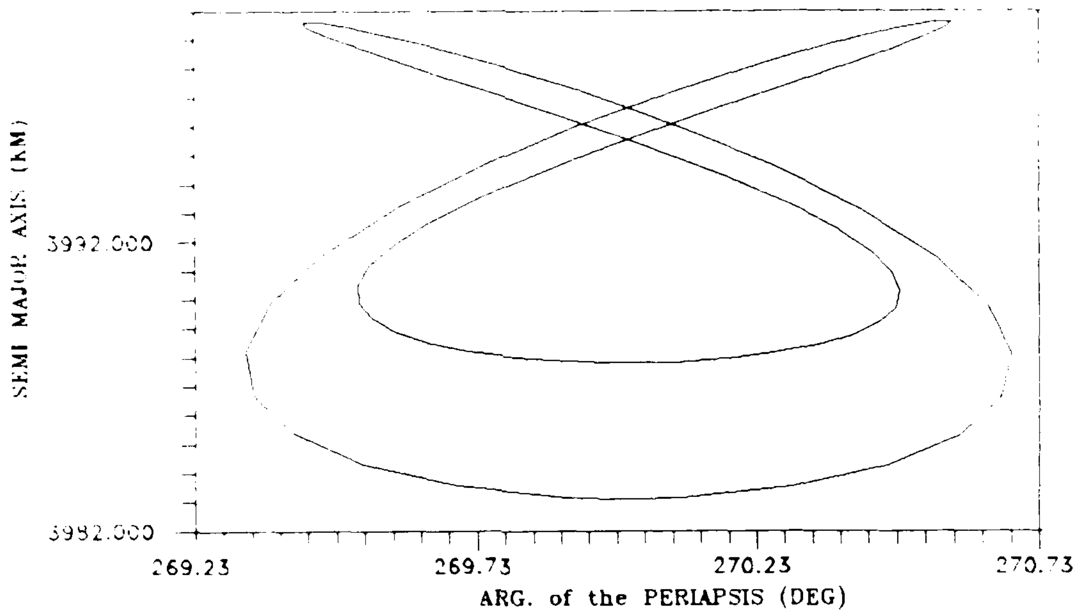

ω vs. a Over One Orbital Period for Critical Value of i

Figure 4.10

A look at the change in ω over one axial period was not made because of the extremely long axial period associated with the critical values of i (on the order of 15 years).

Atmospheric Drag. Equation (4.40) describes the change in the semi major axis due solely to atmospheric drag over one orbital period (11:41):

$$\Delta a = -a^2 \delta \int_0^{2\pi} \frac{1 + e\cos E}{1 - e\cos E} \rho \, dE \tag{4.40}$$

where

$$\delta = \frac{F S C_D}{m} \tag{4.41}$$

$$F = \left(1 - \frac{r_{p0}\,\omega}{v_{p0}} \cos i_0\right)^2 \tag{4.42}$$

$$\rho = \rho_{p0} \exp\left\{\frac{1}{H}\left(a_0 - a - ae_0\right) + \frac{1}{H}\, ae \cos E\right\} \tag{4.43}$$

Equation (4.44) describes the change in eccentricity due solely to atmospheric drag over one orbital period (11:41):

$$\frac{de}{dE} = -a\rho\delta\left(\frac{1 + e\cos E}{1 - e\cos E}\right)^{\frac{1}{2}} \left(1 - e^2\right) \cos E \tag{4.44}$$

Putting equation (4.44) into integral form yields:

$$\Delta e = -a\delta \int_0^{2\pi}\left(\frac{1 + e\cos E}{1 - e\cos E}\right)^{\frac{1}{2}} \rho\left(1 - e^2\right) \cos E \, dE \tag{4.45}$$

Equations (4.40) and (4.45) where solved using an 8th order Gaussian-Legendre quadrature method (see program Dsemi in Appendix E), and the resulting output compared to ASAP. The results showed that the above equations and ASAP give reasonably close answers.

V. Analysis

The Mars Geoscience Climatology Phasing Orbit

The Mars Geoscience Climatology Orbiter (MGCO) phasing orbit is a frozen orbit planned for the next U.S. space mission to Mars. Table 5.1 list the elements of this orbit. The Longitude of the Ascending Node (Ω) of the actual orbiter will be set by the approach asymptote, which, for the purposes of this analysis will be 90 degrees.

Orbital Elements for the MGCO Phasing Orbit (17:3)

Table 5.1

Input Orbital Elements for:	a km	e	i degrees	Ω degrees	ω degrees	ν degrees
MGCO Phasing Orbit	3747.2	0.0081	90.00	90.00	270.00	90.00

In order to determine the predominant characteristics of a frozen orbit the above elements were inputted into ASAP, propagated for one and three orbital periods, and for one axial period using both a 6 X 0 and a 6 X 6 gravity field (with and without atmospheric drag). The axial period was estimated by using:

$$\frac{d\omega}{dt} \cong \frac{3}{2}\frac{J_2 R_p^2}{\left[a\left(1-e^2\right)\right]^2}\left(2-\frac{5}{2}\sin^2 i\right)\sqrt{\frac{\mu}{a^3}} \tag{5.1}$$

Equation (5.1) was derived from the Lagrange Planetary Equations using only the second zonal harmonic of equation (2.91). Analysis on the output revealed that over one orbital period the atmospheric drag has no appreciable effect. However, for a 6 X 0 gravity field the decrease in the semi major axis over one axial period is 0.5 meters more when drag is present than when absent. For a 6 X 6 gravity field, atmospheric drag causes the semi major axis to decrease by 0.1 meters more than the presence of a 6 X 6 gravity field alone.

Figures 5.1 through 5.3 show the effects due to atmospheric drag and a 6 X 0 gravity field, while Figures 5.4 through 5.6 show the effects due to atmospheric drag and a 6 X 6 gravity field. Figures 5.1 and 5.2 are closed curves, asserting that the values of the argument of the periapsis, the eccentricity, and the semi major axis are bounded. In examining Figure 5.3, it should be remembered that the inclination does not change over one orbital period for polar orbits (see equations (4.19) through (4.25)); therefore, Figure 5.3 shows that the values of the argument of the periapsis and the angle of inclination are also bounded. This bounded condition implies that the values of the argument of the periapsis, the eccentricity, the semi major axis, and the inclination are periodic over one orbit. This situation changes when a 6 X 6 gravity field is introduced. Figure 5.4 reveals that the initial value and the final value of both the argument of the periapsis and the eccentricity are not the same. Over one orbital period the argument of the periapsis changes from ω = 275.67128 degrees to ω = 276.55445 degrees, a change of approximately .32 percent over the initial value. The eccentricity changes from e = .00810551 to e = .00806312, representing a change of .5 percent over the initial value. Figure 5.5 reveals that the the semi major axis changes from a = 3756.23351 km to a = 3756.16521 km, giving a change of approximately .00182 percent. Although Figure 5.6 shows no discernible difference from Figure 5.3, an analysis of the data shows that there is a 0.04756 degree change in inclination over one orbital period when in a 6 X 6 gravity field. These changes in the orbital parameters indicate that the above orbital parameters are not periodic over one orbital period when in the presence of a 6 X 6 gravity field. To test these conclusions, the MGCO phasing orbit was propagated over three orbital periods for a 6 X 0 gravity field and a 6 X 6 gravity field, both with drag. For a 6 X 0 gravity field, Figures 5.7 through 5.9 show that the orbit continues to exhibit the same periodic behavior in the argument of the periapsis, the eccentricity, the semi major axis, and the inclination over three orbital periods as was established in the first orbit. This confirms the predictions made from Figures 5.1 through 5.3.

The values for the argument of the periapsis, the eccentricity, the semi major axis, and the inclination for a 6 X 6 gravity field over three orbital periods are shown in Figures 5.10 through 5.12. As predicted, the values in these graphs are not periodic over one orbital period.

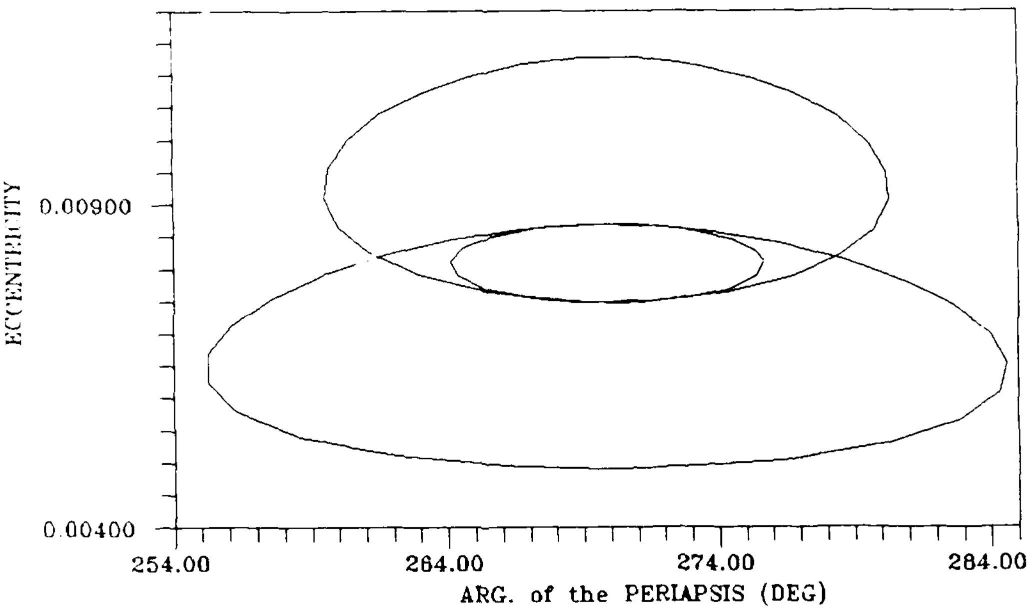

ω vs. e, One Orbital Period, MGCO Orbit, 6X0 Gravity Field, with Drag

Figure 5.1

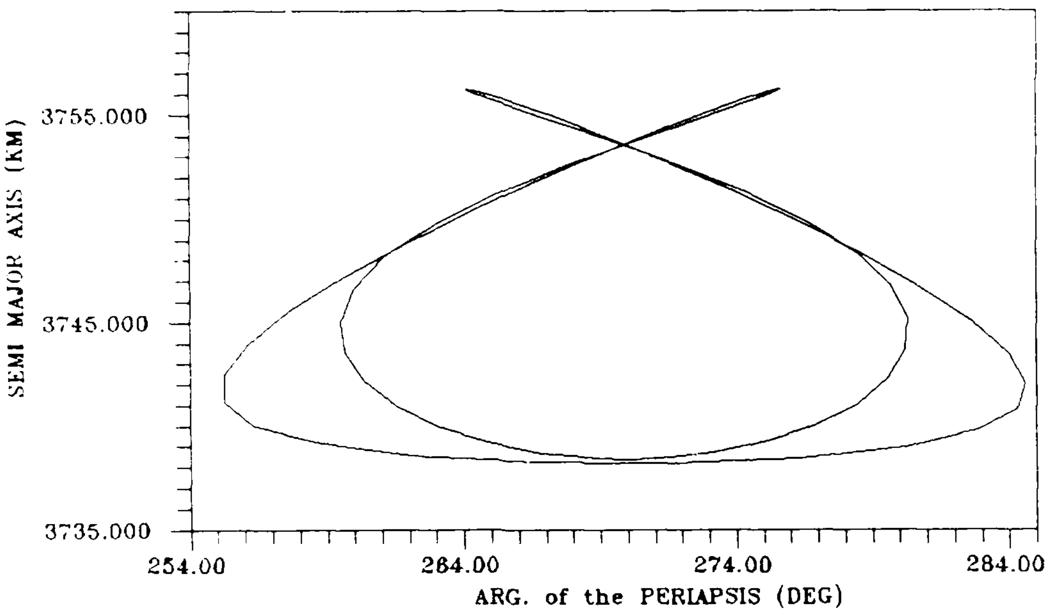

ω vs. a, One Orbital Period, MGCO Orbit, 6X0 Gravity Field, with Drag

Figure 5.2

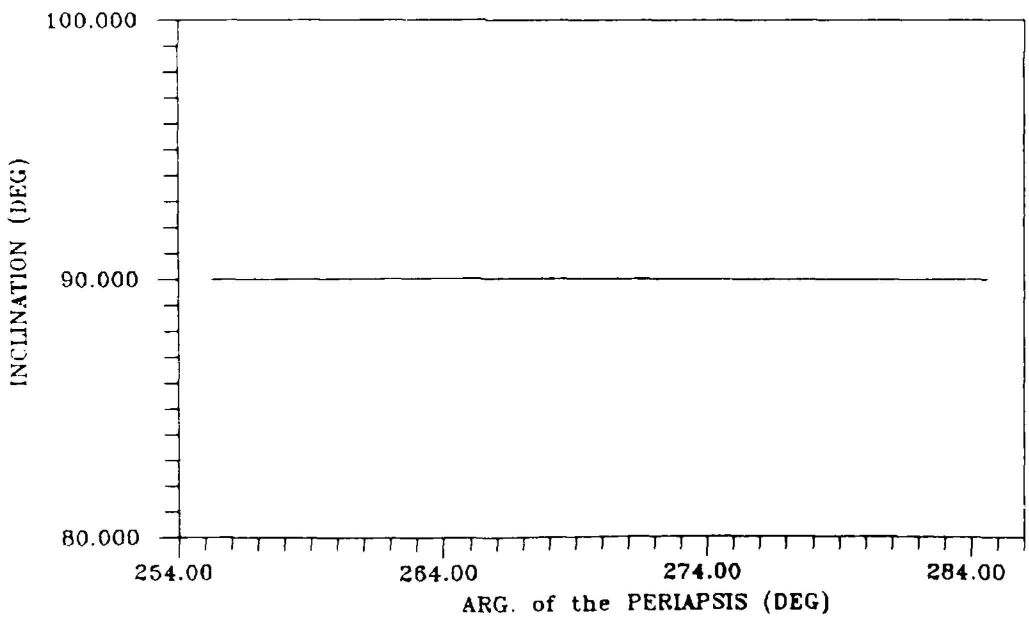

ω vs. i, One Orbital Period, MGCO Orbit, 6X0 Gravity Field, with Drag

Figure 5.3

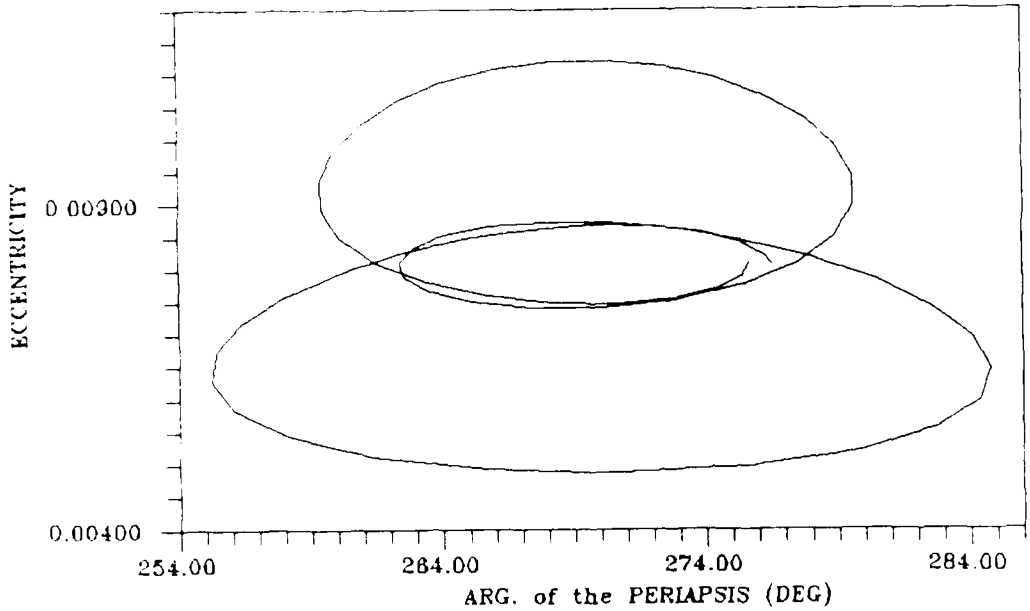

ω vs. e, One Orbital Period, MGCO Orbit, 6X6 Gravity Field, with Drag

Figure 5.4

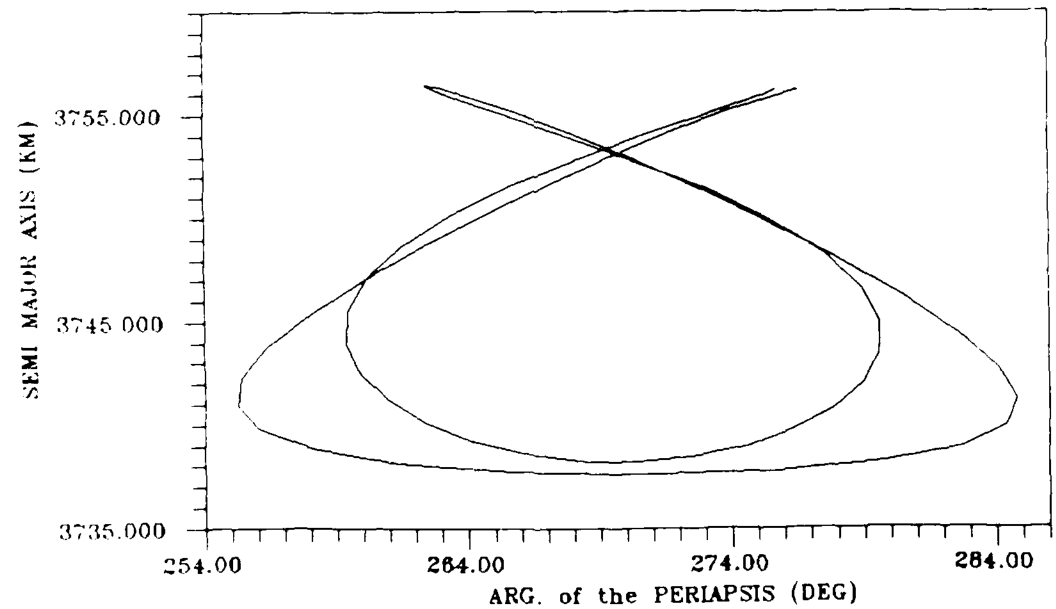

ω vs. a, One Orbital Period, MGCO Orbit, 6X6 Gravity Field, with Drag

Figure 5.5

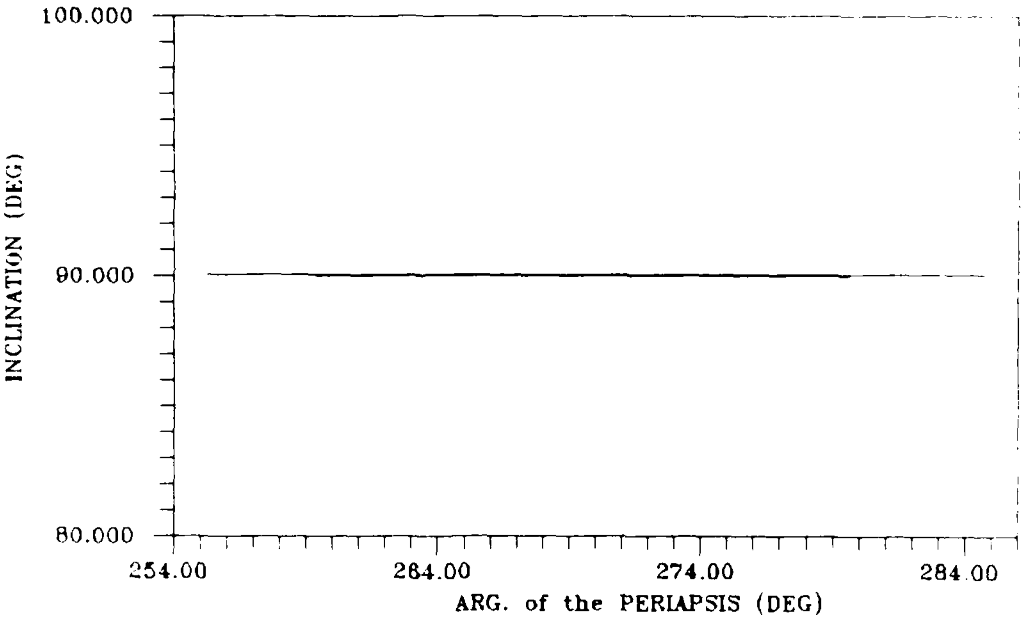

ω vs. i, One Orbital Period, MGCO Orbit, 6X6 Gravity Field, with Drag

Figure 5.6

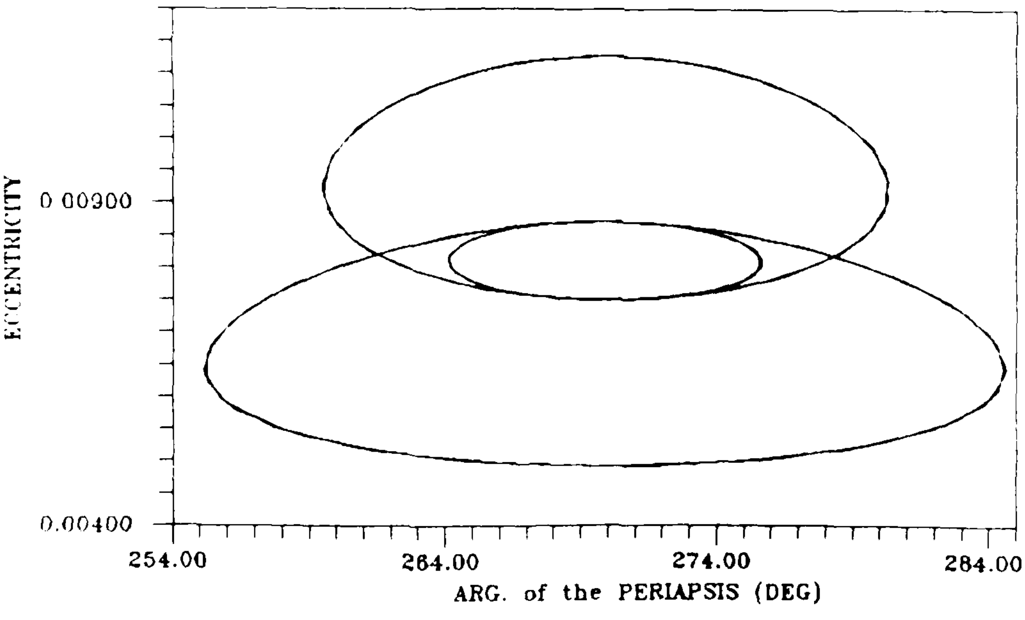

ω vs. e, Three Orbital Periods, MGCO Orbit, 6X0 Gravity Field, with Drag

Figure 5.7

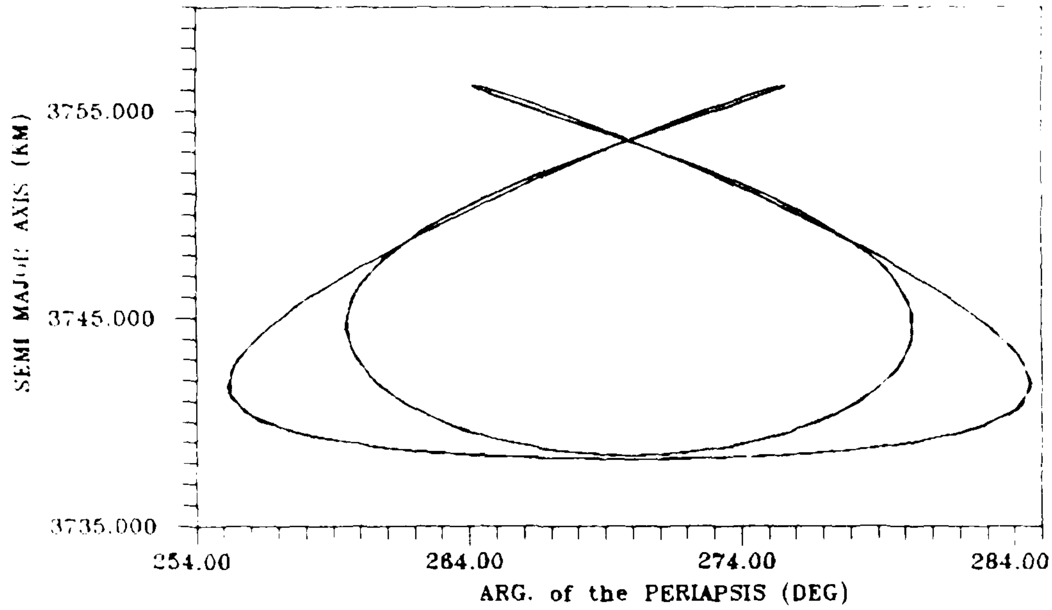

[illegible] vs. [illegible], Three Orbital Periods, MGCO Orbit, 6X0 Gravity Field, with Drag

Figure 5.8

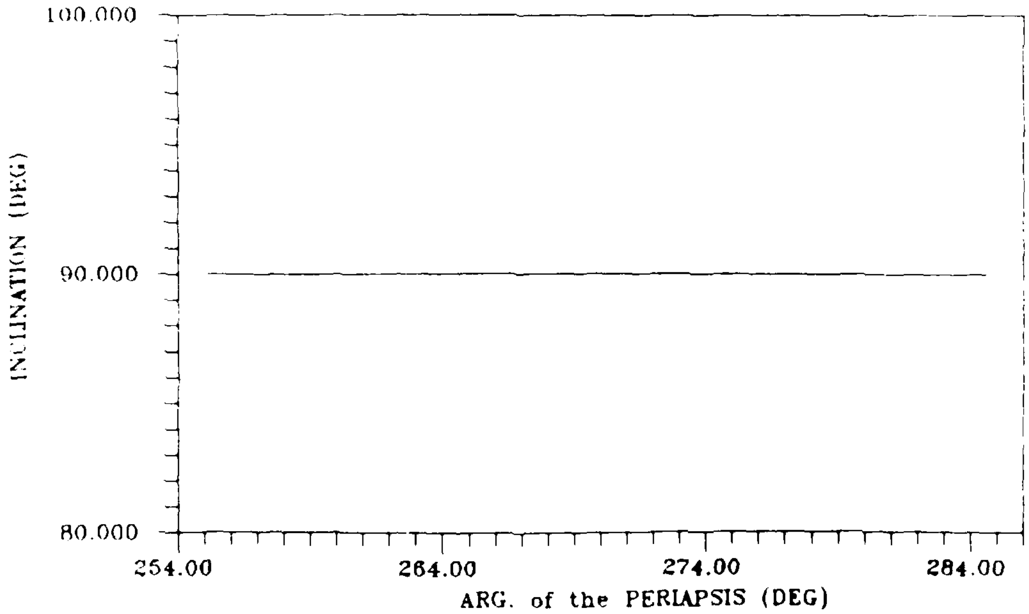

[illegible] vs. [illegible], Three Orbital Periods, MGCO Orbit, 6X0 Gravity Field, with Drag

Figure 5.9

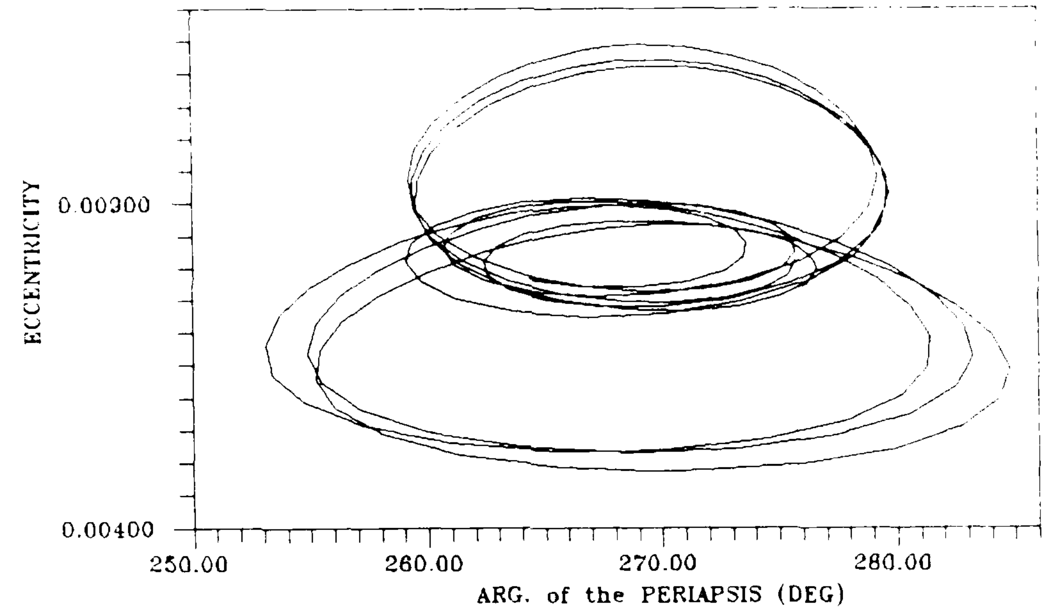

ω vs. e, Three Orbital Periods, MGCO Orbit, 6X6 Gravity Field, with Drag

Figure 5.10

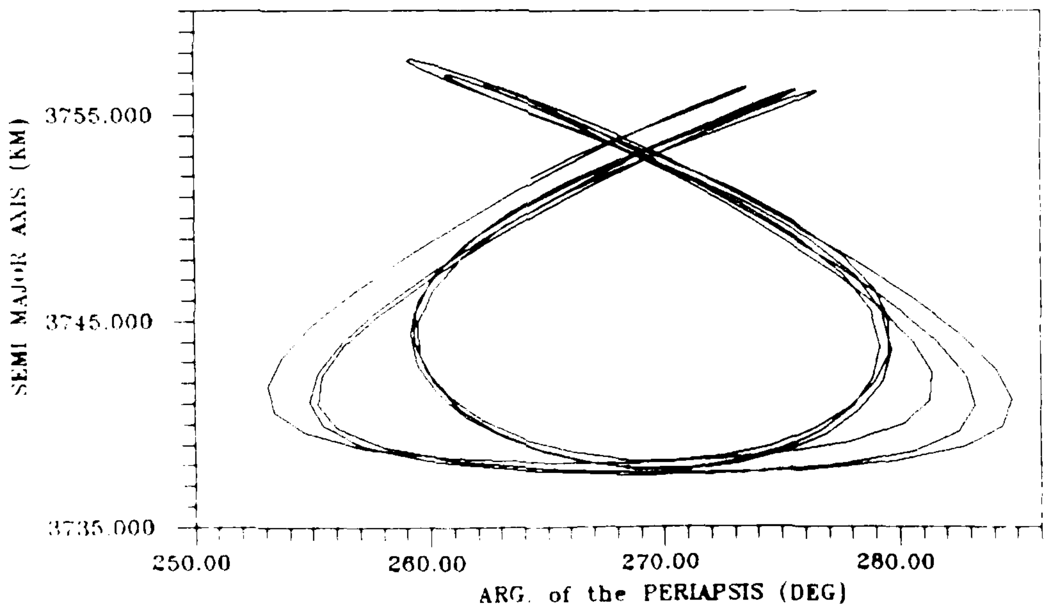

ω vs. a, Three Orbital Periods, MGCO Orbit, 6X6 Gravity Field, with Drag

Figure 5.11

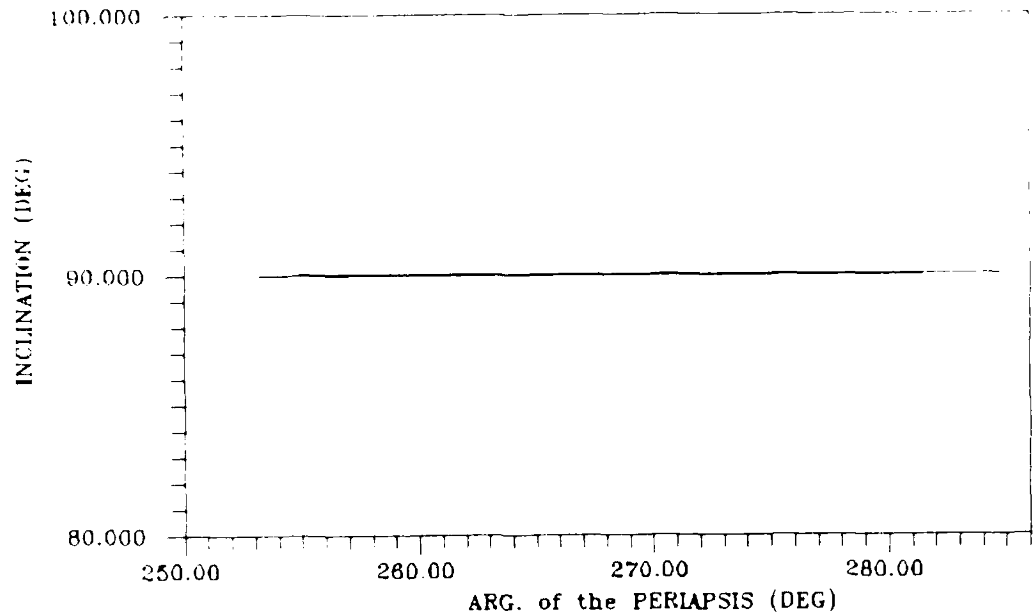

i vs. ω, Three Orbital Periods, MGCO Orbit, 6X6 Gravity Field, with Drag

Figure 5.12

In the next step of this analysis, the phasing orbit was propagated over one axial period. Figure 5.13 shows the effect of a 6 X 0 gravity field, with drag. The figure indicates that the values of the argument of the periapsis, and the eccentricity are not quite periodic over the axial period, which is not correct. The axial period was estimated from Equation (5.1), which does not take into account zonal harmonics greater than two, nor any of the sectoral harmonics; therefore, it does not return the exact axial period. If the input axial period were exact then, Figure 5.13 would be closed. The stair step appearance of Figure 5.13 is due to the inputted computer step size -- the curve is actually smooth.

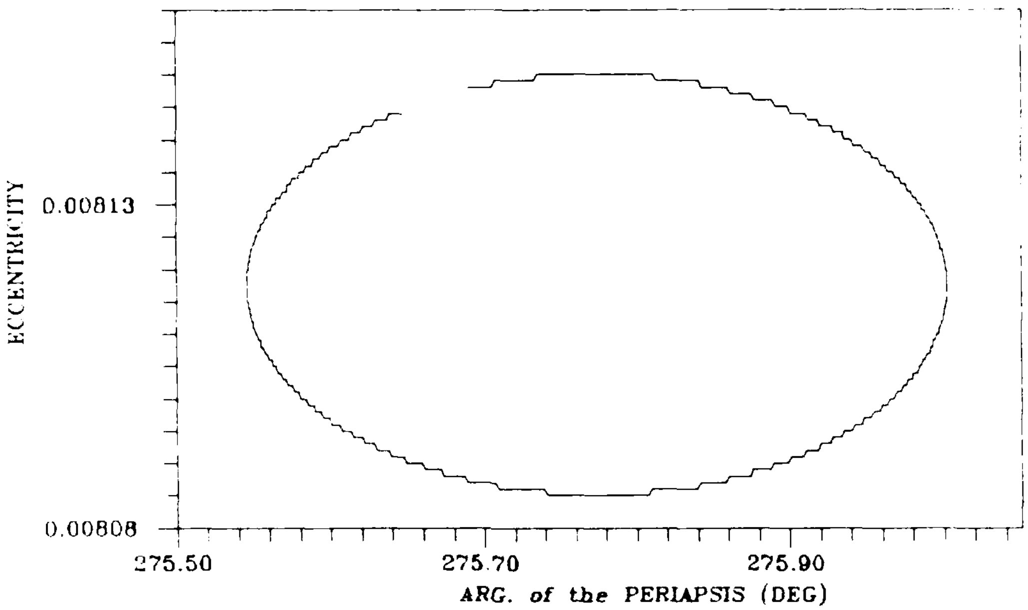

ω vs. e, One Axial Period, MGCO Orbit, 6X0 Gravity Field, with Drag

Figure 5.13

The results of the phasing orbit propagated over one axial period for a 6 X 6 gravity field, with drag, are shown in Figure 5.14. Due to the large amount of data points generated for the 6 X 6 gravity field, data at every 20th ascending nodal passage was plotted; therefore, the appearance of the graph is very erratic. If data were not taken at every 20th ascending nodal passage, but at an interval consistent with Figure 5.13, then Figure 5.14 would appear as a dark mass making analysis difficult. The importance of Figure 5.14 is not in its erratic shape, but like Figure 5.13, the argument of periapsis and the eccentricity both are bounded.

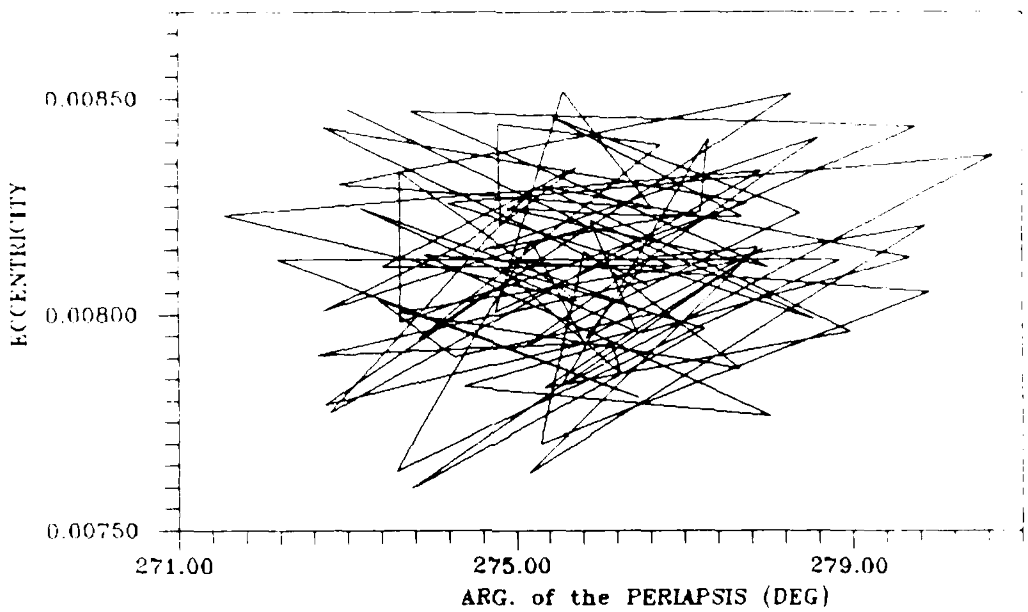

ω vs. e, One Axial Period, MGCO Orbit, 6X6 Gravity Field, with Drag

Figure 5.14

The MGCO phasing orbit was analyzed to gain an understanding of the nature of frozen orbits. As defined in Chapter 1, this thesis considers a frozen orbit as any orbit in which the time rate of change of one or more of the orbital elements is approximately zero, or nonsecular. For example, the above orbit (in a 6 X 6 gravity field) does not possess a single orbital element whose time rate of change is zero; however, the argument of the periapsis oscillates about its original position, and hence, the phasing orbit is considered frozen. Further analysis will be carried out to determine if other frozen, or stable orbits exist other than that class of polar orbits with the periapsis located over the poles. Further, are there orbits whose time rate of change of one or more orbital elements equals zero? If so, where are these orbits and what are their advantages?

Semi Major Axis Equal to 4393.4 Kilometers

Initially, a value of the semi major axis of 4393.4 km and an eccentricity of .1 was chosen. These values establish a periapsis altitude of approximately 560 km. The first goal is to freeze one of the orbital elements, ω, e, i, or Ω when in a 6 X 6 gravity field. For the MGCO phasing orbit, the argument of the periapsis, and the eccentricity showed the greatest rate of change over one orbital period; therefore, these two elements will be the focus of this step.

With the values of the semi major axis and the eccentricity established, the program Omega (see Chapter IV and Appendix E) was run in order to determine the value of the critical inclination angle [that value of inclination that "freezes" ω over one orbital period] for the case of a 6 X 0 gravity field. With this value of i as a baseline, a 6 X 6 gravity field was introduced and numerous runs of ASAP were made in order to find a critical inclination value of 68.15285662 degrees. This critical inclination, along with the other orbital elements inputted into ASAP define Reference Orbit #1. Reference Orbit #1's input is listed in Table 5.2.

Orbital Elements for Reference Orbit #1

Table 5.2

Input Orbital Elements for:	a km	e	i degrees	Ω degrees	ω degrees	ν degrees
Ref Orbit #1	4393.4	.1	68.15285662	90.00	270.00	90.00

Figures 5.15 through 5.17 indicate that the change in ω for this orbit is indeed zero, while the change in e, and i is not equal to zero. Further, Figure 5.16 indicates that the change in the semi major axis vs. the change in the argument of periapsis is bounded. Figure 5.18 shows Reference Orbit #1 propagated over a 255 day period. Although 255 days is only a fraction of this orbit's axial period (the axial period is on the order of 15 years), it is sufficient to see that the effect of the change in eccentricity and inclination causes the argument of the periapsis to change by approximately 260 degrees. This does not compare favorably with the MGCO phasing orbit.

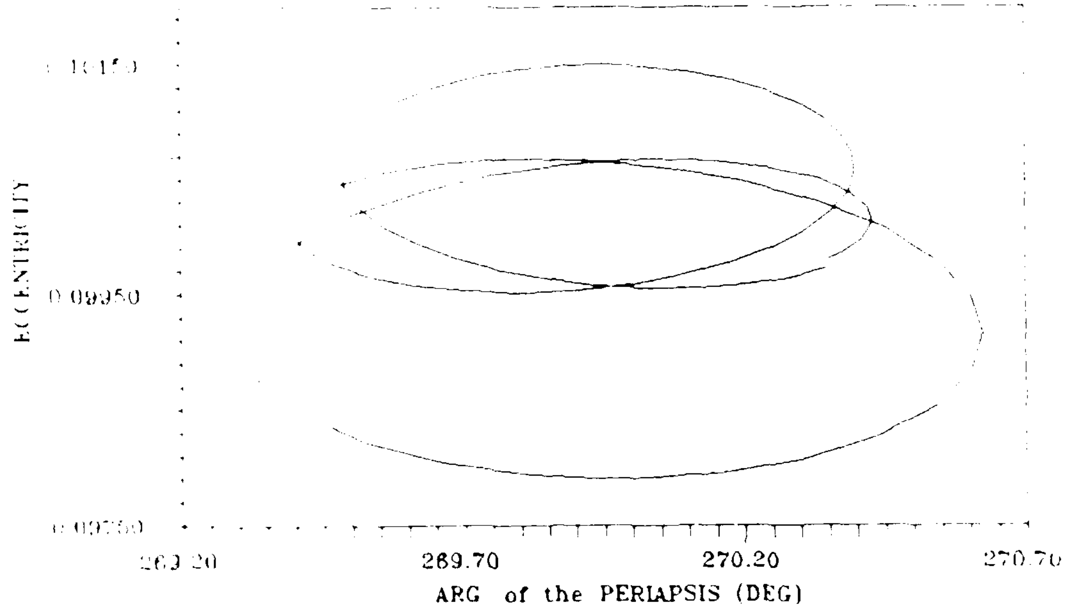

Arg. of the Periapsis vs. Eccentricity, Ref. Orbit #1, One Orbital Period, 6 X 6 Gravity Field

Figure 5.15

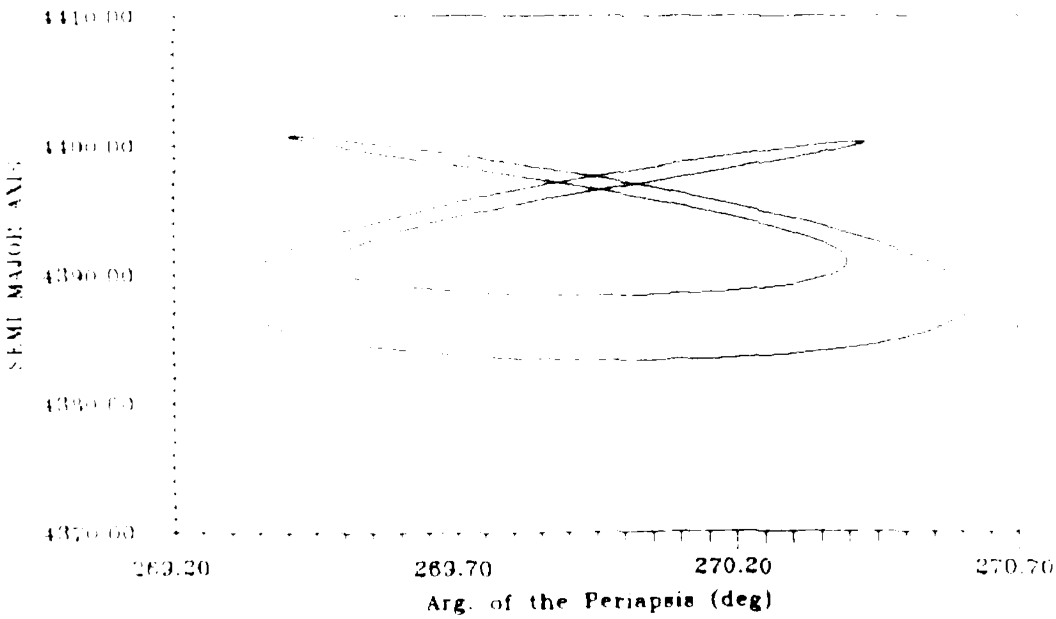

Arg. of the Periapsis vs. a, Ref. Orbit #1, One Orbital Period, 6 X 6 Gravity Field

Figure 5.16

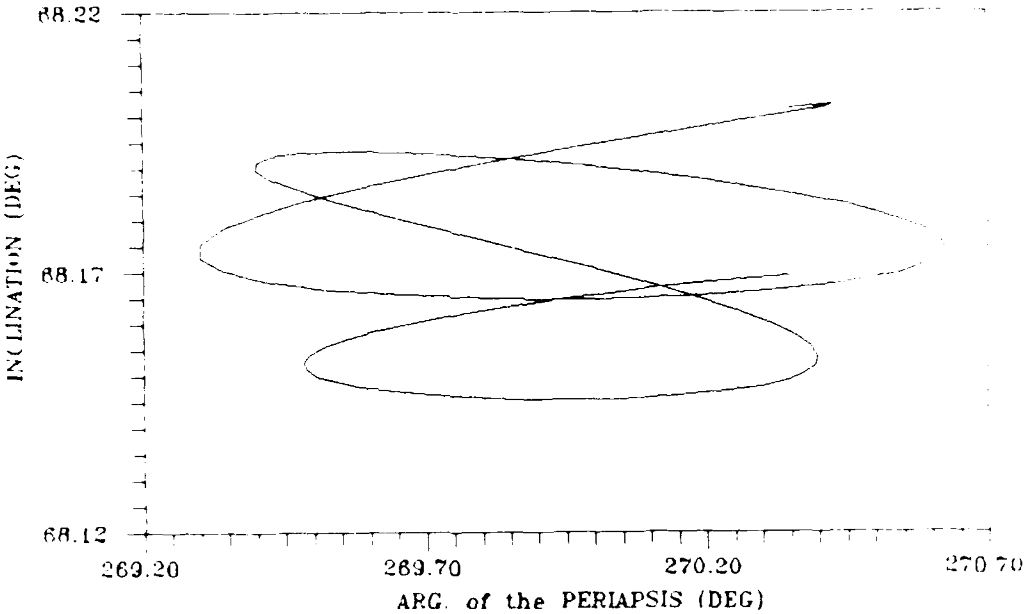

Arg. of the Periapsis vs. Inclination, Ref. Orbit #1, One Orbital Period, 6 X 6 Gravity Field

Figure 5.17

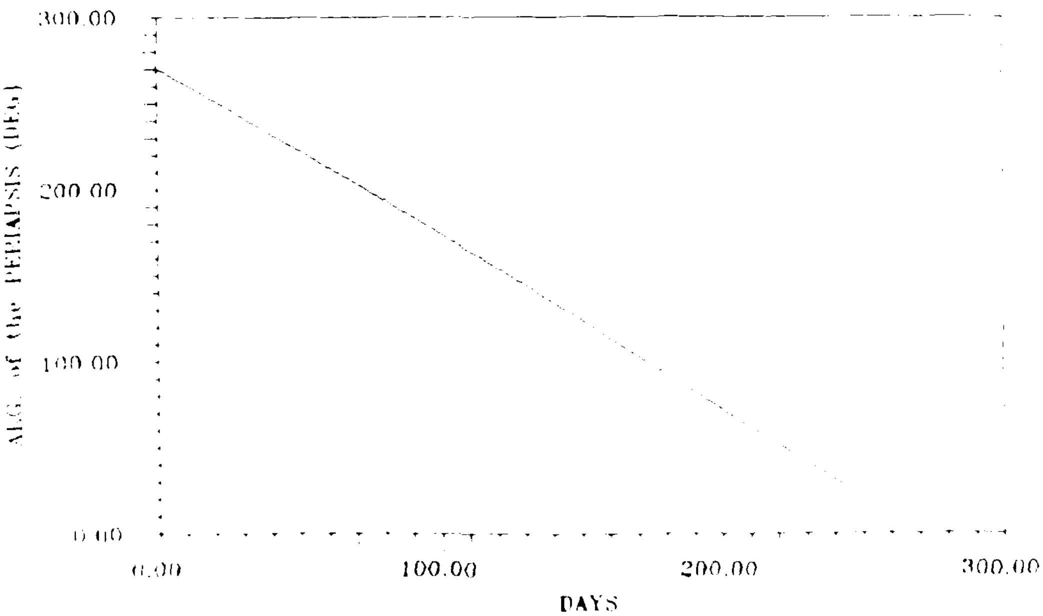

Change in Arg. of the Periapsis Over 255 Days, Ref Orbit #1, 6 X 6 Gravity Field

Figure 5.18

The above figures reveal that the unbounded nature of eccentricity and inclination adversely effect the change in the argument of the periapsis. The analysis indicates the periapsis does not oscillate about a particular point (as in the case of the MGCO phasing orbit), but instead, is unbounded. A search for a input value of the eccentricity which causes the change of the eccentricity and the inclination to be zero over one orbital period was made for values of eccentricity from .01 to 0.7. Figures 5.19 and 5.20 show the results of this search and reveals, for Reference Orbit #1, a value of eccentricity which drives the change in eccentricity and inclination (over one orbital period) to zero does not exist. Note, any eccentricity greater than approximately .227 will cause impact with the planet's surface.

Figure 5.21 reflects the effects of various eccentricities and inclinations upon the change in eccentricity. Since circular orbits facilitate the use of scientific instruments designed to observe the surface of Mars, it is desirable to keep the value of the eccentricity to a minimum. Also, in order to minimize the effects of atmospheric drag a minimum periapsis altitude of 200 km is imposed. Given Figure 5.21 and the above restrictions, analysis revealed that an eccentricity of 0.3 and a semi major axis of 5133.428571 km offers the best compromise between the desire to keep eccentricity to a minimum, and the need for an eccentricity which drives the change in eccentricity over one orbital period to zero.

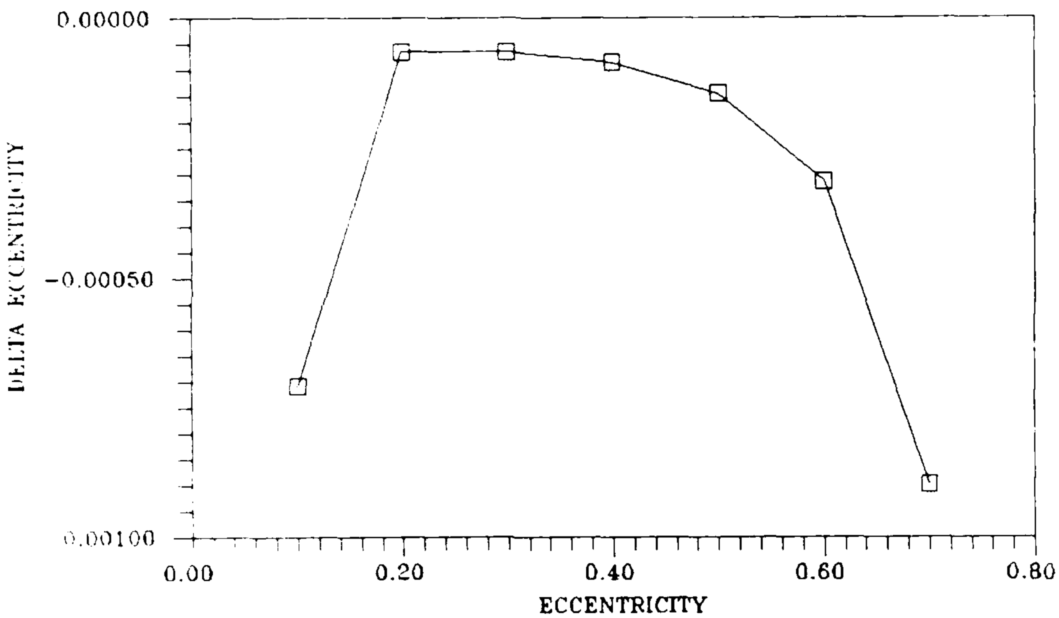

. vs. the Change in e, One Orbital Period, Ref. Orbit #1, 6 X 6 Gravity Field

Figure 5.19

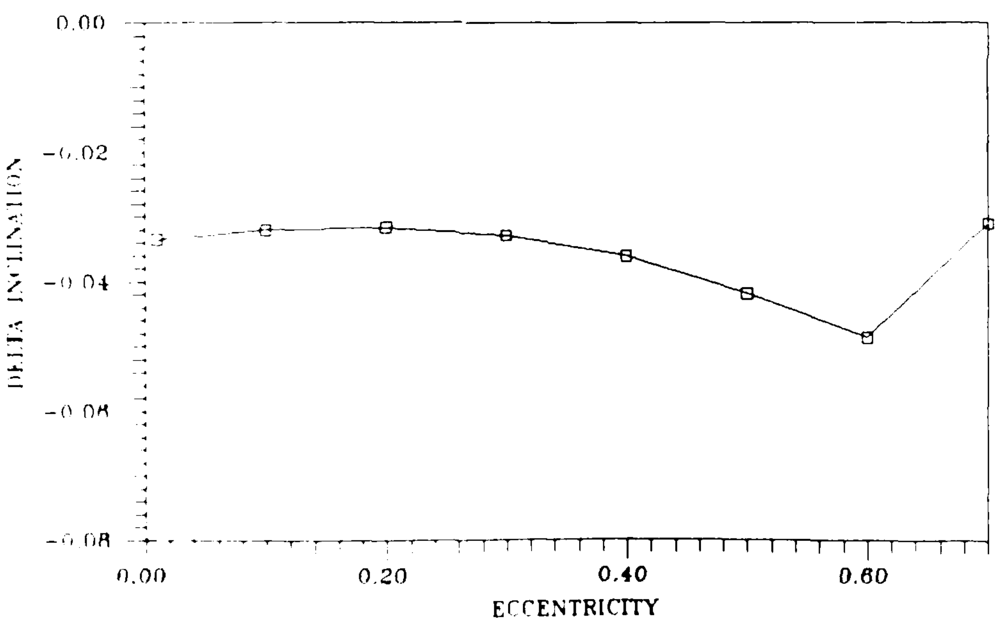

. vs. the Change in i, One Orbital Period, Ref. Orbit #1, 6 X 6 Gravity Field

Figure 5.20

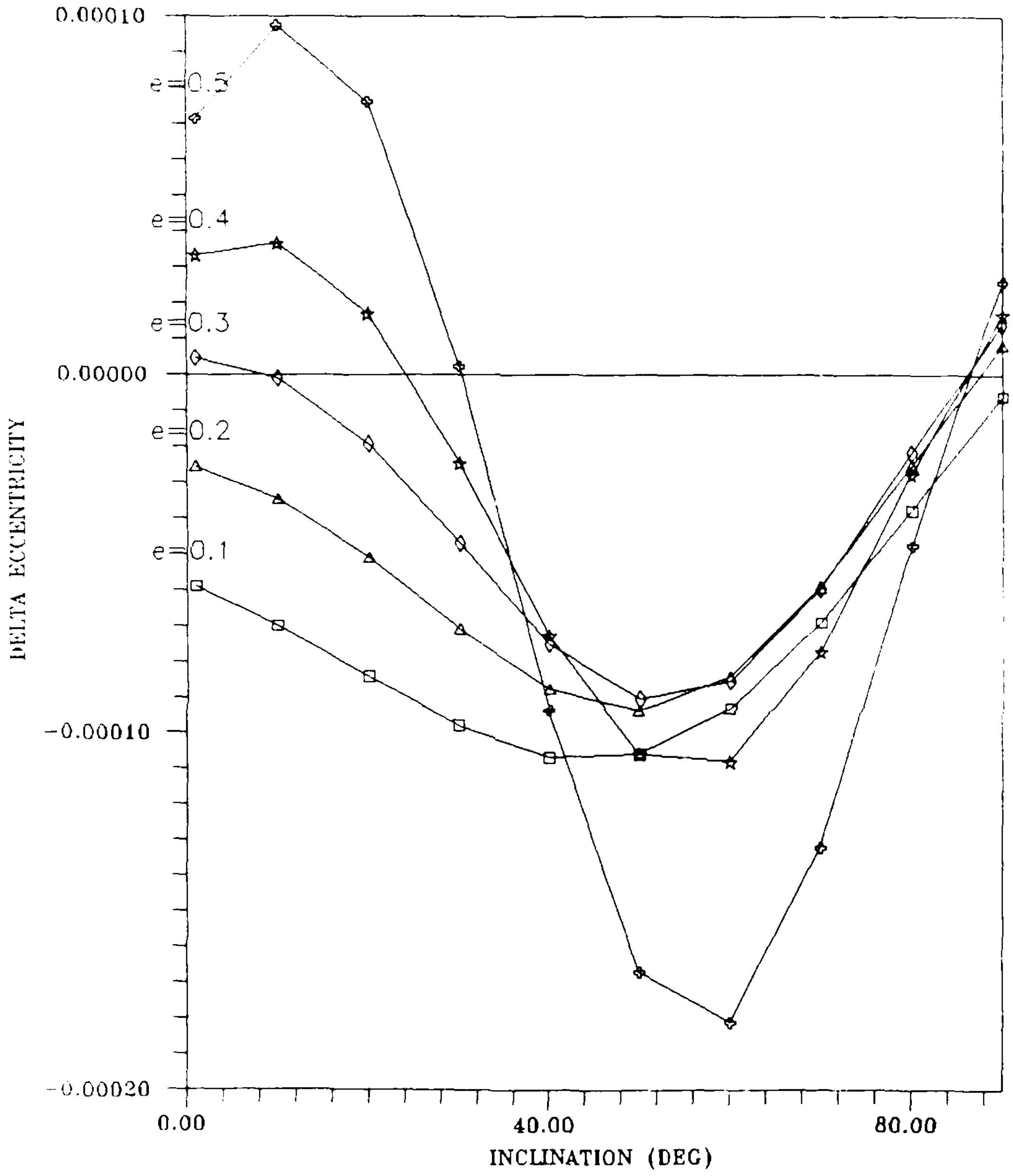

Inclination vs Change in Eccentricity, One Orbital Period, Ref. Orbit #1, 6 X 6 Gravity Field

Figure 5.21

Semi Major Axis Equal to 5133.428571 Kilometers

With the value of the semi major axis established at 5133.428571 km, the value of the eccentricity was swept from e = 0.01 to e = 0.3 for values of inclination ranging from 1 to 90 degrees (see Figures 5.22 and 5.23).

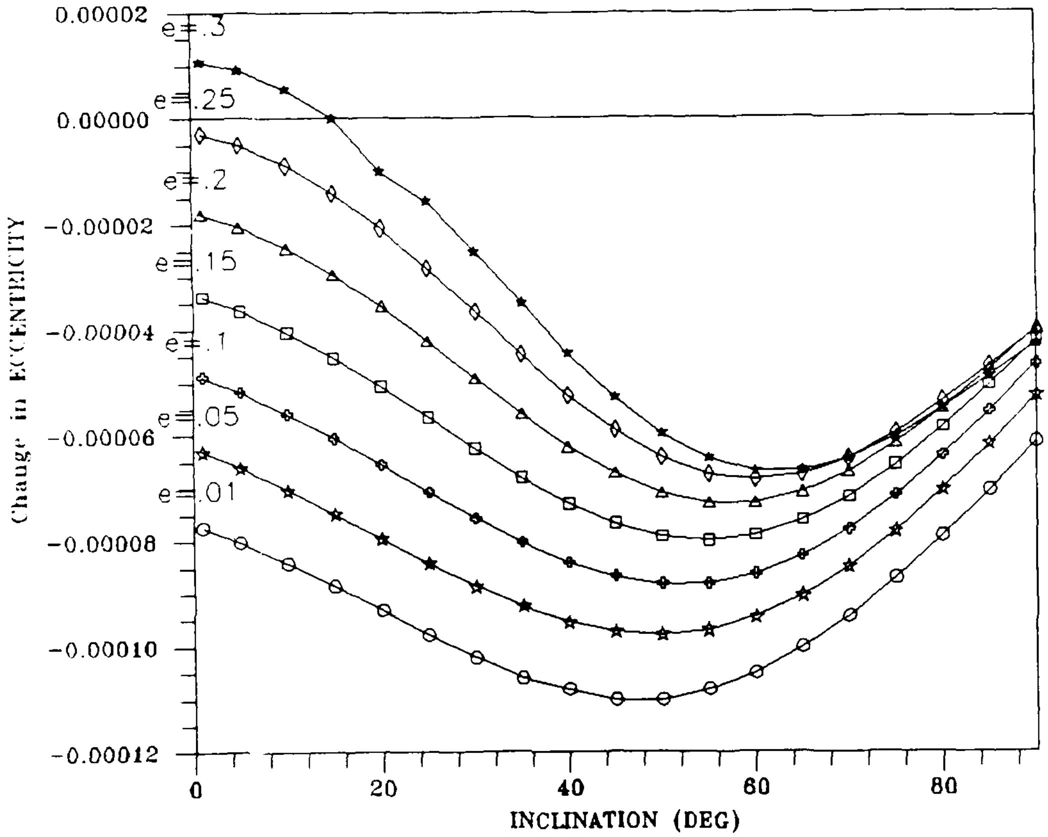

Inclination vs. Change in Eccentricity, One Orbital Period, Ref. Orbit #2, 6 X 6 Gravity Field

Figure 5.22

The above graph shows the effects of various values of eccentricity and inclination on the change in eccentricity over one orbital period. From this graph was determined an inclination angle of 15.05252881 degrees that will cause the change in eccentricity to equal zero over one orbital period. These orbital parameters, along with the other associated input parameters define Reference Orbit #2, and are listed in Table 5.3.

In Figure 5.23 the effect of eccentricity on the change in the argument of the periapsis over one orbital period is investigated. Three important findings stand out. First, there appears to be values of eccentricity near zero such that no matter what the angle of inclination, the change in the argument of the periapsis over one orbital period will never equal zero. Second, there exist values of eccentricity and inclination (from e = 0.03586336 at ι = 90 degrees to e = 0.3 at ι = 65.91286827 degrees) which cause the change in the argument of the periapsis to equal zero over one orbital period. Third, as the eccentricity increases (at least from 0.03586336 to 0.3) the resulting critical inclination angle decreases.

The value of the angle of inclination which causes the change in the argument of the periapsis to equal zero over one orbital period when eccentricity is equal to 0.3, together with the other orbital inputs, defines Reference Orbit #3. The input values for Reference Orbit #3 are listed in Table 5.3

Orbital Elements for Reference Orbits #2 and #3

Table 5.3

Input Orbital Elements for:	a km	e	ι degrees	Ω degrees	ω degrees	M degrees
Ref Orbit #2	5133.428571	.3	15.05252881	90.00	270.00	90.00
Ref Orbit #3	5133.428571	.3	65.91286827	90.00	270.00	90.00

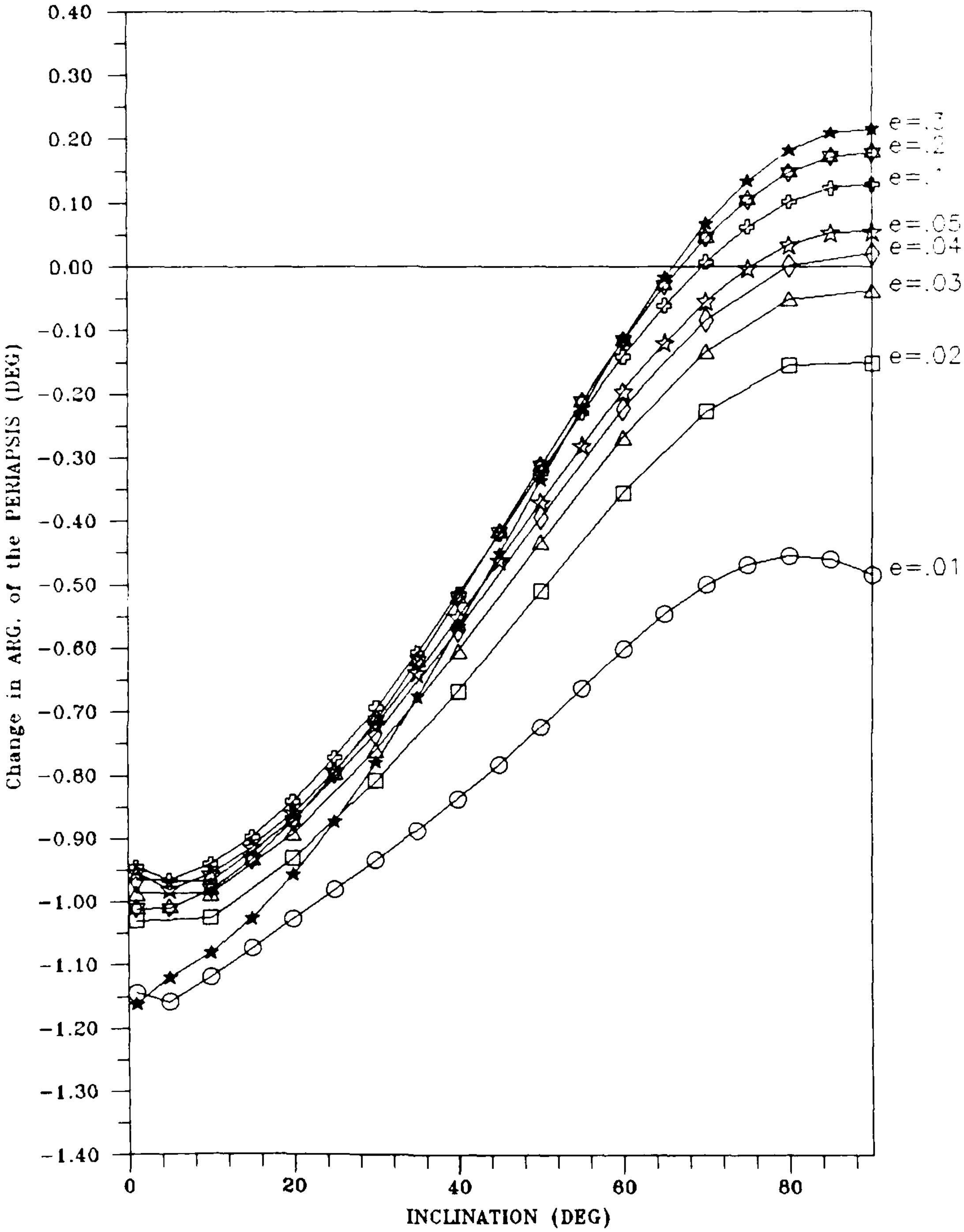

Inclination vs. Change in Arg. of the Periapsis, One Orbital Period, Ref. Orbit #2, 6 X 6 Gravity Field

Figure 5.23

Table 5.4 list the input orbital elements that causes the change in the argument of the periapsis to equal zero over one orbital period when the inclination equals 90 degrees. This orbit is known as Reference Orbit #4.

Orbital Elements for Reference Orbit #4

Table 5.4

Input Orbital Elements for:	a km	e	i degrees	Ω degrees	ω degrees	ν degrees
Ref Orbit #4	5133.428571	.03586336	90.00	90.00	270.00	90.00

Figures 5.24 through 5.26 show Reference Orbit #2 over one orbital period. From these three graphs it can be seen that only the change in eccentricity over one orbital period is zero. Propagating Reference Orbit #2 for 90 days reveals that the argument of the periapsis changes by 720 degrees during this time period (see Figure 5.27).

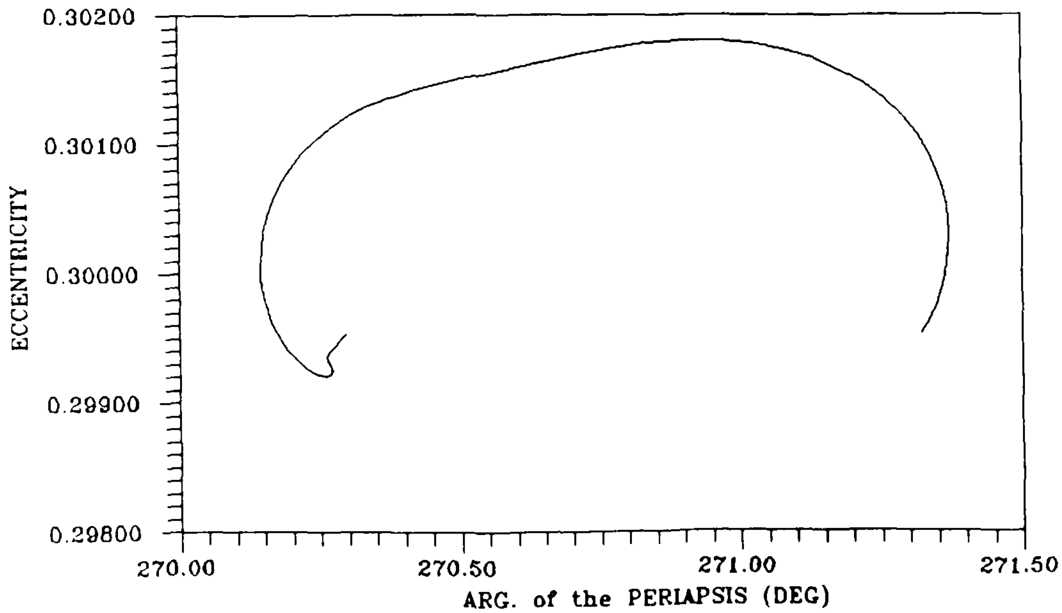

ω vs. e, Ref. Orbit #2, One Orbital Period, 6X6 Gravity Field

Figure 5.24

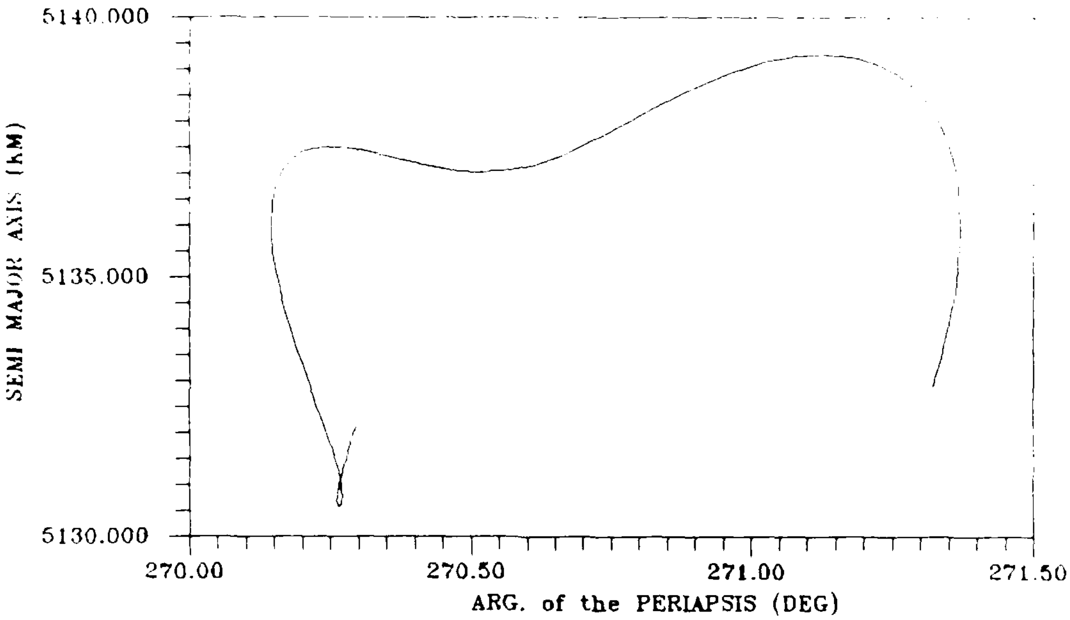

ω vs. a, Ref. Orbit #2, One Orbital Period, 6X6 Gravity Field

Figure 5.25

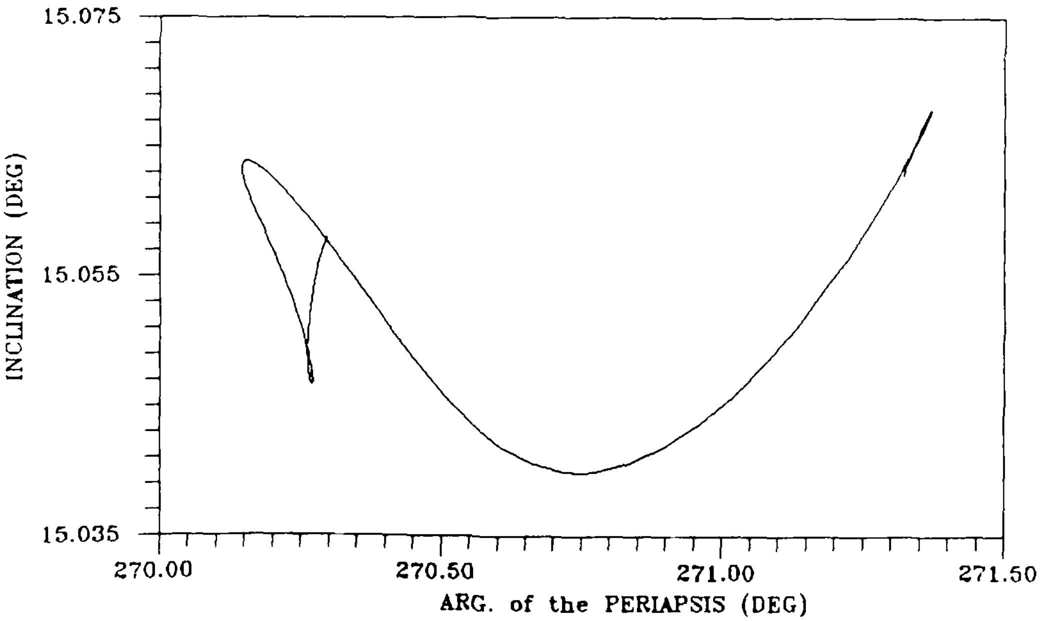

ω vs. i, Ref. Orbit #2, One Orbital Period, 6X6 Gravity Field

Figure 5.26

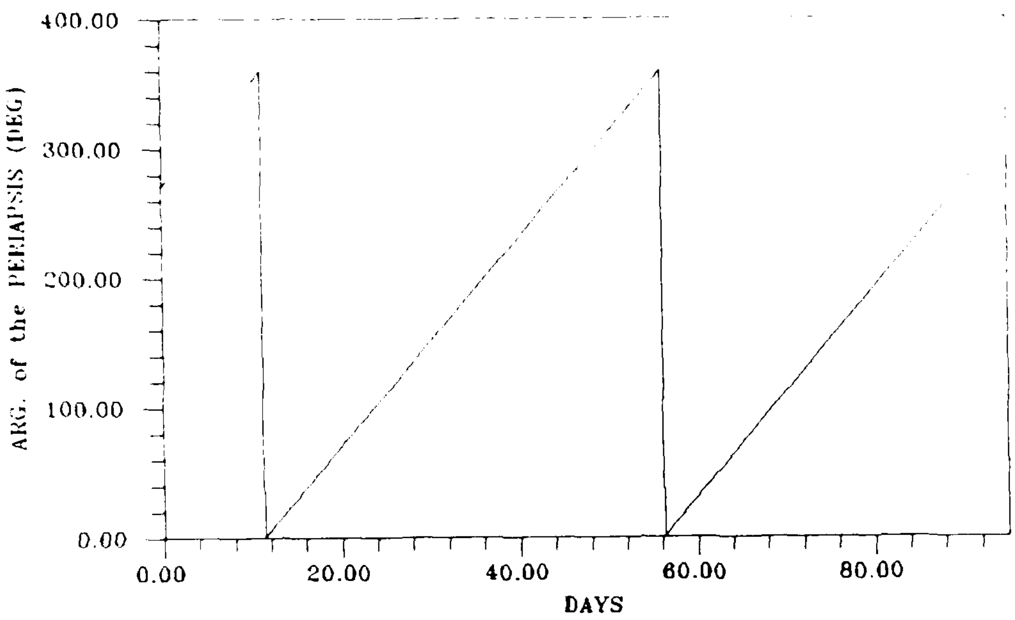

Days vs. ω, Ref. Orbit #2, 6X6 Gravity Field

Figure 5.27

Figures 5.28 through 5.30 show Reference Orbit #3 over one orbital period. Figure 5.31 shows Reference Orbit #3 propagated over 90 days. Here the change in the argument of the periapsis over a 90 day period is only 34 degrees.

Comparing Reference Orbits #2 and #3 shows that the change in the argument of the periapsis and the semi major axis are significantly larger for Reference Orbit #2. The change in the argument of periapsis for Reference Orbit #2 is approximately 1.5 degrees, while the change for Reference Orbit #3 is zero. Likewise, the change in the semi major axis for Reference Orbit #2 is approximately 0.5 kilometers, compared to approximately zero change for Reference Orbit #3. The situation reverses when looking at the eccentricity and the inclination. The change in eccentricity over one orbital period for Reference Orbit #2 is equal to zero, while the change in eccentricity for Reference Orbit #3 is approximately 0.00005. For inclination, Reference Orbit #3 experiences a change that is approximately 10 times greater than that of Reference Orbit #2.

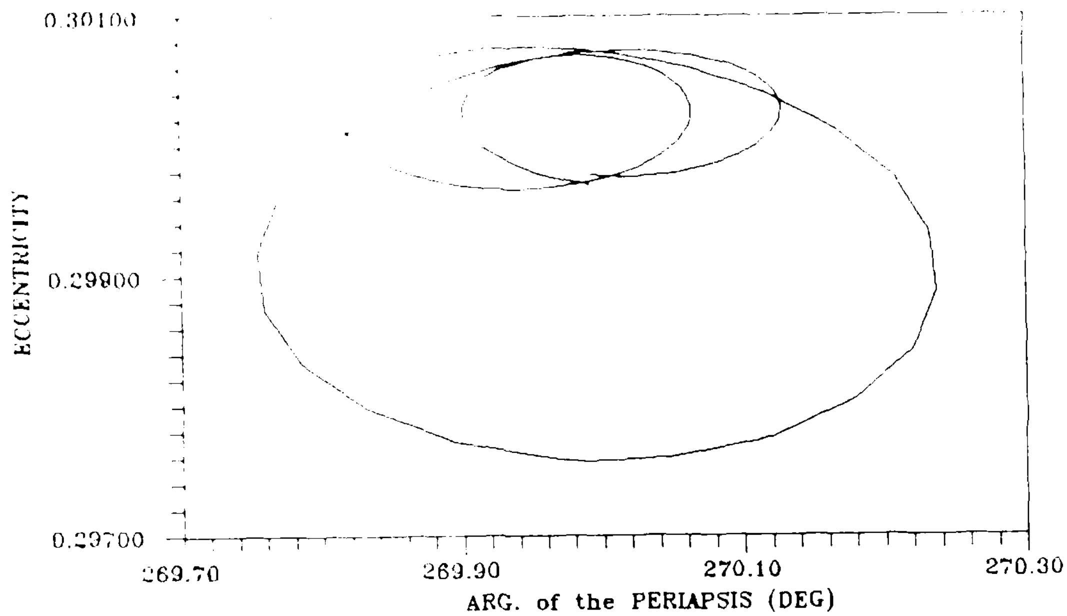

ω vs. e, Ref. Orbit #3, One Orbital Period, 6X6 Gravity Field

Figure 5.28

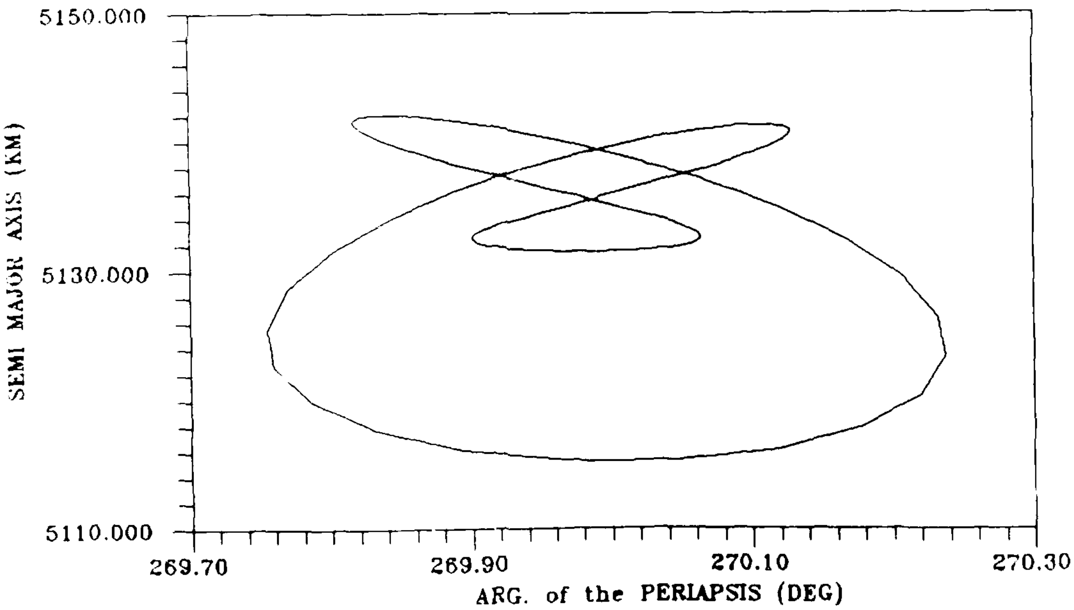

ω vs. a, Ref. Orbit #3, One Orbital Period, 6X6 Gravity Field

Figure 5.29

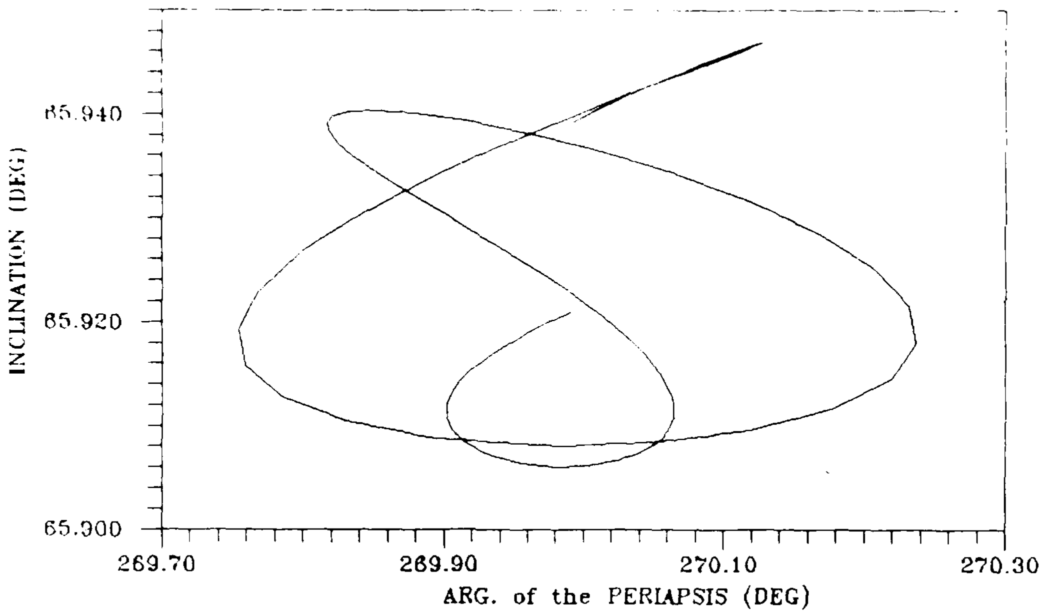

ω vs. ι, Ref. Orbit #3, One Orbital Period, 6X6 Gravity Field

Figure 5.30

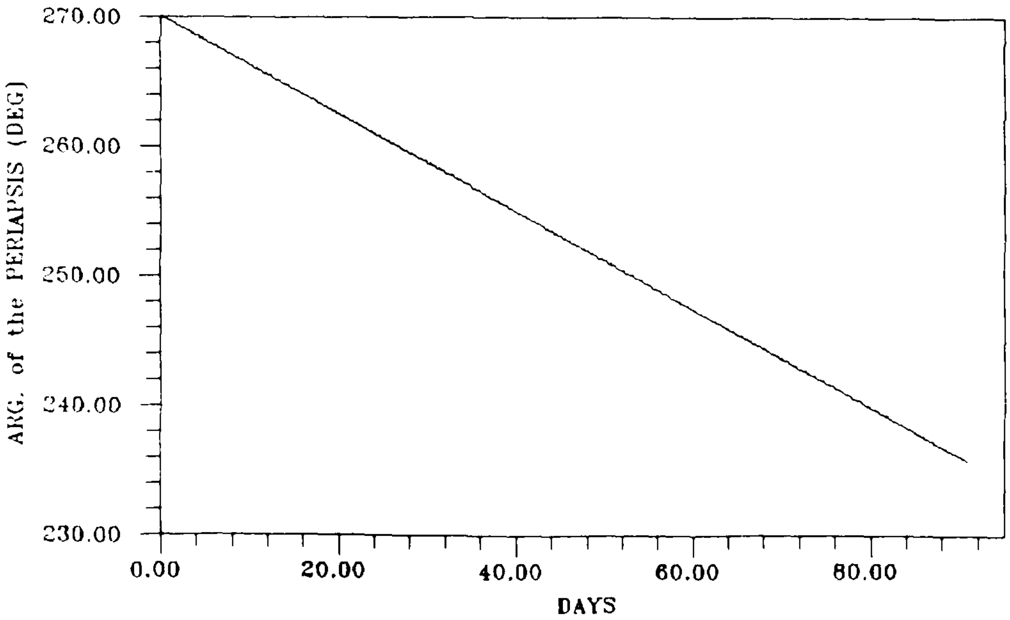

Days vs. ω, Ref. Orbit #3, 6X6 Gravity Field

Figure 5.31

Figures 5.32 through 5.34 show the changes for one orbital period associated with Reference Orbit #4. The magnitude of the change of the argument of the periapsis, the eccentricity, the semi major axis, and the inclination are all of the same order as those changes for Reference Orbit #3; however, for Reference Orbit #4, the the argument of the periapsis changes by 150 degrees per 90 days (see Figure 5.35), as opposed to 34 degrees per 90 days for Reference Orbit #3. The reason can be seen in Figure 5.22. For Reference Orbit #3 the inclination is increasing with each orbit causing an increasing smaller change in the eccentricity for each successive orbit. For Reference Orbit #4 the inclination is effectively decreasing with each orbit causing an increasing larger change in the eccentricity for each successive orbit. Figure 5.23 shows that an increase in eccentricity and inclination (as is the case for Reference Orbit #3), and an increase in eccentricity associated with a decrease in inclination (Reference Orbit #4) both induce a positive change in the argument of the periapsis over one orbital period. Since the change in the argument of the periapsis is calculate by subtracting the final value from the initial value, a positive change implies that the starting value for the argument of the periapsis is greater than the value of the argument of the periapsis one orbit later; therefore, both Reference Orbits #3 and #4 are experiencing a decrease in the argument of the periapsis. The difference in the magnitude of these decreases is due to the initial value of the inclination angle.

For Reference Orbit #3, the inclination value starts out being the critical inclination. The effect of the increase of eccentricity is to decrease the value of the critical inclination (see Figure 5.23). At the start of each orbital period, Reference Orbit #3's inclination has increased over the starting value of the previous orbital period (see Figure 5.30). The combined effect is that Reference Orbit #3's inclination becomes slightly greater than the critical inclination angle. This causes the change in the argument of periapsis over one orbital period to be slightly positive, thus causing the argument of the periapsis to slowly decrease.

Because of the initial value of Reference Orbit #4's inclination (= 90 degrees), the argument of the periapsis wants to decrease at its maximum rate. The only parameter holding it back is the initial eccentricity. This eccentricity increases with time, and with this increase in eccentricity, a positive change (as discussed above) in the argument of the periapsis occurs. This positive change in the argument of the periapsis enhances the natural tendency for an orbit of this inclination to decrease the argument of the periapsis in value. Thus, causing the change in the argument of the periapsis to be much greater than that of Reference Orbit #3.

At this value of the semi major axis and eccentricity, either the change in the argument of the periapsis or the change in the eccentricity over one orbital period can be set to zero, but not both. Figures 5.24 and 5.27 indicate that selecting an inclination which drives the change in eccentricity to zero will result in a rapid change in the argument of the periapsis. Thus, in the effort to control the argument of the periapsis, there is no advantage to driving only the change over one orbital period in the eccentricity to zero.

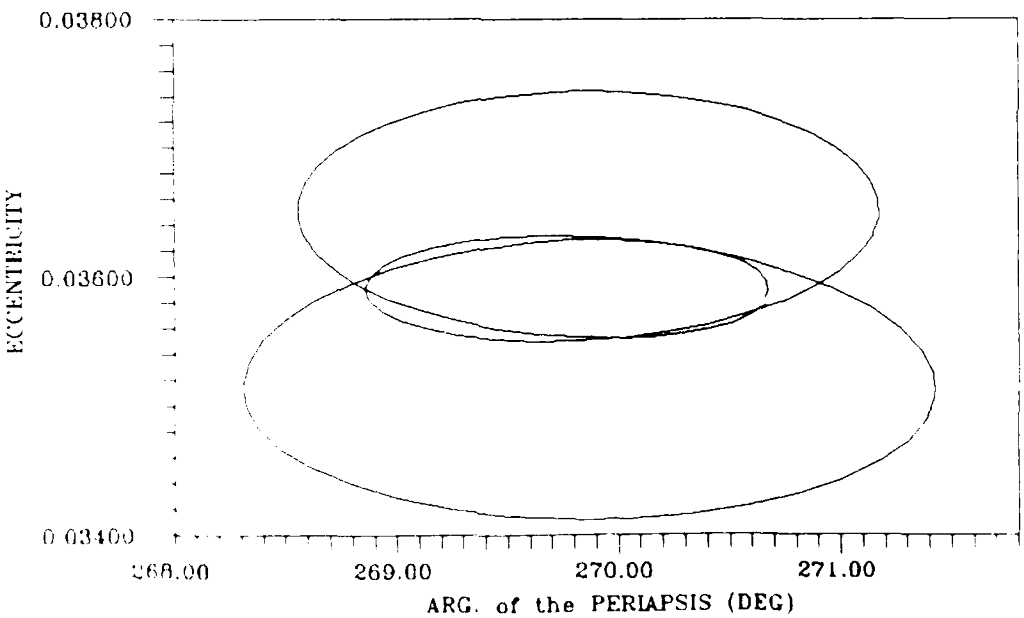

e vs ω, Ref. Orbit #4, One Orbital Period, 6X6 Gravity Field

Figure 5.32

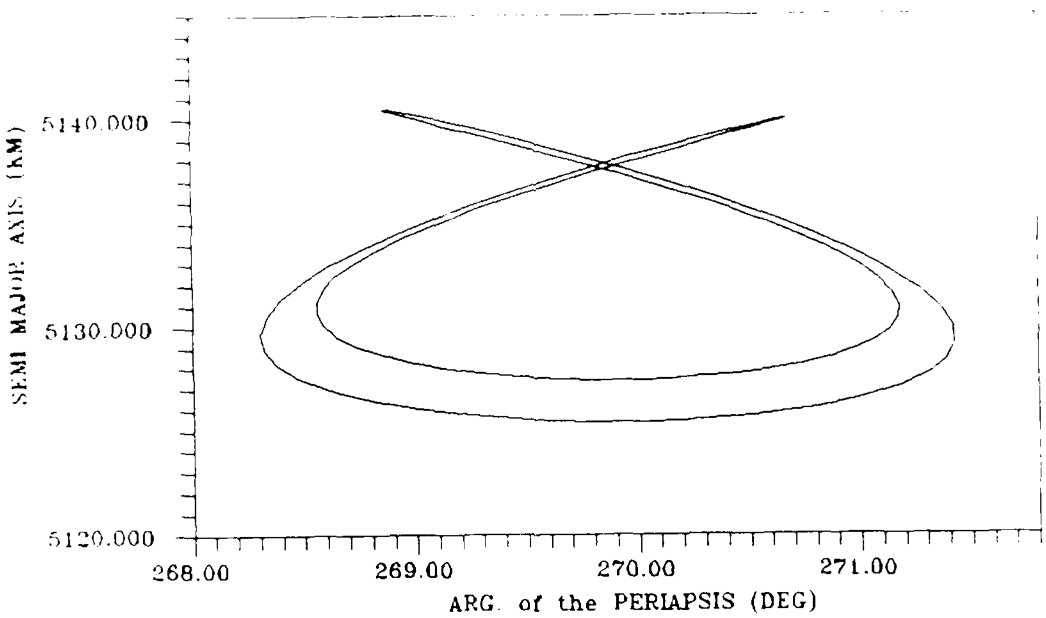

ω vs. a, Ref. Orbit #4, One Orbital Period, 6X6 Gravity Field

Figure 5.33

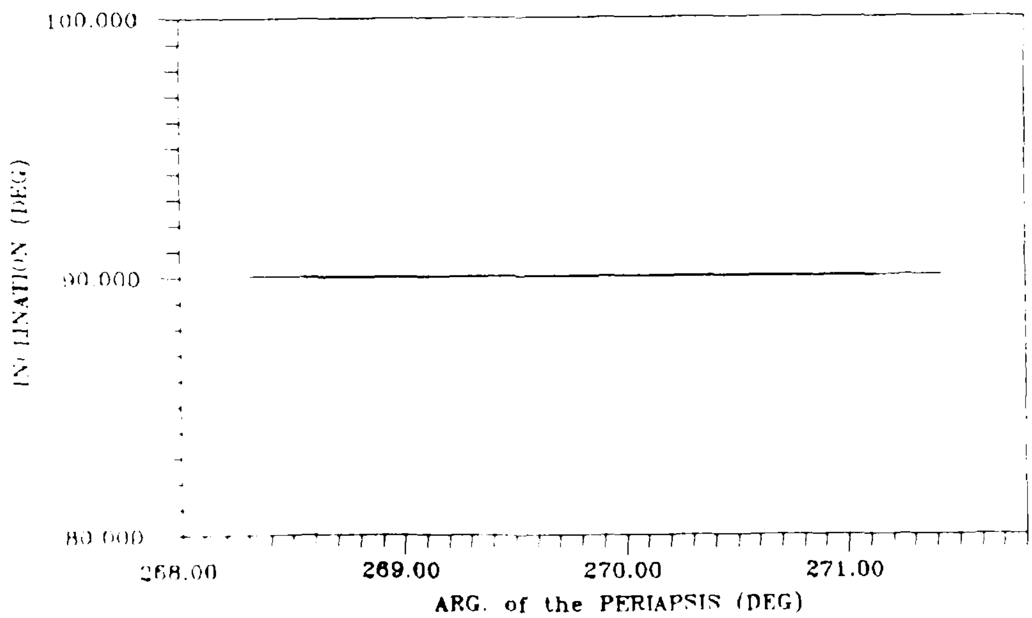

vs , Ref Orbit #4, One Orbital Period, 6X6 Gravity Field

Figure 5.34

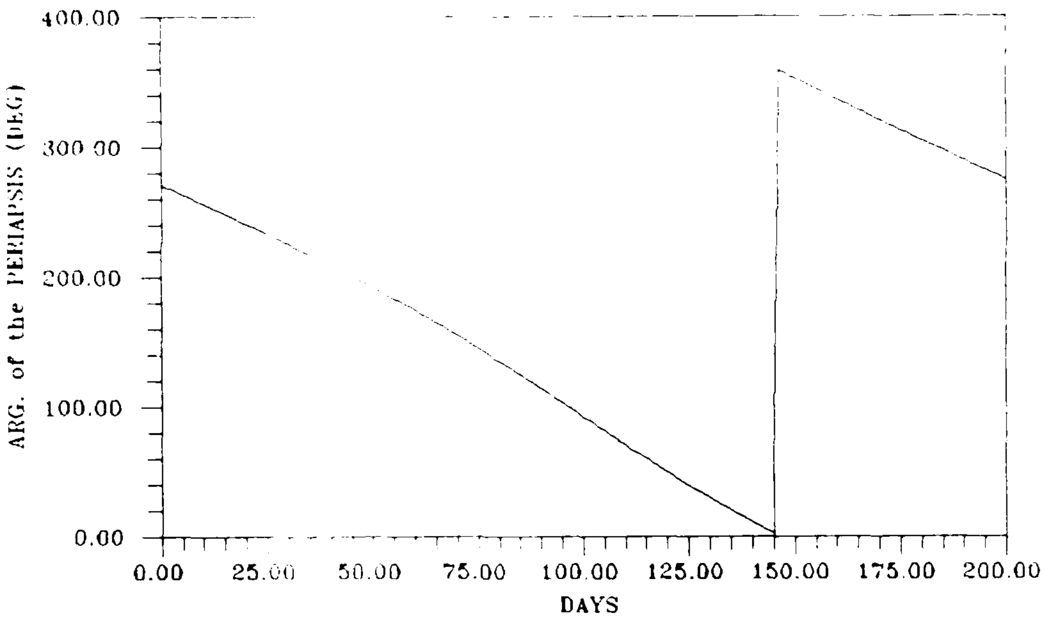

Days vs. ., Ref. Orbit #4, 6X6 Gravity Field

Figure 5.35

Figure 5.23 shows that the value of the critical angle of inclination is dependent upon the value of the eccentricity. However, because the change over one orbital period of the eccentricity is non zero for all the possible values of the critical inclination (see Figure 5.22), the value of the critical inclination is itself changing over time, thus inducing a change in the argument of the periapsis. The change in the argument of the periapsis is the slowest at the maximum allowable eccentricity (e = 0.3), and the fastest at the minimum allowable eccentricity (e = 0.03586336) . The question arises, for e = 0.3 is there a semi major axis value such that the change in the argument of the periapsis, the eccentricity, the semi major axis, and the inclination are all equal to zero? If so, what are the characteristics of this orbit, and what effect does a change in eccentricity have upon such an orbit? The next part of this analysis will focus upon these questions.

Analysis From 5133 KM Out To Geosynchronous

Sweeping the value of the semi major axis from 5133 km to 20,000 km, for inclination values from 1 to 90 degrees, and noting the change over one orbital period of the argument of the periapsis, eccentricity, inclination, and semi major axis yields the figures shown in Appendix F through H. (Note, for Mars, geosynchronous occurs at 20,400 km.) Although the inclination was advanced in increments of 5 degrees, an increment of 10 degrees is sufficient to show the trend, and is used in presenting these figures. The most interesting results occur at an inclination of approximately 70 degrees. Figures 5.36 through 5.38 highlight these results.

At a semi major axis value of approximately 17,000 km, and an inclination of approximately 70 degrees, Figure 5.36 shows the change in the argument of the periapsis and the change in the eccentricity are both approximately zero.

Further analysis showed that the zero change over one orbital period of these two parameters (argument of the periapsis, and eccentricity) actually occurs when the semi major axis is 17,190 km and the inclination is 69.9750 degrees. These parameters, together with the other associated input parameters define Reference Orbit #5, and are shown in Table 5.5

Orbital Elements for Reference Orbit #5

Table 5.5

Input Orbital Elements for:	a km	e	i degrees	Ω degrees	ω degrees	ν degrees
Ref Orbit #5	17,190.0	.3	69.9750	90	[illegible]	[illegible]

AD-A189 574 FROZEN ORBIT ANALYSIS IN THE MARTIAN SYSTEM(U) AIR FORCE INST OF TECH WRIGHT-PATTERSON AFB OH SCHOOL OF ENGINEERING J W FOISTER DEC 87 AFIT/GSO/AA/87D-2

2/2

UNCLASSIFIED F/G 3/3 NL

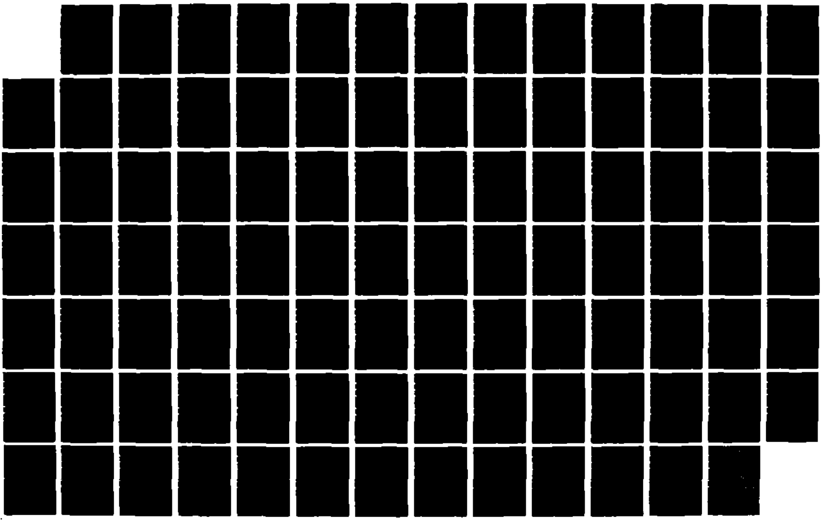

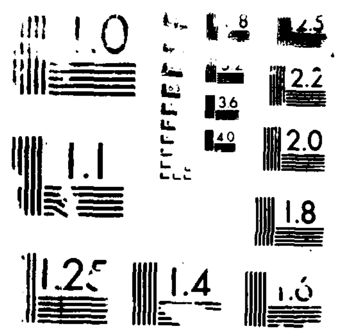
1.0
2.2
3.6
4.0
2.0
1.1
1.8
1.4

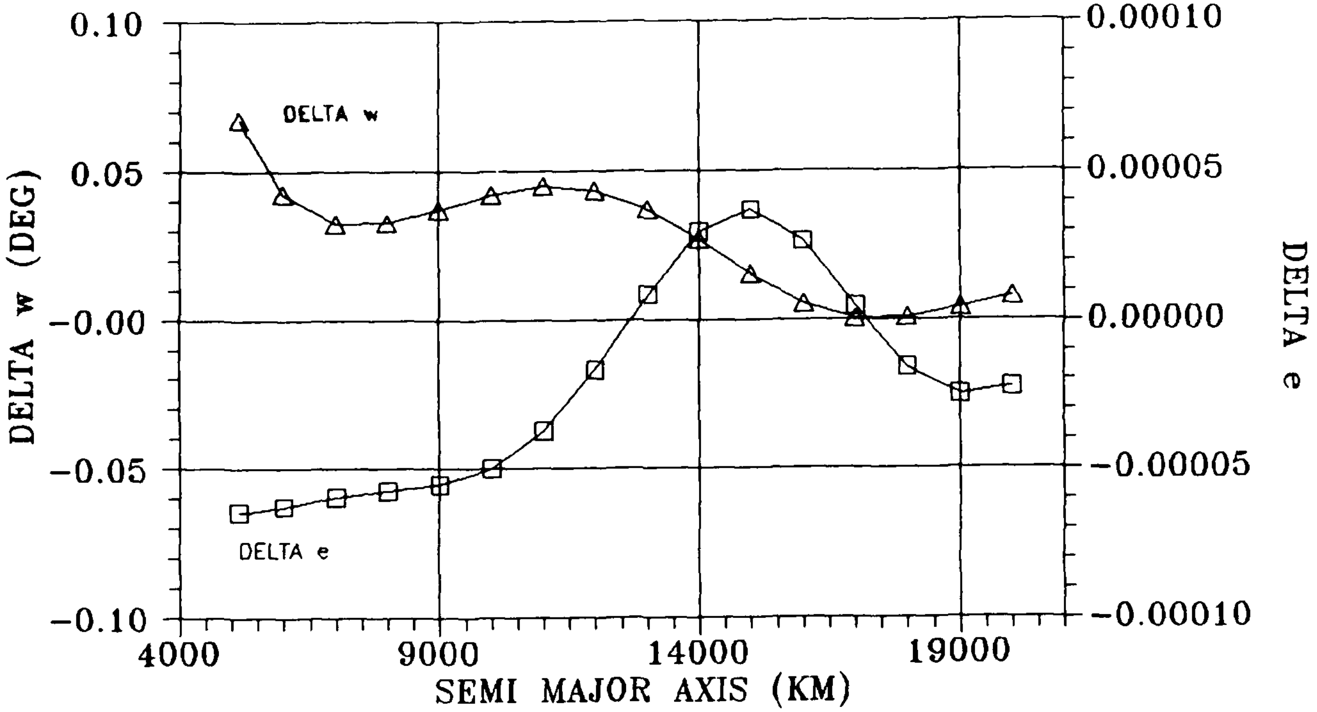

DELTA e, DELTA w vs. SEMI MAJOR AXIS for e = .3, i = 70
Figure 5.36

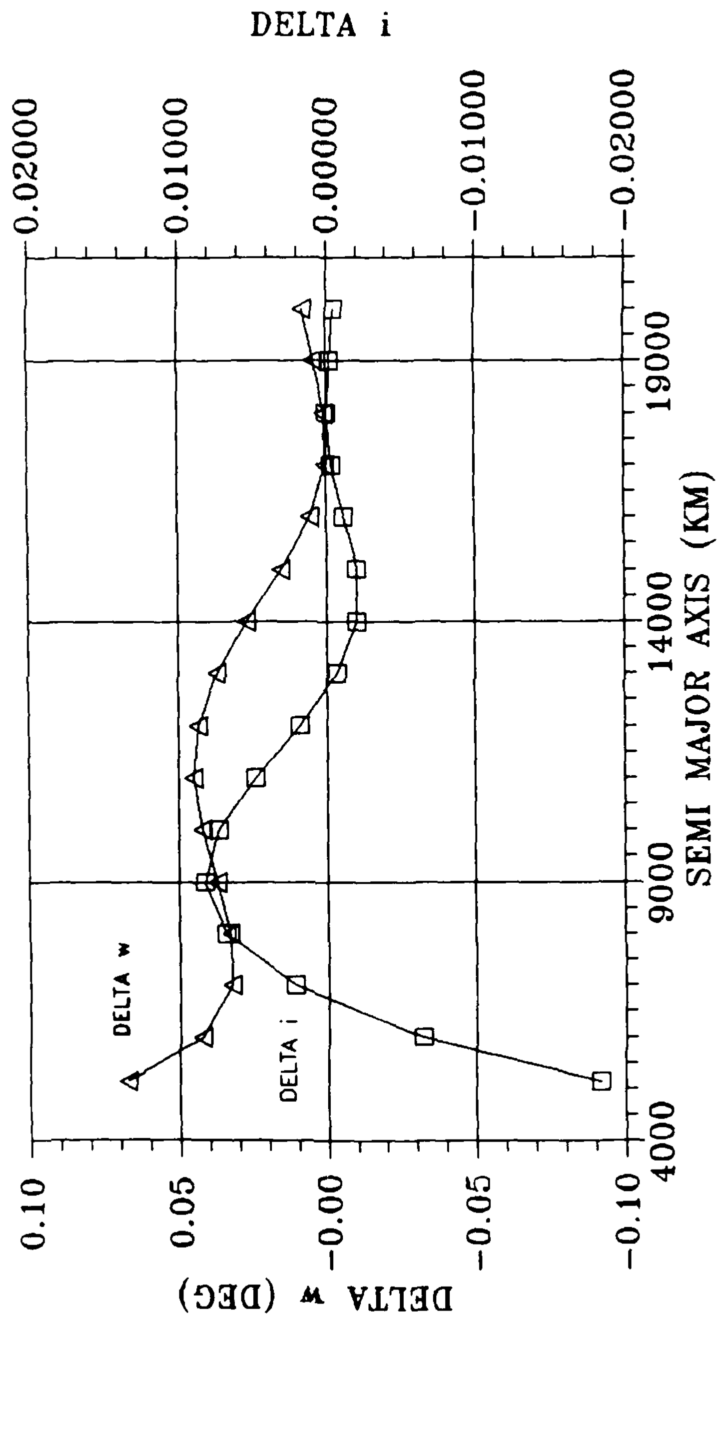

DELTA i, DELTA w vs. SEMI MAJOR AXIS for e = .3, i = 70
Figure 5.37

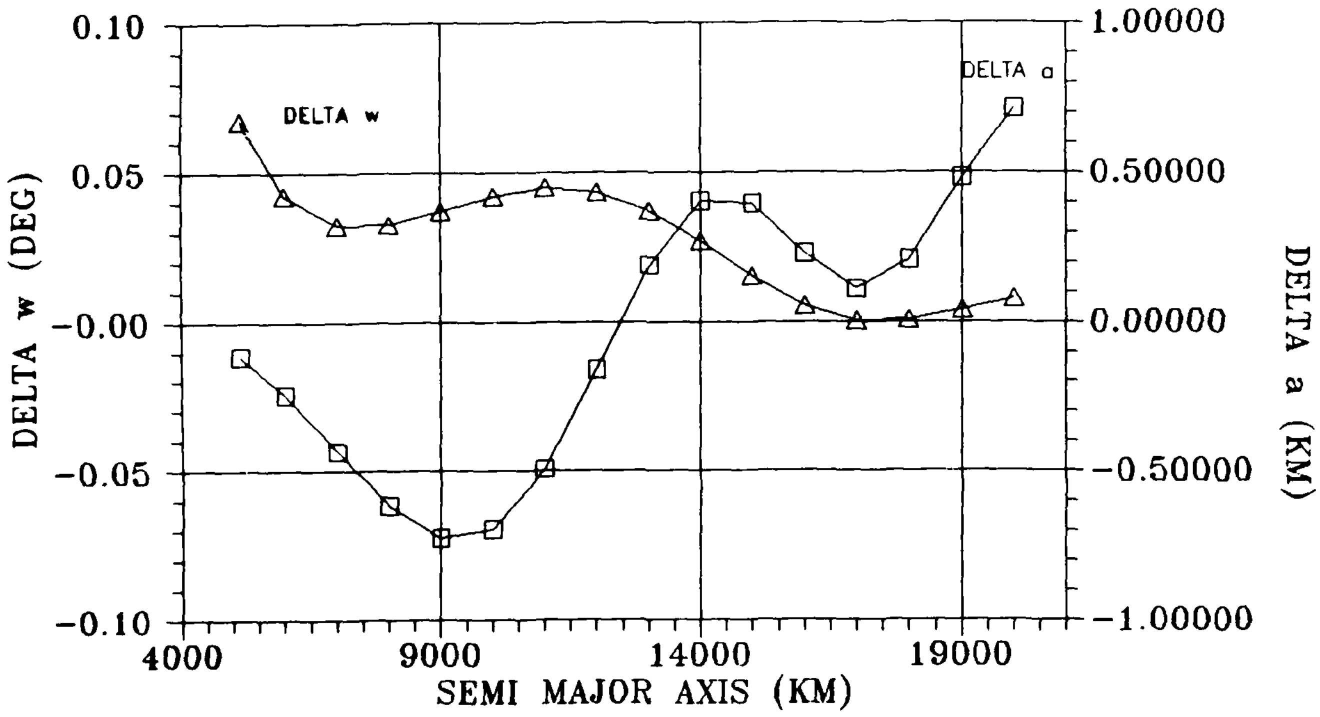

DELTA a, DELTA w vs. SEMI MAJOR AXIS for e = .3, i = 70
Figure 5.38

The time rate of change of the argument of the periapsis, the eccentricity, the semi major axis, and the inclination for Reference Orbit #5 are shown by Figures 5.39 through 5.41. Figure 5.42 reveals that although the change in the argument of the periapsis is zero over one orbital period, over an extended time the argument of the periapsis decreases at the rate of 1.15 degrees per 90 days. This is because of the combined effect of the change in the semi major axis, on the order of 0.1 km per orbit (see Figure 5.40), and the 0.00026 degree per orbit change in the inclination (see Figure 5.41). From Figure 5.36 it can be seen that a small decrease from the semi major axis value of 17,000 km will induce a slow decrease in the eccentricity and the argument of the periapsis. Comparing Figures 5.36 and F.9 (see Appendix F) reveals an increase in inclination will, at this particular value of the semi major axis, also result in a slight decrease in the argument of the periapsis over time. Figures 5.36 through 5.38 show that as the semi major axis slowly decreases, the change in the argument of the periapsis, the change in the eccentricity, the change in the inclination, and the change in the semi major axis will progressively increase. Due to Reference Orbit #5's long orbital period (approximately 20 hours) a 0.1 km decrease in the semi major axis per orbit results in only an approximate 44 km decrease in the semi major axis per year. Hence, although the change in the above orbital elements occurs at a progressively increasing rate, the increase in rate is painstakingly slow. This accounts for the constant slope of Figure 5.42.

Equation (5.1) shows the predominant effect of an increase in the semi major axis is a decrease in the rate of change of the argument of the periapsis. Therefore, the slow rate of Reference Orbit #5's change in the argument of the periapsis, when compared to Reference Orbit #3, is not due entirely to any special effects of one change in an orbital parameter cancelling the effects of the change in another orbital parameter. Figure 5.43 shows the change in the argument of the periapsis for an orbit of the same semi major axis as Reference Orbit #5, but at 45 degrees inclination. A comparison of Figures 5.42 and 5.43 reveals Reference Orbit #5 experiences the same magnitude of change in one year as the change experience over a 90 day period for the orbit in Figure 5.43. Thus indicating Reference Orbit #5 is the more stable orbit.

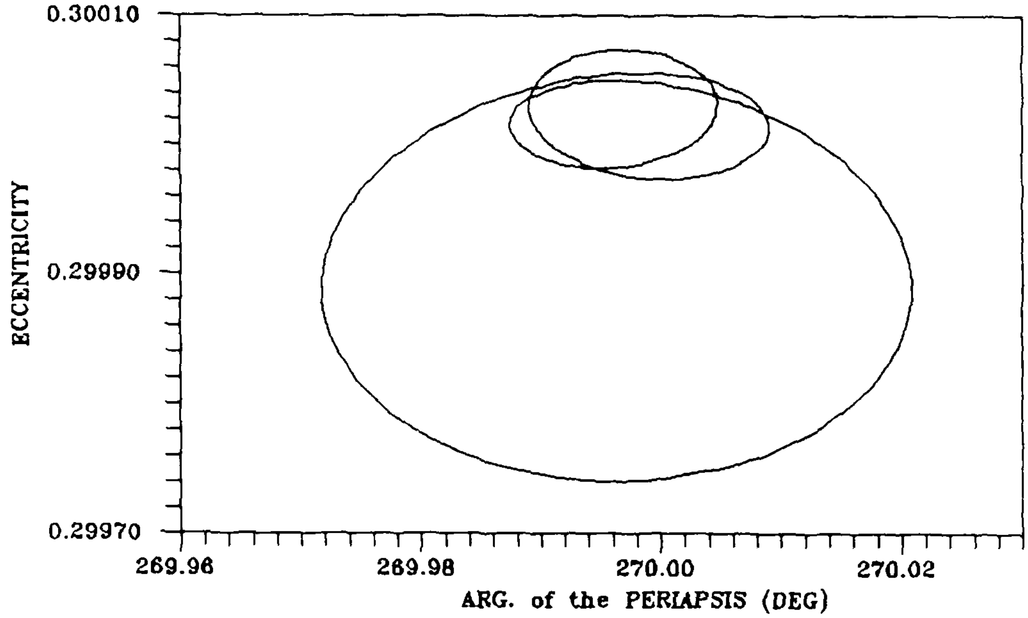

ω vs. e, Ref. Orbit #5, One Orbital Period, 6X6 Gravity Field

Figure 5.39

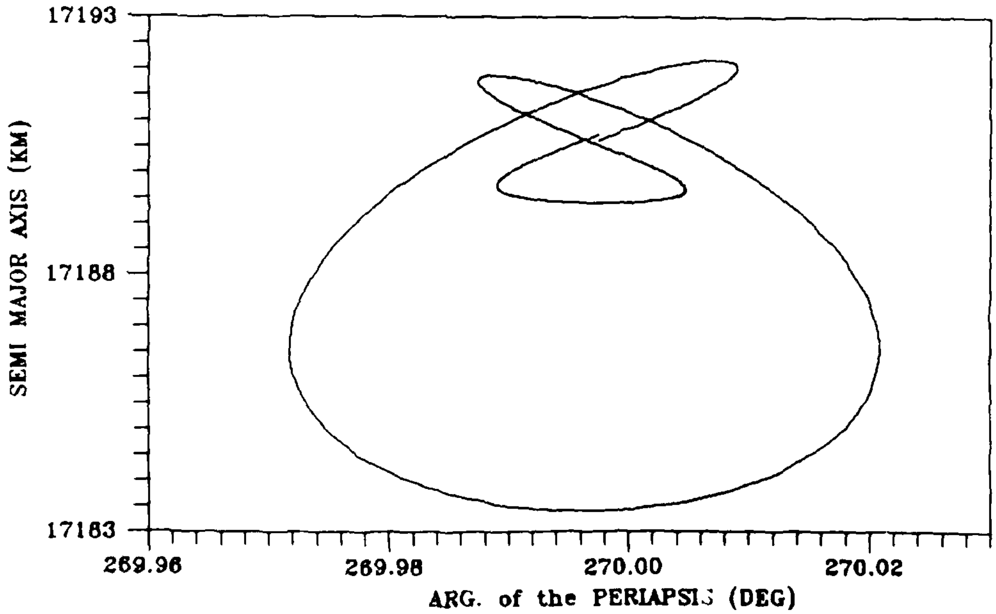

ω vs. a, Ref. Orbit #5, One Orbital Period, 6X6 Gravity Field

Figure 5.40

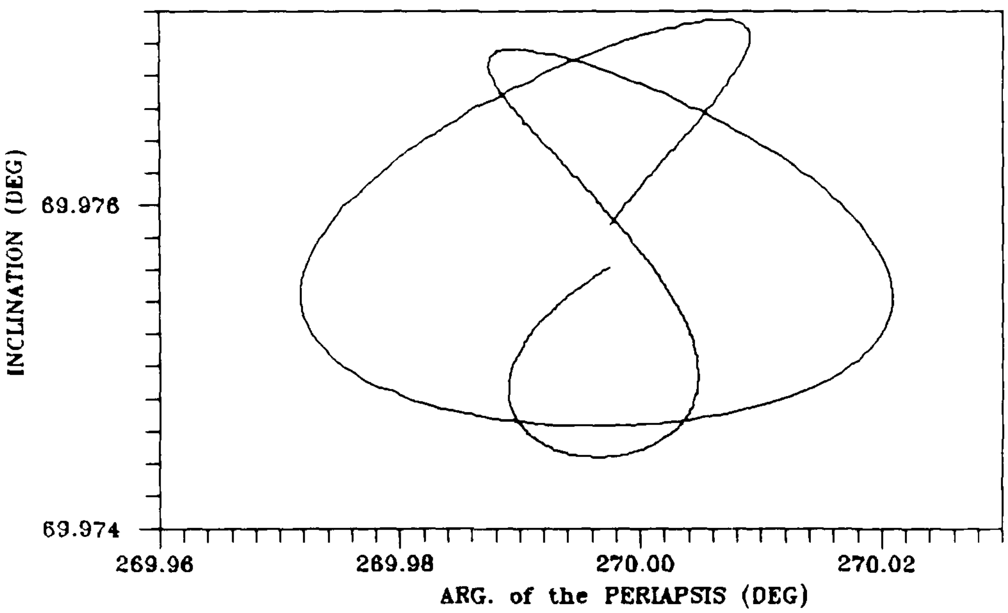

ω vs. ι, Ref. Orbit #5, One Orbital Period, 6X6 Gravity Field

Figure 5.41

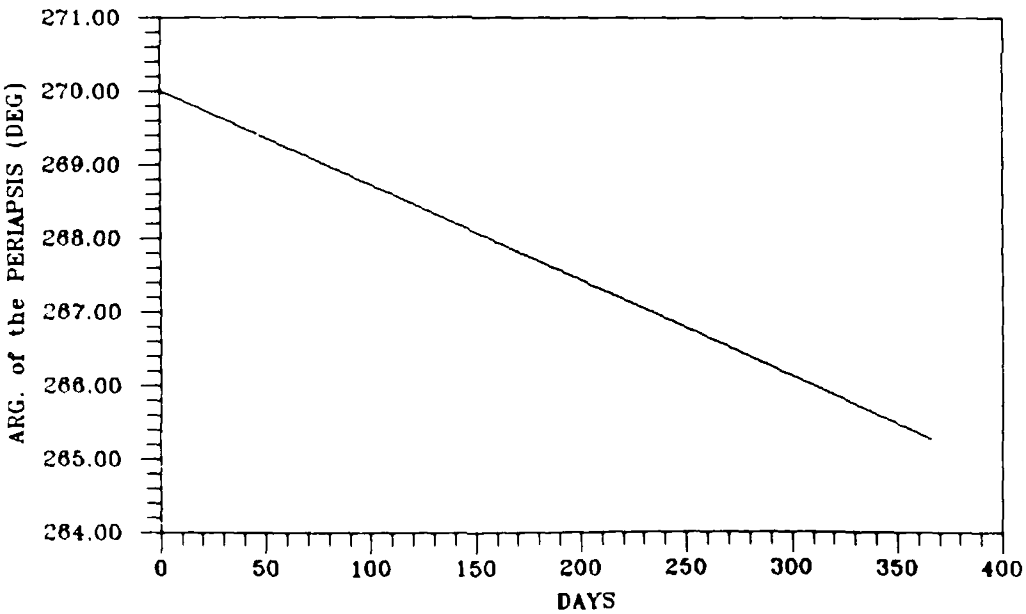

Days vs. ω, Ref. Orbit #5, 6X6 Gravity Field

Figure 5.42

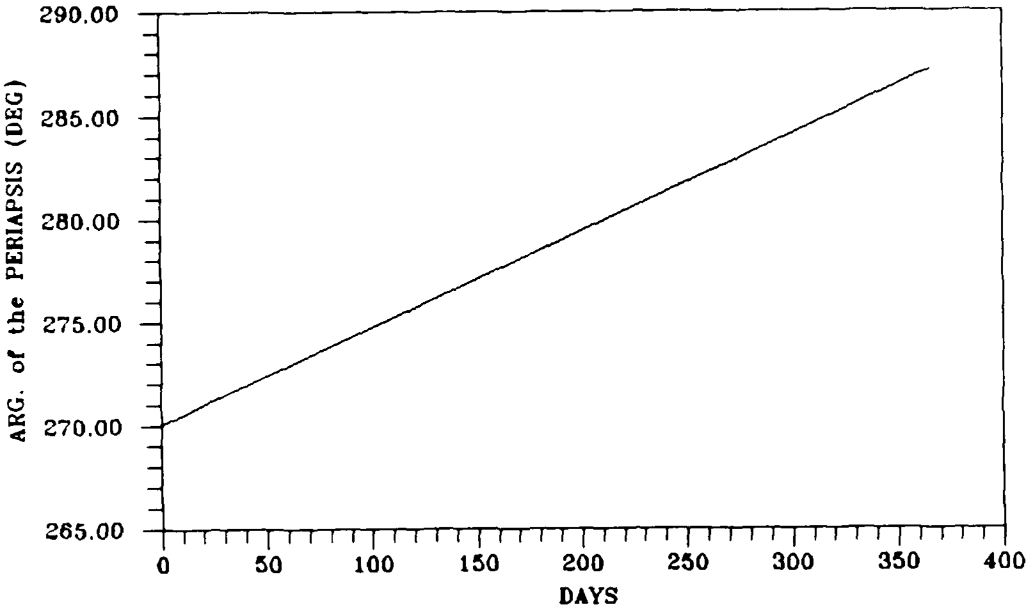

Days vs. ω, $a = 17{,}190$ KM, $i = 45$ Degrees, 6X6 Gravity Field

Figure 5.43

Appendices I through K show the effects of varying the eccentricity and semi major axis upon the change in the argument of the periapsis, the eccentricity, the inclination angle, and the semi major axis. Throughout these figures the input inclination angle remains 70 degrees. These appendices offer trend information, and because not all combinations of eccentricity and semi major axis exist without causing impact with the planet Mars, caution must be exercised in using these figures. From Appendix I it can be seen that for eccentricities from 0.01 to 0.3 (see Figure 5.36), the change in the argument of the periapsis over one orbital period has its zero value between approximately 17,000 and 18,000 kilometers. For eccentricities between 0.01 and 0.6 the change in eccentricity will also become zero somewhere between 17,000 and 18,000 km. As previously mentioned, only when the eccentricity is 0.3 is there one value of the semi major axis that simultaneously drives both values to zero. Further, between the semi major axis values of approximately 12,000 and 13,000 km there is another region where the change in eccentricity over one orbital period becomes zero.

Appendix J shows that at an eccentricity of 0.01 (Figure J.1) the change in inclination is fairly insensitive to changes in the semi major axis from approximately 13,000 to 17,000 km. As eccentricity increases, Figures J.1 through J.6 show that the change in the inclination becomes more sensitive to the value of the semi major axis; however, although not exactly zero, the change in the inclination over one orbital period remains relatively constant, and approximately zero in the semi major axis region of 17,000 to 18,000 km. Also, starting at an eccentricity of approximately .1, the change in inclination over one orbital period is approximately zero between semi major axis values of approximately 12,500 and 13,000 km.

In Appendix K, the change in the semi major axis over one orbital period appears to be fairly sensitive to changes in both the semi major axis and the eccentricity. Through out the range of values of the eccentricity there appears two regions where the zero change in the semi major axis exist. These regions exist from a semi major axis of approximately 12,200 to 13,200 km, and approximately 16,000 to 18,000 km.

Atmospheric Drag

In the next phase of this analysis, atmospheric drag was introduced to the above orbits. In all cases the atmospheric drag showed no appreciable effect over one orbital period. Reference Orbit #3 was propagated over a one year period, both with and without atmospheric drag. The results show that when in the presence of drag, the eccentricity decreased by 0.00002986, and the semi major axis decreased by 798 meters more than if atmospheric drag were not present. Reference Orbit #5 was also propagated over a one year period. Here the results showed no appreciable effects when in the presence of drag. This finding is not surprising given that the periapsis altitude of Reference Orbit #5 is approximately 8,600 km. Because of the height of the orbits investigated, atmospheric drag effects are minimal.

VI. Conclusions and Recommendations

Conclusions

From the analysis section, two general classifications of results were found. The first involves the characteristics of the orbital parameters effecting the control of the argument of the periapsis, and the second involves the two regions of relative orbital stability.

Characteristics of the Orbital Parameters Effecting the Control of the Argument of the Periapsis. For the MGCO phasing orbit none of the orbital elements (ω, e, a, and ι) experienced a zero time rate of change over one orbital period when in the presence of a 6 X 6 gravity field. Yet, the values of the argument of the periapsis and the eccentricity are bounded. The first step of the analysis sought to discover the nature of the argument of the periapsis when the time rate of change of the argument of the periapsis is zero over one orbital period. Through a careful selection of the inclination angle, the change in the argument of the periapsis was driven to zero over one orbital period. The results showed that a zero change in the argument of the periapsis has associated with it a non zero change in the eccentricity and the inclination angle (see figures 5.15 through 5.18). These two non zero parameters induce a long period change in the argument of the periapsis that is not bounded, but rather periodic. Further, from Figure 5.23 it can be seen that the critical inclination angle has a range of values, dependent upon the eccentricity of the orbit. From Figures 5.31 and 5.35 it is revealed that the rate of change in the argument of the periapsis that is induced by the change in eccentricity and inclination is, as in the case of a 6 X 0 gravity field, very sensitive to the initial value of the critical angle of inclination. If the eccentricity is such that a critical angle of inclination has a value that is close to 90 degrees, the rate of change induced in the argument of the periapsis will be much greater than the case where the critical inclination is near some lower value of inclination. Thus, driving only the change in the argument of the periapsis to zero is not sufficient, when in the presence of a 6 X 6 gravity field, to control the argument of the periapsis.

In the next step of the analysis, a value of the semi major axis and the inclination was selected that allows the time rate of change over one orbital period of the eccentricity to be driven to zero. Figure 5.24 shows that for this orbit there is a large change over one orbital period in the argument of the periapsis; hence, driving the time rate of change in the eccentricity to zero will not result in the desired bounded condition of the argument of the periapsis.

Searching values of the semi major axis ranging from 5133 km to 20,000 km, for inclinations ranging from 1 to 90 degrees lead to the discovery of an orbit in which both the argument of the periapsis and the eccentricity are zero over one orbital period. Figure 5.39 shows that the argument of the periapsis and the eccentricity are indeed bounded; however, the semi major axis and the angle of inclination are not bounded. Figures 5.36 through 5.38 indicate how the unbounded nature of the semi major axis and the inclination effect the argument of the periapsis and the eccentricity. The results indicate that in the presence of a 6 X 6 gravity field, control of the argument of the periapsis is not gained by driving the short term perturbations in the argument of the periapsis and the eccentricity to zero.

<u>Regions of Relative Orbital Stability</u>. From this analysis it is evident that driving the short term perturbations of one or two of the orbital elements is not sufficient to control the argument of the periapsis. Rather, the short term perturbations for the change in the argument of the periapsis, the eccentricity, the semi major axis, and the angle of inclination must all be driven to zero. Appendices F through K show that at eccentricities from 0.01 to 0.6 an orbit that freeze the argument of the periapsis, the eccentricity, the semi major axis, and the inclination does not exist. The best that can be obtained is that the change in three out of four of the orbital elements can be driven to approximately zero. Appendices F through K indicate that this takes place in two distinct regions. The first being for a semi major axis from approximately 17,000 km to 18,000 km, with an eccentricity ranging from approximately 0.01 to 0.6 and an inclination value of approximately 70 degrees. Within this region the change in the argument of the periapsis, the change in the eccentricity, and the change in the inclination can be driven to approximately zero, while the change in the semi major axis

prominently remains non zero. The second region exist for semi major axis values from approximately 12,000 km to 13,000 km, with an eccentricity ranging from 0.01 to 0.6 and an inclination value of approximately 70 degrees. Within this region the change in the eccentricity, the semi major axis and the inclination can be made approximately zero, but the change in the argument of the periapsis can not be driven to approximately zero.

Atmospheric Drag. At the beginning of this research it was thought that the locations for the frozen and stable orbits that might be found would be near the planet's surface. This was not the case. In fact the orbits looked at were of sufficient height that the atmospheric drag, even when propagated over a one year period had only very slight effects on the semi major axis, and no discernible effects on the eccentricity.

Recommendations

Examining the MGCO phasing orbit reveals that the change in the argument of the periapsis and the inclination are both negative (values increase over one orbital period), while the change in the eccentricity and the semi major axis are both positive (values decrease over one orbital period). Appendices F through H show that for an eccentricity of 0.3, a region exist from a semi major axis of approximately 13,000 km to 17,100 km, and an inclination value of approximately 35 degrees to 65 degrees where the same characteristics of change in the argument of the periapsis, eccentricity, semi major axis, and the inclination exist as exist for the MGCO phasing orbit. The next step in any follow on study ought to focus on this region. If this region does prove to have bounded changes in the argument of the periapsis, then further analysis needs to be made at other values of the eccentricity.

It is interesting to note that the above region, and the regions of relative orbital stability described earlier occur between the moons of Mars, Phobos (mean distance of 9,380 km) and Deimos (mean distance of 23,474 km). Although the mass of these moons are slight, they will have a perturbative effect upon the regions of relative orbital stability that needs further analysis. Also, further analysis upon the regions of stability needs to be performed taking into account resonance effects, solar pressure and third body effects.

Appendix A: Derivation of Poisson's and Laplace's Equations

Let the entire mass of the planet exist as a point in space; then surround this point with a "simple" surface S. The surface S is called simple if it has a finite area and does not have points that intersect or touch other points on this surface. (see Figure A1) Each small area of the surface (da) will have an associated normal vector $\hat{n}$. The procedure is to determine how much of the acceleration (due to the mass M) is along the normal of each infinitesimal area of surface, and then to integrate over the entire area of the surface S. This will yield the amount of acceleration which mass M exerts over the entire surface S (19:49).

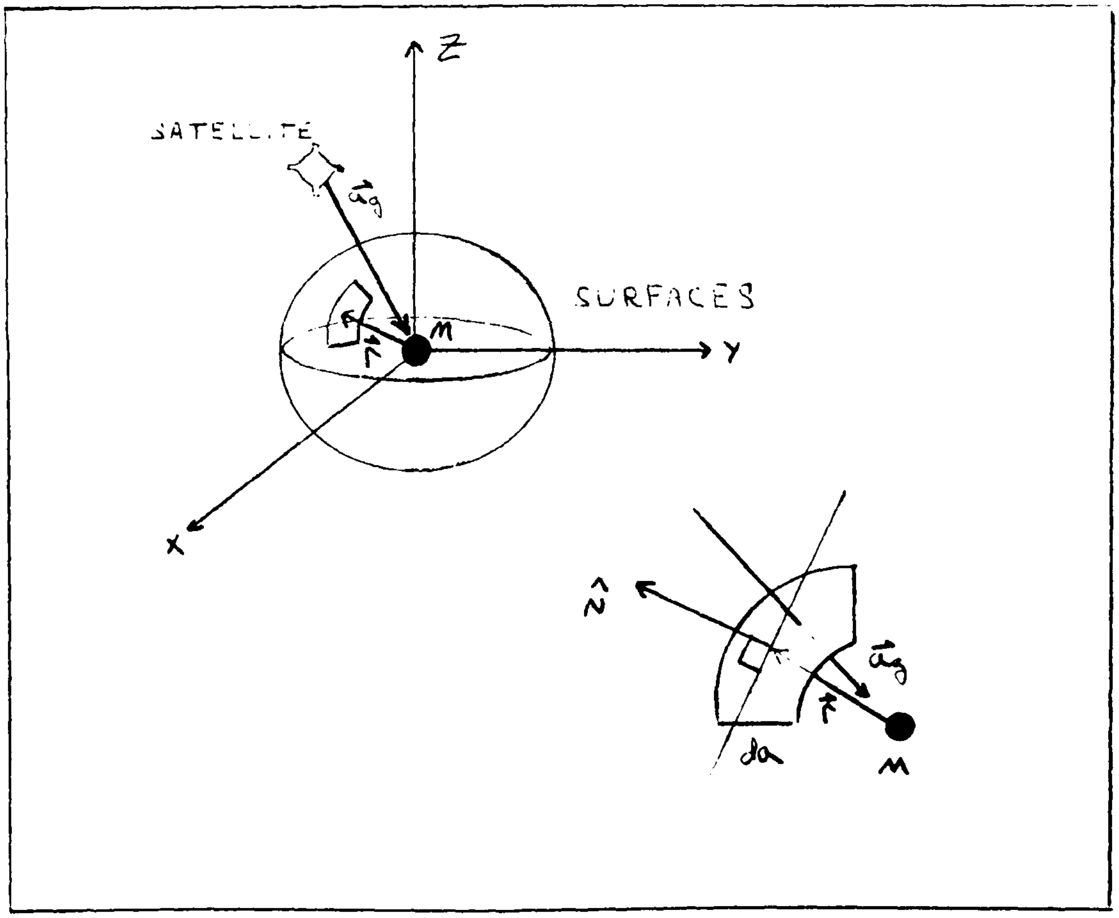

Point Mass Enclosed by a Simple Surface (19:49)

Figure A.1

Mathematically this process is modeled as:

$$\oint_S \vec{a}_g \cdot \hat{n}\, da = \oint_S -\frac{GM}{r^3}\vec{r} \cdot \hat{n}\, da = -GM \oint_S \frac{\vec{r}}{r^3} \cdot \hat{n}\, da \tag{A1.1}$$

Since S is a simple surface, the value of the above integral will not be dependent upon the size of the surface. Therefore, let S be a unit sphere. Then

$$\oint_S \vec{a}_g \cdot \hat{n}\, da = -GM \oint_S da = -GM(4\pi r^2) \tag{A1.2}$$
$$= -GM(4\pi)$$

Employing the Divergence Theorem of Gauss (12:440):

$$\oint_S \vec{a}_g \cdot \hat{n}\, da = \int_V \nabla \cdot \vec{a}\, dV \tag{A1.3}$$

equation (A1.2) becomes:

$$\oint_S \vec{a}_g \cdot \hat{n}\, da = \int_V \nabla \cdot \vec{a}_g\, dV = -4\pi GM \tag{A1.4}$$

where V equals the volume enclosed by the surface S.

The above equation assumes the entire mass of the planet exists as a point mass located at the center of a unit sphere. This restriction is removed by assuming that the mass of the planet is evenly distributed throughout the unit sphere by allowing:

$$m = \int_V \rho\, dV \tag{A1.5}$$

where ρ equals the density of the mass. Equation (A1.4) becomes:

$$\int_V \nabla \cdot \vec{a}_g\, dV = -4\pi G \int_V \rho\, dV \tag{A1.6}$$

Because equation (A1.6) is independent of the size or shape of the volume, equate the integrands to obtain:

$$\nabla \cdot \vec{a}_g = -4\pi G \rho \tag{A1.7}$$

but

$$\vec{a}_g = \nabla V \tag{A1.8}$$

so equation (A1.7) becomes:

$$\nabla \cdot \nabla V = -4\pi G \rho \tag{A1.9}$$

$$\nabla^2 V = -4\pi G \rho$$

Equation (A1.9) is known as Poisson's Equation. This equation is only valid for regions within the planet's interior (5:108). Since the satellite will be orbiting outside the planet's surface, ρ becomes zero, and equation (A1.9) becomes:

$$\nabla^2 V = 0 \tag{A1.10}$$

Equation (A1.10) is Laplace's Equation.

Appendix B: Trigonometric Manipulations

Identities

$$\cos(a+b) = \cos a\cos b - \sin a\sin b \tag{B1.1}$$

$$\sin(a+b) = \sin a\cos b + \cos a\sin b \tag{B1.2}$$

$$\cos(a-b) = \cos a\cos b + \sin a\sin b \tag{B1.3}$$

$$\sin(a-b) = \sin a\cos b - \cos a\sin b \tag{B1.4}$$

$$\cos a\cos b = \frac{1}{2}[\cos(a+b) + \cos(a-b)] \tag{B1.5}$$

$$\sin a\sin b = \frac{1}{2}[\cos(a-b) - \cos(a+b)] \tag{B1.6}$$

$$\sin a\cos b = \frac{1}{2}[\sin(a+b) + \sin(a-b)] \tag{B1.7}$$

$$\cos a\sin b = \frac{1}{2}[\sin(a+b) - \sin(a-b)] \tag{B1.8}$$

Euler's equations are:

$$\sin a = \frac{e^{ja} - e^{-ja}}{2j} \tag{B1.9}$$

$$\cos a = \frac{e^{ja} + e^{-ja}}{2} \tag{B1.10}$$

where $j = \sqrt{-1}$

$$e^{ja} = \cos a + j\sin a \tag{B1.11}$$

Binomial Expansions of cos mx and sin mx

Let (3:2)

$$\cos mx = \text{real part } (e^{jmx}) = \text{RE } e^{jmx} \tag{B2.1}$$

$$\cos mx = \text{RE } (e^{jx})^m \tag{B2.2}$$

$$\cos mx = \text{RE } (\cos x + j\sin x)^m \tag{B2.3}$$

Noting that (1:11)

$$(a + b)^n = \sum_{s=0}^{n} \binom{n}{s} a^{n-s} b^s \tag{B2.4}$$

Equation (B2.3) can be written as:

$$\cos mx = \text{RE } \sum_{s=0}^{m} \binom{m}{s} j^s \cos^{m-s} x \sin^s x \tag{B2.5}$$

Let

$$\sin mx = \text{RE } (-je^{jmx}) \tag{B2.6}$$

Then, equation (B2.6) becomes:

$$\sin mx = \text{RE } \sum_{s=0}^{m} \binom{m}{s} j^{s-1} \cos^{m-s} x \sin^s x \tag{B2.7}$$

Expansions of Sin ^{a} mx Cos ^{b} mx

Multiplying equtions (B1.9), and (B1.10) yields:

$$\sin^a mx \cos^b mx = \left(\frac{e^{jx} - e^{-jx}}{2j}\right)^a \left(\frac{e^{jx} + e^{-jx}}{2}\right)^b \tag{B3.1}$$

$$\sin^a mx \cos^b mx = \left(\frac{(-j)^a}{2^a} \sum_{c=0}^{a} \binom{a}{c} e^{jx(a-c)} e^{-jxc} (-1)^c \right) \tag{B3.1a}$$

$$\times \left(\frac{1}{2^b} \sum_{d=0}^{b} \binom{b}{d} e^{jx(b-d)} e^{-jxd} \right)$$

which becomes

$$\sin^a x \cos^b x = \frac{(-1)^a j^a}{2^{a+b}} \sum_{c=0}^{a} \sum_{d=0}^{d} \binom{a}{c} \binom{b}{d} (-1)^c e^{jx(a+b-2c-2d)} \tag{B3.2}$$

where

$$e^{jx(a+b-2c-2d)} = \cos(a+b-2c-2d)x + j\sin(a+b-2c-2d)x \tag{B3.3}$$

In equation (B3.3), let $a = L-m-2t+s$ and $b = m-s$ (Born:5). Then (B3.3) becomes:

$$e^{jx(a+b-2c-2d)} = \cos(L-2t-2c-2d)x + j\sin(L-2t-2c-2d)x \tag{B3.4}$$

Appendix C: The Inclination and Eccentricity Functions

Table C.1 The Inclination Function

L	m	p	$F_{Lmp}(i)$
2	0	0	$-\frac{3}{8}\sin^2\iota$
2	0	1	$\frac{3}{4}\sin^2\iota - \frac{1}{2}$
2	0	2	$-\frac{3}{8}\sin^2\iota$
2	1	0	$\frac{3}{4}\sin\iota(1+\cos\iota)$
2	1	1	$-\frac{3}{2}\sin\iota\cos\iota$
2	1	2	$\frac{3}{4}\sin\iota(-1+\cos\iota)$
2	2	0	$\frac{3}{4}(1+\cos\iota)^2$
2	2	1	$\frac{3}{2}\sin^2\iota$
2	2	2	$\frac{3}{4}(1-\cos\iota)^2$
3	0	0	$-\frac{5}{16}\sin^3\iota$
3	0	1	$\frac{15}{16}\sin^3\iota - \frac{3}{4}\sin\iota$
3	0	2	$-\frac{15}{16}\sin^3\iota + \frac{3}{4}\sin\iota$
3	0	3	$\frac{5}{16}\sin^3\iota$
3	1	0	$-\frac{15}{16}\sin^2\iota(1+\cos\iota)$

Table C.1 cont. The Inclination Function

L	m	p	$F_{Lmp}(i)$
3	1	1	$\frac{15}{16}\sin^2 i(1+3\cos i)-\frac{3}{4}(1+\cos i)$
3	1	2	$\frac{15}{16}\sin^2 i(1-3\cos i)-\frac{3}{4}(1-\cos i)$
3	1	3	$-\frac{15}{16}\sin^2 i(1-\cos i)$
3	2	0	$\frac{15}{8}\sin i(1+\cos i)^2$
3	2	1	$\frac{15}{8}\sin i(1-2\cos i-3\cos^2 i)$
3	2	2	$-\frac{15}{8}\sin i(1+2\cos i-3\cos^2 i)$
3	2	3	$-\frac{15}{8}\sin i(1-\cos i)^2$
3	3	0	$\frac{15}{8}(1+\cos i)^3$
3	3	1	$\frac{15}{8}(3+3\cos i-3\cos^2 i-3\cos^3 i)$
3	3	2	$\frac{15}{8}(3-3\cos i-3\cos^2 i+3\cos^3 i)$
3	3	3	$\frac{15}{8}(1-\cos i)^3$
4	0	0	$\frac{35}{128}\sin^4 i$
4	0	1	$-\frac{35}{32}\sin^4 i+\frac{15}{16}\sin^2 i$
4	0	2	$\frac{3}{8}\left(\frac{35}{8}\sin^4 i-5\sin^2 i+1\right)$
4	0	3	$-\frac{35}{32}\sin^4 i+\frac{15}{16}\sin^2 i$

Table C.1 cont. The Inclination Function

L	m	p	$F_{Lmp}(i)$
4	0	4	$\frac{35}{128}\sin^4 i$
4	1	0	$-\frac{35}{32}\sin^3 i(1+\cos i)$
4	1	1	$\frac{35}{16}\sin^3 i(1+2\cos i)-\frac{15}{8}\sin i(1+\cos i)^2$
4	1	2	$\cos i\left(\frac{15}{4}\sin i-\frac{105}{16}\sin^3 i\right)$
4	1	3	$-\frac{35}{16}\sin^3 i(1-2\cos i)+\frac{15}{8}\sin i(1-\cos i)$
4	1	4	$\frac{35}{32}\sin^3 i(1-\cos i)$
4	2	0	$-\frac{105}{32}\sin^2 i(1+\cos i)^2$
4	2	1	$\frac{105}{8}\sin^2 i\cos i(1+\cos i)-\frac{15}{8}(1+\cos i)^2$
4	2	2	$\frac{105}{16}\sin^2 i(1-3\cos^2 i)-\frac{15}{4}(1-\cos^2 i)$
4	2	3	$-\frac{105}{8}\sin^2 i\cos i(1-\cos i)-\frac{15}{8}(1-\cos i)^2$
4	2	4	$-\frac{105}{32}\sin^2 i(1-\cos i)^2$
4	3	0	$\frac{105}{16}\sin i(1+\cos i)^3$
4	3	1	$\frac{105}{8}\sin i(1-3\cos^2 i-2\cos^3 i)$
4	3	2	$-\frac{315}{8}\sin^3 i\cos i$
4	3	3	$-\frac{105}{8}\sin i(1-3\cos^2 i+2\cos^3 i)$

Table C.1 cont. The Inclination Function

L	m	p	$F_{Lmp}(i)$
4	3	4	$-\frac{105}{16}\sin\iota(1-\cos\iota)^3$
4	4	0	$\frac{105}{16}(1+\cos\iota)^4$
4	4	1	$\frac{105}{4}\sin^2\iota(1+\cos\iota)^2$
4	4	2	$\frac{315}{8}\sin^4\iota$
4	4	3	$\frac{105}{4}\sin^2\iota(1-\cos\iota)^2$
4	4	4	$\frac{105}{16}(1-\cos\iota)^4$

Table C.2 The Eccentricity Funtion (10:38)

L	p	q	L	p	q	$G_{Lpq}(e)$
2	0	-2	2	2	2	0
2	0	-1	2	2	1	$-\frac{1}{2}e + \frac{1}{16}e^3 + \cdots$
2	0	0	2	2	0	$1 - \frac{5}{2}e^2 + \frac{13}{16}e^4 + \cdots$
2	0	1	2	2	-1	$\frac{7}{2}e - \frac{123}{16}e^3 + \cdots$
2	0	2	2	2	-2	$\frac{17}{2}e^2 - \frac{115}{6}e^4 + \cdots$
2	1	-2	2	1	2	$\frac{9}{4}e^2 + \frac{7}{4}e^4 + \cdots$
2	1	-1	2	1	1	$\frac{3}{2}e + \frac{27}{16}e^3 + \cdots$
			2	1	0	$1 - e^2 \; {}^{-3/2}$
3	0	-2	3	3	2	$\frac{1}{8}e^2 + \frac{1}{48}e^4 + \cdots$
3	0	-1	3	3	1	$-e + \frac{5}{4}e^3 + \cdots$
3	0	0	3	3	0	$1 - 6e^2 + \frac{423}{64}e^4 + \cdots$
3	0	1	3	3	-1	$5e - 22e^3 + \cdots$
3	0	2	3	3	-2	$\frac{127}{8}e^2 - \frac{3065}{48}e^4 + \cdots$
3	1	2	3	2	-2	$\frac{53}{8}e^2 + \frac{39}{16}e^4 + \cdots$
4	0	-2	4	4	2	$\frac{1}{2}e^2 - \frac{1}{3}e^4 + \cdots$

L	p	q	L	p	q	$G_{Lpq}(e)$
4	0	-1	4	4	1	$-\frac{3}{2}e + \frac{75}{16}e^3 + \cdots$
4	0	0	4	4	0	$1 - 11e^2 + \frac{199}{8}e^4 + \cdots$
4	0	1	4	4	-1	$\frac{13}{2}e - \frac{765}{16}e^3 + \cdots$
4	0	2	4	4	-2	$\frac{51}{2}e^2 - \frac{321}{2}e^4 + \cdots$
4	1	-2	4	3	2	$\left(\frac{3}{4}e^2\right)(1-e^2)^{-7/2}$
4	1	-1	4	3	1	$\frac{1}{2}e + \frac{33}{16}e^3 + \cdots$
4	1	0	4	3	0	$1 + e^2 + \frac{65}{16}e^4 + \cdots$
4	1	1	4	3	-1	$\frac{9}{2}e - \frac{3}{16}e^3 + \cdots$
4	1	2	4	3	-2	$\frac{53}{4}e^2 - \frac{179}{24}e^4 + \cdots$
4	2	-2	4	2	2	$5e^2 + \frac{155}{12}e^4 + \cdots$
4	2	-1	4	2	1	$\frac{5}{2}e + \frac{135}{16}e^3 + \cdots$
			4	2	0	$\left(1 + \frac{3}{2}e^2\right)(1-e^2)^{-7/2}$

Appendix D: Atmospheric Density

Figure D1 shows a small element of unit volume of atmosphere.

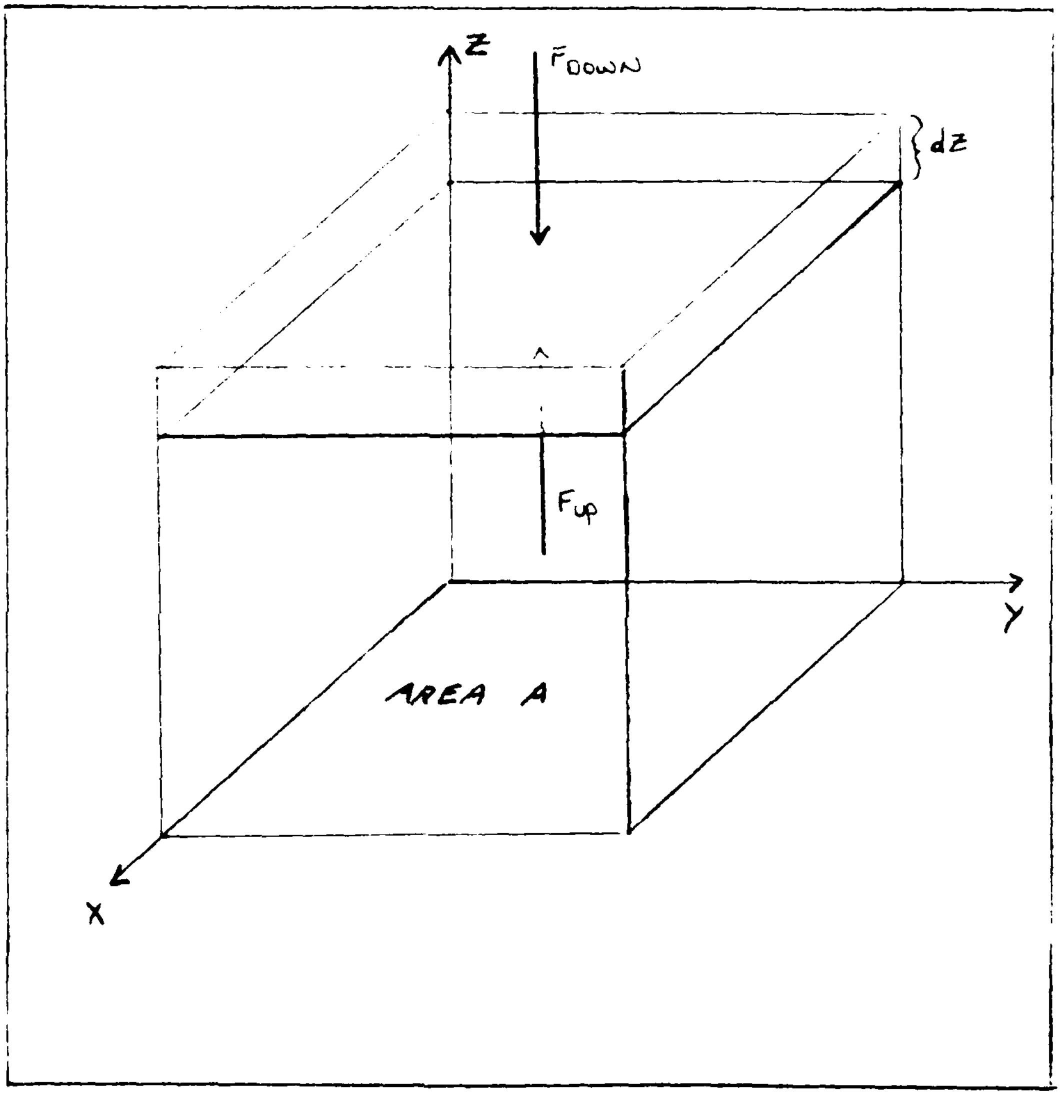

Unit Volume Element of Atmosphere (7:1)

Figure D.1

Let the mass of the unit volume of atmosphere be denoted by m. Then (7:2):

$$\underline{m} = \frac{\sum N_i M_i}{\sum N_i} \tag{D1.1}$$

where m = the mean molecular mass of the unit volume atmosphere

N_i = the number of molecules of type i per unit volume

M_i = the molecular mass of type i molecule

Since the unit volume element of the atmosphere is stationary (i.e. no thermal effects are being considered):

$$F_{UP} + F_{DOWN} = 0 \tag{D1.2}$$

where

$$F_{UP} = A\left[P(z+dz) - P(z)\right] \tag{D1.3}$$

$$F_{DOWN} = \left(\sum N_i M_i\right)(A dz)g$$

Applying equations (D1.3) to (D1.2) yields:

$$P(z+dz) - P(z) = -\left(\sum N_i M_i\right)(dz)g \tag{D1.4}$$

$$dP = -g\left(\sum N_i M_i\right)dz$$

where P = the total pressure of the atmosphere at height z

A = the area on the surface of the planet subtended by the unit volume of atmosphere

g = the acceleration due to gravity

From the ideal gas law an expression for the total pressure can be written as (9:12):

$$P = \frac{\left(\sum N_i\right)RT}{V} \tag{D1.5}$$

where R = the universal gas constant

T = the temperature

V = the volume

But

$$\frac{\sum N_i}{V} = \rho = density \tag{D1.6}$$

So equation (D1.5) becomes:

$$P = \rho RT \tag{D1.7}$$

Writing equation (D1.4) in terms of equation (D1.7) yields:

$$\rho(z+dz)RT = -g\left(\sum N_i M_i\right)dz \tag{D1.8}$$

$$\rho(z+dz) = -\frac{g\sum N_i M_i}{RT}dz$$

$$d\rho = -\frac{g\sum N_i M_i}{RT}dz$$

Noting that for the unit volume element, $V=1$, dividing equation (D1.8) by equation (D1.6), and applying equation (D1.1) yields:

$$\frac{d\rho}{\rho} = -\frac{g\sum N_i M_i}{\sum N_i RT}dz \tag{D1.9}$$

$$= -\frac{g\overline{m}}{RT}dz$$

Taking the integral of both sides of equation (D1.9) yields:

$$\ln\rho = -\frac{g\overline{m}}{RT}z + c \tag{D1.10}$$

When $z=0$, $c=\ln\rho_0$. As a result equation (D1.10) becomes:

$$\ln\left(\frac{\rho}{\rho_0}\right) = -\frac{g\overline{m}}{RT}z \tag{D1.11}$$

Taking the exponential of both sides of equation (D1.11) yields:

$$\rho = \rho_0 \exp\left\{ -\frac{gm}{RT} z \right\} \tag{D1.12}$$

Program Mars1

```
C234567*********************************************************
C     This program calculates the geopotential field around    *
C     the planet Mars.  It writes data into file MARSGRAV.DAT  *
C     in three columns (corresponding to X,Y,Z coordinates)    *
C     where                                                    *
C     X = Longitude                                            *
C     Y = Latitude                                             *
C     Z = the value of the Geopotential                        *
C                                                              *
CWritten by  J. W. Foister, III                                *
CDate                 10 Sept 87                               *
C                                                              *
C234567*********************************************************
$NOFLOATCALLS
      PROGRAM MARS1
      REAL*8 C(19,19),S(19,19),LP(19,19),LAT,PHI,PI,
     1 MU,RP,R,LONG,V,PT(91,91),B
C234567*********************************************************
C     C    = The nondimensional c coefficient to the grav model *
C     S    = The nondimensional s coefficient to the grav model *
C     LP   = The values of the Legendre, and associated Legendre*
C            polynomials                                        *
C     LAT  = The latitude                                       *
C     PHI  = The sin of the latitude                            *
C     PI   = The classic irrational number                      *
C     MU   = The universal gravitational constant multiplied by *
C            the mass of the planet Mars                        *
C     RP   = the equatorial radius of Mars                      *
C     R    = The distance from the center of Mars at which it is*
C            desired to calculate the geopotential              *
C     LONG = The longitude                                      *
C     V    = An intermediate value of the geopotential (calculat*
C            ion not yet complete)                              *
C     PT   = The value of the geopotential at a particular point*
C     B    = Intermediate step in calculating geopotential      *
C234567*********************************************************
C
C
C
      INTEGER i,j,k,m,n
C234567***** Determine/Set the intial values *******************
      PI=4.D0*DATAN(1.D0)
      MU=4.2828287D4
      RP=3393.4D0
      R=3893.4D0
      LAT=-90.D0
      LONG=0.D0
      V=0.D0
C234567
      OPEN(1,FILE='MGRAV',STATUS='OLD')
C234567   This file contains an 18 by 18 gravity model of Mars
C         Source: Jet Porpulsion Laboratory, EM 312/87-153
C                                             20 April 1987
C234567
      C(1,1)=1.D0
      S(1,1)=0.D0
      C(2,1)=0.D0
      S(2,1)=0.D0
      C(2,2)=0.D0
      S(2,2)=0.D0
      DO 10 i=3,19
         DO 20 j=1,i
         READ(1,'(25X,F15.13,15X,F15.13)') C(i,j),S(i,j)
20       CONTINUE
10    CONTINUE
C234567
```

```
67        CLOSE(1)
68        OPEN(1,FILE='MARSGRAV.DAT')
69  C        This file will contain this programs output
70  C234567************************************************************
71  C Start with the latitude and longitude established in line 52  *
72  C and 53 of this program.  Then for each value of latitude cal  *
73  C ulate the Legendre polynomials, and step from 0 longitude to  *
74  C 360 by 4 degree increments calculating the geopotential as    *
75  C you go.  When caluclations are complete for a particular lat  *
76  C itude, increment latitude by 2 degrees and start all over agai*
77  C234567************************************************************
78        WRITE(*,150)
79  150   FORMAT(20X,'LAT =-90 DEGREES   LONG = 0.0 DEGREES')
80        LAT=LAT*(PI/180.D0)
81        DO 30 i=1,91
82           PHI=DSIN(LAT)
83  C234567************************************************************
84  c collect all the legendre poly. assosicated with the latitude
85  C This subroutine was written by J. H. Kwok as part of ASAP      *
86        CALL LEGEND(18,18,PHI,LP)
87  C234567************************************************************
88  c now establish a particular latitude and step through all
89  c values of longitude for that latitude
90         DO 60 j=1,91
91               V=0.D0
92            DO 70 n=1,19
93               DO 80 m=1,n
94                B=C(n,m)*DCOS((m-1)*LONG)+S(n,m)*DSIN((m-1)*LONG)
95                V=LP(n,m)*B+V
96  80           CONTINUE
97            V=((RP/R)**(n))*V
98  70        CONTINUE
99         PT(i,j)=-(MU/R)*V
100        LONG=LONG*(180.D0/PI)+4.D0
101          WRITE(*,220) LONG
102 220      FORMAT(40X,'LONG = ',F30.15)
103        LONG=LONG*(PI/180.D0)
104 60     CONTINUE
105       LONG=0.D0
106        LAT=LAT*(180.D0/PI)+2.D0
107           WRITE(*,230) LAT
108 230       FORMAT(20X,'LAT = ',F30.15)
109        LAT=LAT*(PI/180.D0)
110 30    CONTINUE
111 C234567********  Routine to write data to data file  ************
112       LAT=-90.D0
113       LONG=0.D0
114       DO 90 i=1,91
115             LONG=0.D0
116          DO 100 j=1,91
117             WRITE(*,200) LAT,LONG,PT(i,j)
118             WRITE(1,200) LAT,LONG,PT(i,j)
119 200         FORMAT(1X,F30.15,1X,F30.15,1X,F30.15)
120             LONG=LONG+4.D0
121 100      CONTINUE
122             LAT=LAT+2.D0
123 90    CONTINUE
124 C234567
125       STOP
126       END
```

Data File MGRAV, Mars Gravity Model

The following is an 18 by 18 gravity model of Mars (see reference 13).

L	m	C	S
2	0	-.196045446D-02	.000000000D+00
2	1	.000000000D+00	.000000000D+00
2	2	-.547326856D-04	.313950595D-04
3	0	-.314492574D-04	.000000000D+00
3	1	.447686230D-05	.268959963D-04
3	2	-.557915148D-05	.289455551D-05
3	3	.484500981D-05	.360651187D-05
4	0	.188943678D-04	.000000000D+00
4	1	.349376617D-05	.398991302D-05
4	2	-.207679791D-06	-.219936945D-05
4	3	.417451933D-06	.162519077D-07
4	4	-.361428569D-08	-.276521879D-06
5	0	-.266924852D-05	.000000000D+00
5	1	.894766531D-07	.308526456D-05
5	2	-.720193726D-06	-.293288206D-06
5	3	.832996054D-07	.149487871D-07
5	4	-.385168584D-07	-.207595805D-07
5	5	-.109219527D-07	.919565583D-08
6	0	.134075698D-05	.000000000D+00
6	1	.271525423D-05	-.246253833D-05
6	2	.213067102D-06	.181410819D-06
6	3	.223152945D-07	.445497372D-07
6	4	.483156237D-08	.823473177D-08
6	5	.160879585D-08	.123736685D-08
6	6	.657537516D-09	.228632415D-09
7	0	.953741475D-05	.000000000D+00
7	1	-.206001412D-06	.763581399D-06
7	2	.250370055D-06	.191207892D-07
7	3	.867979547D-08	-.245968398D-07
7	4	.438492756D-08	-.119730141D-08
7	5	-.173195787D-09	-.680670137D-09
7	6	-.221682749D-10	-.122380471D-09
7	7	.119528233D-10	-.441439878D-10
8	0	-.193679382D-05	.000000000D+00
8	1	-.252155307D-06	-.440871508D-07
8	2	.198283464D-06	-.222818552D-07
8	3	-.744492089D-08	.168273842D-07
8	4	.180188344D-08	.870606083D-09
8	5	-.416374748D-09	-.288259952D-09
8	6	-.285094540D-10	-.426112296D-10
8	7	-.359107648D-11	.831516583D-11
8	8	.131693828D-13	-.907998398D-12
9	0	.297973316D-05	.000000000D+00
9	1	.792173764D-06	-.173565293D-06
9	2	.811195624D-07	.371532024D-07
9	3	-.111353505D-07	-.178980646D-07
9	4	-.393202454D-09	.159736275D-08
9	5	-.208064442D-09	-.181003288D-09
9	6	.130134517D-11	.346518782D-11
9	7	-.239656251D-12	.155142518D-11
9	8	.846636412D-13	-.134516525D-13
9	9	-.129159190D-12	.669405839D-13
10	0	-.214587140D-05	.000000000D+00
10	1	.505175679D-06	-.467074615D-06
10	2	.216973907D-07	-.463249130D-07
10	3	.367957903D-08	.917348832D-08
10	4	-.538542186D-09	-.585013360D-09
10	5	.392417842D-10	-.356486582D-10
10	6	.763183573D-11	-.288267583D-11
10	7	-.120760979D-12	.141799288D-12
10	8	.106724719D-12	.120979573D-12
10	9	-.254490861D-13	-.308310394D-13
10	10	-.522230377D-14	.280057675D-14

11	0	-.276297743D-05	.000000000D+00
11	1	-.422119586D-06	-.641987552D-06
11	2	-.273903461D-07	-.494207165D-07
11	3	.679530071D-09	-.249855717D-08
11	4	-.442569660D-09	-.343286924D-09
11	5	.850675190D-11	.155014669D-10
11	6	.594002688D-12	.406059896D-11
11	7	.631782969D-12	-.273273893D-12
11	8	-.261659977D-13	-.275980967D-13
11	9	-.102229153D-13	.104867061D-14
11	10	.254299637D-15	.192200463D-14
11	11	.408741643D-16	-.187645208D-15
12	0	.724509650D-06	.000000000D+00
12	1	-.665441647D-06	-.783022446D-07
12	2	.412814620D-07	.176086232D-07
12	3	-.228523486D-08	-.259996939D-08
12	4	-.138990748D-09	-.324803100D-11
12	5	.430141608D-10	-.200578698D-11
12	6	-.281462344D-11	-.179903336D-11
12	7	.422558135D-13	.405214999D-12
12	8	-.606810280D-14	.127944398D-13
12	9	.401661164D-14	-.440694307D-14
12	10	.184496962D-15	.354385774D-15
12	11	.476538999D-16	-.786062825D-16
12	12	-.295776875D-17	.802086213D-17
13	0	-.543198032D-05	.000000000D+00
13	1	-.105510215D-08	.877020886D-09
13	2	.111588505D-07	-.197347899D-07
13	3	.313552813D-08	.212305884D-08
13	4	.141892690D-09	.825861835D-10
13	5	.213535691D-10	-.585077221D-11
13	6	-.758128724D-12	-.192699340D-11
13	7	-.193744173D-12	.936949857D-14
13	8	-.889208276D-14	-.130598439D-14
13	9	.161895047D-14	.165232772D-14
13	10	.248001154D-16	-.126971688D-15
13	11	.138791059D-16	.104356450D-17
13	12	-.639743167D-18	-.796208536D-18
13	13	.107263536D-18	.340715758D-18
14	0	.478772159D-06	.000000000D+00
14	1	-.332426980D-06	.297621694D-06
14	2	-.435088996D-08	-.356872650D-07
14	3	.169891626D-08	-.207647667D-08
14	4	.139919334D-09	-.255099836D-10
14	5	-.430148645D-11	-.154072699D-10
14	6	-.525284102D-12	.574060758D-12
14	7	.171152471D-13	.332481028D-13
14	8	.548898505D-16	-.135105153D-14
14	9	.277704867D-15	.168216163D-15
14	10	.396465938D-16	-.311637989D-16
14	11	-.497691886D-17	.106379919D-17
14	12	-.390690533D-19	.164038719D-18
14	13	.217992662D-19	.934648560D-19
14	14	.132110275D-19	-.559726427D-20
15	0	-.148268106D-05	.000000000D+00
15	1	-.104584515D-06	.227412119D-07
15	2	.477029989D-08	.595709129D-09
15	3	-.672384900D-09	-.240384972D-08
15	4	-.260831862D-10	-.984258303D-10
15	5	-.154606226D-11	-.110921013D-10
15	6	-.537048685D-12	.415150164D-12
15	7	.423676862D-13	.428137862D-13
15	8	.359166823D-14	-.856596602D-15
15	9	-.999521187D-16	.319062543D-17
15	10	-.104419170D-16	.480719744D-18
15	11	-.101354149D-17	.901416487D-18
15	12	.125915532D-18	.123448148D-18
15	13	-.107031158D-20	.778559537D-20
15	14	-.235822167D-20	-.306632691D-20
15	15	-.436863339D-21	.775293774D-23
16	0	.210341751D-05	.000000000D+00
16	1	.241073171D-06	-.110457364D-06

16	2	-.182440905D-08	-.303832411D-07
16	3	.857232052D-09	-.444078356D-09
16	4	-.682555079D-10	-.510326275D-10
16	5	.433793270D-11	.302290752D-11
16	6	.136323587D-12	-.104891886D-12
16	7	-.121384042D-13	.112850738D-13
16	8	-.244945719D-16	-.621086011D-15
16	9	.783639045D-16	-.183450204D-16
16	10	.253503225D-17	.524889864D-17
16	11	-.240362445D-18	.933612186D-19
16	12	-.256512352D-20	.346539446D-19
16	13	-.497431552D-20	.221065646D-20
16	14	.104731289D-21	-.922733087D-21
16	15	-.115474494D-21	.449029743D-23
16	16	-.132508126D-22	.736531139D-24
17	0	.632588722D-06	.000000000D+00
17	1	-.352520530D-06	.804202741D-07
17	2	-.647275359D-08	.316134760D-08
17	3	-.368277640D-09	-.596912836D-09
17	4	-.162888684D-10	.635013369D-10
17	5	.317766095D-11	.589913917D-13
17	6	.178400288D-12	.362066925D-12
17	7	.222378189D-13	-.442859983D-14
17	8	-.858389410D-15	-.105498786D-14
17	9	-.836249338D-16	-.300267024D-16
17	10	.163218614D-17	.305185874D-17
17	11	.401578743D-21	.185824464D-19
17	12	.346096770D-21	.193848107D-19
17	13	.114615315D-21	-.845205020D-21
17	14	-.506255786D-22	-.845367336D-22
17	15	-.184195390D-22	.681759100D-23
17	16	.212302575D-23	-.148479434D-23
17	17	.332518713D-24	.447497480D-25
18	0	.794786830D-06	.000000000D+00
18	1	.142558531D-07	-.997992732D-07
18	2	.625982398D-08	.172674827D-07
18	3	-.139155110D-11	.242854118D-10
18	4	.267161837D-11	.567965311D-10
18	5	.196738667D-11	-.943658879D-12
18	6	-.104261777D-12	-.947694516D-13
18	7	-.708729256D-14	-.505267640D-15
18	8	.339408632D-15	-.579459532D-15
18	9	-.343122925D-16	.186741541D-16
18	10	.149402749D-17	.411773895D-17
18	11	.292146270D-19	.323201624D-19
18	12	.240629777D-20	-.891144216D-20
18	13	-.447926768D-22	-.399393250D-22
18	14	.518577432D-23	-.679543490D-22
18	15	.742435657D-24	.660693902D-23
18	16	.637594803D-24	.194527232D-24
18	17	-.442155409D-26	-.126956739D-24
18	18	.184429013D-25	.110393602D-25

Program Omega

```
C234567****************************************************************
C     Omega is a program that finds the roots to delta omega          *
C     where the equations for delta omega (change in arg. of the      *
C     periapsis) are found in THE MOTION OF A SATELLITE IN AN AXI-    *
C     SYMMETRIC GRAVITATIONAL FIELD, by R. H. MERSON.  As found in    *
C     the Geophysical Journal Vol 4, 1961, p.17. This program finds*
C     the roots of delta omega as a function of f, f=(sin i)**2.      *
C     The primary equation is: delta omega = cf**3+bf**2+af+d=0.      *
C     Where a,b,c, and d are constants depending on the semi major *
C     axis and the eccentricity                                       *
C                                                                     *
C WRITTEN BY J.W. FOISTER, III                                        *
C DATE   AUG 5 1987                                                   *
C                                                                     *
C     J(1) =                                                          *
C     J(2) = C20 coefficient                                          *
C     J(3) =                                                          *
C     J(4) = C40 coefficient                                          *
C     J(5) =                                                          *
C     J(6) = C60 coefficient                                          *
c234567****************************************************************
$NOFLOATCALLS
      PROGRAM OMEGA
C
C
C234567**********  DEFINE THE VARIABLES ****************************
      REAL*8 J(6),LAT,A,B,C,D,E,F(3),EC,DLTA,P,Q,R,X(3),Y,THETA(3),
     1  SEMI,PI,W(3),TP,AHLD
C
C
C234567
      INTEGER i,k,COUNTER
C
      PI=4.D0*DATAN(1.D0)
      R=1.D0
C234567*******     Following values are for the planet Mars   ********
      J(2)=-0.196045446D-02
      J(4)=0.188943678D-04
      J(6)=0.134075698D-05
C
      OPEN(1,FILE='LPT1')
200   FORMAT(1X,'f = ',F30.15)
210   FORMAT(1X,'f',i1,' = ',F30.15)
C
C234567*******     INPUT THE DATA ************************************
      WRITE(*,100)
100   FORMAT(1X,'Semi Major axis equals... in KMs...(F30.15)....',\)
      READ(*,'(F30.15)') SEMI
      WRITE(1,105) SEMI
105   FORMAT(1X,'The Semi Major axis in Km is ',F30.15)
      WRITE(*,105) SEMI
C234567 convert from KM to Du's this is for a Mars orbit
      SEMI=SEMI/3393.4
C234567
      WRITE(*,110)
110   FORMAT(1X,'Eccentricity equals ... (F30.15)......',\)
      READ(*,'(F30.15)') EC
      AHLD=(3.D0/2.D0)
      TP=(2*PI)*(SEMI**AHLD)
C234567****** This converts from Mars Time Units to Minutes *******
      TP=TP*(15.9197403800)
C
      WRITE(*,120) SEMI,TP,EC
      WRITE(1,120) SEMI,TP,EC
120   FORMAT(1X,'For the Semi Major axis = ',F30.15,
     1 ' the period (in minutes) is ',F30.15,/,
     2 ' and Eccentricity = ',F30.15)
C234567********* CALCULATE THE VALUES OF THE COEFFICIENTS **********
      LAT=SEMI*(1-EC**2)
```

```
C SEMI = semi major axis, LAT = semi latus rectum
      J(1)=J(4)*((R/LAT)**4)
      J(3)=J(6)*((R/LAT)**6)
      J(5)=(J(2)**2)*((R/LAT)**4)
C  A through D are coefficients described in line 8 of this program
      A=(-(15.D0/4.D0)*J(2)*((R/LAT)**2))
      A=A+J(1)*((930.D0/32.D0)+(945.D0/32.D0)*EC**2)
      A=A+J(3)*((-33600.D0/320.D0)-((22575.D0/64.D0)*EC**2)
     1  -((14175.D0/128.D0)*EC**4))
      A=A+J(5)*((855.D0/48.D0)-((27.D0/32.D0)*EC**2))
C234567
      B=J(1)*((-735.D0/32.D0)-((2835.D0/128.D0)*EC**2))
      B=B+J(3)*((541800.D0/2560.D0)+((343350.D0/512.D0)*EC**2)
     1  +((51975.D0/256.D0)*EC**4))
      B=B+J(5)*((-4005.D0/192.D0)-((135.D0/128.D0)*EC**2))
C234567
      C=J(3)*((-1247400.D0/10240.D0)-((381150.D0/512.D0)*EC**2)
     1  -((225225.D0/2048.D0)*EC**4))
C234567
      D=3.D0*J(2)*((R/LAT)**2)+J(1)*((-240.D0/32.D0)
     1  -((270.D0/32.D0)*EC**2))+J(3)*((4200.D0/320.D0)
     2  +((3150.D0/64.D0)*EC**2)+((1050.D0/64.D0)*EC**4))
     3  +J(5)*((63.D0/48.D0)*EC**2)
C234567
      P=((A/C)-((B/C)**2)/3.D0)
      Q=((2.D0/27.D0)*((B/C)**3)-((A*B)/(3.D0*C**2))+(D/C))
C234567
      DLTA=(-27.D0*Q**2)-(4.D0*P**3)
C
      IF (DLTA .LT. 0.0) THEN
C one real root exist
          GOTO 500
      ELSEIF (DLTA .GE. 0.0) THEN
C all roots are real, if dlta = 0 then two of the roots are the same
c                     if dlta > 0 then all three roots are different
          GOTO 700
      ELSE
      ENDIF
C234567*******  NEWTON - RAPHSON METHOD ***************************
500   COUNTER=0
C234567set inital guess of f value
      X(1)=0.5D0
503   IF (COUNTER .GT. 100) THEN
         WRITE(1,505) COUNTER
505      FORMAT(1X,'After ',i3,' iterations')
         F(1)=X(2)
         GOTO 800
      ELSE
      ENDIF
      W(1)=(2.D0*C*X(1)**3)+(B*X(1)**2)-D
      W(2)=(3.D0*C*X(1)**2)+(2.D0*B*X(1))+A
      IF (W(2) .EQ. 0.0) THEN
         WRITE(1,510)
510      FORMAT(1X,'First derivative = 0, program stopped')
         GOTO 900
      ELSE
      ENDIF
C234567
      X(2)=W(1)/W(2)
      X(3)=X(2)-X(1)
      X(3)=DABS(X(3))
      IF (X(3) .LE. 1.D-12) THEN
Cthe root to the equation is X(2)
         F(1)=X(2)
         COUNTER=0
         GOTO 800
      ELSEIF (DABS(X(3)) .GT. 1.D-12) THEN
Cthe root has yet to be identified
         COUNTER=COUNTER+1
         X(1)=X(2)
         GOTO 503
      ELSE
```

```
      ENDIF
C234567**********  ROUTINE TO FIND CUBIC ROOT *****************
700   THETA(1)=(3.D0*DSQRT(3)*Q)/(2.D0*P*DSQRT(-P))
      THETA(1)=(DACOS(THETA(1)))/3.D0
      THETA(2)=THETA(1)+((2.D0*PI)/3.D0)
      THETA(3)=THETA(1)-((2.D0*PI)/3.D0)
      E=DSQRT((-4.D0*P)/3.D0)
      X(1)=E*DCOS(THETA(1))
      X(2)=E*DCOS(THETA(2))
      X(3)=E*DCOS(THETA(3))
      F(1)=X(1)-(B/(3.D0*C))
      F(2)=X(2)-(B/(3.D0*C))
      F(3)=X(3)-(B/(3.D0*C))
      DO 10 i=1,3
         WRITE(1,210) i, F(i)
         WRITE(*,210) i, F(i)
10    CONTINUE
      GOTO 900
C234567**********************************************************
800   WRITE(1,810) F(1), X(3)
      WRITE(*,810) F(1), X(3)
810   FORMAT(1X,'The root is  ',F30.15,/,' The error is ',F30.15)
C234567**********************************************************
900   STOP
      END
```

Program Capmega

```
C234567***********************************************************
C     CAPMEGA is a program that finds the root to delta cap        *
C     omega, the equation delta cap omega being defined in         *
C     The Motion of a satellite in an Axi-symmetric Gravitational  *
C     Field, by R. H. Merson .  As found in the Geophysical Journal*
C     Vol 4, 1961, p.17.  This program finds the roots of delta    *
C     omega as a function of f, where f=(sin i)**2.  The  primary  *
C     equation is : delta cap omega = Af**2 + Bf + C = 0.  Where   *
C     A,B,and C are constants depending on the semi major axis and *
C     the Eccentricity                                             *
C                                                                  *
C WRITTEN BY J.W. FOISTER, III                                     *
C DATE   AUG 21 1987                                               *
C                                                                  *
C     J(1) =                                                       *
C     J(2) = C20 coefficient                                       *
C     J(3) =                                                       *
C     J(4) = C40 coefficient                                       *
C     J(5) =                                                       *
C     J(6) = C60 coefficient                                       *
c234567***********************************************************
$NOFLOATCALLS
      PROGRAM CAPMEGA
C
C
C234567********** DEFINE THE VARIABLES ***************************
      REAL*8 J(6),LAT,A,B,C,D,E,F(3),EC,DLTA,P,Q,R,X(3),Y,THETA(3),
     1  SEMI,PI,W(3),TP,AHLD,RP
C
C
C234567
      INTEGER i,k,COUNTER
C
      PI=4.D0*DATAN(1.D0)
      R=1.D0
C234567
      J(2)=-0.196045446D-02
      J(4)=0.188943678D-04
      J(6)=0.134075698D-05
C
      OPEN(1,FILE='LPT1')
200   FORMAT(1X,'f = ',F30.15)
210   FORMAT(1X,'f',i1,' = ',F30.15)
C
C234567*******    INPUT THE DATA ***********************************
      WRITE(*,100)
100   FORMAT(1X,'Semi Major axis equals... in KMs...(F30.15)....',)
      READ(*,'(F30.15)') SEMI
      WRITE(*,110)
11)
      READ(*,'(F30.15)') EC
C234567 find the Radius of the Periapsis
      RP=SEMI*(1-EC)
      WRITE(*,105) SEMI,RP
      WRITE(1,105) SEMI,RP
105   FORMAT(/,1X,'The Semi Major axis in Km is ',F30.15,/,
     1 ' The Radius of Periapsis in Km is ',F30.15)
C234567 convert from KM to Du's this is for a Mars orbit
      SEMI=SEMI/3393.4D0
C234567
      AHLD=(3.D0/2.D0)
      TP=(2.D0*PI)*(SEMI**AHLD)
      TP=TP*(15.9197403800)
C
      WRITE(*,120) SEMI,TP,EC
      WRITE(1,120) SEMI,TP,EC
120   FORMAT(1X,'For the Semi Major axis = ',F30.15,
     1 ' the period (in minutes) is ',F30.15,/,
     2 ' and Eccentricity = ',F30.15)
```

```
C234567********* CALCULATE THE VALUES OF THE COEFFICIENTS **********
      LAT=SEMI*(1.D0-EC**2)
C
      J(1)=J(4)*((R/LAT)**4)
      J(3)=J(6)*((R/LAT)**6)
      J(5)=(J(2)**2)*((R/LAT)**4)
C234567
      A=((-51975.D0/1024.D0)*EC**4)-((17325.D0/128.D0)*EC**2)
     1  -(3465.D0/128.D0)
      A=J(3)*A
C
      B=J(3)*(((14175.D0/256.D0)*EC**4)+((4725.D0/32.D0)*EC**2)+
     1(945.D0/32.D0))+(J(1)*(((-315.D0/32.D0)*EC**2)-(105.D0/16.D0)
     2 ))+(J(5)*(((-45.D0/32.D0)*EC**2)-(15.D0/2.D0)))
C
      C=J(3)*(((-1575.D0/128.D0)*EC**4)-((-525.D0/16.D0)*EC**2)
     1 -(105.D0/16.D0))+(J(1)*(((45.D0/8.D0)*EC**2)+(15.D0/4.D0)))
     2 +(J(5)*(((-3.D0/8.D0)*EC**2)+(9.D0/8.D0)))
      C=C+(J(2)*((R/LAT)**2))*(-3.D0/2.D0)
C234567
      W(1)=(B**2)-(4.D0*A*C)
      IF (W(1) .LT. 0.0) THEN
         WRITE(*,300)
         WRITE(1,300)
300      FORMAT(1X,'THE ROOTS ARE IMAGINARY!')
         W(2)=-B/(2.D0*A)
         W(3)=W(1)/(2.D0*A)
         WRITE(*,310) W(2),W(3)
         WRITE(1,310) W(2),W(3)
310   FORMAT(1X,'ROOT 1 = ',F30.15,' + i ',F30.15)
         WRITE(*,320) W(2),W(3)
         WRITE(1,320) W(2),W(3)
320   FORMAT(1X,'ROOT 2 = ',F30.15,' - i ',F30.15)
         GOTO 900
      ELSE
      ENDIF
C
      F(1)=(-B+DSQRT(W(1)))/(2.D0*A)
      F(2)=(-B-DSQRT(W(1)))/(2.D0*A)
      WRITE(*,330) F(1),F(2)
      WRITE(1,330) F(1),F(2)
330   FORMAT(1X,'ROOT 1 = ',F30.15,/,' ROOT 2 = ',F30.15)
C234567
900   STOP
      END
```

Program Dsemi

```
C234567**********************************************************
C      This program solves for the change in the semi major axis, *
C      and the change in the eccentricity over one orbital period *
C      with the change due solely to air drag.  Equation 4.14 and *
C      equation 4.11 from Desmond King-Hele's book, THEORY OF     *
C      SATELLITE ORBITS IN AN ATMOSPHERE are used as the          *
C      expression of change in semi major axis, and eccentricity  *
C      These equations include integrals, and therefore requrires *
C      an integration.  A standard 8th order Gaussian-Legendre    *
C      quadrature method is used to perform this integration.     *
C      The interval of integration (from 0 to 2 pi) will be broken*
C      up into four intervals (from 0 to pi/2, from pi/2 to pi    *
C      from pi to 3pi/2, from 3pi/2 to 2pi) and the Gaussian -    *
C      Legendre quadrature will be applied to each interval.  This*
C      will improve the accuracy of this routine.                 *
C                                                                 *
CWritten by J. W. Foister, III                                    *
C                                                                 *
CDate        22 Sept. 1987                                        *
C                                                                 *
C234567**********************************************************
$NOFLOATCALLS
      PROGRAM DSEMI
C
      REAL*8 A,AK(4),EK(4),PI,RHO,RHOO,DELTA,F,INCL,RPO,VPO,
     1 S,CD,M,EC,H,MU,W,DA,DE,E,YE,XE,INT
C234567*****DEFINITION OF VARIABLES******************************
C      A     = intial value of the semi major axis  (km)          *
C      AK(4) = the Gaussian quadrature coefficients               *
C      EK(4) = the values of E, the independent varialbe where    *
C              f(E) = 0.                                          *
C      PI    = the irrational number pie.                         *
C      RHO   = the density of the atmosphere in (kg)/(km**3)      *
C      RHOO  = the reference density of the atmosphere            *
C      DELTA = the surface area of the satellite times the coeff. *
C              of drag divided by the mass of the satellite, with *
C              the entire quanity multiplied by a correction      *
C              factor that converts the velocity of the satellite *
C              wrt the center of the planet, to a velocity wrt the*
C              atmosphere in which it is moving. (F)              *
C      RPO   = the reference periapsis (km)                       *
C      F     = the conversion factor that changes the velocity    *
C              term from one relative to the center of the planet *
C              to one relative to the atmosphere                  *
C      INCL  = the angle of inclination   (radians)               *
C      VPO   = the velocity of the satellite at RPO (km)/(sec)    *
C      S     = the reference area of the satellite (km**2)        *
C      CD    = the coefficient of drag                            *
C      M     = the mass of the satellite  (kg)                    *
C      EC    = the eccentricity                                   *
C      H     = the scale height  (km)                             *
C      MU    = the gravitational constant times the radius of the *
C              planet  (km**3)/(sec**2)                           *
C      W     = the rotational velocity of the planet (rad/sec)    *
C      DA    = the change in A                                    *
C      DE    = the change in Eccentricity                         *
C      YE    = the integrand for change in A equation             *
C      XE    = the integrand for change in Eccentricity equation  *
C      DE    = the change in eccentricity over one orbital period *
C      INT   = the constant need inorder to perform the needed    *
C              change in varialbe required by the interval        *
C234567**********************************************************
C
       INTEGER i,j,k
C
C
       DATA EK/.96028986D0,.79666648D0,.52553241D0,.18343464D0/
C
       DATA AK/.10122854D0,.22238103D0,.31370665D0,.36268378D0/
```

```
C
      OPEN(1,FILE='LPT1')
C
C234567*************DEFINE THE CONSTANTS*************************
      PI=4.D0*DATAN(1.D0)
      RHO0=3.3D-3
      S=1.D-5
      CD=2.D0
      M=1000.D0
      H=14.13867049D0
      RPO=3593.4D0
      MU=4.2828287D4
      VPO=DSQRT(MU/RPO)
      W=(4.061249803D-3)*(PI/180.D0)
      INCL=(45.D0)*(PI/180.D0)
      F=(1.D0-(RPO/VPO)*W*DCOS(INCL))**2
      A=5133.428571D0
      EC=.3D0
      DELTA=(F*S*CD)/M
      WRITE(*,500) PI,RHO0,S,CD,M,H,RPO,MU
      WRITE(1,500) PI,RHO0,S,CD,M,H,RPO,MU
500   FORMAT(1X,'PI= ',F30.15,' RHO0= ',F30.15,/
     1         ,' S= ',F30.15,'  CD=   ',F30.15,/,
     2          ' M= ',F30.15,'  H=    ',F30.15,/,
     3          ' RPO=',F30.15,' MU=   ',F30.15)
      WRITE(*,600) VPO,W,INCL,F,A,EC,DELTA
      WRITE(1,600) VPO,W,INCL,F,A,EC,DELTA
600   FORMAT(1X,'VPO= ',F30.15,' W= ',F30.15,/,
     1          ' INCL=',F30.15,' F= ',F30.15,/,
     2          ' A =  ',F30.15,' EC=',F30.15,/,
     3          ' DELTA = ',F30.15)
C234567**********************************************************
      DA=0.D0
      DE=0.D0
C234567*********determine the interval*************************
      DO 10 i=1,4
         IF (i .EQ. 1) THEN
            INT=1.D0
         ELSEIF (i .EQ. 2) THEN
            INT=3.D0
         ELSEIF (i .EQ. 3) THEN
            INT=5.D0
         ELSEIF (i .EQ. 4) THEN
            INT=7.D0
         ELSE
         ENDIF
C234567********start the quadrature***************************
      DO 20 j=1,4
         DO 30 k=1,2
            IF (k .EQ. 1) THEN
               E=(PI/4.D0)*(EK(j)+INT)
            ELSEIF (k .EQ. 2) THEN
               E=(PI/4.D0)*(-EK(j)+INT)
            ELSE
            ENDIF
         RHO=RHO0*DEXP(((-A*EC)/H)*(1.D0-DCOS(E)))
         YE=(1.D0+EC*DCOS(E))**(1.5)
         YE=(YE/DSQRT(1.D0-EC*DCOS(E)))*RHO
         XE=RHO*(1.D0-EC**2)*DCOS(E)
         XE=XE*DSQRT((1.D0+EC*DCOS(E))/(1.D0-EC*DCOS(E)))
         DA=(AK(j)*YE)+DA
         DE=(AK(j)*XE)+DE
30       CONTINUE
20    CONTINUE
10    CONTINUE
C234567
      DA=-(A**2)*DELTA*(PI/4.D0)*DA
      DE=-A*DELTA*(PI/4.D0)*DE
C234567
      WRITE(*,100) DA,DE
      WRITE(1,100) DA,DE
100   FORMAT(1X,'Delta semi major axis = ',F30.15,/,
```

```
     1          ' Delta eccentricity    = ',F30.15)
C234567********************************************************
      STOP
      END
```

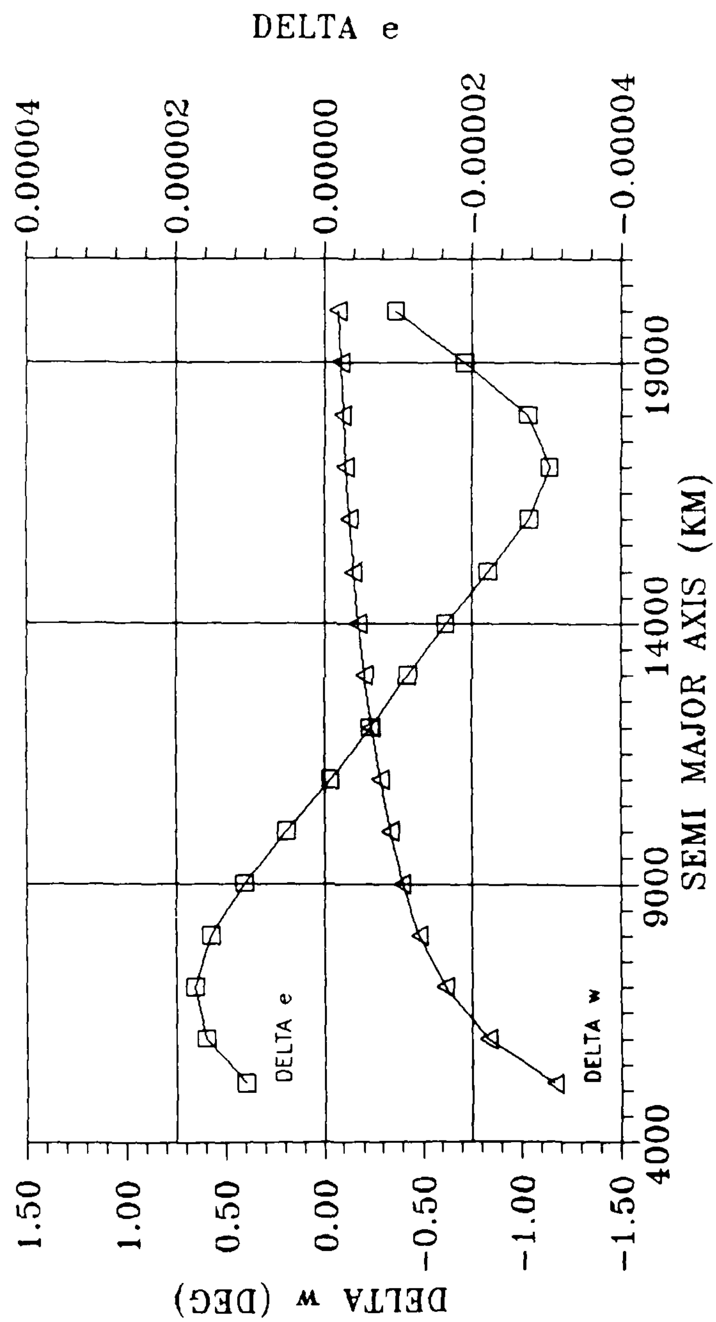

DELTA e, DELTA w vs. SEMI MAJOR AXIS for e = .3, i = 1

Figure F.1

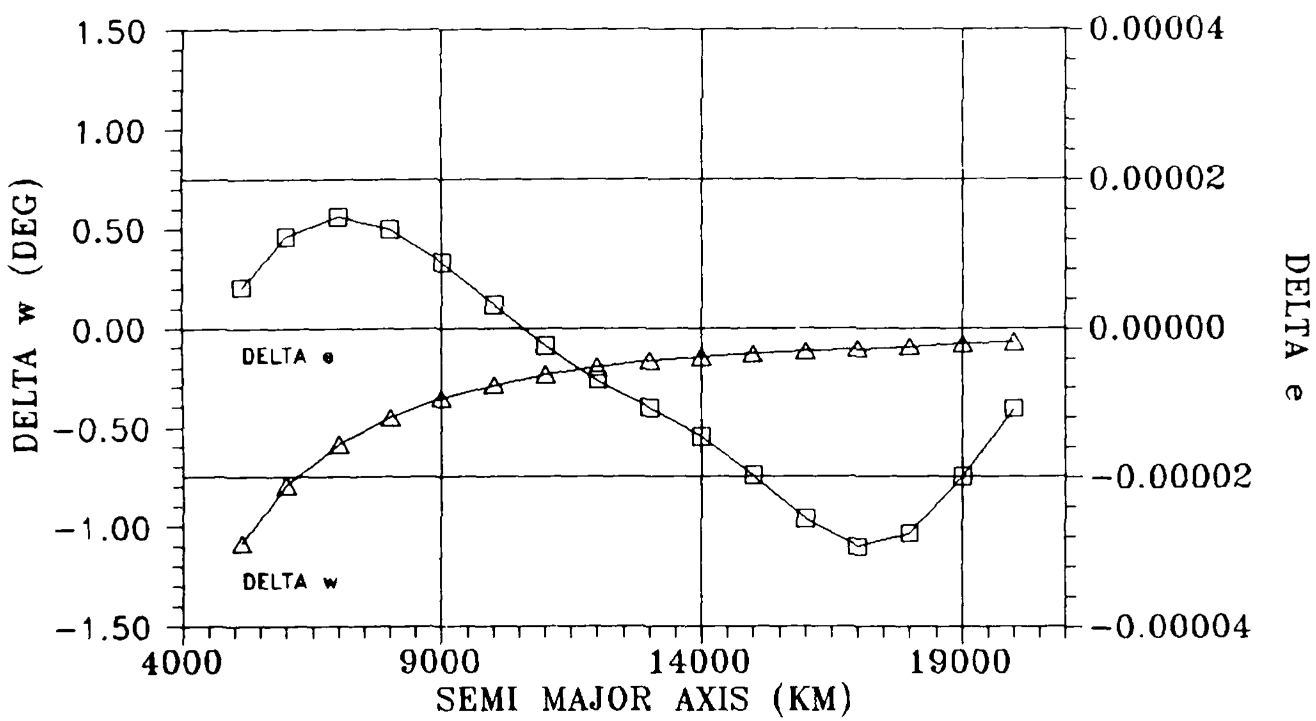

DELTA e, DELTA w vs. SEMI MAJOR AXIS for e = .3, i = 10
Figure F.2

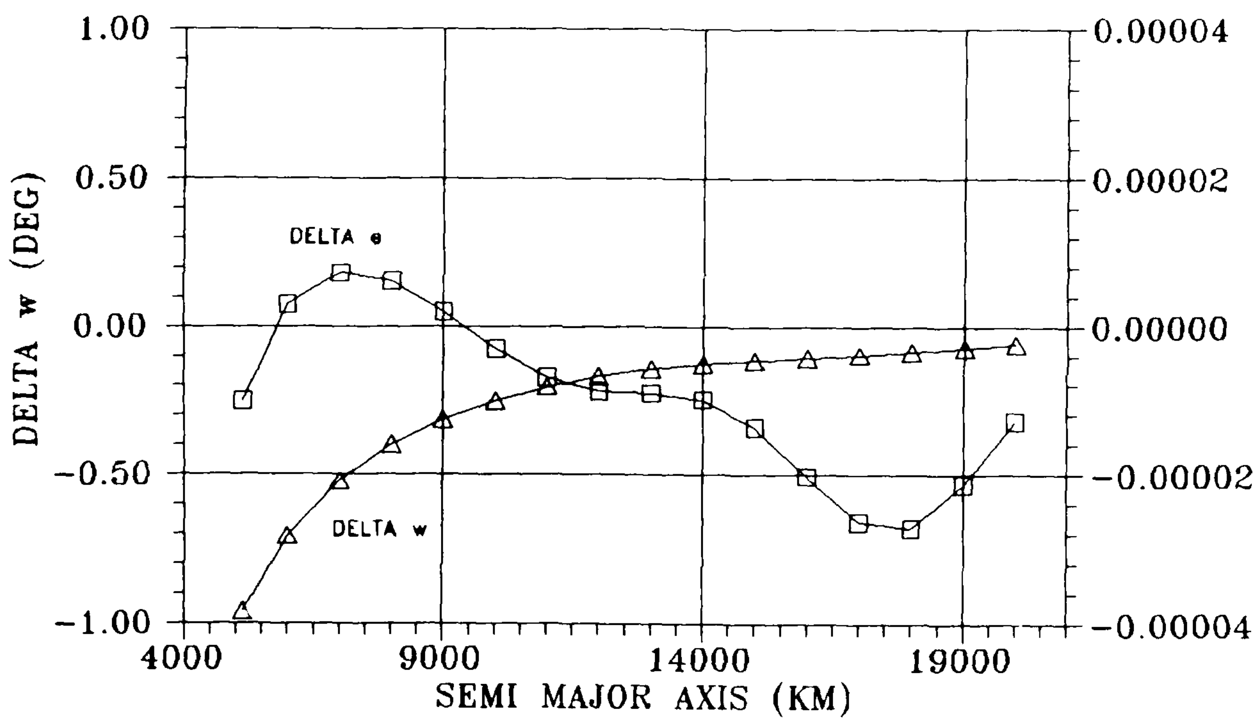

DELTA e, DELTA w vs. SEMI MAJOR AXIS for e = .3, i = 20
Figure F.3

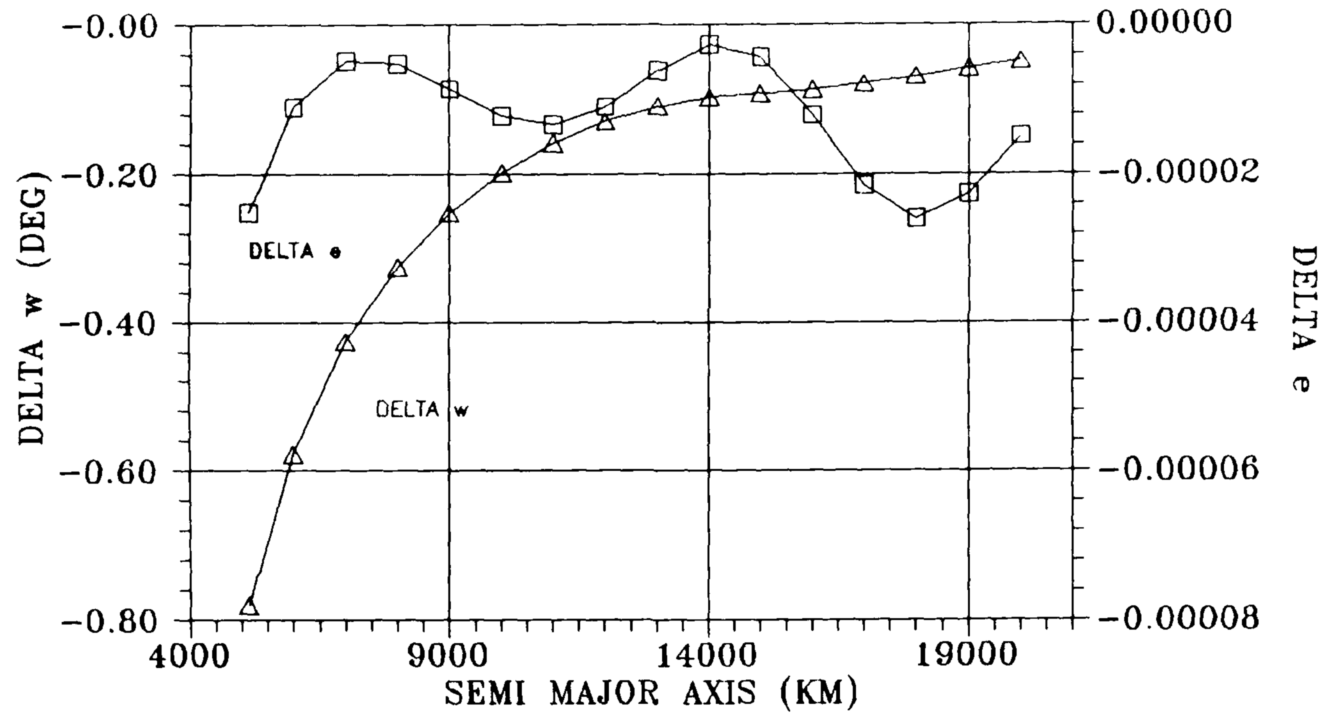

DELTA e, DELTA w vs. SEMI MAJOR AXIS for e = .3, i = 30
Figure F.4

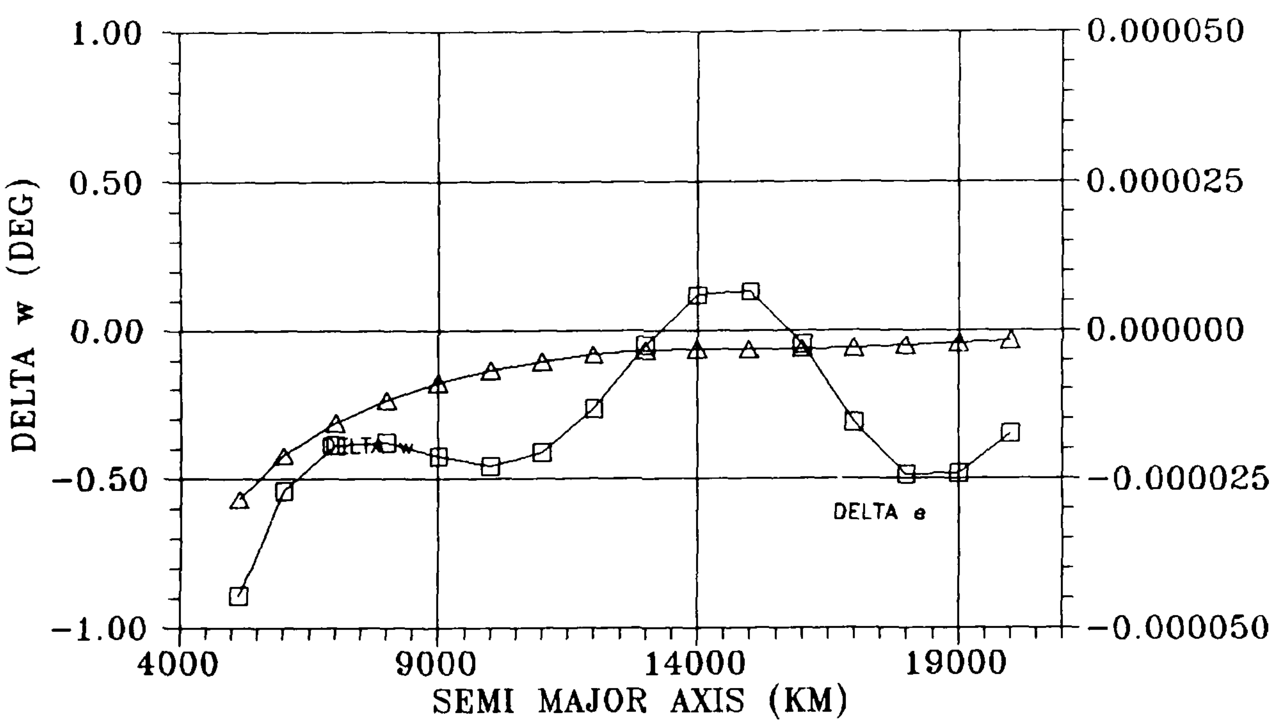

DELTA e, DELTA w vs. SEMI MAJOR AXIS for e = .3, i = 40
Figure F.5

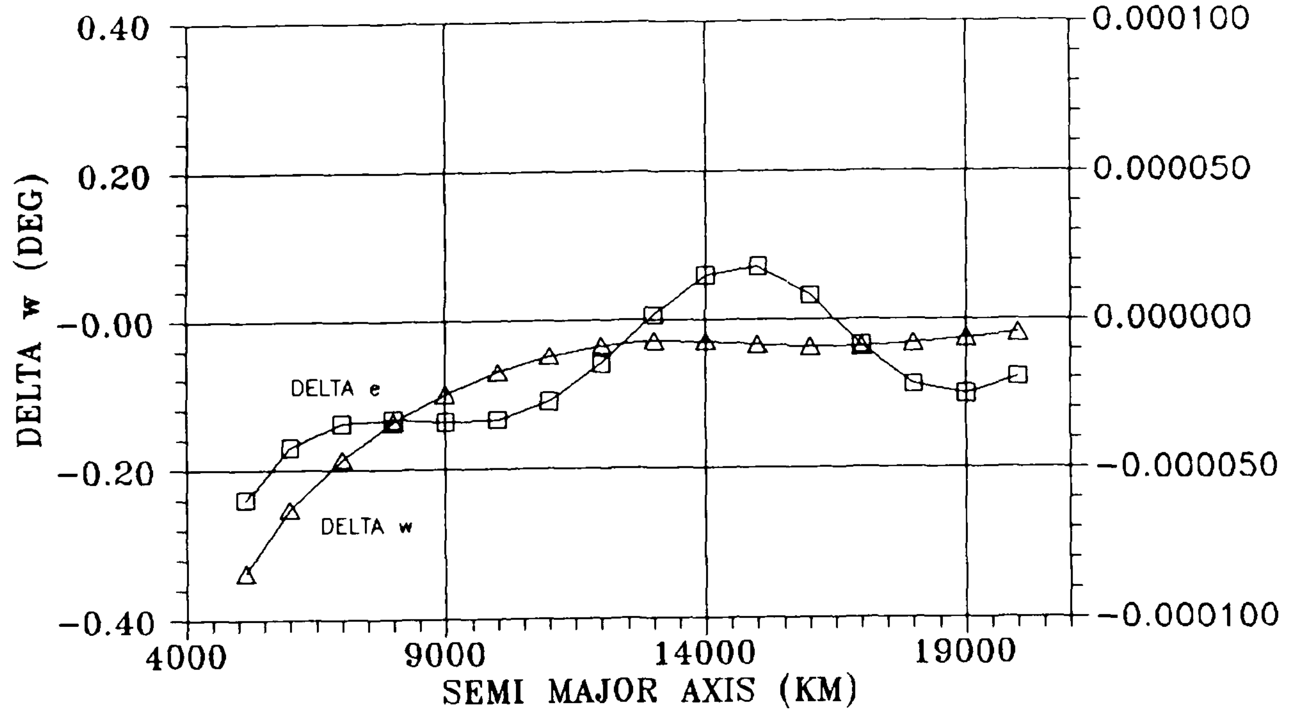

DELTA e, DELTA w vs. SEMI MAJOR AXIS for e = .3, i = 50
Figure F.6

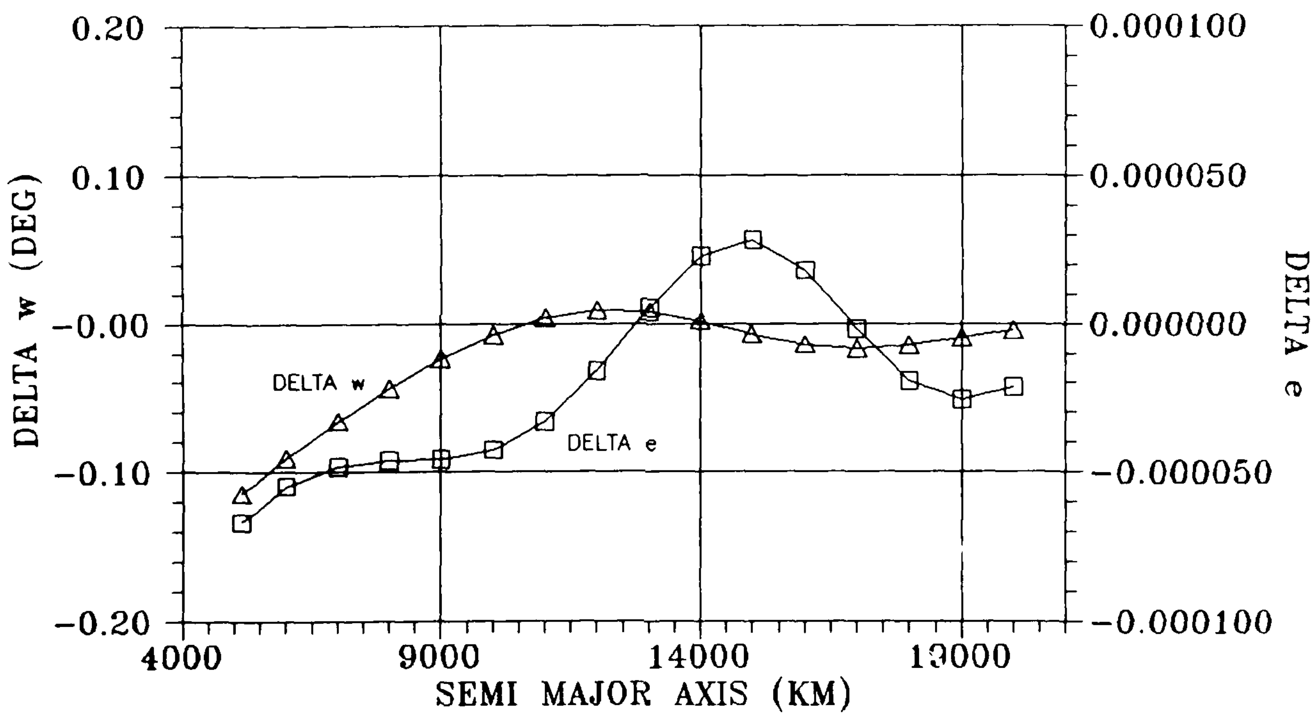

DELTA e, DELTA w vs. SEMI MAJOR AXIS for e = .3, i = 60
Figure F.7

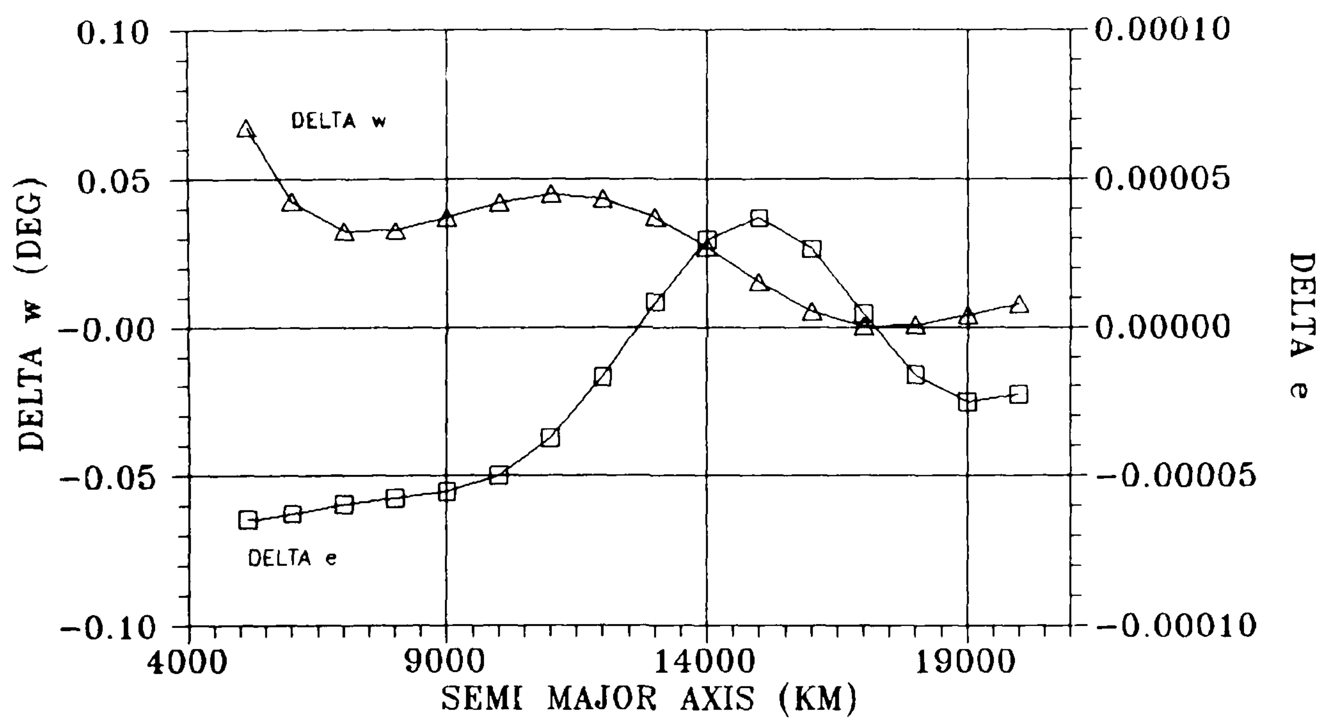

DELTA e, DELTA w vs. SEMI MAJOR AXIS for e = .3, i = 70
Figure F.8

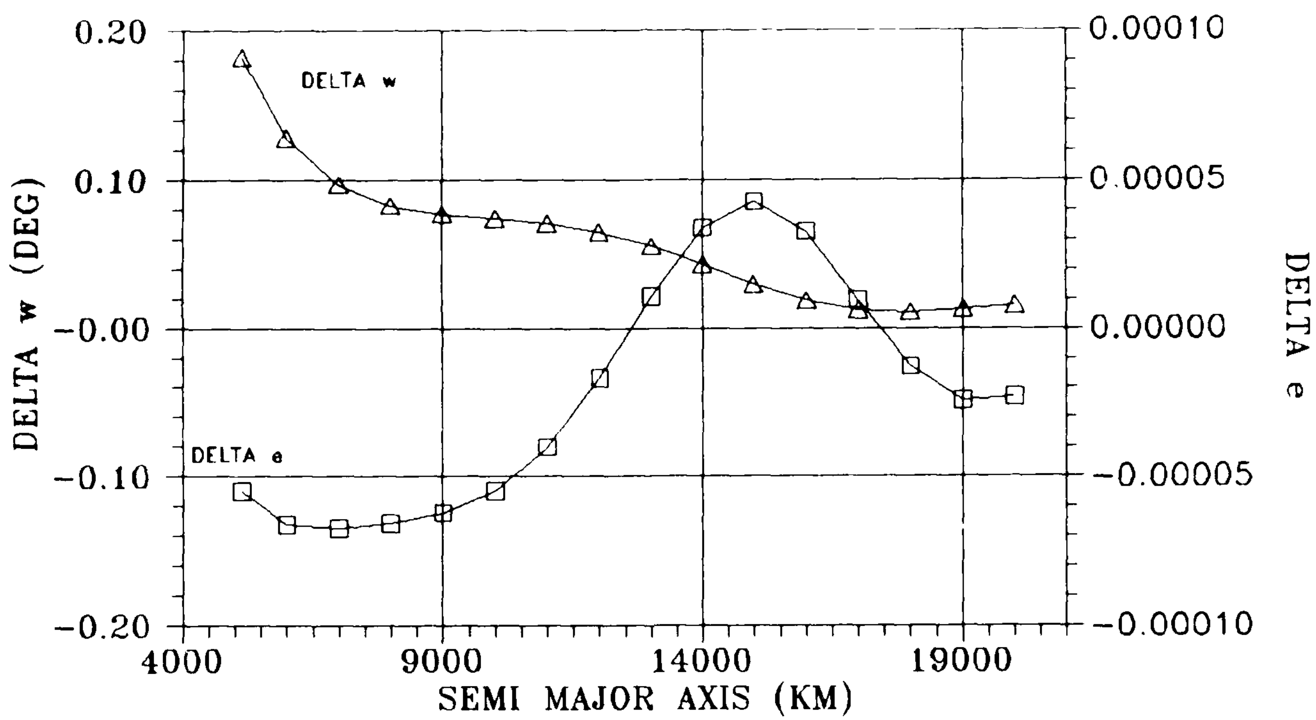

DELTA e, DELTA w vs. SEMI MAJOR AXIS for e = .3, i = 80
Figure F.9

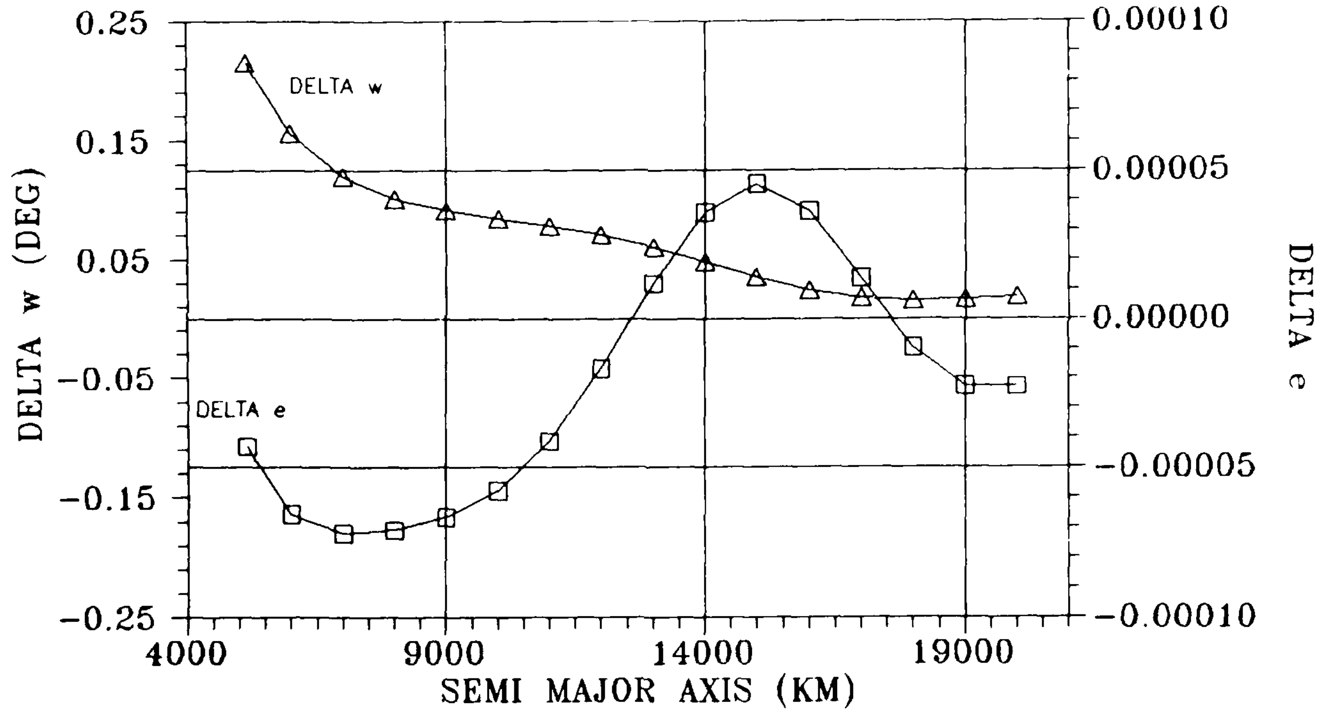

DELTA e, DELTA w vs. SEMI MAJOR AXIS for e = .3, i = 90
Figure F.10

Appendix G: Delta ι, Delta ω, vs. Semi Major Axis

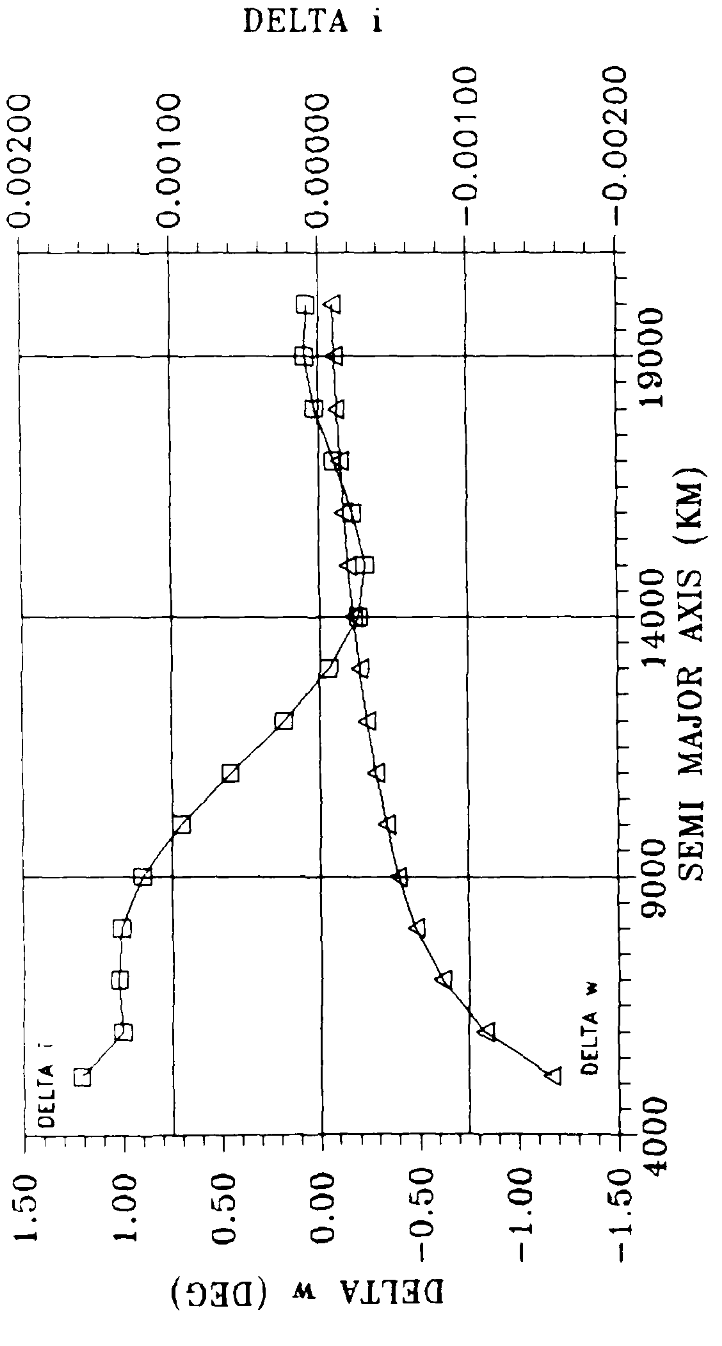

DELTA i, DELTA w vs. SEMI MAJOR AXIS for e = .3, i = 1
Figure G.1

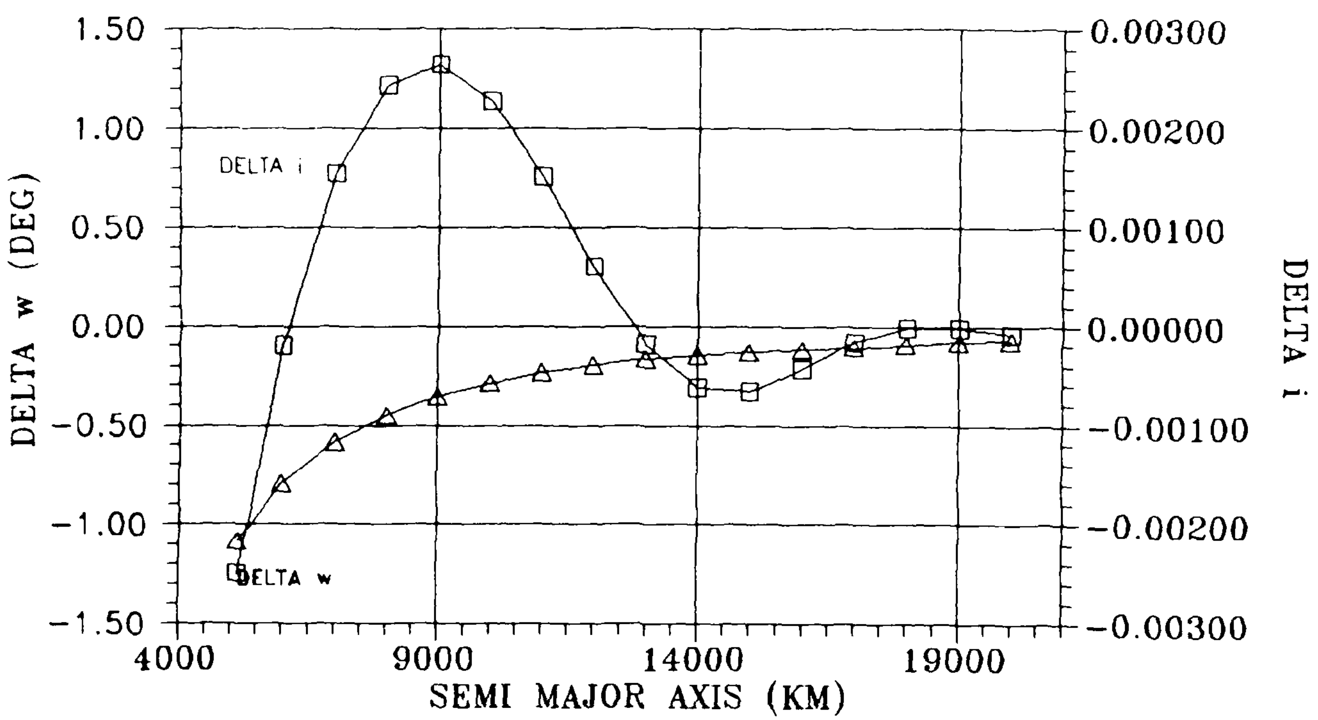

DELTA i, DELTA w vs. SEMI MAJOR AXIS for e = .3, i = 10
Figure G.2

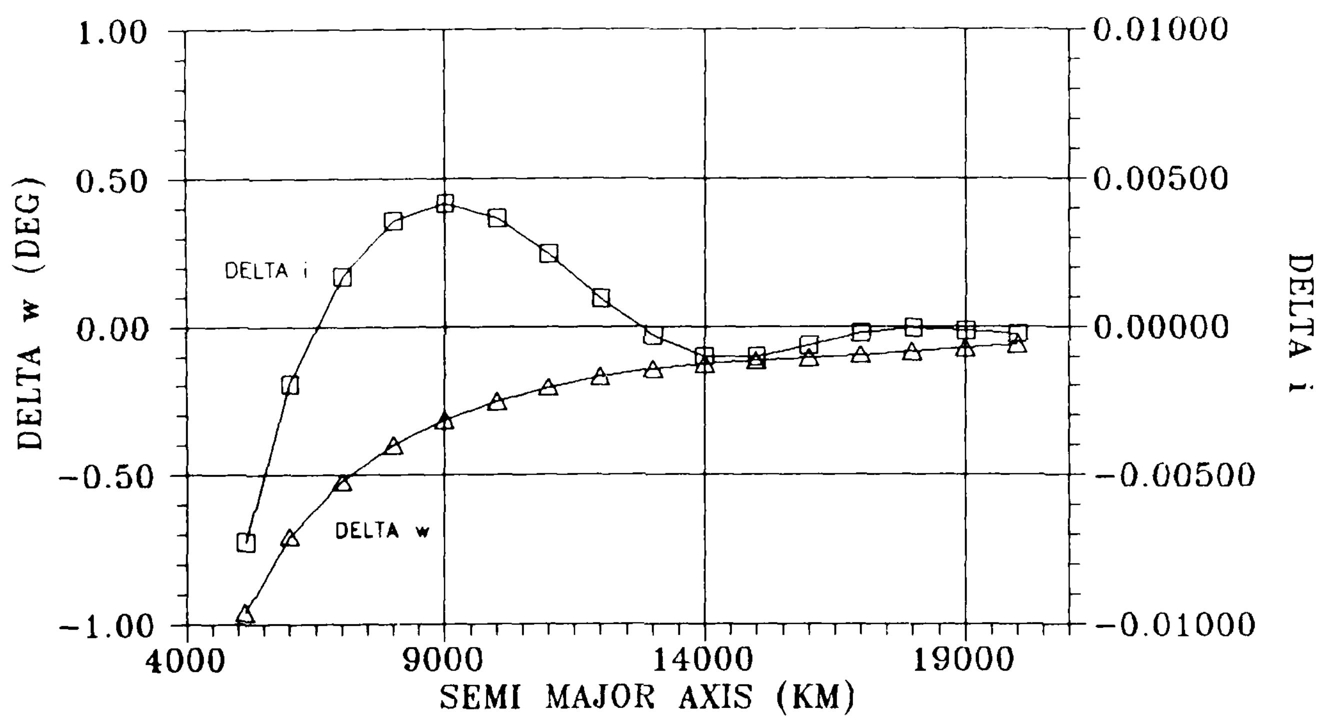

DELTA i, DELTA w vs. SEMI MAJOR AXIS for e = .3, i = 20
Figure G.3

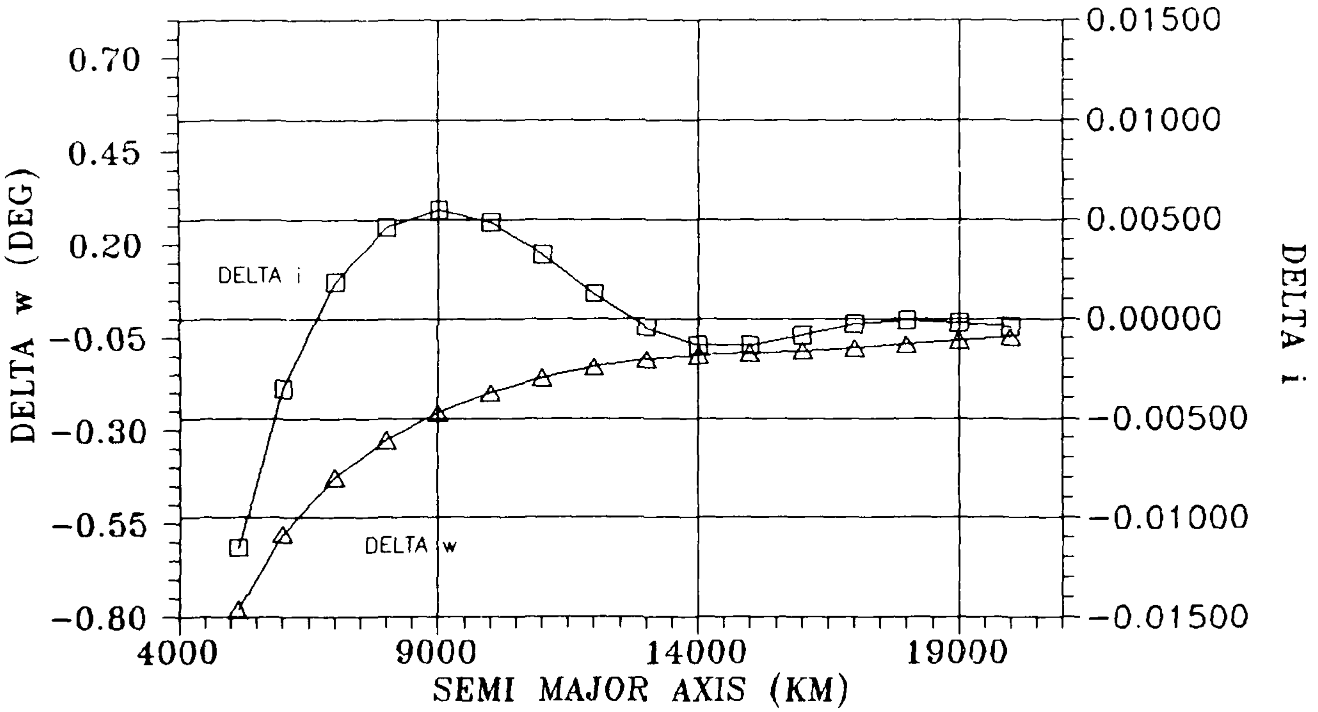

DELTA i, DELTA w vs. SEMI MAJOR AXIS for e = .3, i = 30
Figure G.4

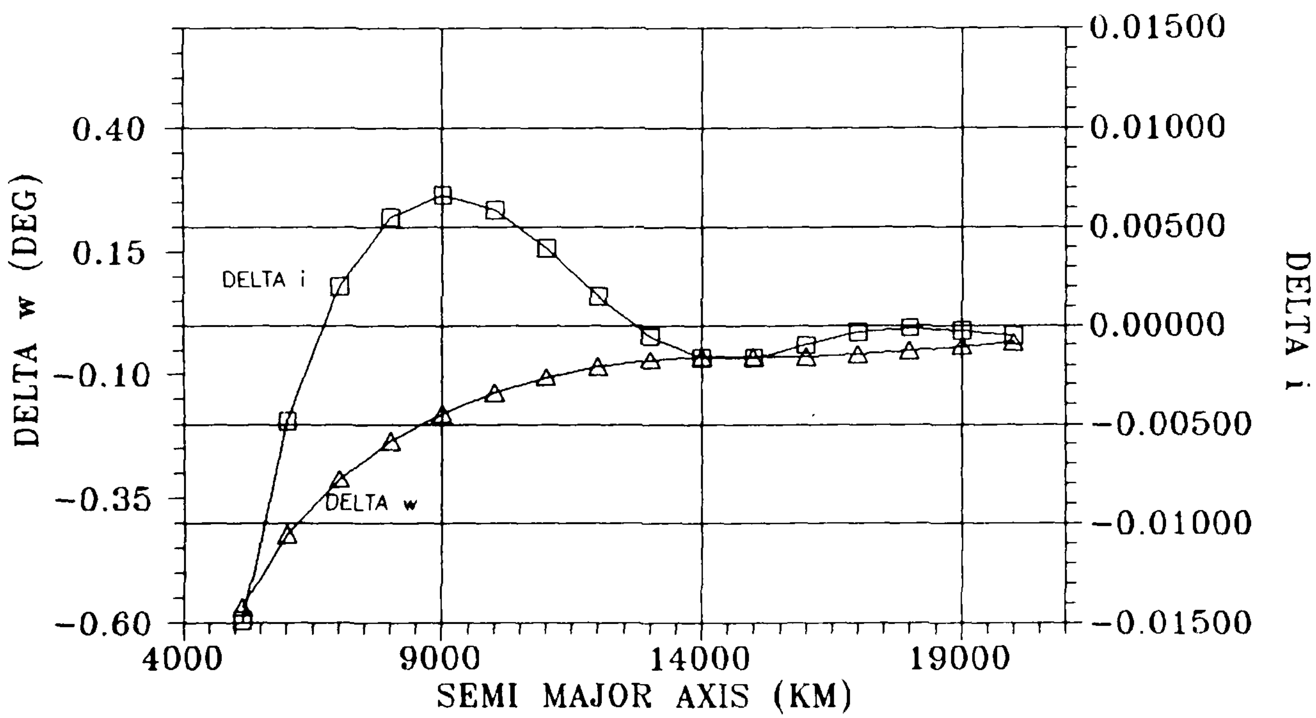

DELTA i, DELTA w vs. SEMI MAJOR AXIS for e = .3, i = 40
Figure G.5

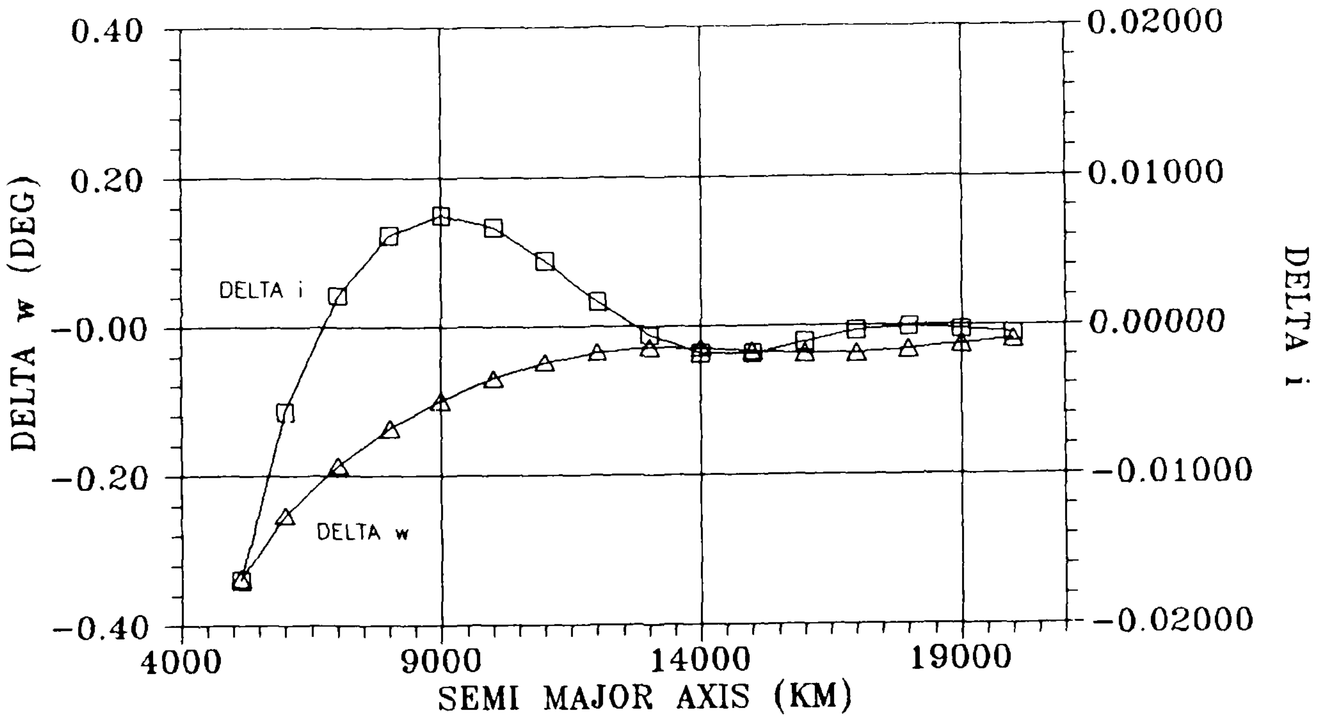

DELTA i, DELTA w vs. SEMI MAJOR AXIS for e = .3, i = 50
Figure G.6

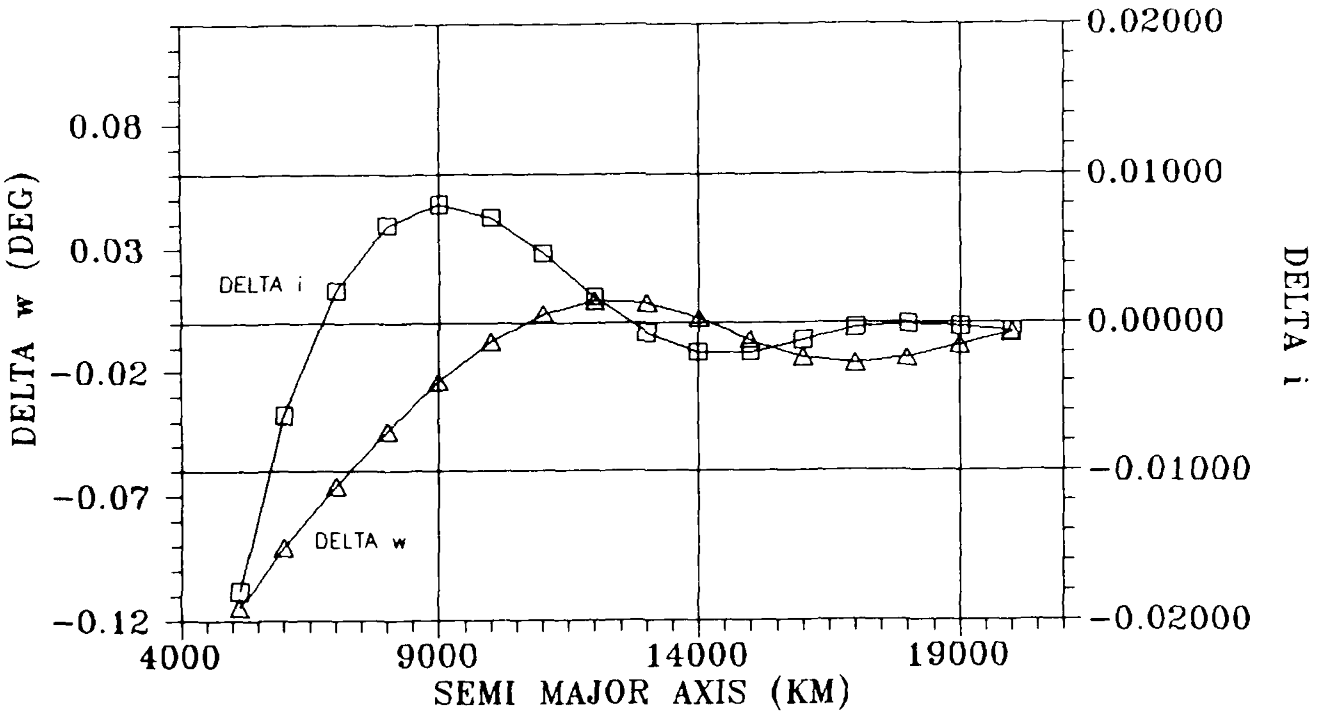

DELTA i, DELTA w vs. SEMI MAJOR AXIS for e = .3, i = 60
Figure G.7

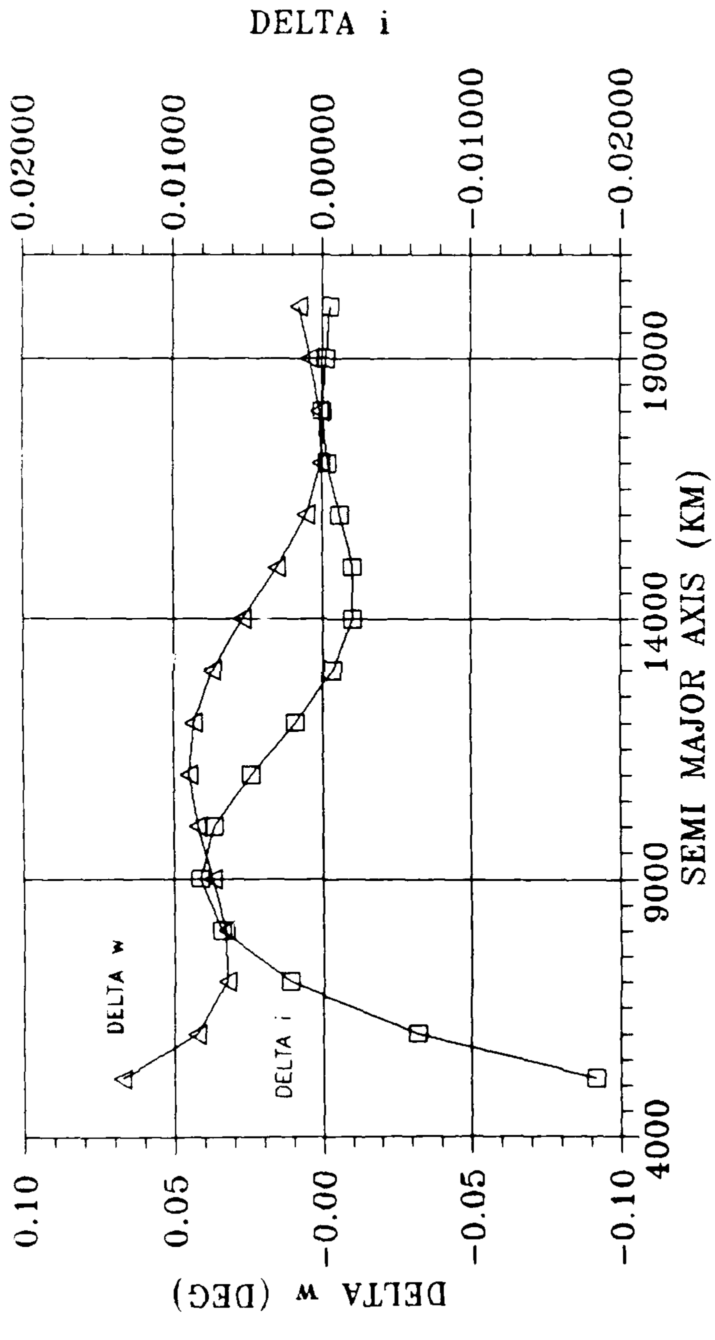

DELTA i, DELTA w vs. SEMI MAJOR AXIS for e = .3, i = 70
Figure G.8

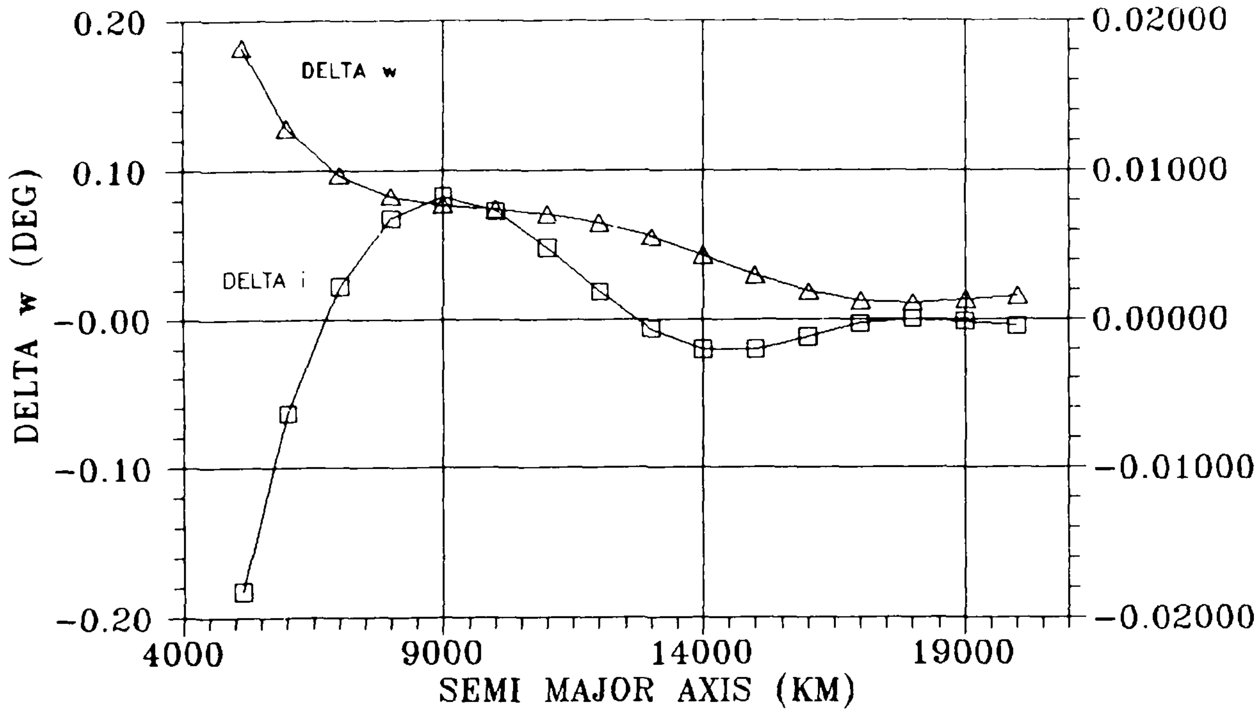

DELTA i, DELTA w vs. SEMI MAJOR AXIS for e = .3, i = 80
Figure G.9

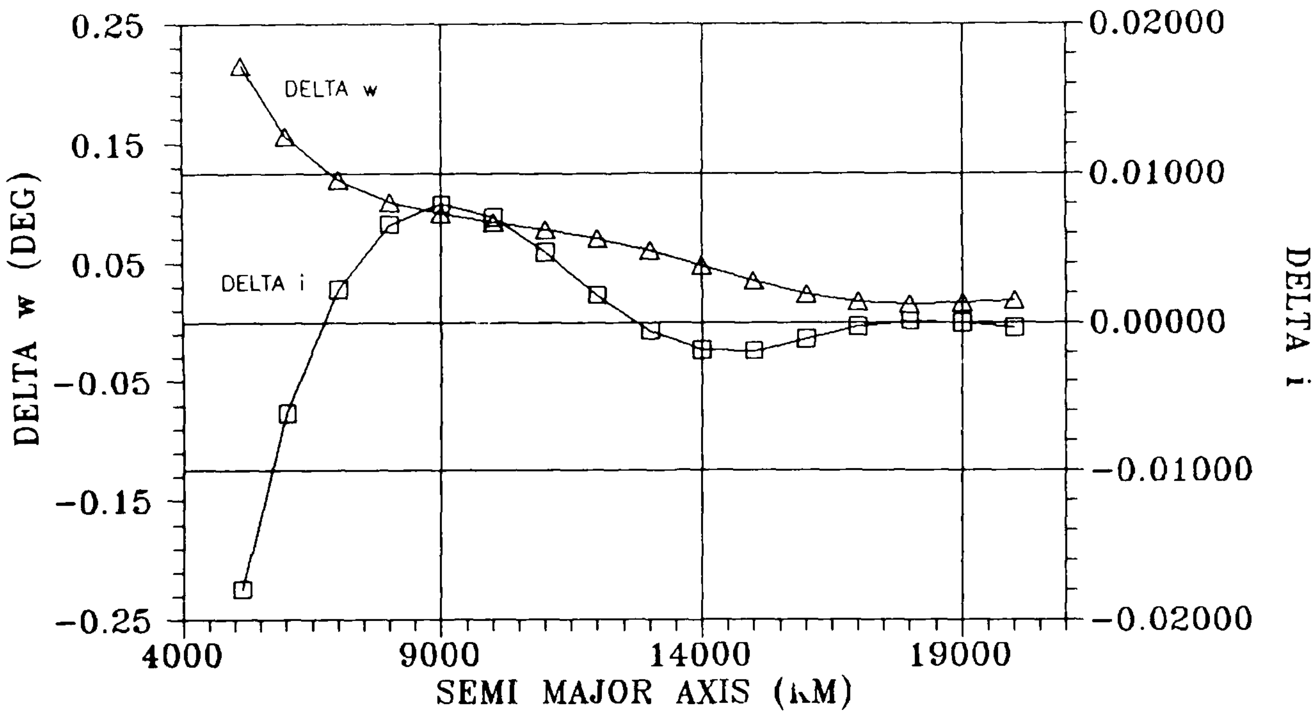

DELTA i, DELTA w vs. SEMI MAJOR AXIS for e = .3, i = 90
Figure G.10

Appendix H: Delta a, Delta ω, vs. Semi Major Axis

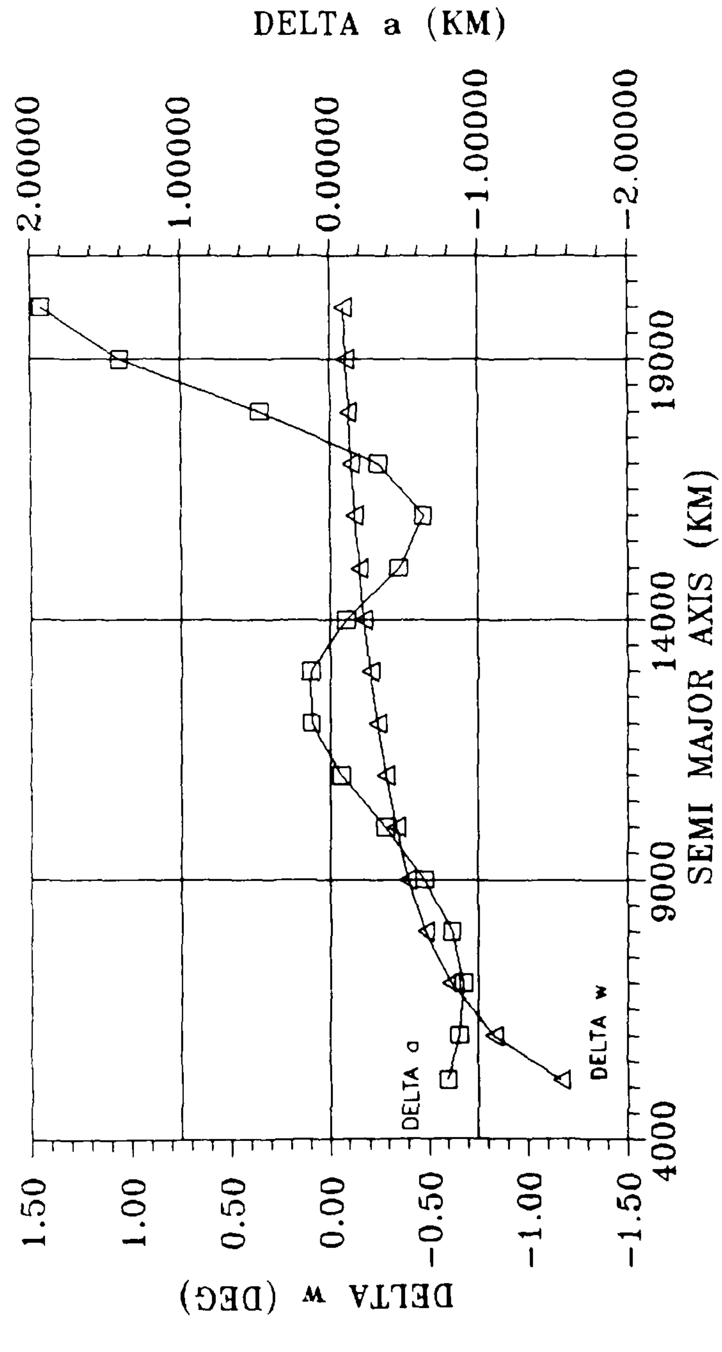

DELTA a, DELTA w vs. SEMI MAJOR AXIS for e = .3, i = 1
Figure H.1

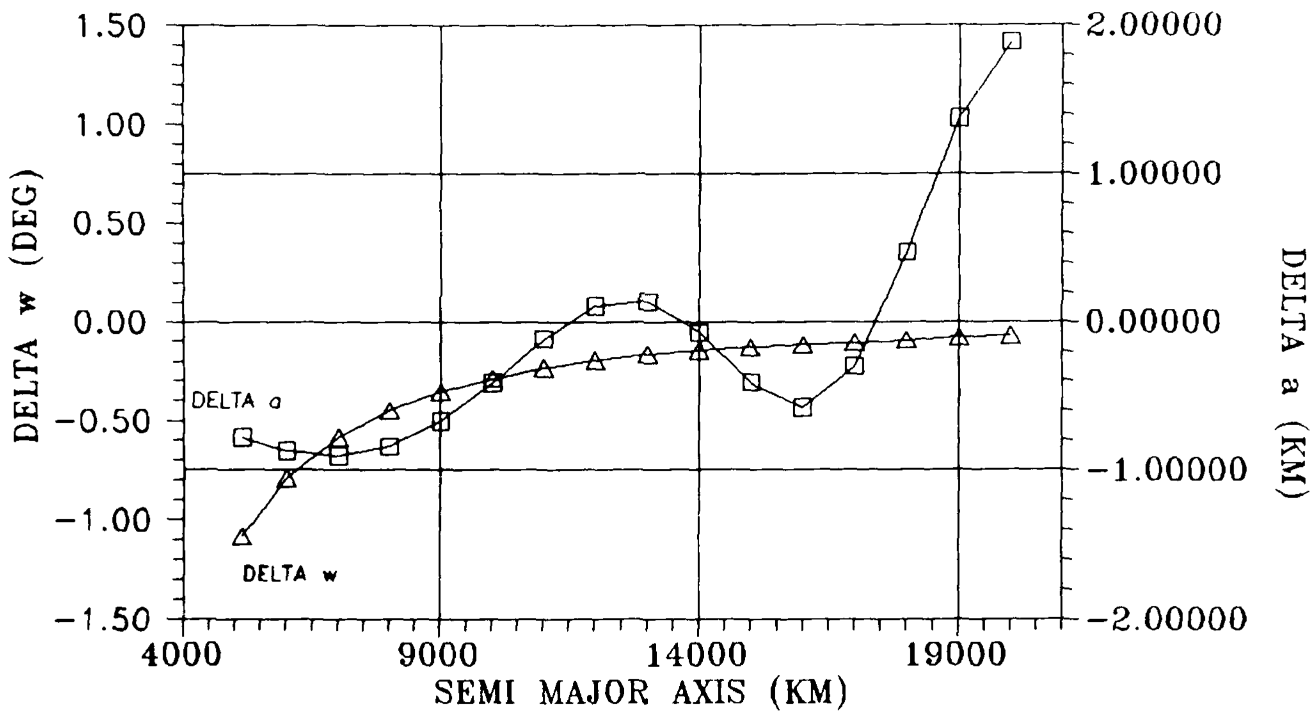

DELTA a, DELTA w vs. SEMI MAJOR AXIS for e = .3, i = 10
Figure H.2

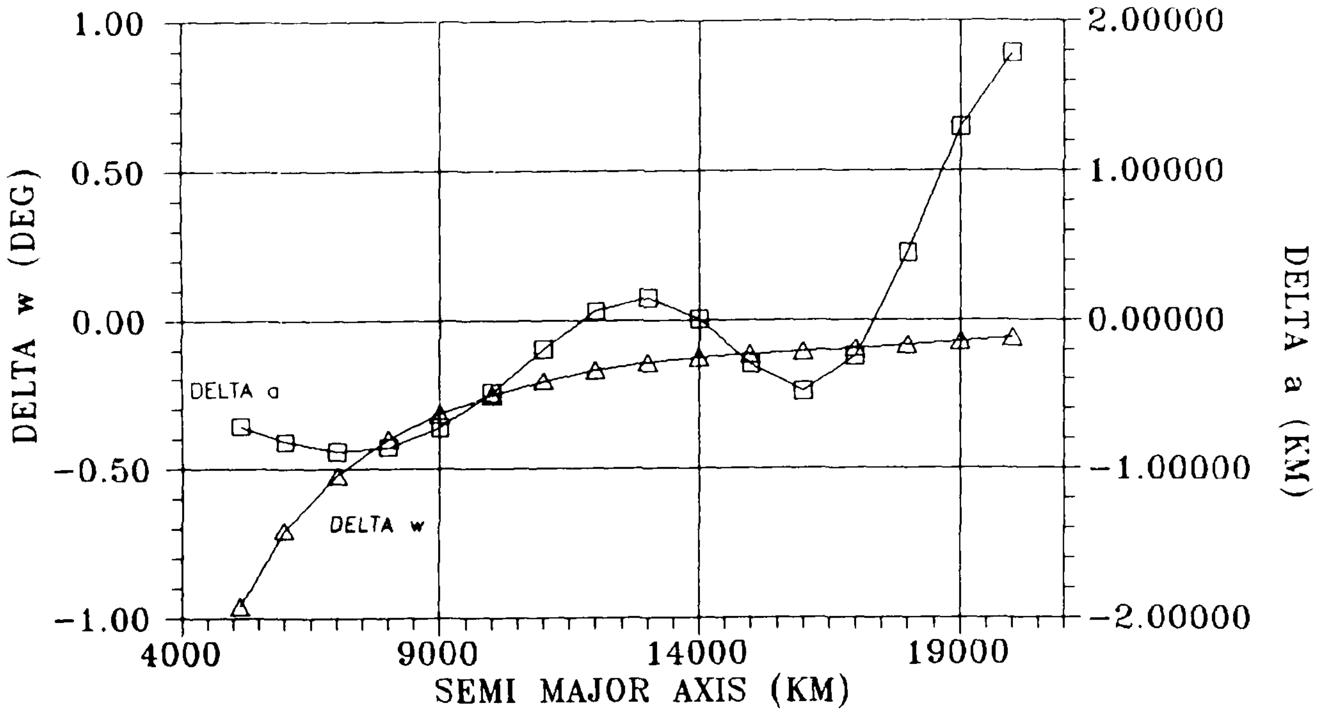

DELTA a, DELTA w vs. SEMI MAJOR AXIS for e = .3, i = 20
Figure H.3

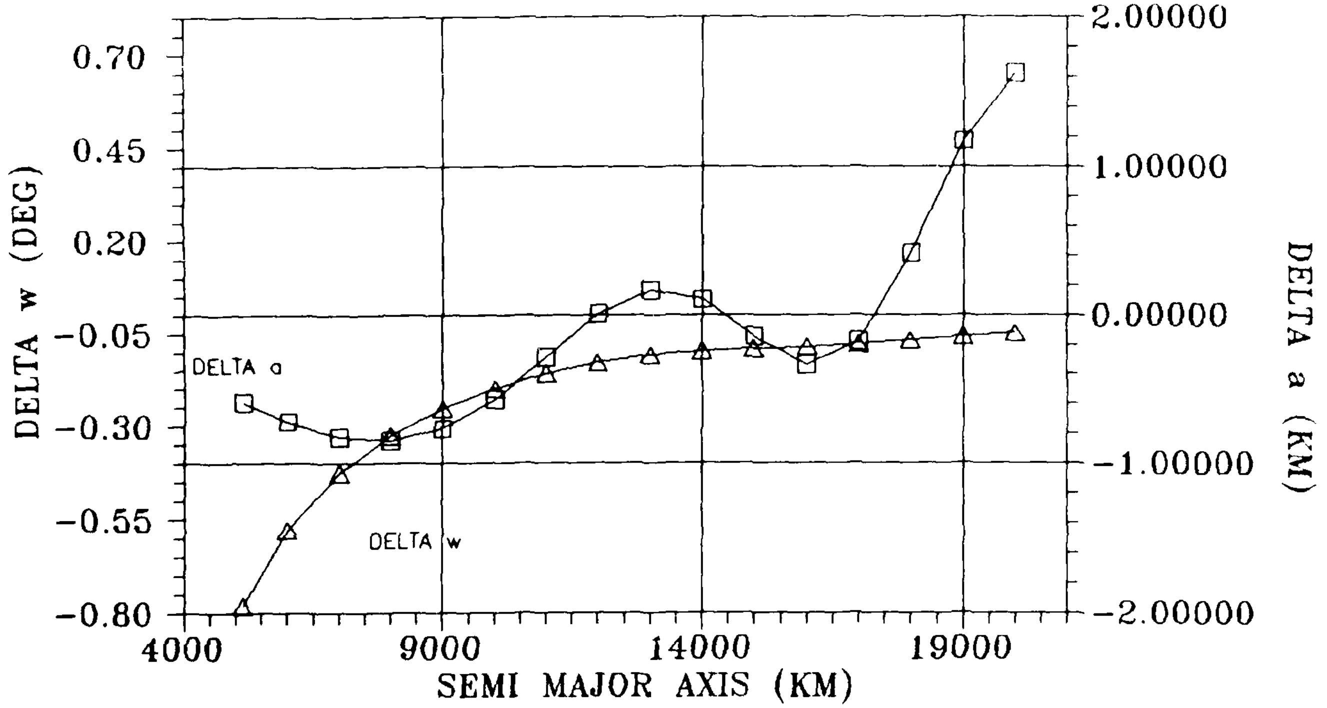

DELTA a, DELTA w vs. SEMI MAJOR AXIS for e = .3, i = 30
Figure H.4

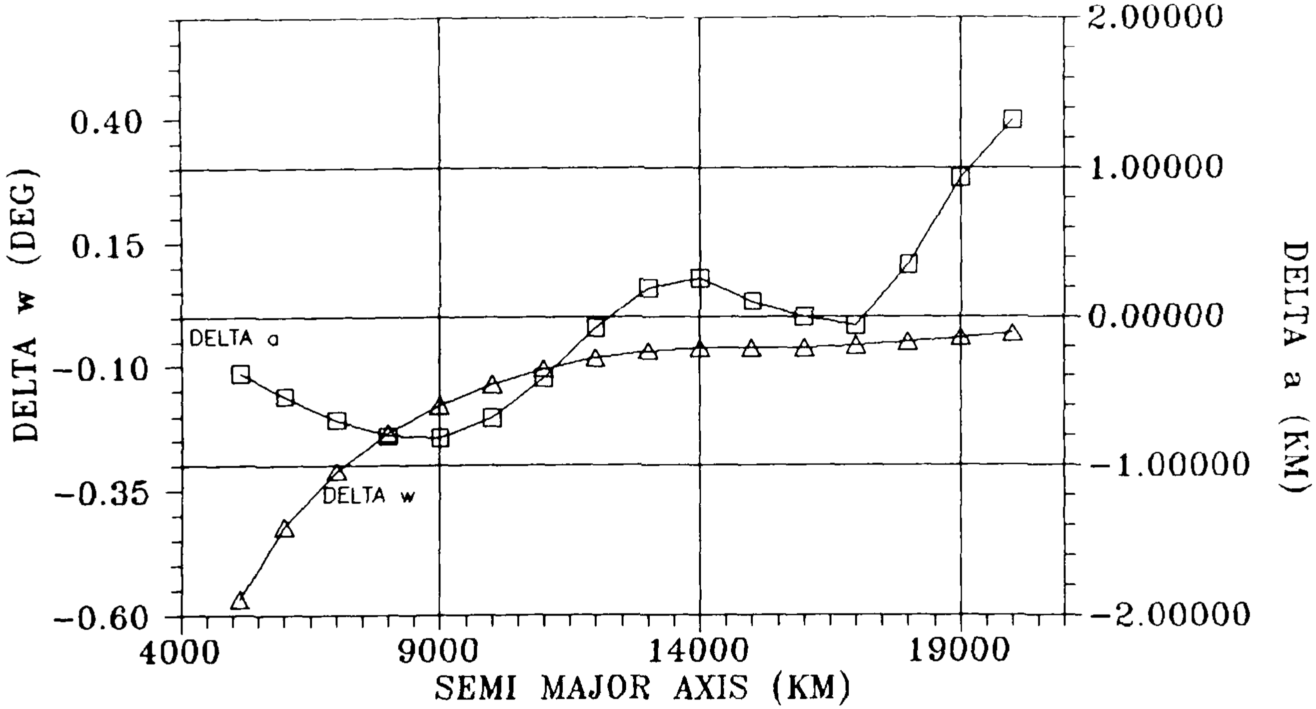

DELTA a, DELTA w vs. SEMI MAJOR AXIS for e = .3, i = 40
Figure H.5

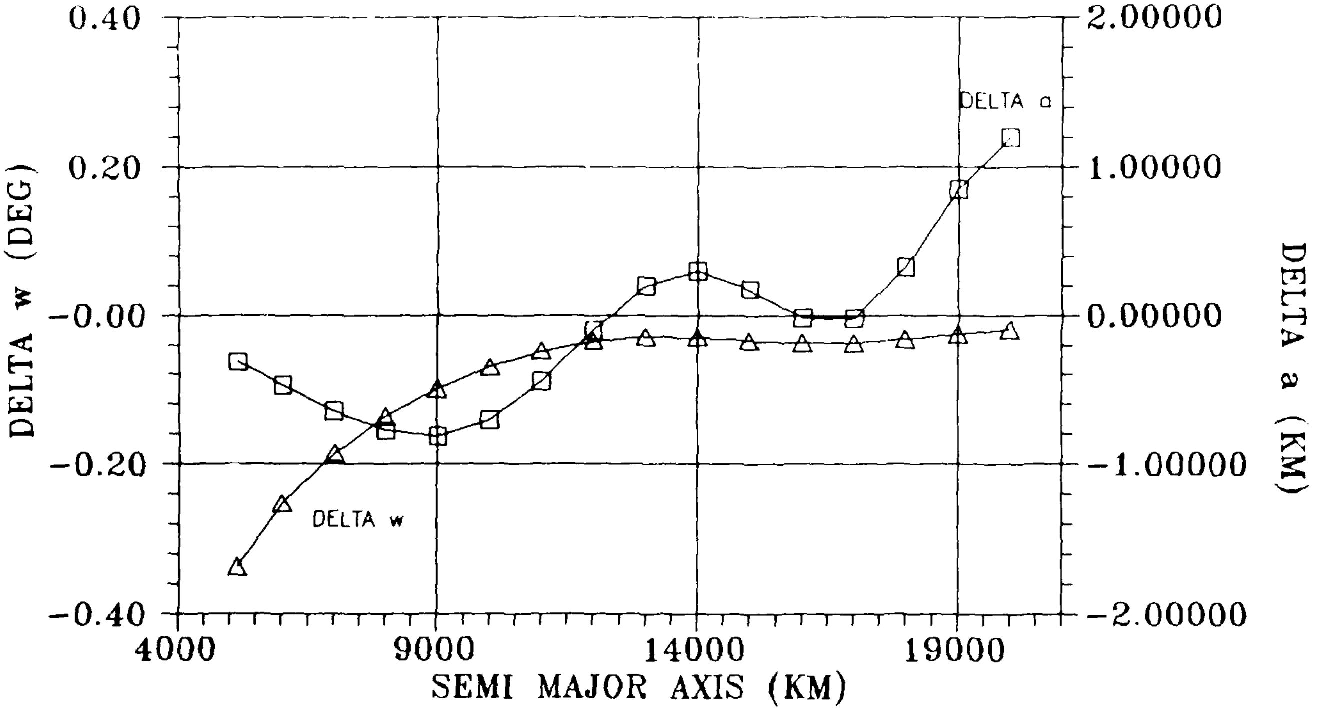

DELTA a, DELTA w vs. SEMI MAJOR AXIS for e = .3, i = 50
Figure H.6

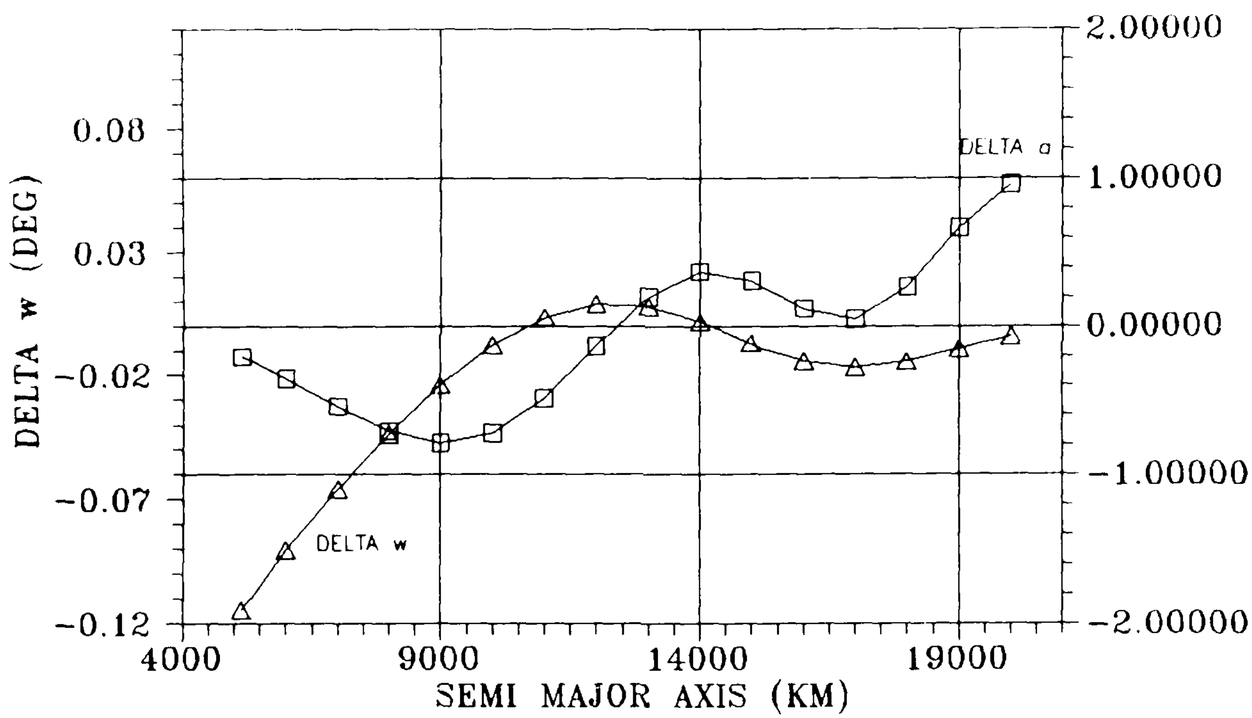

DELTA a, DELTA w vs. SEMI MAJOR AXIS for e = .3, i = 60
Figure H.7

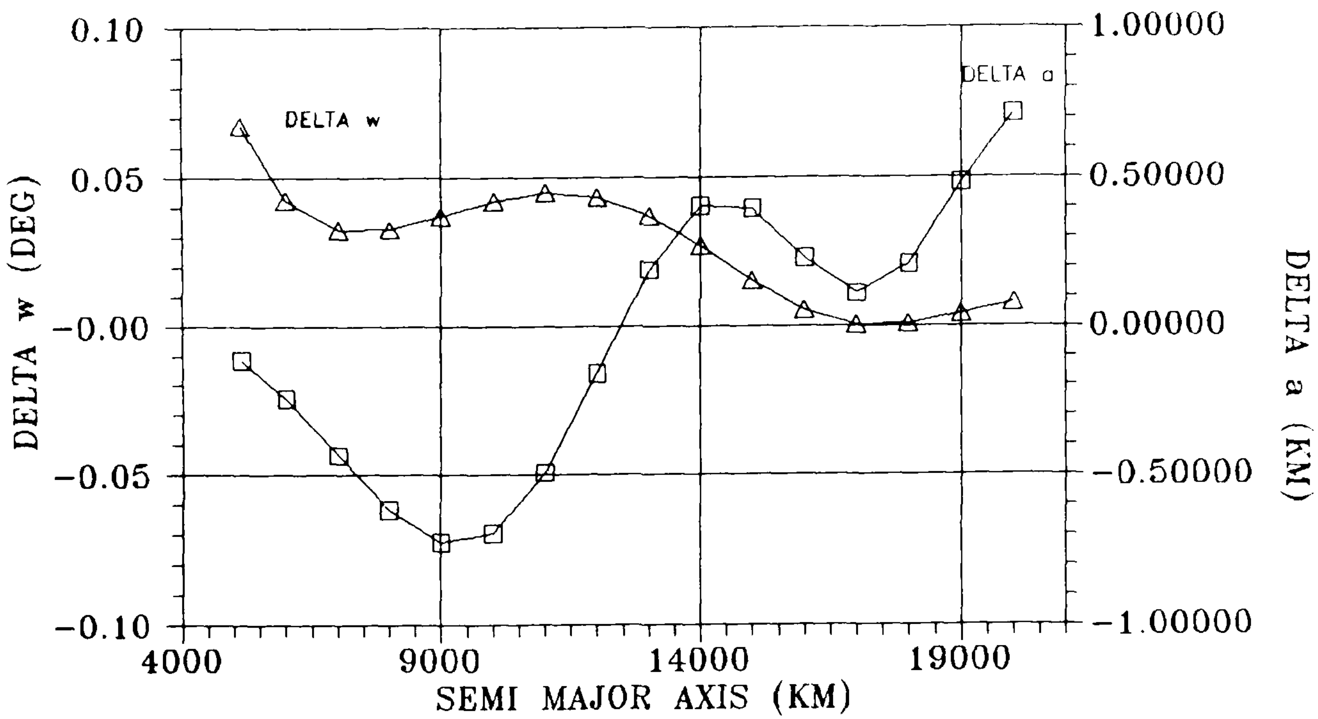

DELTA a, DELTA w vs. SEMI MAJOR AXIS for e = .3, i = 70
Figure H.8

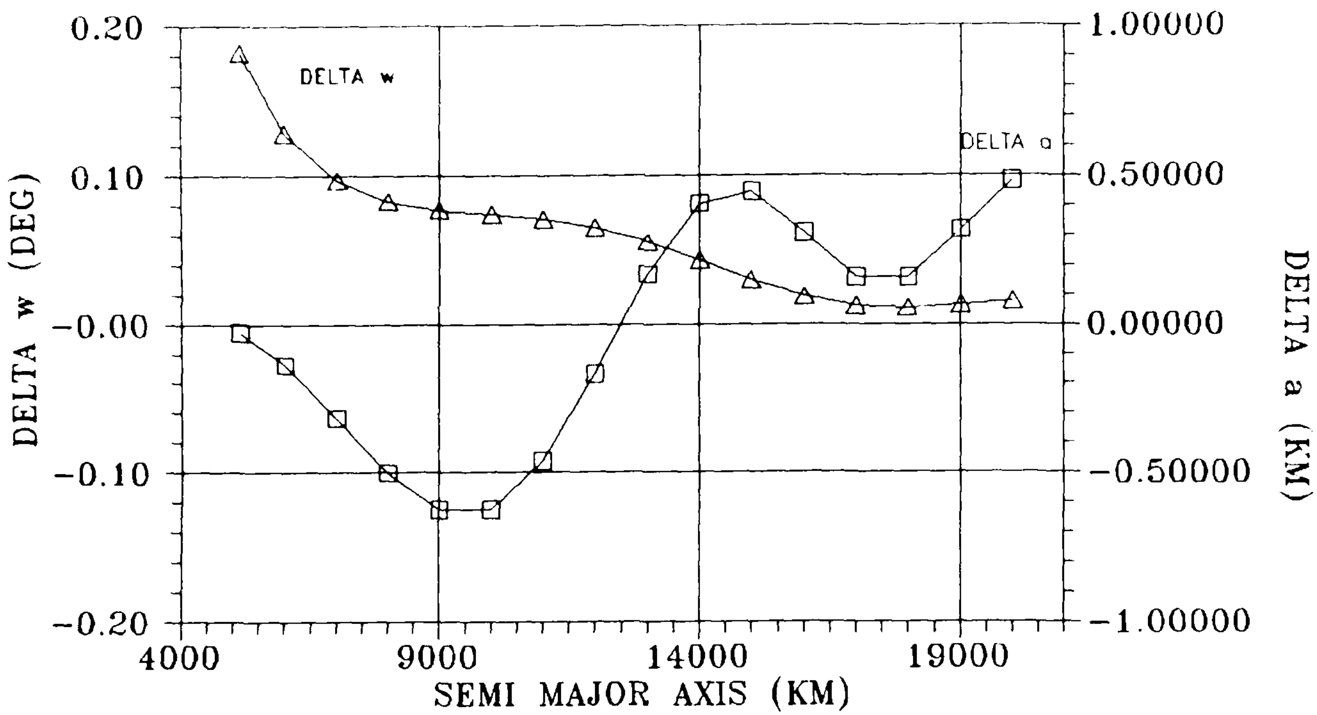

DELTA a, DELTA w vs. SEMI MAJOR AXIS for e = .3, i = 80
Figure H.9

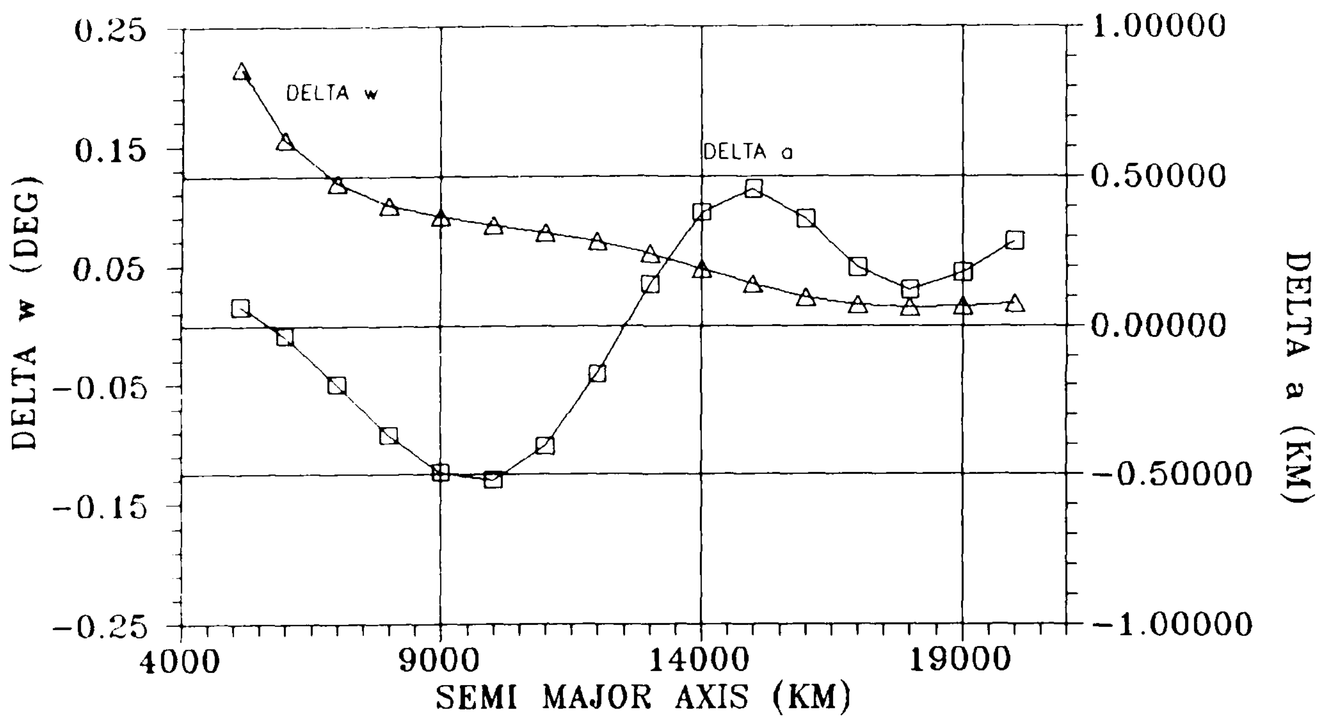

DELTA a, DELTA w vs. SEMI MAJOR AXIS for e = .3, i = 90
Figure H.10

Appendix I: Delta e, Delta ω, vs. Semi Major Axis for Various Eccentricities

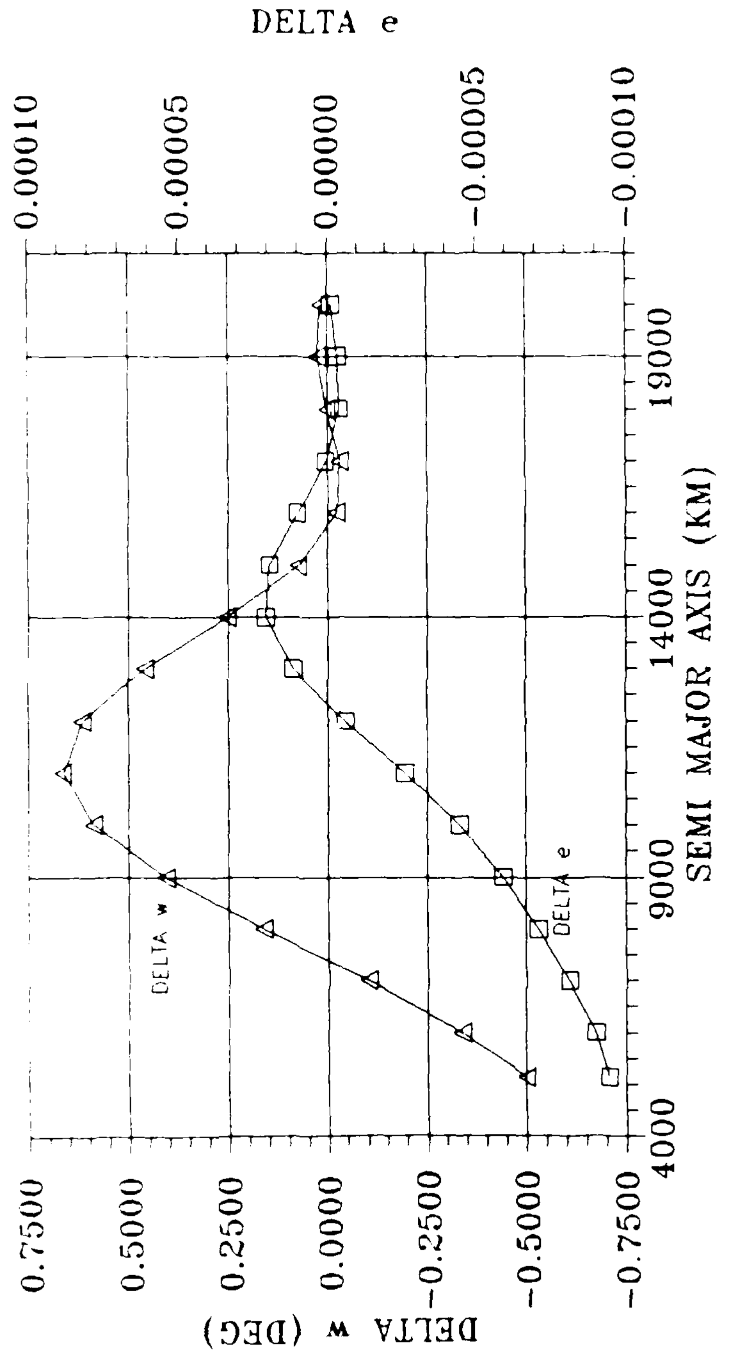

DELTA e, DELTA w vs. SEMI MAJOR AXIS for i = 70, e = .01

Figure I.1

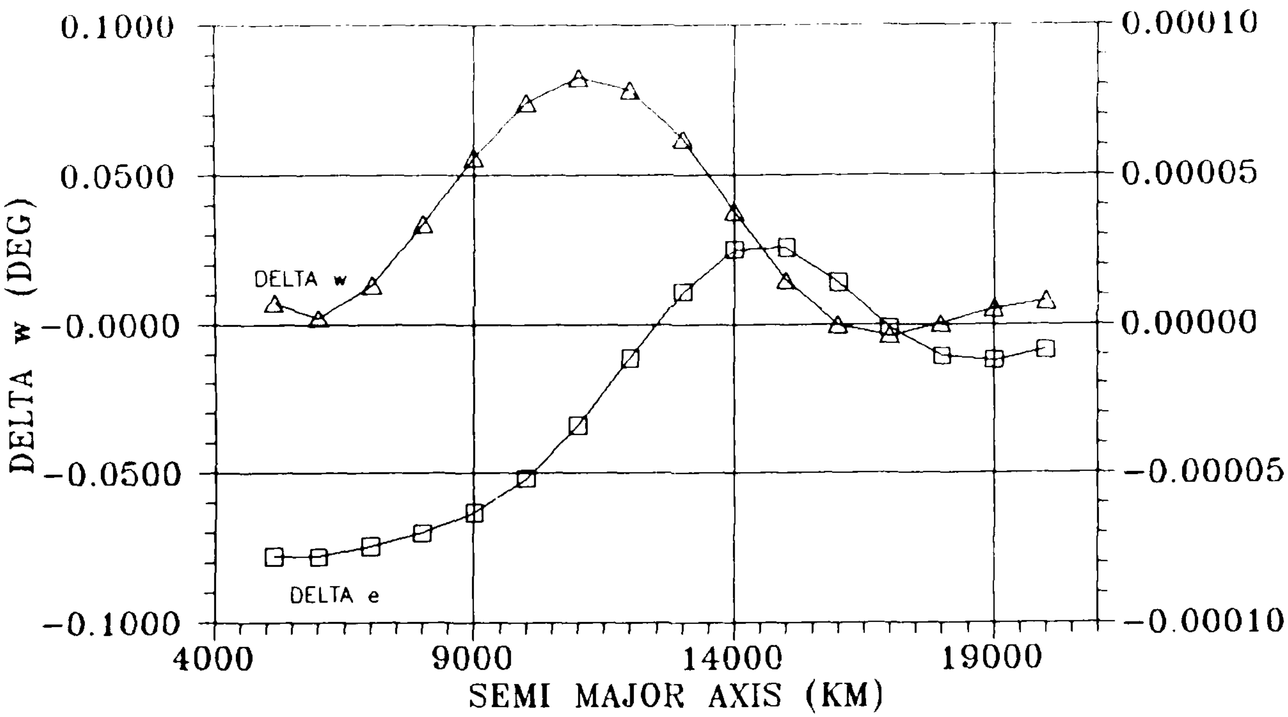

DELTA e, DELTA w vs. SEMI MAJOR AXIS for i = 70, e = .1
Figure I.2

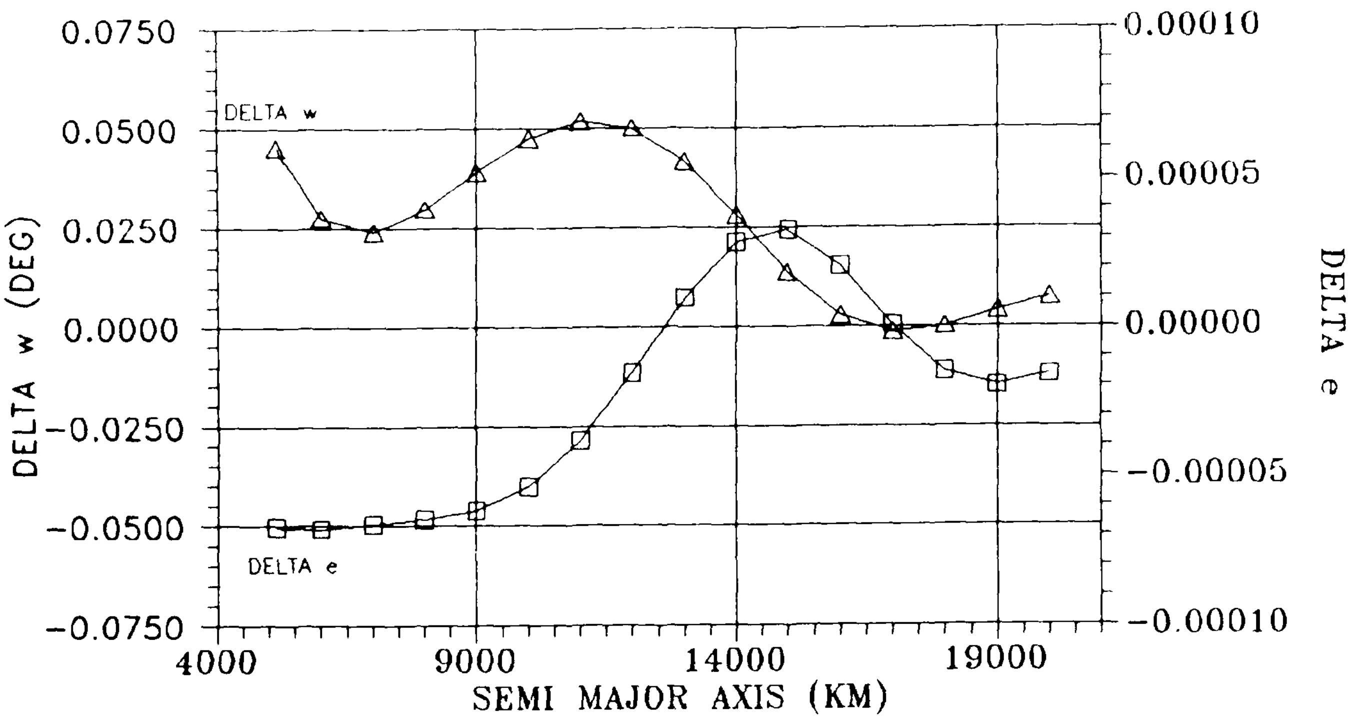

DELTA e, DELTA w vs. SEMI MAJOR AXIS for i = 70, e = .2
Figure I.3

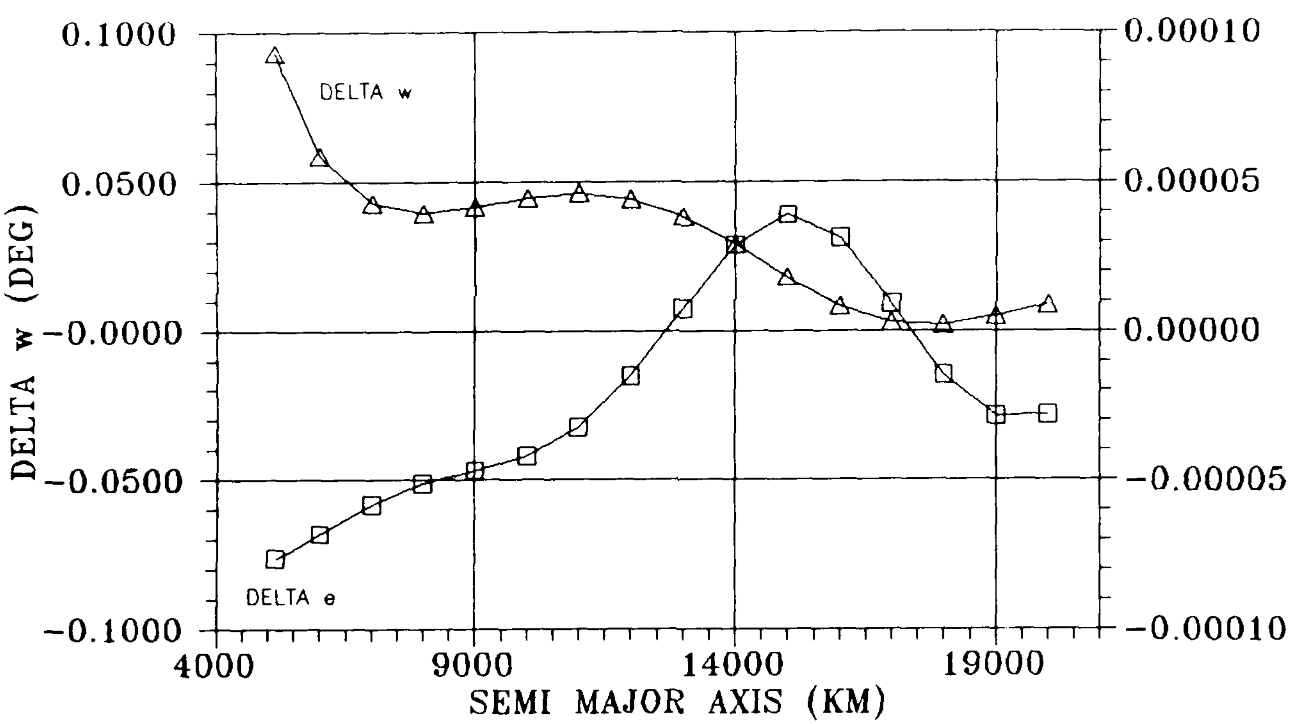

DELTA e, DELTA w vs. SEMI MAJOR AXIS for i = 70, e = .4
FIGURE I.4

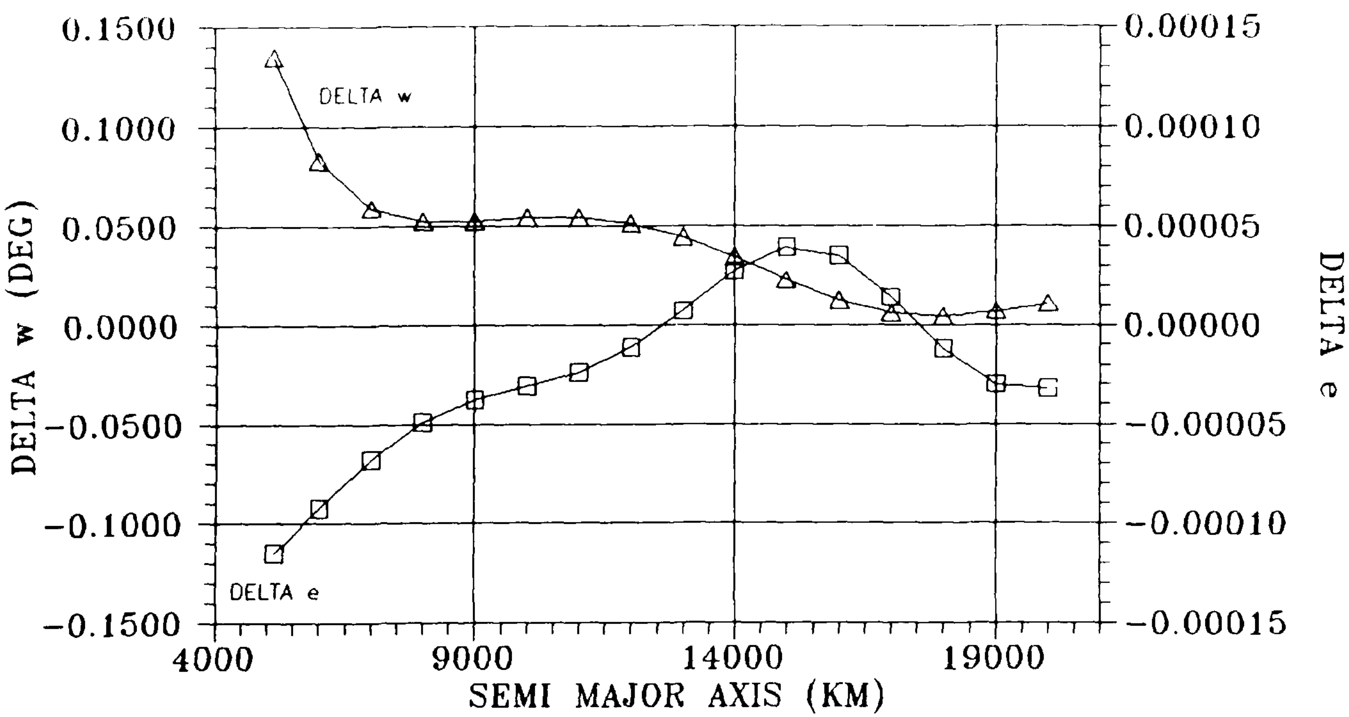

DELTA e, DELTA w vs. SEMI MAJOR AXIS for i = 70, e = .5
Figure I.5

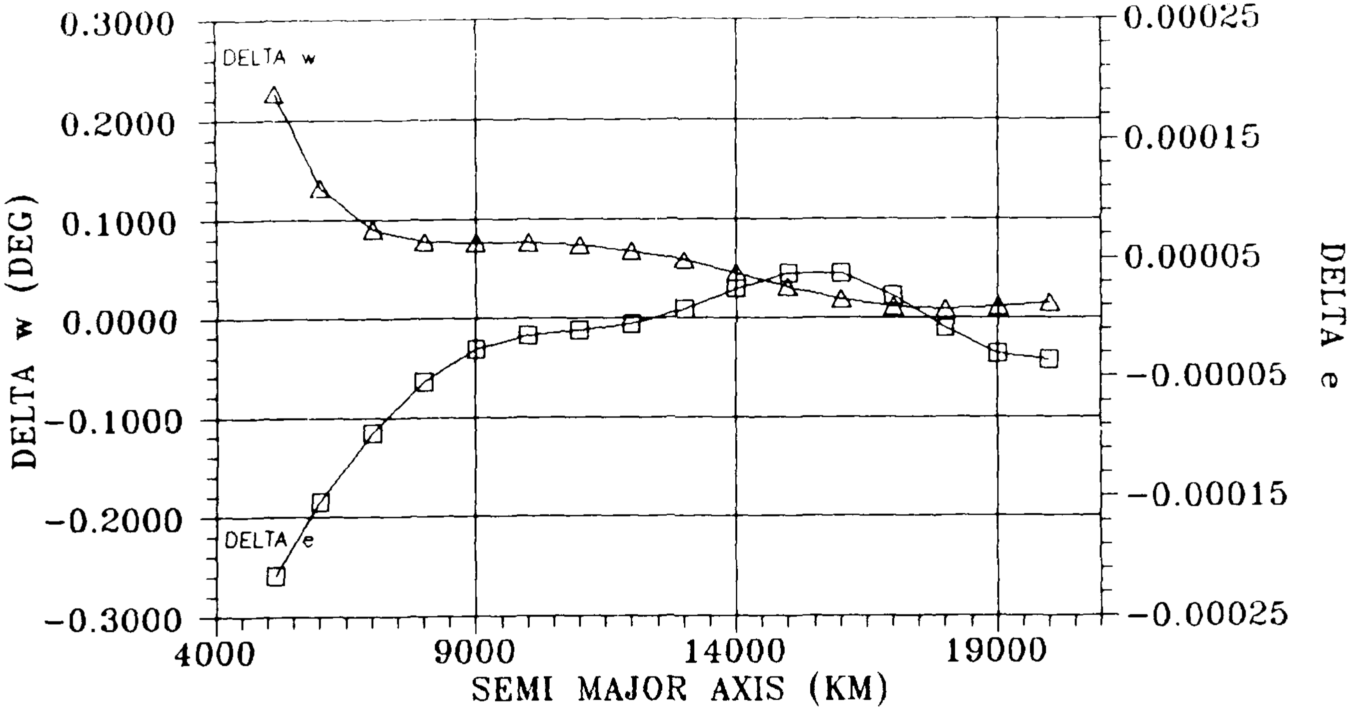

DELTA e, DELTA w vs. SEMI MAJOR AXIS for i = 70, e = .6
Figure I.6

Appendix J: Delta i, Delta ω, vs. Semi Major Axis for Various Eccentricities

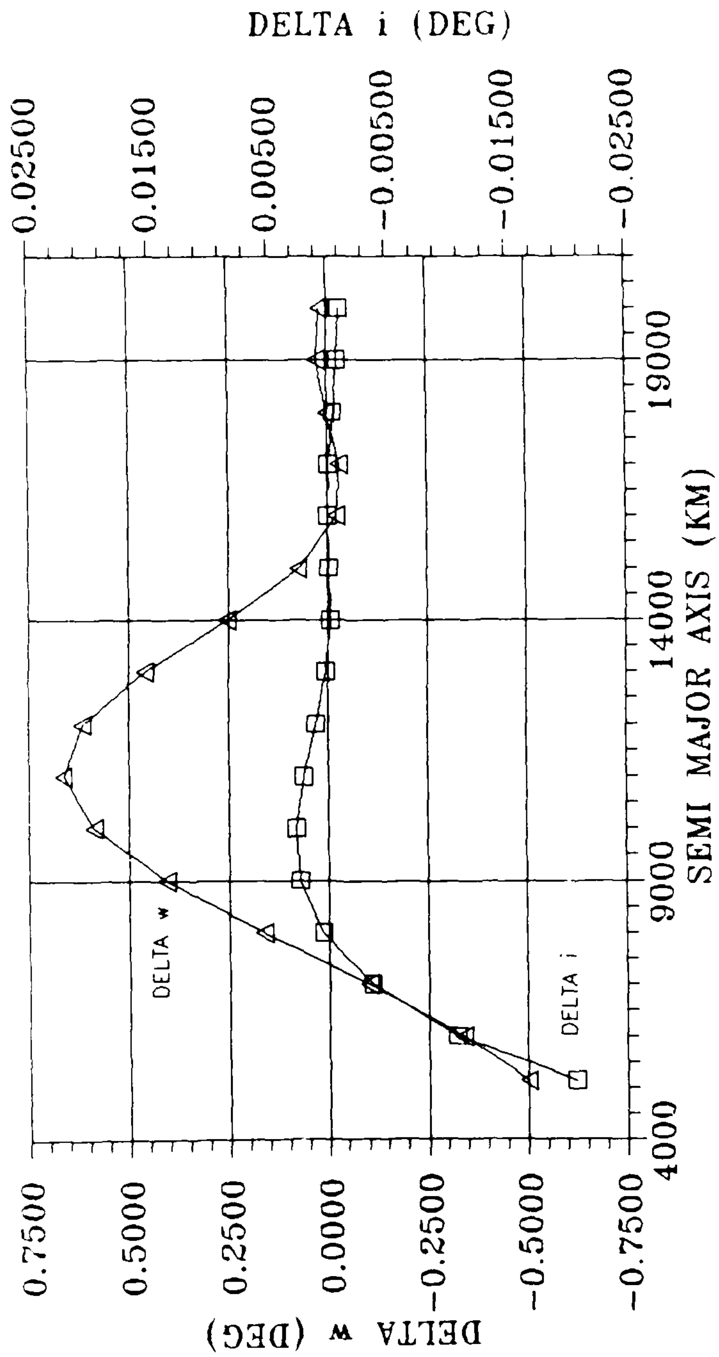

DELTA i, DELTA w vs. SEMI MAJOR AXIS for i = 70, e = .01
Figure J.1

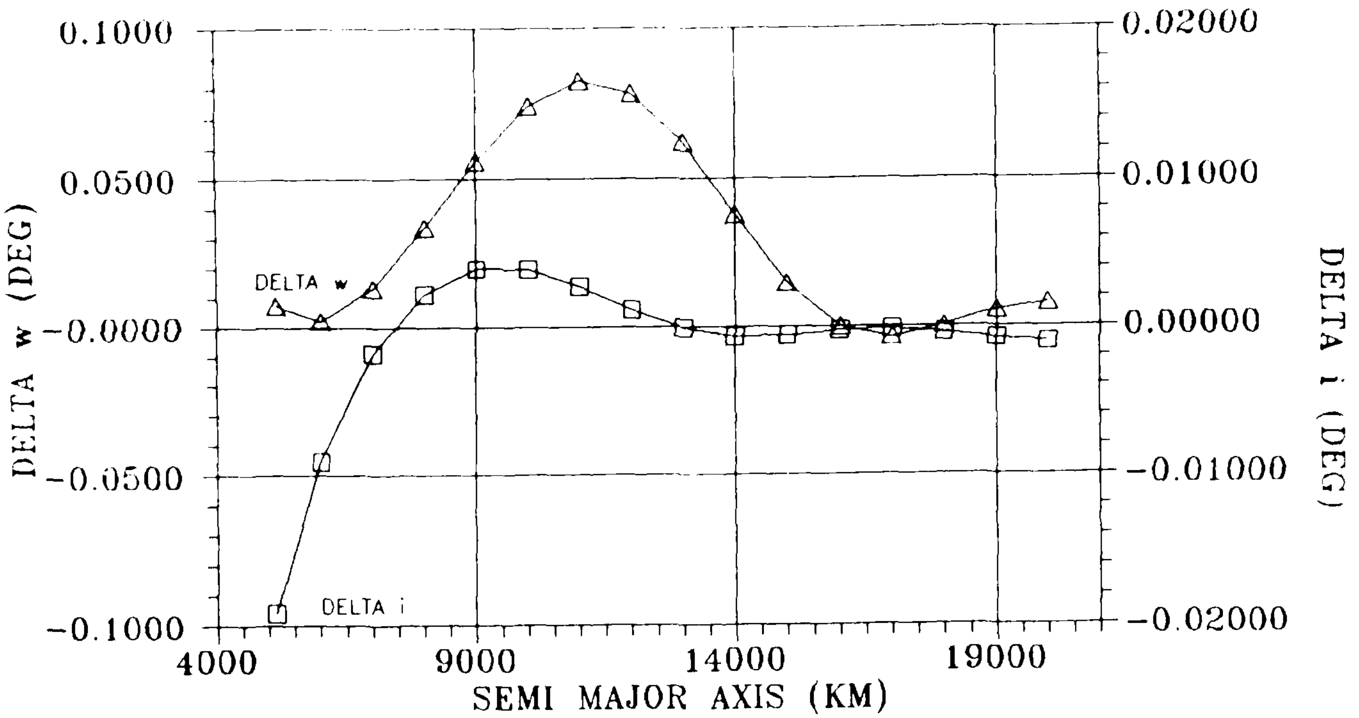

DELTA i, DELTA w vs. SEMI MAJOR AXIS for i = 70, e = .1
Figure J.2

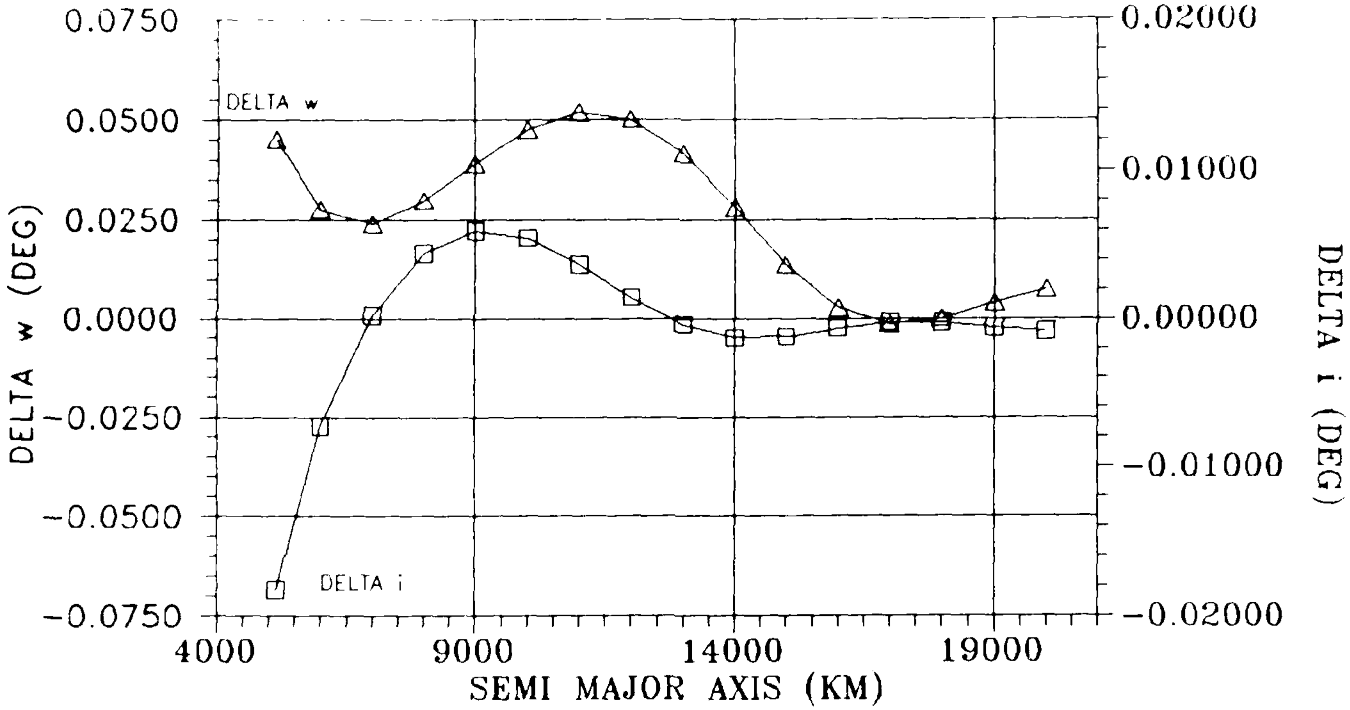

DELTA i, DELTA w vs. SEMI MAJOR AXIS for i = 70, e = .2
Figure J.3

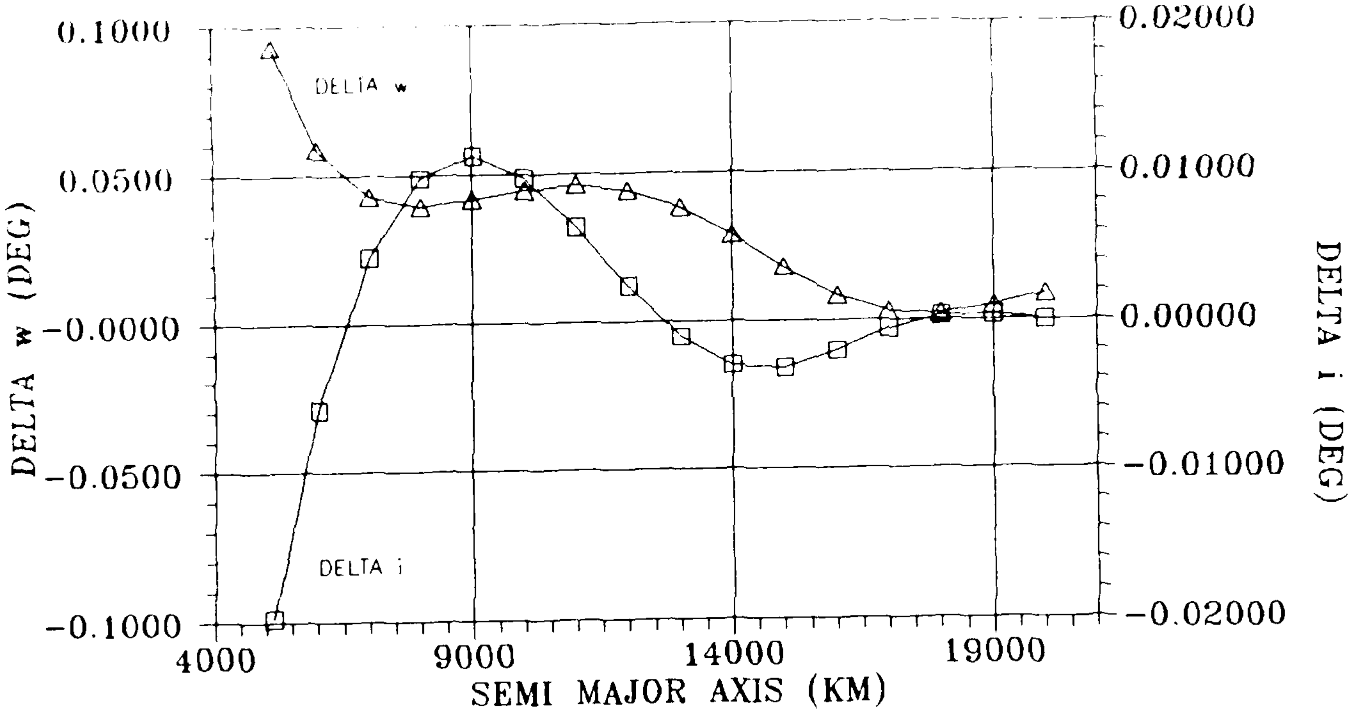

DELTA i, DELTA w vs. SEMI MAJOR AXIS for i = 70, e = .4
Figure J.4

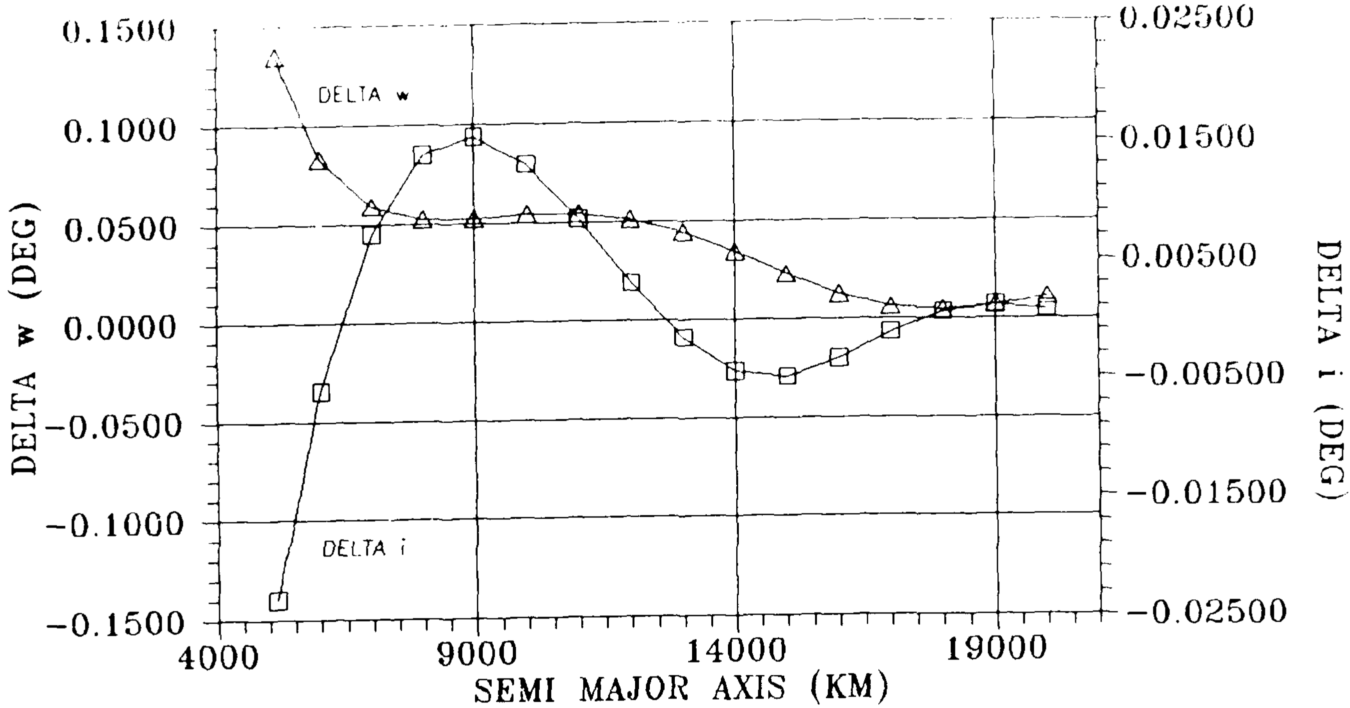

DELTA i, DELTA w vs. SEMI MAJOR AXIS for i = 70, e = .5
Figure J.5

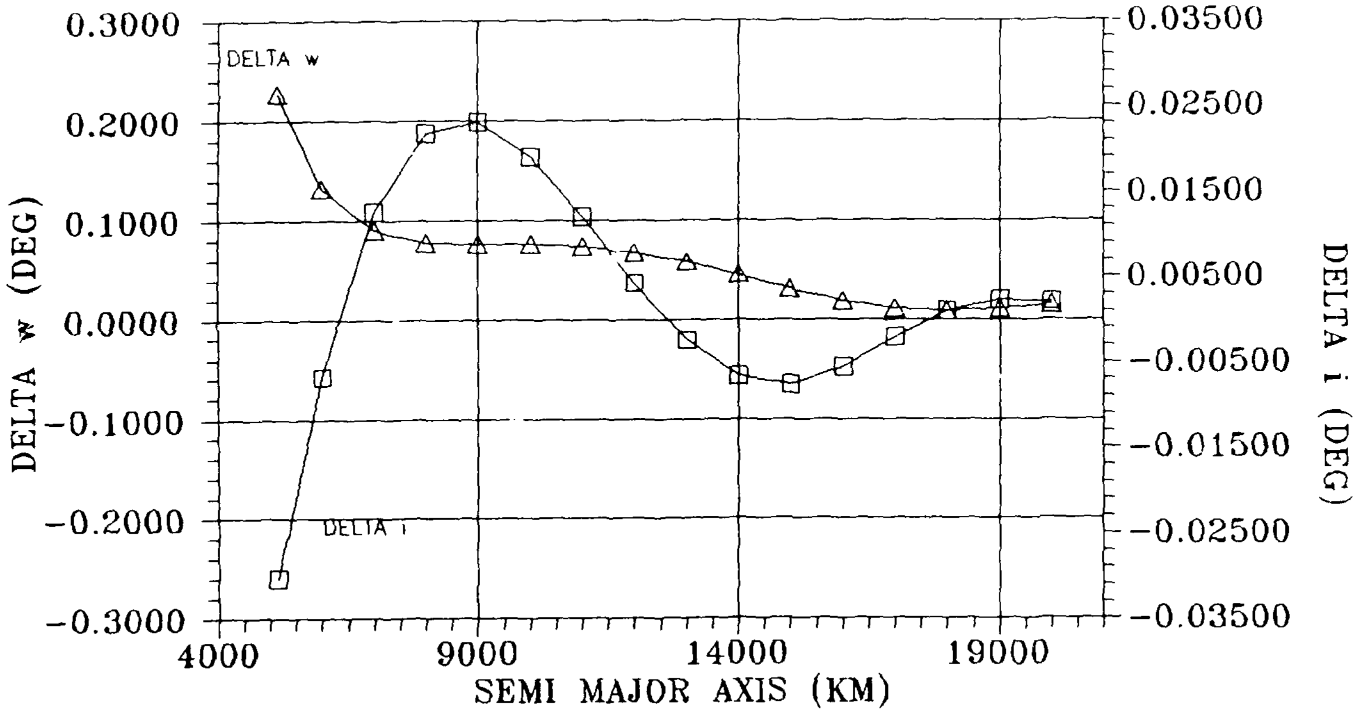

DELTA i, DELTA w vs. SEMI MAJOR AXIS for i = 70, e = .6
Figure J.6

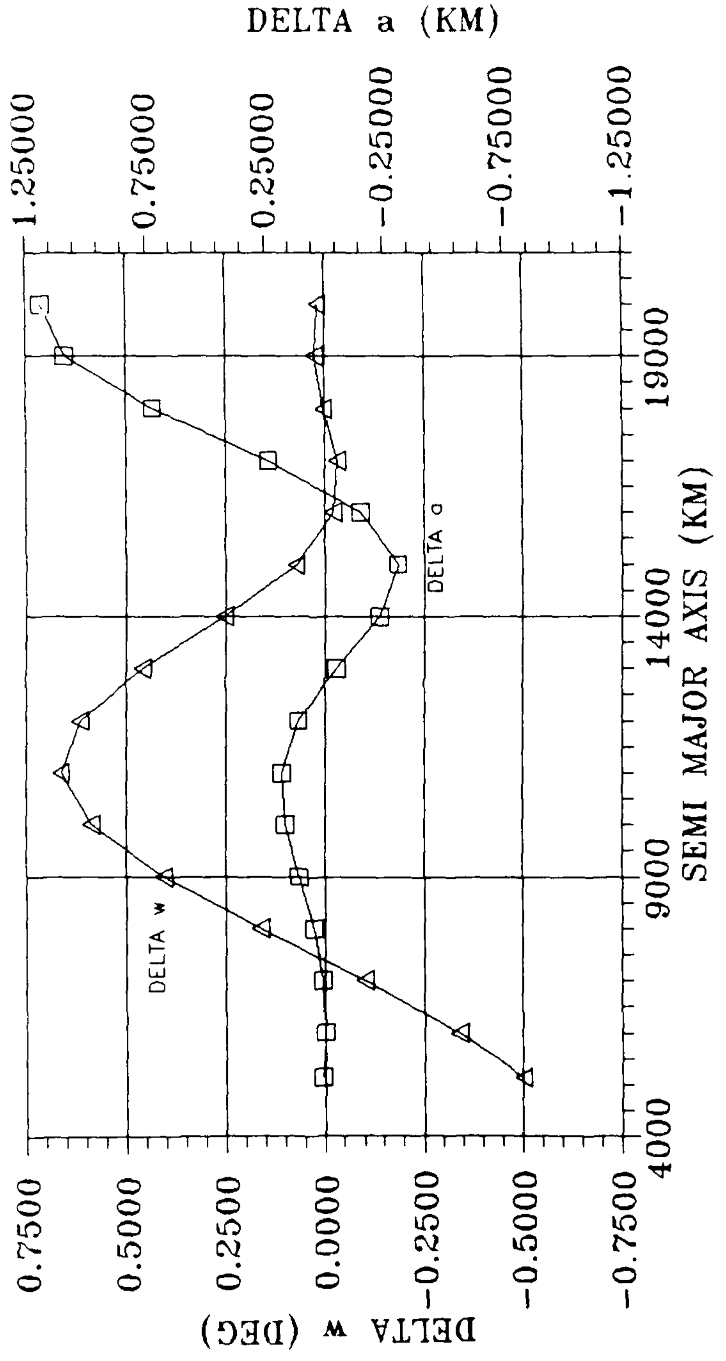

DELTA a, DELTA w vs. SEMI MAJOR AXIS for i = 70, e = .01
Figure K.1

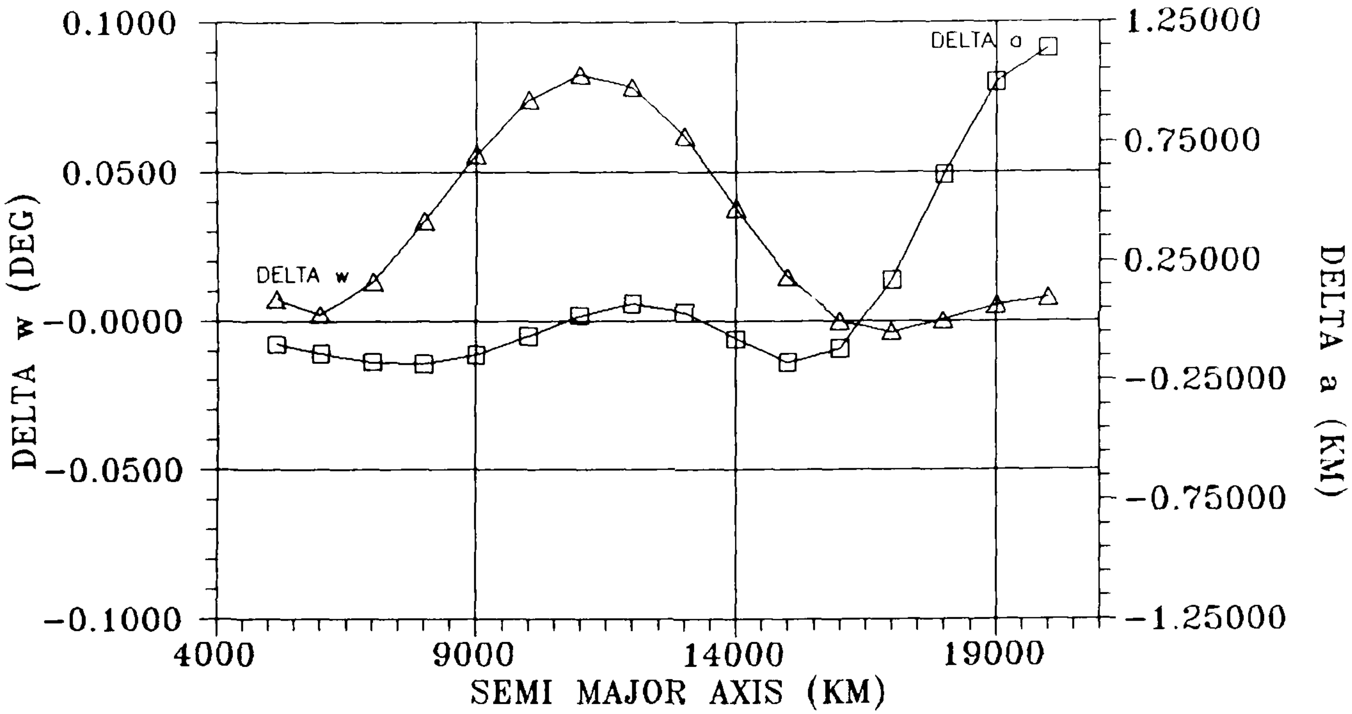

DELTA a, DELTA w vs. SEMI MAJOR AXIS for i = 70, e = .1
Figure K.2

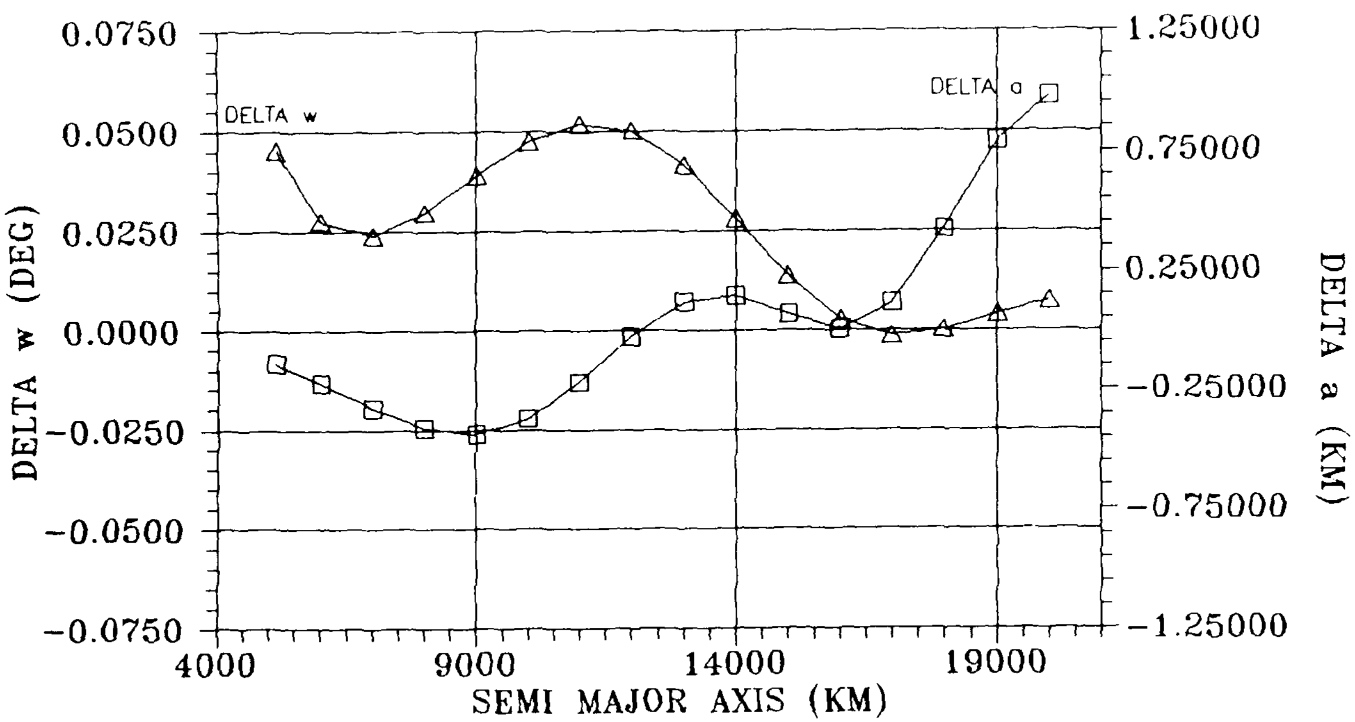

DELTA a, DELTA w vs. SEMI MAJOR AXIS for i = 70, e = .2
Figure K.3

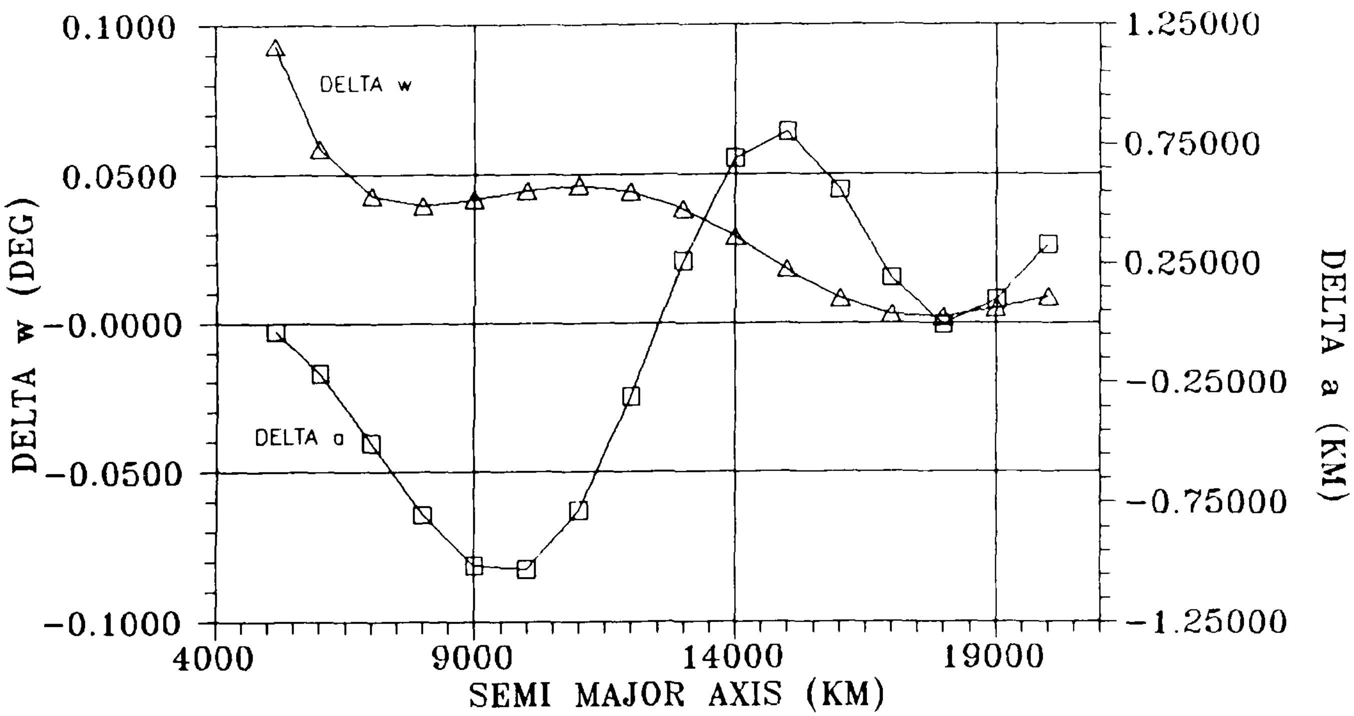

DELTA a, DELTA w vs. SEMI MAJOR AXIS for i = 70, e = .4
Figure K.4

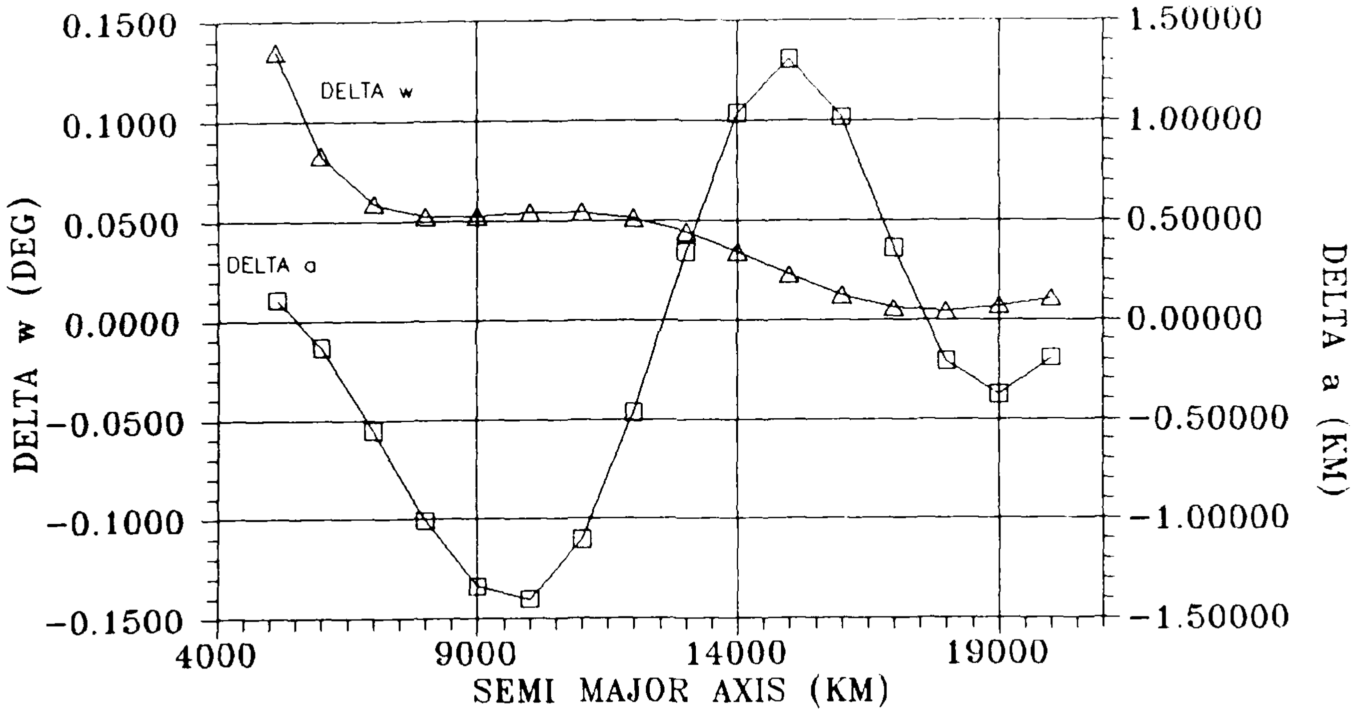

DELTA a, DELTA w vs. SEMI MAJOR AXIS for i = 70, e = .5
Figure K.5

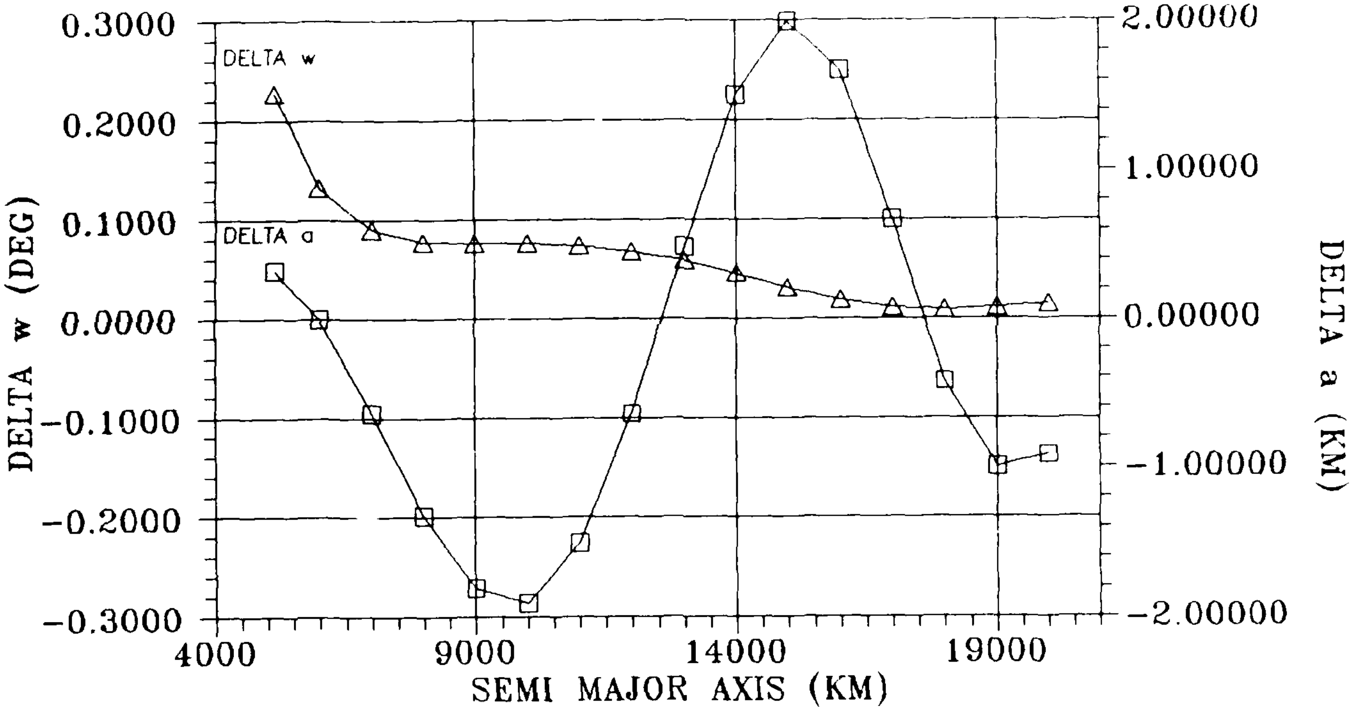

DELTA a, DELTA w vs. SEMI MAJOR AXIS for i = 70, e = .6
Figure K.6

Bibliography

1. Andrews, Larry C. Special Functions for Engineers and Applied Mathematicians. New York: Macmillan Publishing Co., 1985.

2. Bain, Rodney D. Lecture notes prepared for Advanced Astrodynamic II. School of Engineering, Air Force Institute of Technology (AU), Wright-Patterson AFB OH. July 1987.

3. Born, George H. and Hildebrand, Claude E. Jr. The Conversion of the Spherical Harmonic and Third Body Potential to Keplerian Elements, 2 May 1967. NASA Manned Spacecraft Center Contract 9-2619.

4. Cook, A. H. Gravity and the Earth. London: Wykeham Publications Ltd., 1969.

5. Danby, J. M. A. Fundamentals of Celestial Mechanics. New York: Macmillian Publishing Co., 1964.

6. Escobal, Pedro R. Methods of Orbit Determination. Malabar, Florida: Robert E. Krieger Publishing Company, 1985.

7. Evans, Howard., *Class handout distributed* in Physics 519, The Near Earth Space Enviroment. School of Engineering, Air Force Institute of Technology (AU), Wright-Patterson AFB OH, July 1986.

8. Greenwood, Donald T. Principles of Dynamics. Englewood Cliffs, N.J.: Prentice-Hall Inc., 1965.

9. Hansen, Arthur G. Fluid Mechanics. New York: John Wiley and Sons, Inc., 1967.

10. Kaula, William M. Theory of Satellite Geodesy. Waltham, Massachusetts: Blaisdell Publishing Co., 1966.

11. King-Hele, Desmond. Theory of Satellite Orbits in an Atmosphere. London, England: Butterworths Mathematical Texts, 1964.

12. Kreyszig, Erwin. Advanced Engineering Mathematics (Fifth Edition). New York: John Wiely & Sons, 1983.

13. Kwok, Johnny H. The Artificial Satellite Analysis Program (ASAP) (Version 2). COSMIC catalog #NPO-16731. Athens, Georgia: The University of Georgia, 1987.

14. Merson, R. H. "The Motion of a Satellite in an Axi-symmetric Gravitational Field," Geophysic Journal, Vol. 4, pp 17-52 (1961).

15. Roy, A. E. Orbital Motion (Second Edition). Bristol, England: Adam Hilger Ltd., 1982.

16. Seiff, Alvin and Donn B. Kirk. "Structure of the Atmosphere of Mars in Summer at Mid-Latitudes," Journal of Geophysical Research, Vol. 82, No. 28, pp 4364-4378 (September 30, 1977).

17. Uphoff, C. "Orbit Selection for Mars Geoscience/Climatology Orbiter," Proceeding of the American Institute of Aeronautics and Astronautics 22nd Aerospace Sciences Meeting. AIAA-84-0318. New York: American Institute of Aeronautics and Astronautics, 1984.

18. Vinh, Nguyen X. et al. Hypersonic and Planetary Entry Flight Mechanics. Ann Arbor, Mich.: The University of Michigan Press, 1980.

19. Wiesel, William. Class handout distributed in Mech 636, Advanced Astrodynamics. School of Engineering, Air Force Institute of Technology (AU), Wright-Patterson AFB OH, October 1986.

VITA

Captain James W. Foister, III received his commission and a B. S. degree in Aeronautical Engineering in June 1977 from the U. S. Air Force Academy. Upon graduating from pilot training in June 1978, Capt. Foister flew the F-4 D and E model with: 561st Tactical Fighter Squadron, George A.F.B., California, 18th Tactical Fighter Squadron, Elmendorf A.F.B., Alaska, 36th Tactical Fighter Squadron, Osan A.F.B., Korea, and the 497th Tactical Fighter Squadron, Taegu A.B., Korea. In May 1982, Capt. Foister was assigned to the 65th Aggressor Squadron, Nellis A.F.B., Nevada where he flew the F-5 E and F model. Before entering the School of Engineering, Air Force Institute of Technology, Capt. Foister would spend four years at Nellis, the last of which he served as the Chief of Red Force Operations for the 4440th Tactical Fighter Training Group (Red Flag).

UNCLASSIFIED
SECURITY CLASSIFICATION OF THIS PAGE

AD-A189 574

REPORT DOCUMENTATION PAGE

Form Approved
OMB No 0704-0188

1a. REPORT SECURITY CLASSIFICATION: UNCLASSIFIED

1b. RESTRICTIVE MARKINGS:

2a. SECURITY CLASSIFICATION AUTHORITY:

2b. DECLASSIFICATION / DOWNGRADING SCHEDULE:

3. DISTRIBUTION / AVAILABILITY OF REPORT: Approved for public release; distribution unlimited.

4. PERFORMING ORGANIZATION REPORT NUMBER(S): AFIT/GSO/AA/87D-2

5. MONITORING ORGANIZATION REPORT NUMBER(S):

6a. NAME OF PERFORMING ORGANIZATION: School of Engineering

6b. OFFICE SYMBOL (If applicable): AFIT/ENS

7a. NAME OF MONITORING ORGANIZATION:

6c. ADDRESS (City, State, and ZIP Code):
Air Force Institute of Technology
Wright-Patterson AFB, Ohio 45433-6583

7b. ADDRESS (City, State, and ZIP Code):

8a. NAME OF FUNDING / SPONSORING ORGANIZATION:

8b. OFFICE SYMBOL (If applicable):

9. PROCUREMENT INSTRUMENT IDENTIFICATION NUMBER:

8c. ADDRESS (City, State, and ZIP Code):

10. SOURCE OF FUNDING NUMBERS

PROGRAM ELEMENT NO	PROJECT NO.	TASK NO	WORK UNIT ACCESSION NO.

11. TITLE (Include Security Classification): FROZEN ORBIT ANALYSIS IN THE MARTIAN SYSTEM (unclassified)

12. PERSONAL AUTHOR(S): James W. Foister, III Captain, USAF

13a. TYPE OF REPORT: MS Thesis

13b. TIME COVERED: FROM ______ TO ______

14. DATE OF REPORT (Year, Month, Day): 1987, Dec., 7

15. PAGE COUNT: 189

16. SUPPLEMENTARY NOTATION:

17. COSATI CODES

FIELD	GROUP	SUB-GROUP
22	01	

18. SUBJECT TERMS (Continue on reverse if necessary and identify by block number):
Trajectories Orbits
Mars
Frozen Orbits

19. ABSTRACT (Continue on reverse if necessary and identify by block number)

Thesis Chariman: Rodney D. Bain, Captain, USAF
Instructor of Astronautical Eng.

31 Dec 87

20. DISTRIBUTION / AVAILABILITY OF ABSTRACT: ☒ UNCLASSIFIED/UNLIMITED ☐ SAME AS RPT ☐ DTIC USERS

21. ABSTRACT SECURITY CLASSIFICATION: UNCLASSIFIED

22a. NAME OF RESPONSIBLE INDIVIDUAL: Rodney D. Bain, Captain, USAF

22b. TELEPHONE (Include Area Code): 513-255-3633

22c. OFFICE SYMBOL: AFIT/ENY

DD Form 1473, JUN 86 — Previous editions are obsolete

SECURITY CLASSIFICATION OF THIS PAGE
UNCLASSIFIED

FROZEN ORBIT ANALYSIS IN THE MARTIAN SYSTEM.
The purpose of this study is to determine where about Mars there may exist regions of orbital stabilities similar to those of the known polar frozen orbits. Only perturbative effects due to a 6 X 6 gravity field and atmospheric drag are considered. The geopotential equation is developed for both spherical coordinates and the classical orbital elements. An atmospheric model is also developed. The Fortran computer model ASAP (Artificial Satellite Analysis Program) is validated for accuracy, and used to perform a major portion of the analysis. Finally, recommendations are made for future study.

END
DATE
FILMED
3-1988
DTIC